Origin of Island Dolostone: Case Study of Cayman Formation (Miocene), Grand Cayman, British West Indies

by

Min Ren

A thesis submitted in partial fulfillment of the requirements for the degree of

Doctor of Philosophy

Department of Earth and Atmospheric Sciences
University of Alberta

ABSTRACT

Grand Cayman is located on an isolated fault block that is part of the Cayman Ridge that defines the southern margin of the North American Plate. The exposed part of the Oligocene to Pleistocene carbonate succession that forms the island comprises the Bluff Group (Brac Formation, Cayman Formation, Pedro Castle Formation) and Ironshore Formation. The Cayman Formation (Miocene), which is up to ~140 m, is formed of dolostones and limestones. Analyses of numerous dolostone samples from numerous wells drilled on the eastern part of the island show that there are no obvious stratigraphic variations in the dolostones. In contrast, there are significant geographic variations in the petrography, dolomite stoichiometry, and stable isotope signatures of these dolostones. Thus, from a geographic perspective, the Cayman Formation can be divided into the concentrically arranged peripheral dolostone, transitional dolostone, interior dolostone, and interior (dolomitic) limestone zones. $^{87}Sr/^{86}Sr$ ratios from the dolostones indicate that they probably resulted from two major phases of dolomitization that occurred during the late Miocene to early Pliocene and late Pliocene to early Pleistocene. Dolomitization was mediated by seawater as it flowed from the coast inland. As it migrated inland the composition of the water progressively changed as it interacted with the host rock and mixed with meteoric water. These changes were responsible for the landward variations in the petrographic and geochemical signatures of the dolostones. This model for the origin of island dolostones stresses the geographic variability in the dolostones and dolomitizing fluids that are controlled by various intrinsic and extrinsic factors.

Over the last 1 Ma, the Cayman Formation has experienced rapid and frequent

changes in diagenetic environments because of the frequent and rapid glacio-eustatic changes in sea level. The diagenetic fabrics evident in the dolostones and limestones of the formation, however, do not record all of these diagenetic regimes.

The Cayman Model for island dolomitization can be applied to many island dolostone succession found throughout world. The extent and distribution of the concentrically arranged zones vary from island to island because their development is controlled by many different intrinsic and extrinsic factors. The Cayman Model, highlights the complexity of the dolomitization processes, clearly illustrates that geographic and stratigraphic variations must be integrated into any proposed dolomitization model. This study suggests that dolomitization models should not be based on a single geographic location because the progressive lateral changes in the dolomitizing fluids and environmental conditions cannot be assessed.

PREFACE

This thesis is an original work by Min Ren under the supervision of Professor Brian Jones. The PhD thesis project started in September 2013.

The research conducted for this thesis forms part of a research project, led by Professor B. Jones at the University of Alberta. The research project received funding support from the Natural Sciences and Engineering Research Council of Canada (grant No. ZA635) to Professor B. Jones.

Chapters two and three of this thesis have been published as:

Ren, M., Jones, B., 2017, "Spatial variations in the stoichiometry and geochemistry of Miocene dolomite from Grand Cayman: Implications for the origin of island dolostone", *Sedimentary Geology* 348, 69-93.

Ren, M., Jones, B., 2016, "Diagenesis in limestone-dolostone successions after 1 million years of rapid sea-level fluctuations: a case study from Grand Cayman, British West Indies", *Sedimentary Geology* 342, 15–30.

Chapter four of this thesis has been submitted as:

Ren, M., Jones, B., "New insights into Cenozoic island dolostones: geometries, and spatial variations", *Sedimentary Geology*.

The initial theme of the thesis was outlined by Professor Brian Jones, and the concept of each chapter was developed through discussions between both of us. The thesis is based on samples that were collected by Dr. Jones and the database that has been assembled by Dr. Jones over the last thirty years and supplemented by data that I obtained during my research. I analyzed the compiled data and wrote the initial drafts of the manuscripts with input from both authors. Both authors discussed the results and edited the manuscripts.

To the memory of my Grandfather

ACKNOWLEDGEMENTS

I would like to express my sincere gratitude to my supervisor Dr. Brian Jones for letting me fulfill my dream of being a student of his. I am thankful to him for introducing me to carbonate research. I am indebted to his encouragement, guidance, and patience, and the valuable things I learned from him. He pushed me further than I thought I could go.

I am thankful to the members of my thesis committee, Drs. Murray Gingras, Nicholas Harris, Long Li, and Hairuo Qing (external) for their valuable guidance and encouragement.

I would like to thank the Natural Sciences and Engineering Research Council of Canada for the funding provided to Dr. Brian Jones that helped the completion of this thesis. I express my thanks to the drilling crews from Industrial Services and Equipment Ltd., who drilled many of the wells, and numerous staff members from the Water Authority, Cayman Islands, who helped collect the samples used in this study.

I wish to thank many people in the Department of Earth and Atmospheric Sciences at the University of Alberta: Diane Caird for running the XRD analyses, Martin Von Dollen and Mark Labbe for preparing the thin sections, Nathan Gerein for helping on the SEM, Dr. Robert Creaser for the strontium analyses, and David Chesterman and Lisa Budney for helping with my TAs.

Thanks to the great carbonate research group – Josh, Rong, Ting, Megan, Erjun, and Simone for the delightful academic discussions and chitchats. Thank you to my fellow classmates Merilie and Yuhao for the help they offered in the classroom and in my research.

Thank you to all my family members for their faith and love in me, especially my loving grandmother. Thank you to my dear friends – you have always been there for me and shaped up a better me.

TABLE OF CONTENTS

LIST OF TABLES

LIST OF FIGURES

CHAPTER ONE

INTRODUCTION

1. Introduction

Dolomite [$CaMg(CO_3)_2$], which is a common mineral that forms dolostone, is found throughout Precambrian to Cenozoic strata and has been studied for over two centuries (see Van Tuyl, 1914; Hardie, 1987; Land, 1985, 1992; Warren, 2000; Machel, 2004; McKenzie and Vasconcelos, 2009; Gregg et al., 2015). Research on dolomite and dolostone flourished during the late 20th century, due largely to the discovery of its economic importance as hydrocarbons reservoirs (e.g., Devonian reef, Alberta) and ore host rocks (e.g., Machel, 2004). The dolomitization mechanisms and models proposed during that period contributed significantly to our understanding of dolomite and the process of dolomitization. During the early part of the 21st century, however, the study of dolomite continued because the controversy over the origin of dolomite still existed. Many geologists have tried to develop new approaches to resolving the dolomite mystery. These include, for example, numerical hydrological and dolomitization reaction modeling (e.g., Whitaker et al., 2004), laboratory experiments to synthesize dolomite under high temperature and pressures (Kaczmarek and Sibley, 2011; Gregg et al., 2015) or under ambient conditions in the presence of bacteria (Mazzullo, 2000; McKenzie and Vasconcelos, 2009; Roberts et al., 2013), and the application of non-traditional geochemical analyses (e.g., Azmy et al., 2013). Advances in our understanding of dolomite formation have been made because of these diverse approaches and significant advances in analytical techniques. Nevertheless, debate on the origin of dolomite is still ongoing.

The dolomite problem (Van Tuyl, 1914; Fairbridge, 1957) is essentially a question of the origin of thick dolostone successions that have formed throughout geological history. The main problems encountered in trying to resolve this problem are as follows.

- To date, it has proved impossible to precipitate dolomite in the laboratory under

ambient, abiotic conditions. This means that it has been impossible to develop equations and distribution coefficients that can be used to interpret stable isotope and trace element data under low temperature conditions. Instead, these parameters have been extrapolated from high temperature and pressure experiments even though it is not known if they are truly applicable to ambient conditions.

- The role of microbial activity in dolomitization is open to debate. Many authors have synthesized microbially mediated "dolomite" and suggested that organic compounds can reduce the hydration of Mg^{2+} ions and thus kinetically promote dolomitization (e.g., Vasconcelos and McKenzie, 1997; Burns et al., 2000). This assertion has been questioned because it is not clear if (1) the product is nonstoichiometric dolomite or simply high magnesium calcite (e.g., Gregg et al., 2015), and (2) the dolomite-producing bacteria have the capability of producing thick, laterally extensive dolostone bodies that are analogous to those found in the geological record.
- It is difficult to explain the reasons for the considerable variations in dolostone abundance throughout geological time and the paucity of dolostone in Holocene sediments. This reflects, at least in part, the lack of precise knowledge of the conditions that were responsible for dolomitization.
- Although numerous dolomitization models have been proposed, the ones that have the highest potential of producing thick, laterally extensive dolostone bodies remain a matter of debate.

An important approach to the dolomite problem involves the selection of dolostone samples that reflect the signatures of dolomitization rather than signals of later diagenetic modifications. In this regard, Cenozoic island dolostones are ideal for addressing the dolomite problem. "Island dolomite" refers to those dolomites found on oceanic islands, atolls, and carbonate platforms where carbonate sediments were deposited and subsequently dolomitized during the Cenozoic. Although the term was first coined by Budd (1997),

"island dolomites" found on many Caribbean and Pacific islands had been the focus of numerous studied since 1960 because they offered various advantages over older dolostones found in continental settings. As pointed out by Budd (1997), the Cenozoic island dolostones provide a natural laboratory for studying the dolomite problem because (1) the hydrological conditions during dolomitization can be reasonably inferred, (2) the dolomitization temperature can be constrained to a narrow range, (3) they are young and hence allow precise dating of dolomitization, and (4) there is little post-dolomitization diagenesis that could have altered the petrographic and geochemical properties of the original dolostones.

Many dolomitization models have been proposed for the origin of island dolostones. These include, for example, reflux dolomitization, mixing zone dolomitization, and hydrothermal dolomitization. All these models are categorized as the general "seawater dolomitization model" (e.g., Tucker, 1990), which indicates that seawater, whether diluted, concentrated, or normal, is the source of the Mg needed for dolomitization of the island carbonates (Fig. 1.1A). The seawater dolomitization model in Tucker (1990) includes all of the hydrological mechanisms that can drive seawater into carbonate islands including ocean current pumping, reflux of slightly hypersaline lagoon waters, tidal pumping along shorelines, and Kohout convection (Fig. 1.1A). The seawater dolomitization model proposed by Budd (1997) is divided into elevation-head-driven seawater dolomitizations (including tidal pumping, seepage influx, and differential sea-surface elevation), and density-head-driven seawater dolomitizations (brine reflux, coastal mixing zone and outlying zone of entrained seawater, and thermal convection) (Fig. 1.1B). Apparently, all the proposed models for island dolomitization are fluid chemistry and flow models but rather models that reflect the attributes of dolostones themselves.

An effective seawater circulation mechanism that guarantees sufficient magnesium supply is critical to island dolomitization. Thus, most dolomite models invoked to explain island dolomitization have tried to link various parameters of the dolostones to the hydrological conditions and the geochemistry of dolomitizing fluid (Fig. 1.1; see Budd,

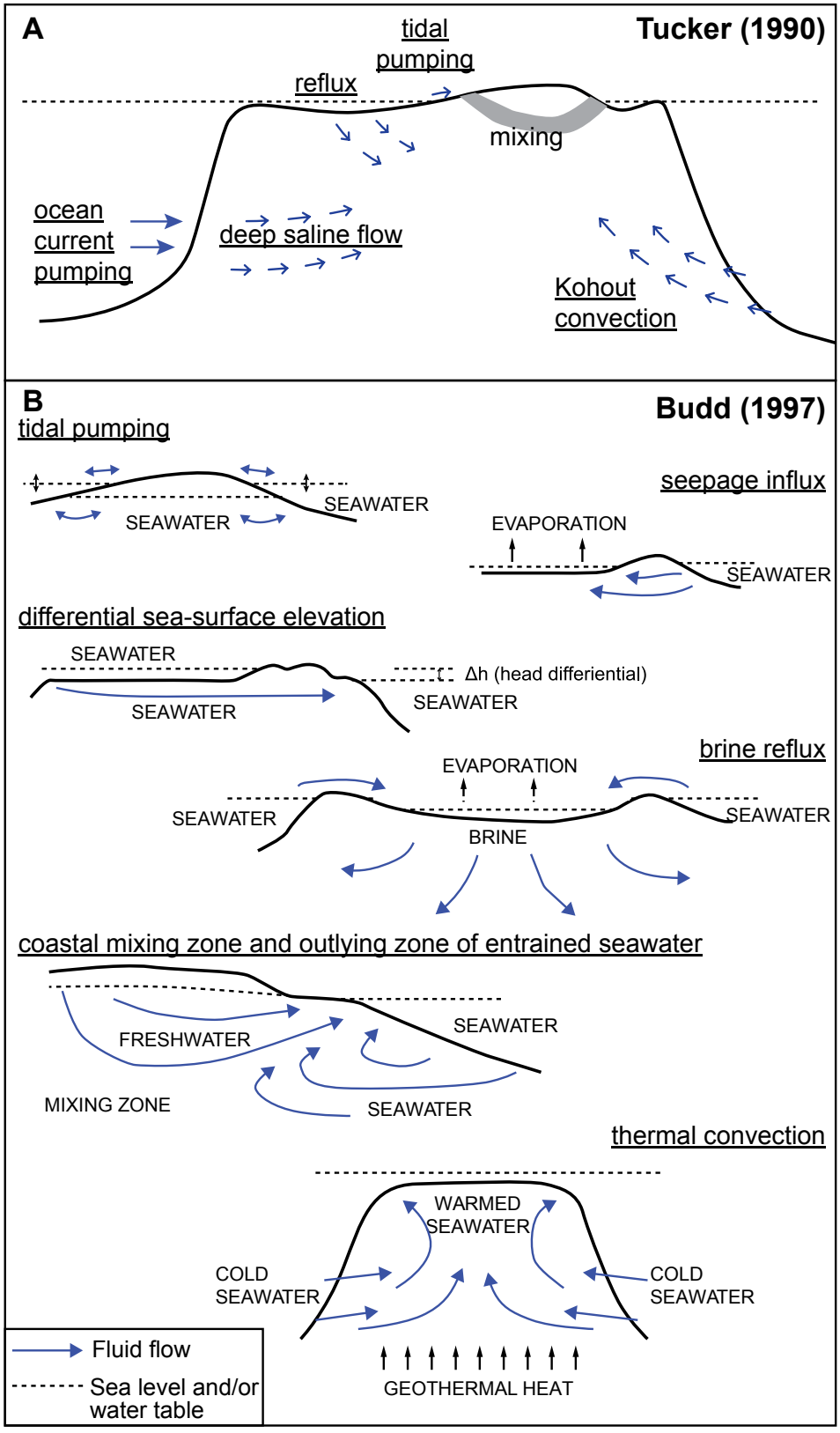

Fig. 1.1. Seawater dolomitization model for the origin of island dolostones as summarized by (A) Tucker (1990) and (B) Budd (1997). See text for details.

1997). As a result, less attention has been focused on the dolostones themselves. Thus, the three-dimensional spatial variability in the properties of the dolostones within individual dolostone bodies has received little attention. A dolomitization model should incorporate and reflect as many aspects of the dolostones as possible. This viewpoint is a key point in this study, which is designed to address to dolomite problem.

The Cayman Formation (Miocene), which is found on the east end of Grand Cayman, is ideal for studying the dolomite problem for following reasons.

- On the east end of Grand Cayman, the Cayman Formation are up to 140 m thick and laterally extensive.
- After thirty years of research on the geology of the Cayman Islands, a large database has been established that includes the surface and subsurface geological and hydrological information for the eastern part of Grand Cayman. This includes data from 32 wells and 1788 samples of dolostone and limestone on the east end of Grand Cayman (Table 1.1; Fig. 1.2). This allows a detailed view of the lateral and vertical variations and trends in the distribution, petrography, and geochemistry of the dolostones.
- The stratigraphy and sedimentology of the Cayman Formation have been well established in previous studies (e.g., Jones et al., 1994a, b; Der, 2012).

2. Geological setting

Grand Cayman, the largest of the Cayman Islands, is located south of Cuba, east of the Yucatan Peninsula, and northwest of Jamaica (Fig. 1.3A). The island is about 35 km long and up to 14 km wide with an area of 196 km^2 (Fig. 1.3B). The interior of the island, which is typically less than 3 m above sea level is, on the east end of the island, surrounded by a coastal ridge that rises up to 15 m above sea level.

Tectonically, Grand Cayman is located on the Cayman Ridge, a large uplifted fault block that developed as an island arc north of the Cayman Trench (Fig. 1.3C). There are

Table 1.1. Information for the wells on the east end of Grand Cayman in this study.

#	Well	Drilling year	Depth (m)	Sample type	#XRD Samples
1	QHW-1	1992	60.0	?	39
2	BOG-1	1994	39.6	Core	6
3	RWP-2	1998	94.7	Core	62
4	NSC-1	2005	150.0	Cutting/Core	126
5	BAC-1	2006	39.6	Cutting	37
6	RTR-1	2006	138.7	Cutting	91
7	AIR-1	2007	49.4	Cutting	33
8	DTE-1	2007	46.3	Cutting	30
9	FSR-11	2007	52.4	Cutting	35
10	HRQ-1	2007	61.6	Cutting	80
11	CKC-1	2008	67.2	Cutting	45
12	FFM-1	2008	64.8	Cutting	41
13	HMB-1	2008	57.9	Cutting	37
14	EER-1	2009	140.2	Cutting	92
15	EEV-2	2009	101.8	Cutting	67
16	EER-2	2009	117.3	Cutting	77
17	RAD-1	2009	18.3	?	17
18	EEZ-1	2010	87.6	Core/Cutting	66
19	LBL-1	2010	94.5	Cutting	70
20	EEZ-2	2010	86.9	Cutting	57
21	GFN-1	2011	121.9	Cutting	84
22	HHD-1	2011	61.0	Cutting	43
23	HRQ-2	2011	128.0	Cutting	84
24	GMR-2	2011	46.0	?	28
25	ESS-1	2012	77.4	Core/Cutting	49
26	CLZ-1	2012	77.0	Core/Cutting	61
27	HRQ-3	2013	80.8	Cutting	53
28	GFN-2	2014	92.2	Core	59
29	HRQ-4	2014	64.0	Cutting	42
30	HRQ-5	2014	76.2	Cutting	50
31	HRQ-6	2014	76.2	Cutting	51
32	HRQ-7	2014	39.6	Cutting	26
33	HRQ-8	2014	76.2	Cutting	50
Total	33	-	2585.2	-	1788

numerous isolated banks and islands on the ridge, including the Cayman Islands. The Cayman Ridge began to subside during the Eocene at an average rate of 6 cm/1,000 yr (Perfit

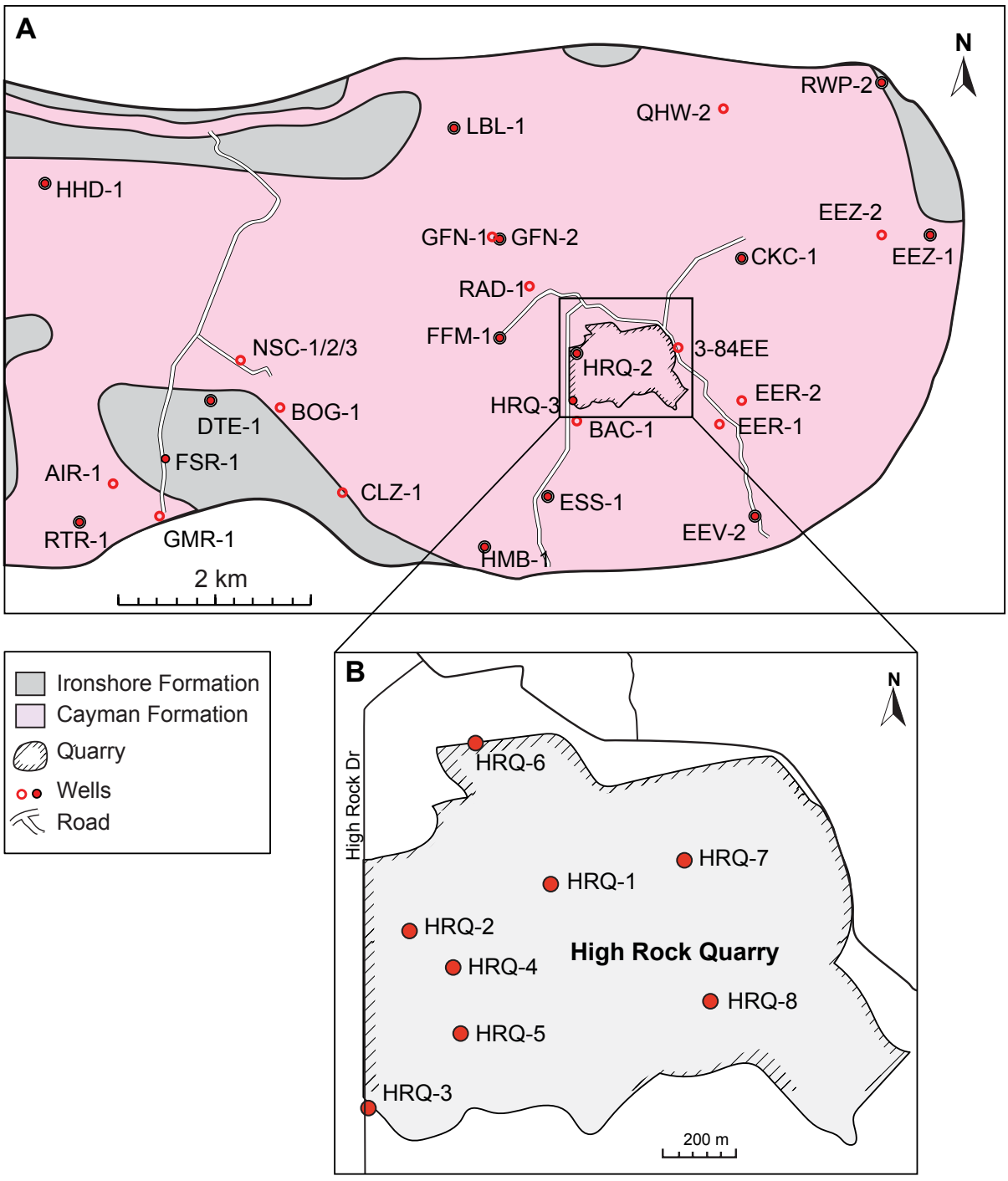

Fig. 1.2. Locations of wells incorporated in this study on the east end of Grand Cayman. (A) Locations of the wells (Detailed lithological columns and cross sections are presented in the following chapters for those wells indicated as solid red dots). (B) Locations of eight wells drilled in High Rock Quarry (HRQ).

and Heezen, 1978). This subsidence caused progressive restriction of carbonate banks and reefs to a few isolated islands and algal pinnacles (Perfit and Heezen, 1978). The Cayman Trench is bordered by a transform fault zone that separates the southwest-moving North American Plate and the northeast-moving Caribbean Plate. The Cayman Trench opened during the Eocene (Perfit and Heezen, 1978; Leroy et al., 2000). In the middle of the

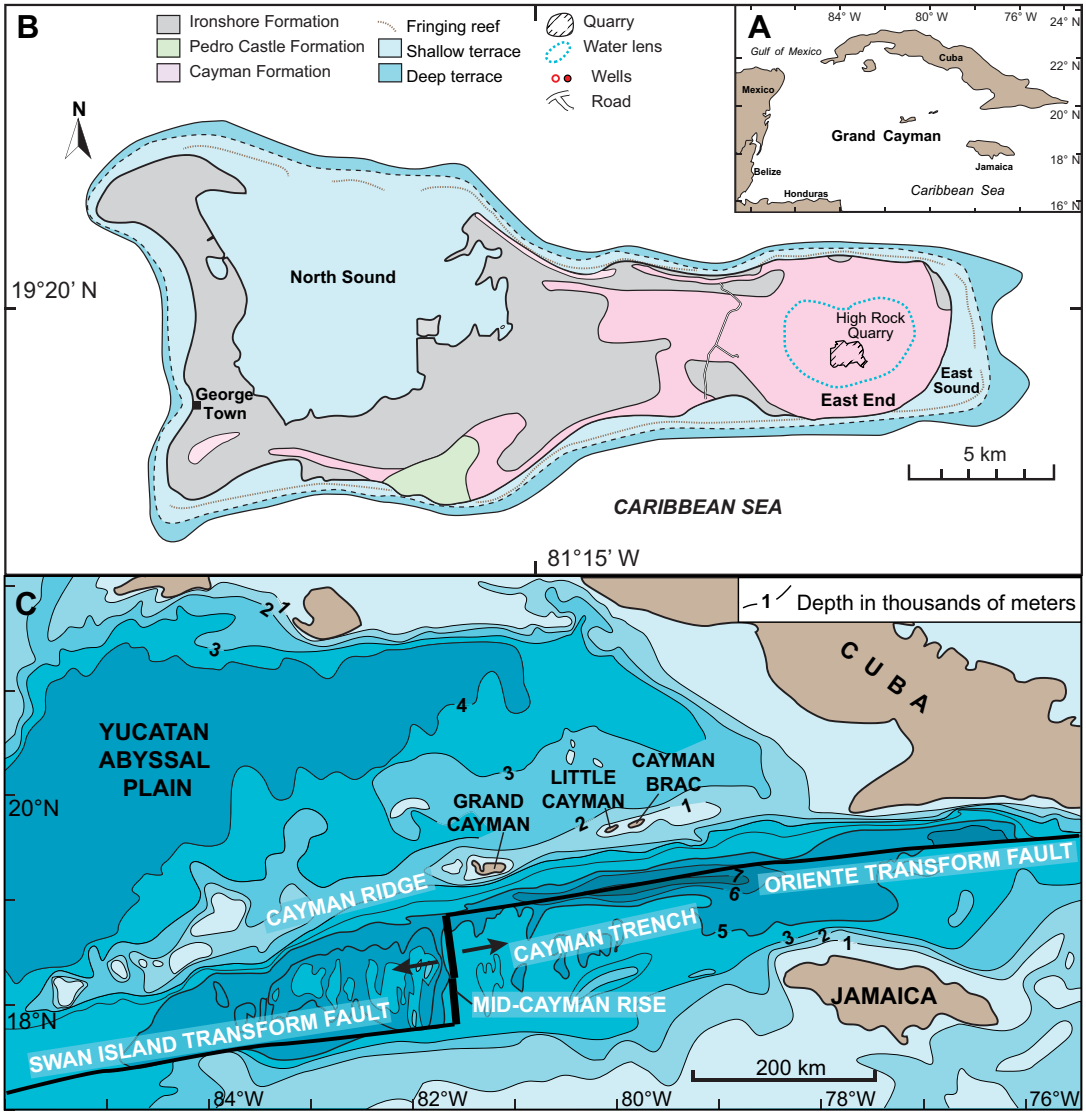

Fig. 1.3. Geological and tectonic settings of Grand Cayman. (A) Location of Grand Cayman in Caribbean Sea. (B) Geological map of Grand Cayman showing the distribution of the Cayman Formation, the Pedro Castle Formation, the Ironshore Formation, and the East End Lens. Modified from Jones (1994) and Ng (1991). (C) Tectonic and bathymetric map showing the location of the Cayman Islands on the Cayman Ridge. Modified from Jones (1994) based on Perfit and Heezen (1978) and MacDonald and Holcombe (1978).

Cayman Trench is the Mid-Cayman spreading center that is located off the southwest corner of the Grand Cayman. The spreading center, which is still active today, spreads at a rate of 15-17 mm/yr (Hayman et al., 2011).

Carbonate sediments have accumulated on Grand Cayman since the Oligocene (at latest) and possibly earlier (Fig. 1.3). A deep well drilled close to the middle southern coast reveals shallow marine limestone of Oligocene age to a depth of 401 m (Emery and Milliman, 1980). Wells drilled over the last 20 years, with a maximum depth of 243 m on Grand Cayman, have also penetrated the Oligocene carbonate strata. The carbonate successions that are exposed and evident in wells are divided into the Brac Formation (Oligocene), the Cayman Formation (Miocene), the Pedro Castle Formation (Pliocene), and the Ironshore Formation (Holocene) that are bounded by unconformities that developed during sea level lowstands (Jones et al., 1994a) (Fig. 1.4). With the exception of the Brac Formation, all of these formations are exposed at the surface on Grand Cayman (Fig. 1.3B).

The Cayman Formation covers most of the surface on the east end of Grand Cayman. The formation was initially defined as a thick (≥ 130 m) dolostone succession (Jones et al., 1994a, Jones and Luth, 2003a), formed largely of fabric-retentive and microcrystalline (average crystal length of 10-30 μm with most < 50 μm long) dolostones (Jones, 1994, 2005; Fig. 1.5). The succession consists largely of dolomitized mudstones, skeletal wackestones, skeletal packstones, and skeletal grainstones (Jones and Luth, 2003a). Biota in the formation is dominated by corals (branching, platy, domal), bivalves, gastropods, red algae, foraminifera, *Halimeda*, and rhodoliths (Jones, 1994a). According to the distribution of *Porites*, *Stylophora*, and *Montastrea*, Der (2012) defined eight sedimentary facies. Depositional environments were thought to range from deep to shallow (water 10 to 30 m deep) environments on an unrimmed bank (Der, 2012).

3. Previous study of dolostones from the Cayman Islands

On Grand Cayman and Cayman Brac, the dolostones (dolomitic limestones) found

in the Brac Formation, the Cayman Formation, the Pedro Castle Formation, and the Ironshore Formation have been studied by Jones (1989), Pleydell et al. (1990), Ng (1990), Wignall (1995), Willson (1998), Jones et al., (2011), Jones and Luth (2002, 2003a, b), MacNeil and Jones (2003), Jones (2005), Jones (2007), Zhao and Jones (2012, 2013a, b), Jones (2013), and Li and Jones (2014). These studies focused on the characteristics of the dolostones (petrography, stoichiometry and geochemistry), and their modes of origin (types of dolomitizing fluid, and timing of dolomitization). The dolostones from these different formations and islands share similarities and differences.

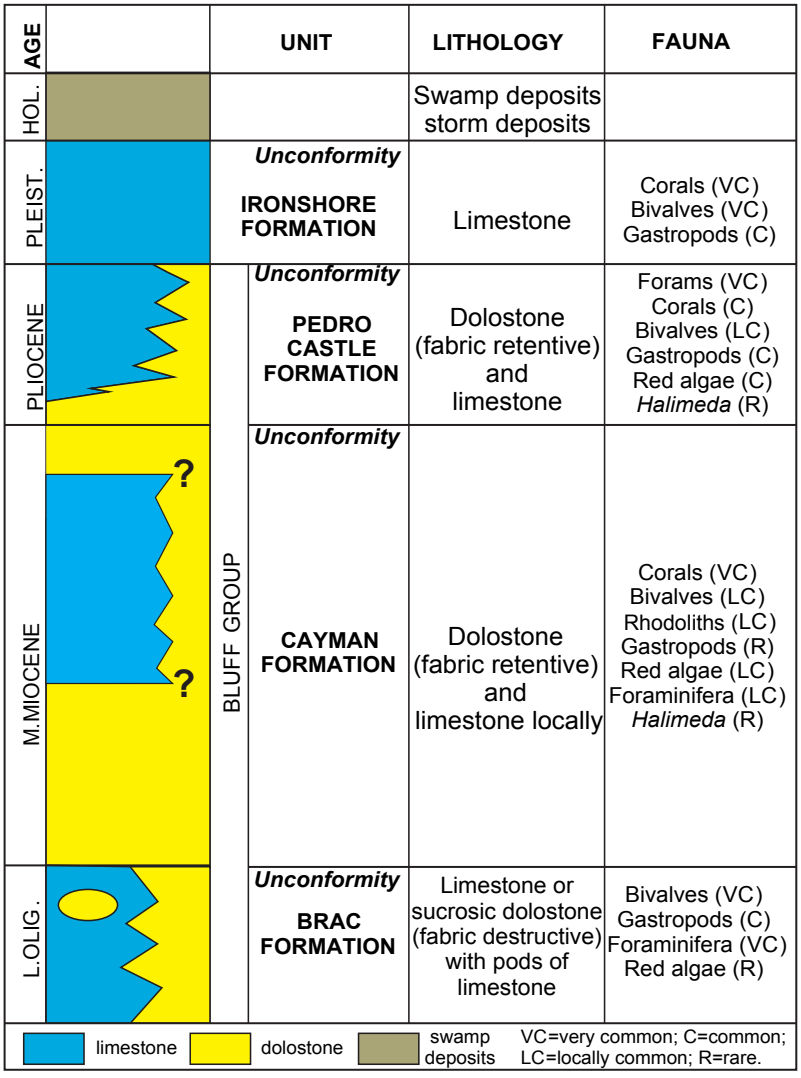

Fig. 1.4. Stratigraphic succession on the Cayman Islands. Modified from Jones (1994).

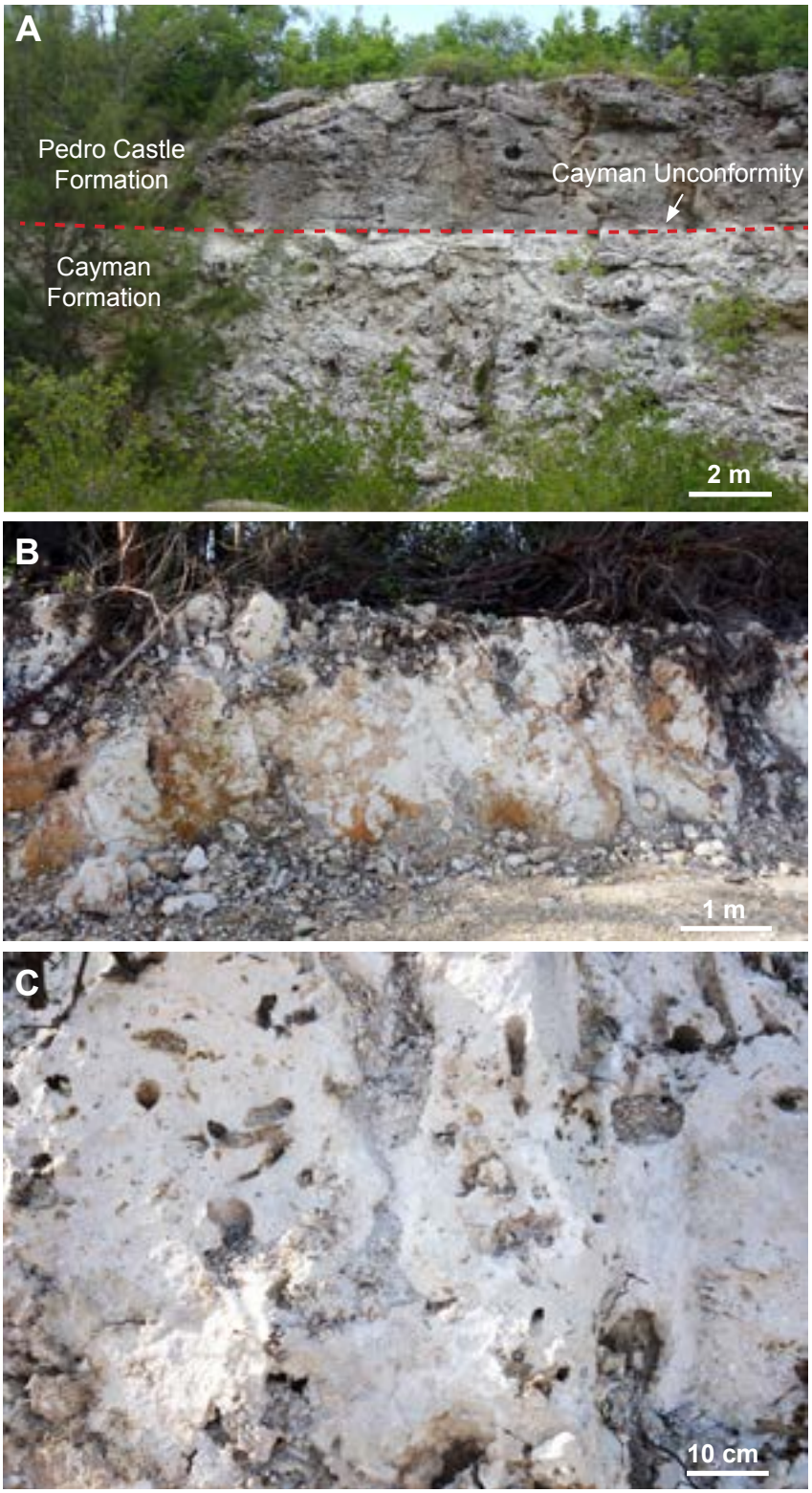

Fig. 1.5. Field photographs of Cayman Formation on Grand Cayman. (A) West wall of Pedro Castle Quarry showing Cayman Formation, Pedro Castle Formation and Cayman Unconformity. (B) NW corner of High Rock Quarry showing exposure of the upper Cayman Formation. (C) Close view of the dolostone in (B). Note the leached fossils.

3.1. The Brac Formation

The Brac Formation, found at the surface and in the subsurface on Cayman Brac is > 20 m thick and partly dolomitized. The exposed cliff faces at the east coast show that the formation is dominated by dolostone with pods of limestones on the south coast and limestones on the north coast (Jones et al., 1994; Uzelman, 2009; Zhao and Jones, 2012b). In the subsurface, the formation is formed largely of dolomitic limestones (Zhao and Jones, 2012b). Dolostones of the formation are fabric destructive and dolomite cements are very common. In the matrix, dolomite crystal size ranges from 50–1500 μm (Zhao and Jones, 2012b). Petrographic and geochemical features of the dolostones suggest that dolomitization of the formation was mediated by slightly modified seawater during the Late Miocene and Pliocene-Early Pleistocene (Zhao and Jones, 2012b). According to Zhao and Jones (2012a, b), the first episode also led to dolomitization of the basal part of the Cayman Formation.

3.2. The Cayman Formation

On Grand Cayman, the Cayman Formation is ~140 m thick and formed of dolostones and limestones (Der, 2012), whereas on Cayman Brac (~3-50 m thick) it is formed entirely of dolostone (Jones et al., 1994; Zhao and Jones, 2012a). The dolostones are predominately fabric-retentive with crystals typically < 50 μm long (Jones et al. 1994; Jones and Luth, 2002). It has been suggested that the formation was dolomitized by slightly modified seawater (e.g., Ng, 1990; Jones and Luth, 2003b; Zhao and Jones, 2012a). Although there is some debate regarding the number of phases of dolomitization and their time, it is now commonly accepted that the Cayman Formation has experienced 2-3 dolomitization events (Jones and Luth, 2003b; Jones, 2005; Zhao and Jones, 2012a).

3.3. The Pedro Castle Formation

The Pedro Castle Formation, < 20 m thick, is found on the surface and subsurface of the western ends of Grand Cayman and Cayman Brac. On Grand Cayman, the formation is formed of dolostone, dolomitic limestone, and limestone (Jones and Luth, 2002).

Dolomitization is patchy with no apparent pattern to its distribution. Similarly, the Pedro Castle Formation on Cayman Brac includes dolostone, dolomitic limestone, and limestone. There, the dolomite content decreases towards to the top of the formation. The dolostones in the basal part of the formation, which are similar to those in the Cayman Formation, are fabric retentive on Grand Cayman and fabric retentive and destructive on Cayman Brac (e.g., Jones, 1994; MacNeil, 2001; MacNeil and Jones, 2003).

The dolostones and dolomitic limestones in the Pedro Castle Formation may have same origin as those in the Cayman Formation. Seawater, slightly modified by evaporation and/or water-rock interaction, was probably responsible for the dolomitization (Jones and Luth, 2002, 2003a, b; MacNeil and Jones, 2003). Dolostone of the Pedro Castle Formation formed through three phases of dolomitization as suggested by MacNeil and Jones (2003).

3.4. The Ironshore Formation

The Ironshore Formation contains minor (up to 12%) amounts of dolomite in some units (Li and Jones, 2013). On the northeast coast of Grand Cayman, 12% dolomite was found in the limestone matrices in Unit A in well RWP-14, and 3% dolomite in Units D and F in well BJC-3 (Li and Jones, 2013). The dolomites, with crystals ~1 μm long, occur as individual rhombs associated with blocky calcite, or in thin layers that coat the allochems. The origin of this dolomite is open to debate.

4. Methods

This study focuses on the Cayman Formation on the east end of Grand Cayman. As such, it includes that part of the island that is located to the east of Lower Valley (Fig. 1.3B). There are 33 wells in the area that are available for study (Table 1.1; Fig. 1.2). For the purpose of the study, two deep wells (RWP-2, 94.7 m; GFN-2, 92.2 m) with continuous high-recovery-rate cores were critically important. The other deep wells, including for example, HRQ-2 (128.0 m), and HRQ-3 (80.0 m), were the main focus of the study because that (1) most of the wells (> 90 m) span the Cayman Formation, and (2) their locations

are representative of different sedimentary and diagenetic environments. Well cuttings obtained over 0.76 m (2.5 ft) intervals from other wells provided important samples for X-ray diffraction, oxygen and carbon isotopes, and strontium isotope analyses.

Fieldwork, including well drillings and sample collections (cores, well cuttings, groundwater) were directed and carried out by Professor Brian Jones during the past 30 years (Table 1.1; Fig. 1.2). A large database of geological information for the Cayman Islands, established from field and laboratory research on surface and subsurface samples from the Cayman Islands, provided the data used in this thesis. Information for individual wells includes but not limited to the well locations, drilling details, and formations penetrated, rock compositions as established from X-ray diffraction (XRD) analyses, oxygen and carbon stable isotopes, strontium isotope, trace elements and REE, whole rock porosity and permeability, and groundwater (geochemistry, and temperature). This database was supplemented by new data acquired during this study (wells GFN-1, GFN-2, HRQ-3, HRQ-4, HRQ-5, HRQ-6, HRQ-7, HRQ-8, and CLZ-1).

The petrography of the dolostone and limestones from the Cayman Formation was based on standard thin-section techniques and scanning electron microscopy. One hundred and twenty thin sections were made from wells GFN-2, RWP-2, HRQ-3, and RTR-1. Rock samples were impregnated with blue epoxy and stained with Alizarin Red S. Thicker (40-50 μm) thin sections, made from selected samples from HRQ-2, were prepared for examination on the SEM. The epoxy-impregnated thin sections were polished and etched in 30% HCl for 10-15 seconds following the procedure outlined by Jones (2005). They were then coated with carbon and examined on a Zeiss EVO SEM (LaB_6 electron source, accelerating voltage 15 kV). Backscattered electron (BSE) images were obtained from these samples. Elemental compositions were obtained using a Bruker energy dispersive X-ray spectroscopy (EDS) system with dual silicon drift detectors, each with an area of 60 mm^2 and an energy resolution of 123 eV. The thin sections were prepared by Martin Von Dollen in the Thin Section Laboratory (University of Alberta). The SEM photomicrographs were taken with the help of

Nathan Gerein in the Scanning Electron Microscope Laboratory (University of Alberta).

Mineral compositions of the rock samples and the magnesium-calcium compositions of the dolomite samples were analyzed using X-ray diffraction (XRD) following the protocol of Jones et al. (2001). For each well, core samples or rock cuttings (one every 1.5 m depth), formed largely of matrix dolostone or limestone (fossils and/or cement were avoided), were selected for XRD and isotopic analyses. Each sample was ground into a fine powder using a mortar and pestle. The powder samples were then scanned using a Rigaku Geigerflex 2173 XRD system with Co Kα radiation from 29° to 38° 2θ at 40 kV and 35 mA following the protocol of Jones et al. (2001). Quartz was added to each sample as a standard. The peak-fitting method of Jones et al. (2001) was used to determine the %Ca of the constituent LCD and HCD (± 0.5% accuracy) and the weight percentages of LCD and HCD (± 10% accuracy). All of the XRD analyses were conducted by Diane Caird in the X-Ray Diffraction Laboratory (University of Alberta).

For every other XRD sample (i.e., at 3 m intervals), oxygen and carbon isotopes for the dolomite and calcite were determined separately. A DELTA^{Plus} XL Isotope Ratio Mass Spectrometer (IRMS) coupled with a ConFlo III interface and EA1110 Elemental Analyzer was used for the analysis. The isotopes are reported relative to VPDB in per mill (± 0.1‰ accuracy). The isotope data were obtained by the Isotope Tracer Technologies Inc. (Waterloo, Canada).

$^{87}Sr/^{86}Sr$ ratios were obtained for 114 dolostone and limestone samples from wells RWP-2, FFM-1, HMB-1, CKC-1, RTR-1, and GFN-2, using the same procedure as MacNeil and Jones (2003). Mineral compositions and stable isotopes have been analyzed for those samples before the $^{87}Sr/^{86}Sr$ analysis. These samples were selected at a particular depth interval from wells at various localities to reflect the stratigraphic and geographic variabilities of the ratio. All results were corrected for variable mass discrimination (0.1194) and normalized to SRM 987 standard (0.710245). The $^{87}Sr/^{86}Sr$ values have the 2 standard errors range from 0.00001 to 0.00003. The $^{87}Sr/^{86}Sr$ analysis was provided by Dr. Robert Creaser in

the Radiogenetic Isotope Laboratory (University of Alberta).

Groundwater samples collected from RTR-1 (2009), GFN-1 (2011), and HRQ-3 (2014); and seawater samples from Spotts Bay (south coast) collected in each of these years were incorporated into this study. The chemical composition and oxygen isotope analyses were performed for 34 groundwater and 3 seawater samples, within 2 months of collection. Ninety-seven groundwater samples were measured for temperature during drilling of GFN-1, HRQ-2, and EEV-2. The chemical compositions and isotopes of the water samples were analyzed by Saskatchewan Research Council (Saskatoon, Canada) and Isotope Tracer Technologies Inc. (Waterloo, Canada), respectively.

5. Thesis structure

The thesis is presented in a paper-based format. Chapters two to four are based on two published and one submitted peer-viewed papers respectively. These three chapters are closely linked and collectively describe the origin of the Miocene carbonates on Grand Cayman. These chapters focus on the dolomitization and diagenetic evolution of these Cenozoic island carbonates.

Chapter Two delineates the spatial distribution of the dolostones and limestones in the Cayman Formation, the petrographic features of those dolostone and limestones, and the stoichiometric and oxygen, carbon and strontium isotopic properties of the dolostones. In this chapter, a dolomitization model is built that emphasizes the significance of gradual transition and variations in dolomite properties from the coast to the center of the island. These variabilities in the Cayman dolomitization model reflect the feedback between the dolostones and the dolomitizing conditions of a complex dolomitization system. During dolomitization, there were changes in the groundwater geochemistry as it flowed from the coast to the interior of the island caused by water-rock interaction and/or mixture with meteoric water, seawater flux and flow rate, and other environmental parameters. These factors were responsible for the lateral variations in the stoichiometric and isotopic signatures

of the dolostones.

Chapter Three examines the diagenetic modifications in the limestones and dolostones of Cayman Formation that occurred following dolomitization. Ever since the last phase of dolomitization that affected the Cayman Formation (about 1 Ma BP), the formation was repeatedly exposed and submerged as sea level fluctuated rapidly. This chapter discusses the relationship between the diagenesis of island limestone-dolostone and those glacio-eustasic fluctuations.

Chapter Four is designed to test the applicability of the Cayman dolomitization model to other Cenozoic island dolostones that are found throughout the oceans of the world. Like the dolostones of Cayman Formation on Grand Cayman, many Cenozoic island dolostones are characterized by similar lateral variations in dolomite stoichiometry and geochemistry. These include, for example, the Cayman Formation on Cayman Brac, the Brac Formation and Pedro Castle Formation on the Cayman Islands, the Miocene-Pliocene dolostones on the Little Bahama Bank, Pliocene dolostones on Mururoa, and the Miocene-Pliocene dolostones on Kita-daito-jima. Dolostones on those islands can also be divided into geographically defined dolostone zones. Individual island dolostone bodies deviate from the Cayman model due to a variety of intrinsic factors. The fact the Cayman model can be applied to many Cenozoic island dolostone bodies suggests that similar hydrological conditions were responsible for their development.

Chapter Five summarizes the conclusions reached from this study and the significance of the study, and presents the author's final thoughts on dolomite and the dolomite problem.

References

Azmy, K., Lavoie, D., Wang, Z., Brand, U., Al-Aasm, I., Jackson, S., Girard, I., 2013. Magnesium-isotope and REE compositions of Lower Ordovician carbonates from eastern Laurentia: implications for the origin of dolomites and limestones. Chemical Geology 356, 64-75.

Budd, D.A., 1997. Cenozoic dolomites of carbonate islands: their attributes and origin. Earth-Science Reviews 42, 1-47.

Burns, S.J., Mckenzie, J.A., Vasconcelos, C., 2000. Dolomite formation and biogeochemical cycles in the Phanerozoic. Sedimentology 47, 49-61.

Der, A., 2012. Deposition and sea level fluctuation during Miocene times, Grand Cayman, British West Indies. Unpublished M.Sc. thesis, University of Alberta, 101 pp.

Emery, K., Milliman, J., 1980. Shallow-water limestones from slope off Grand Cayman Island. The Journal of Geology 88, 483-488.

Fairbridge, R.W., 1957. The dolomite question. In: Le Blanc R.J., Breeding. J.G. (Eds.) Regional Aspects of Carbonate Deposition. Society of Economic Paleontologists and Mineralogists Special Publication 5, pp. 125-178.

Gregg, J.M., Bish, D.L., Kaczmarek, S.E., Machel, H.G., 2015. Mineralogy, nucleation and growth of dolomite in the laboratory and sedimentary environment: A review. Sedimentology 62, 1749-1769.

Hardie, L.A., 1987. Dolomitization: a critical view of some current views. Journal of Sedimentary Research 57, 166-183.

Hayman, N.W., Grindlay, N.R., Perfit, M.R., Mann, P., Leroy, S., de Lépinay, B.M., 2011. Oceanic core complex development at the ultraslow spreading Mid-Cayman Spreading Center. Geochemistry, Geophysics, Geosystems 12, 1-21.

Jones, B., 1989. Syntaxial overgrowths on dolomite crystals in the Bluff Formation, Grand Cayman, British West Indies. Journal of Sedimentary Petrology 59, 839-847.

Jones, B., 2005. Dolomite crystal architecture: genetic implications for the origin of the

Tertiary dolostones of the Cayman Islands. Journal of Sedimentary Research 75, 177-189.

Jones, B., 2007. Inside-out dolomite. Journal of Sedimentary Research 77, 539-551.

Jones, B., 2013. Microarchitecture of dolomite crystals as revealed by subtle variations in solubility: Implications for dolomitization. Sedimentary Geology 288, 66-80.

Jones, B., Hunter, I.G., 1994. Messinian (late Miocene) karst on Grand Cayman, British West Indies; an example of an erosional sequence boundary. Journal of Sedimentary Research 64, 531-541.

Jones, B., Hunter, I., Kyser, K., 1994a. Revised stratigraphic nomenclature for Tertiary strata of the Cayman Islands, British West Indies. Caribbean Journal of Science 30, 53-68.

Jones, B., Hunter, I.G., Kyser, T.K., 1994b. Stratigraphy of the Bluff Formation (Miocene-Pliocene) and the newly defined Brac Formation (Oligocene), Cayman Brac, British West Indies. Caribbean Journal of Science 30, 30-51.

Jones, B., Luth, R.W., 2002. Dolostones from Grand Cayman, British West Indies. Journal of Sedimentary Research 72, 559-569.

Jones, B., Luth, R.W., 2003a. Petrography of finely crystalline Cenozoic dolostones as revealed by backscatter electron imaging: Case study of the Cayman Formation (Miocene), Grand Cayman, British West Indies. Journal of Sedimentary Research 73, 1022-1035.

Jones, B., Luth, R.W., 2003b. Temporal evolution of Tertiary dolostones on Grand Cayman as determined by $^{87}Sr/^{86}Sr$. Journal of Sedimentary Research 73, 187-205.

Jones, B., Luth, R.W., MacNeil, A.J., 2001. Powder X-ray diffraction analysis of homogeneous and heterogeneous sedimentary dolostones. Journal of Sedimentary Research 71, 790-799.

Kaczmarek, S.E., Sibley, D.F., 2011. On the evolution of dolomite stoichiometry and cation order during high-temperature synthesis experiments: an alternative model for the geochemical evolution of natural dolomites. Sedimentary Geology 240, 30-40.

Land, L.S., 1985. The origin of massive dolomite. Journal of Geological Education 33, 112-125.

Land, L.S. 1992. The dolomite problem: stable and radiogenic isotope clues. In: Clauer, N., Chaudhuri, S. (Eds.), Isotopic Signatures and Sedimentary Records. Springer, Berlin, Heidelberg, pp. 49-68.

Leroy, S., Mauffret, A., Patriat, P., Mercier de Lépinay, B., 2000. An alternative interpretation of the Cayman trough evolution from a reidentification of magnetic anomalies. Geophysical Journal International 141(3), 539-557.

Li, R., Jones, B., 2013. Heterogeneous diagenetic patterns in the Pleistocene Ironshore Formation of Grand Cayman, British West Indies. Sedimentary Geology 294, 251-265.

Machel, H.G., 2000. Dolomite formation in Caribbean Islands: driven by plate tectonics?! Journal of Sedimentary Research 70, 977-984.

Machel, H.G., 2004. Concepts and models of dolomitization: a critical reappraisal. In: Braithwaite, C.J.R., Rizzi, G., Darke, G. (Eds.), The Geometry and Petrogenesis of Dolomite Hydrocarbon Reservoirs. Geological Society of London Special Publication 235, pp. 7-63.

MacNeil, A., 2001. Sedimentology, Diagenesis and Dolomitization of the Pedro Castle Formation on Cayman Brac, BWI. Master Thesis, University of Alberta, 128 pp.

MacNeil, A., Jones, B., 2003. Dolomitization of the Pedro Castle Formation (Pliocene), Cayman Brac, British West Indies. Sedimentary Geology 162, 219-238.

Mazzullo, S. J., 2000. Organogenic dolomitization in peritidal to deep-sea sediments. Journal of Sedimentary Research 70, 10-23.

Mckenzie, J. A., Vasconcelos, C., 2009. Dolomite Mountains and the origin of the dolomite rock of which they mainly consist: historical developments and new perspectives. Sedimentology 56, 205–219.

Ng, K.C., 1990. Diagenesis of the Oligocene-Miocene Bluff Formation of the Cayman Islands -- A petrographic and hydrogeochemical approach. Unpublished PhD thesis,

University of Alberta, 344 pp.

Perfit, M.R., Heezen, B.C., 1978. The geology and evolution of the Cayman Trench. Geological Society of America Bulletin 89, 1155-1174.

Pleydell, S.M., Jones, B., Longstaffe, F.J., Baadsgaard, H., 1990. Dolomitization of the Oligocene-Miocene Bluff Formation on Grand Cayman, British West Indies. Canadian Journal of Earth Sciences 27, 1098-1110.

Roberts, H.H., 1994. Reefs and lagoons of Grand Cayman. In: Brunt, M.A., Davies, J.E. (Eds.), The Cayman Islands: Natural History and Biogeography. Springer, Netherlands, pp. 75-104.

Roberts, J.A., Kenward, P.A., Fowle, D.A., Goldstein, R.H., González, L.A., Moore, D.S., 2013. Surface chemistry allows for abiotic precipitation of dolomite at low temperature. Proceedings of the National Academy of Sciences 110, 14540-14545.

Tucker, M.E., Wright, V.P. 1990. Carbonate Sedimentology. Blackwell Scientific Publications, Oxford, 482 pp.

Uzelman, B.C., 2009. Sedimentology, diagenesis, and dolomitization of the Brac Formation (Lower Oligocene), Cayman Brac, British West Indies. Master Thesis, University of Alberta, 120 pp.

Vahrenkamp, V.C., Swart, P.K., Purser, B., Tucker, M., Zenger, D., 1994. Late Cenozoic dolomites of the Bahamas: metastable analogues for the genesis of ancient platform dolomites. In: Purser, B.H.,Tucker, M.E., Zenger, D.L. (Eds.), Dolomites: A Volume in Honour of Dolomieu. International Association of Sedimentologists Special Publication 21, 133-153.

Van Tuyl, F.M., 1916. New points on the origin of dolomite. American Journal of Science 42, 249-260.

Warren, J., 2000. Dolomite: occurrence, evolution and economically important associations. Earth-Science Reviews 52, 1-81.

Whitaker, F.F., Smart, P.L., Jones, G.D., 2004. Dolomitization: from conceptual to numerical

models. In: Braithwaite, C.J.R., Rizzi, G., Darke, G. (Eds.), The Geometry and Petrogenesis of Dolomite Hydrocarbon Reservoirs. Geological Society of London Special Publication 235, pp. 99-139.

Wignall, B.D., 1995. Sedimentology and Diagenesis of the Cayman (Miocene) and Pedro Castle (Pliocene) Formations at Safe Haven, Grand Cayman, British West Indies. Master Thesis, University of Alberta, 110 pp.

Willson, E.A., 1998. Depositional and Diagenetic Features of the Middle Miocene Cayman Formation, Roger's Wreck Point, Grand Cayman, British West Indies. Master Thesis, University of Alberta, 103 pp.

Zhao, H., Jones, B., 2012a. Origin of "island dolostones": A case study from the Cayman Formation (Miocene), Cayman Brac, British West Indies. Sedimentary Geology 243-244, 191-206.

Zhao, H., Jones, B., 2012b. Genesis of fabric-destructive dolostones: A case study of the Brac Formation (Oligocene), Cayman Brac, British West Indies. Sedimentary Geology 267-268, 36-54.

Zhao, H., Jones, B., 2013. Distribution and interpretation of rare earth elements and yttrium in Cenozoic dolostones and limestones on Cayman Brac, British West Indies. Sedimentary Geology 284-285, 26-38.

CHAPTER TWO

DOLOMITES OF THE CAYMAN FORMATION AND THE CAYMAN DOLOMITIZATION MODEL[1]

1. Introduction

Dolomite [ideally $CaMg(CO_3)_2$], has received considerable attention because of questions that remain about its origin (Land and Moore, 1980; Budd, 1997; Warren, 2000; Machel, 2004; Gregg et al., 2015). Sedimentary dolomites typically contain excess calcium (48-62 mol %$CaCO_3$, hereafter referred to as %Ca), as is the case for most modern and Cenozoic dolostones (e.g., Vahrenkamp et al., 1994; Budd, 1997; Wheeler et al., 1999; Jones and Luth, 2002; Suzuki et al., 2006). Many Phanerozoic dolomites, despite their antiquity, are still non-stoichiometric (e.g., Lumsden and Chimahusky, 1980; Sperber et al., 1984; Reeder, 1991; Drits et al., 2005; Swart et al., 2005). Calcium-rich dolomites are thermodynamically metastable and more reactive than ideal or near-stoichiometric dolomites (e.g., Reeder, 1991; Chai et al., 1995). Thus, in most geological environments high calcium dolomite (HCD, %Ca = 55-62%) is more susceptible to diagenetic modifications than low calcium dolomite (LCD, %Ca = 48-55%) (Jones and Luth, 2002). This includes the preferential dissolution of the calcium-rich cores found in many dolomite crystals. Dolostones formed of hollow crystals generated by this process have high micro-porosity (Jones and Luth, 2002; Jones, 2007) and may be important reservoir rocks. Later precipitation of calcite or dolomite in the hollow crystals leads to the formation of dedolomite (Schmidt, 1965; Folkman, 1969; Jones, 1989; James et al., 1993) or inside-out dolomite (Jones, 2007). At burial, non-stoichiometric dolomite is prone to recrystallization and transformation to stoichiometric, well-ordered dolomites (e.g., Land and Moore,

---

1 This chapter was published as: Ren, M., Jones, B., 2017. Spatial variations in the stoichiometry and geochemistry of Miocene dolomite from Grand Cayman: implications for the origin of island dolostone. Sedimentary Geology 348, 69-93.

1980; Reeder, 1981; Blake et al., 1982; Hardie, 1987; Kaczmarek and Sibley, 2014). Such modifications change the petrographic properties, geochemical signatures, and reservoir potential of the dolostones.

Models developed to explain dolomitization have typically regarded dolostones as being compositionally uniform. In many cases, however, two or more dolomite populations, as defined by their composition, are present (Sperber et al., 1984; Searl, 1994; Wheeler et al., 1999; Jones and Luth, 2002; Drits et al., 2005; Suzuki et al., 2006). If variations in stoichiometry have been considered, it is done from a stratigraphic perspective and the possibility of geographic variations have been ignored (e.g., Dawans and Swart, 1988; Wheeler et al., 1999). The Cenozoic dolostones on the Cayman Islands, which are formed of various mixtures of LCD (%Ca = 48-55%) and HCD (%Ca = 55-62%) (Jones et al., 2001; Jones, 2005, 2013), are ideal for testing the notion that lateral variations in the composition of dolostones may be critical for developing a model to explain their origin. On the east end of Grand Cayman, 32 wells drilled and sampled to depths up to 140 m are ideally suited for establishing the stratigraphic and geographic variations in the %Ca of dolostones on an isolated carbonate island. The model developed to explain the formation of these island dolostones is based on the integration of their petrography, %Ca, stable isotopes, $^{87}Sr/^{86}Sr$ isotopes, and stratigraphic relationships with coeval limestones. The model, which also relies on the chemistry of the present-day groundwater, is also used to test some of the basic concepts of dolomite formation that have been derived from laboratory experiments like those described by Kaczmarek and Sibley (2011, 2014). The conclusions reached by this research have far-reaching implications for the development of island dolostones throughout the world.

2. Geological setting

Grand Cayman, located on the Cayman Ridge in the Caribbean Sea (Fig. 2.1A), is surrounded by a shelf that is < 1 km wide (Fig. 2.1B, C). Sculptured by two submarine

terraces at 0-10 m below sea level (bsl) and 12-40 m bsl (Fig. 2.1D), the shelf formed as a result of reef growth and marine erosion during successive sea-level cycles of the last deglaciation (e.g., Blanchon and Jones, 1995). The island slope, which generally begins at a depth of ~55 m (Roberts, 1994), extends into the deep Cayman Trench to the south and Yucatan Basin to the north. Today, the east end of the island has a N-S width of ~ 6.8 km. The low-lying interior of eastern part of this island, generally < 3 m above sea level (asl), is surrounded by a peripheral rim that is up to 13.5 m asl (e.g., Jones et al., 1994a; Jones and Hunter, 1994; Liang and Jones, 2014).

The carbonate succession on Grand Cayman is divided into the unconformity-bounded Brac Formation, Cayman Formation, Pedro Castle Formation, and Ironshore Formation (Fig. 2.2). Limestones and dolostones of the Cayman Formation (Miocene) are widely exposed over the eastern part of the island (Fig. 2.1B). Fossils in this formation include corals, bivalves, red algae, foraminifera, and *Halimeda* (Jones et al., 1994b; Ren and Jones, 2016) (Fig. 2.2). On the east end, the Cayman Formation has undergone pervasive dolomitization in the coastal areas but minimal dolomitization in the central areas of the island (Der, 2012; Ren and Jones, 2016).

3. Methods

This paper integrates all information from outcrops and 32 wells on the east end of Grand Cayman with focus being placed on 21 wells (Fig. 2.1C, E; Table 2.1), which were selected because they are the deepest wells (40 to 140 m with most > 70 m), and are located

Fig. 2.1. Location and geological setting of study area. (A) Location of Grand Cayman in the Caribbean Sea. (B) Geological map showing the distribution of the Cayman Formation on Grand Cayman (modified from Jones et al., 1994a), the approximate distribution of East End Freshwater Lens on the island (modified from Ng and Jones, 1992), and location of High Rock Quarry. (C) Locations of 32 wells incorporated in this study (wells in solid red dots are the primary wells used in this study). (D) Shelf profile in northeastern corner of the island, modified from Brunt (1994). (E) Distribution of 8 wells in High Rock Quarry.

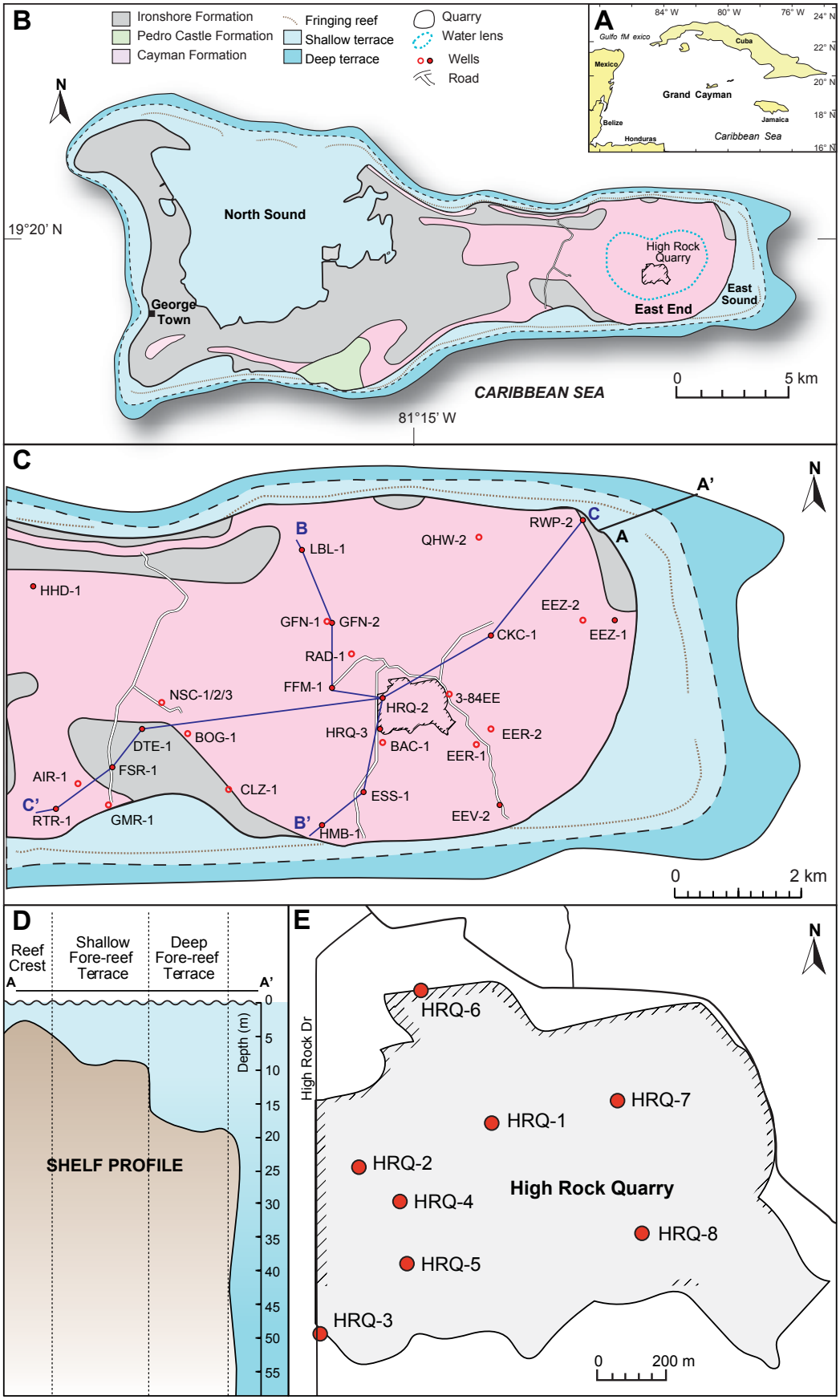
B
Ironshore Formation
Pedro Castle Formation
Cayman Formation
Fringing reef
Shallow terrace
Deep terrace
Quarry
Water lens
Wells
Road
N
A
84° W
80° W
76° W
24° N
22° N
20° N
18° N
16° N
Gulfo fM exico
Cuba
Mexico
Grand Cayman
Jamaica
Belize
Honduras
Caribbean Sea
19°20' N
North Sound
George Town
High Rock Quarry
East End
East Sound
CARIBBEAN SEA
0
5 km
81°15' W
C
A'
B
C
A
RWP-2
LBL-1
QHW-2
HHD-1
EEZ-2
GFN-1
GFN-2
CKC-1
EEZ-1
RAD-1
FFM-1
NSC-1/2/3
3-84EE
HRQ-2
HRQ-3
BOG-1
BAC-1
EER-2
DTE-1
EER-1
AIR-1
FSR-1
CLZ-1
ESS-1
C'
RTR-1
GMR-1
B'
HMB-1
EEV-2
0
2 km
D
Reef Crest
Shallow Fore-reef Terrace
Deep Fore-reef Terrace
A
A'
Depth (m)
0
5
10
15
20
25
30
35
40
45
50
55
SHELF PROFILE
E
N
High Rock Dr
HRQ-6
HRQ-7
HRQ-1
HRQ-2
High Rock Quarry
HRQ-4
HRQ-8
HRQ-5
HRQ-3
0
200 m

Table 2.1. Wells on the east end of Grand Cayman (see Figs. 1, 6 for locations) used this study. Twenty-one wells (in bold) were the primary wells used in this study. Distance to shelf edge is the shortest distances from the well to the northern (N), eastern (E), or southern (S) shelf edge. (PD=peripheral dolostone, TD=transitional dolostone, IL/D=interior limestone/dolostone, IL=interior limestone only).

Well	Zone	Total depth (m)	Distance to shelf edge (km)	%Core	%Cutting
HHD-1	PD	61.0	1.55 / N	0	100
LBL-1	PD	94.5	1.36 / N	0	100
RWP-2	PD	94.6	0.66 / N	97	0
EEZ-1	PD	87.6	1.40 / E	0	100
ESS-1	PD	77.4	1.29 / S	0	100
HMB-1	PD	57.9	0.86 / S	0	100
RTR-1	PD	138.7	1.32 / S	0	100
QHW-1	PD	[a]60.0	1.16 / N		0
EEZ-2	PD	87.6	1.86 / E		100
CKC-1	TD	67.2	3.10 / E	0	100
EEV-2	TD	101.8	1.14 / S	0	100
HRQ-3	TD	80.0	2.48 / S	0	100
FSR-1	TD	[b]52.4	2.21 / S	0	100
EER-1	TD	140.2	2.45 / S	0	100
BAC-1	TD	39.6	2.22 / S	0	100
GMR-2	TD	46.0	1.45 / S	0	100
AIR-1	TD	49.4	1.82 / S	0	100
GFN-2	IL/D	92.2	2.75 / N	63	0
FFM-1	IL/D	64.8	3.42 / S	0	100
HRQ-2	IL/D	128.0	3.00 / S	0	100
HRQ-1	IL/D	61.7	3.23 / S	0	100
HRQ-4	IL/D	64.0	2.95 / S	0	100
HRQ-5	IL/D	76.2	2.78 / S	0	100
HRQ-6	IL/D	76.2	3.55 / S	0	100
HRQ-7	IL/D	39.6	3.29 / S	0	100
HRQ-8	IL/D	76.2	2.90 / S	0	100
DTE-1	IL	[b]46.3	2.88 / S	0	100
GFN-1	IL	122.3	2.75 / N	0	100
RAD-1	IL/D	20.1	3.43 / N	0	100
EER-2	IL/D	115.8	2.73 / S	0	100
BOG-1	IL	39.6	2.75 / S	20	0
NSC-1	IL	[c]243.0	3.35 / S	0	100

[a] Cayman Formation in the lower 20 m (cf., Jones and Luth, 2003b). [b] Cayman Formation starts ~8 m bsl. [c] Cayman formation in the upper ~140 m (cf., Jones et al., 1994; Liang and Jones, 2014).

at various distances from the shoreline. Continuous cores were obtained from wells GFN-2 and RWP-2. Cuttings were collected over 0.76 m (2.5 ft) intervals from all other wells. The depth of each well is accurate to ± 1% whereas the depth intervals represented by each sample of cuttings are ± 2% with the highest variance being on the deeper samples.

Petrographic descriptions are based on standard thin-section techniques and scanning electron microscopy. Thin sections, made from 120 samples from GFN-2, RWP-2, HRQ-3, and RTR-1, were impregnated with blue epoxy to highlight porosity and stained with Alizarin Red S to indicate calcite. Thicker (40-50 µm) thin sections from selected samples from HRQ-2 were prepared for examination on the SEM. After these epoxy-impregnated thin sections were polished and etched in 30% HCl for 10-15 seconds following the procedure outlined by Jones (2005), they were then coated with carbon and examined on a Zeiss EVO

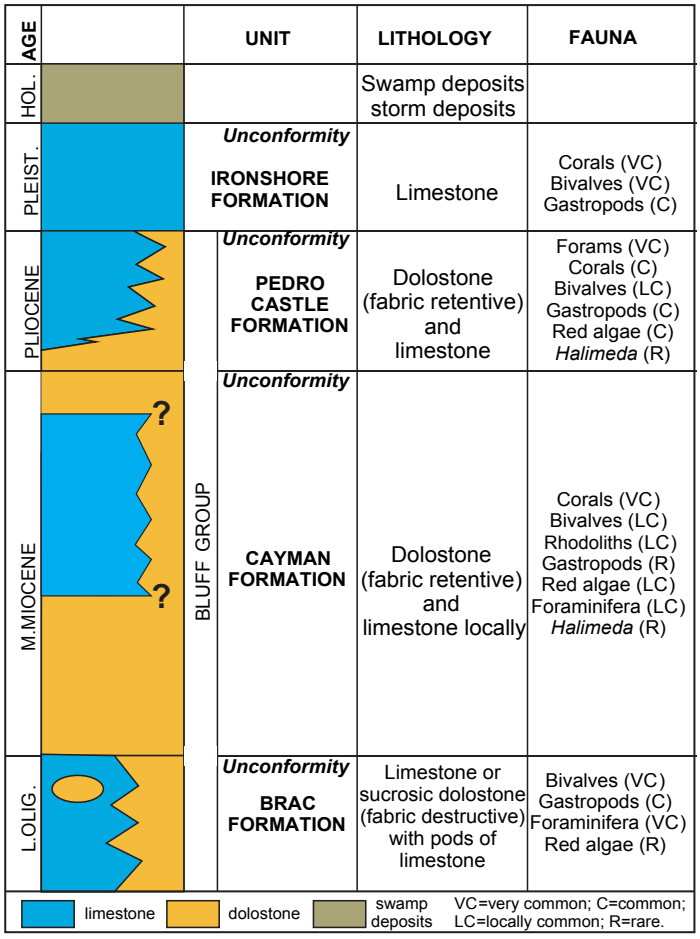

Fig. 2.2. Stratigraphic succession on Grand Cayman (modified from Jones et al., 1994a).

SEM (LaB_6 electron source, accelerating voltage 15 kV). Backscattered electron (BSE) images were obtained from these samples. Elemental compositions were obtained from spots/lines/areas using a Bruker energy dispersive X-ray spectroscopy (EDS) system with dual silicon drift detectors, each with an area of 60 mm^2 and an energy resolution of 123 eV.

Rock cuttings (one every 1.5 m depth), formed largely of matrix dolostone or limestone (fossils and/or cement were avoided), were ground into a fine powder using a mortar and pestle and then subjected to X-ray diffraction (XRD) using a Rigaku Geigerflex 2173 XRD system with Co Kα radiation from 29° to 38° 2θ at 40 kV and 35 mA following the protocol of Jones et al. (2001). The peak-fitting method of Jones et al. (2001) was used to determine the %Ca of the constituent LCD and HCD (± 0.5% accuracy) and the weight percentages of LCD and HCD (± 10% accuracy).

Oxygen and carbon isotopes for the dolomite and calcite were determined for every other XRD sample (i.e., at 3 m intervals) from EEZ-1, CKC-1, LBL-1, HMB-1, HRQ-1, HRQ-2, and HRQ-3. These analyses were undertaken by Isotope Tracer Technologies Inc. (Waterloo, Canada) who used a DELTA^{Plus} XL Isotope Ratio Mass Spectrometer (IRMS) coupled with a ConFlo III interface and EA1110 Elemental Analyzer. No phosphoric acid fractionation factor was applied to the dolomite. The isotopes are reported relative to VPDB in per mill (± 0.1‰ accuracy).

$^{87}Sr/^{86}Sr$ were measured for 114 samples from RWP-2, FFM-1, HMB-1, CKC-1, RTR-1, and GFN-2 in the Radiogenetic Isotope Laboratory, University of Alberta, using the same procedure as MacNeil and Jones (2003). All results were corrected for variable mass discrimination (0.1194) and normalized to SRM 987 standard (0.710245). The 2 standard errors of the $^{87}Sr/^{86}Sr$ values range from 0.00001 to 0.00003.

Groundwater samples were collected from RTR-1 (2009), GFN-1 (2011), and HRQ-3 (2014); and seawater samples from Spotts Bay (south coast) were also collected in each of these years. Chemical composition and oxygen isotope analyses were performed for 34 groundwater and 3 seawater samples by the Saskatchewan Research Council and Isotope

Tracer Technologies Inc., respectively, within 2 months of collection. Saline water is defined using chloride contents (>19,000 mg/L) following Ng et al. (1992). Ninety-seven groundwater samples were measured for temperature during drilling of GFN-1, HRQ-2, and EEV-2.

4. Results

4.1. Sedimentary facies

The Cayman Formation contains numerous fossils including corals (mainly *Stylophora*, *Montastrea*, *Porites*), benthic foraminifera, bivalves, gastropods, red algae, and planktonic foraminifera. Der (2012) and Ren and Jones (2016) recognized the following biofacies: (1) rhodolith-coral-benthic foraminifera, (2) platy and domal coral–benthic foraminifera, (3) branching platy and domal coral–benthic foraminifera, (4) branching coral-benthic foraminifera facies, (5) benthic foraminifera-bivalve, (6) *Halimeda*-benthic foraminifera–coral, and (7) planktonic foraminifera facies (Fig. 2.3). Facies 1 is found only in two coastal wells (RWP-2 and RTR-1), facies 2, 3, and 4 are found in most wells but are most common in the coastal areas, and facies 6 and 7 are present only in GFN-2 and HRQ-2, which are located in the interior of the island (Fig. 2.3).

4.2. Definition and distribution of the dolostone and limestone

The Cayman Formation contains undolomitized limestones, partially dolomitized limestones, and dolostones. Most dolostone is found around the perimeter of the island and in the shallow surface zone in the interior of the island, whereas limestones are restricted to the interior part of the island (Figs. 2.4, 2.5). There is no evidence indicating that the limestone and dolostones belong to different formations (Ren and Jones, 2016).

Key attributes of each succession are the distribution of LCD, HCD, and calcite. Well locations are specified relative to shelf edge rather than the present-day coastline, which is a feature of recent erosion and sea level. Integration of the geographic positions of the wells

and their basic lithological attributes allows delineation of the (1) peripheral dolostone zone, (2) transitional dolostone zone, (3) interior dolostone zone, and (4) interior limestone zone (Fig. 2.6).

The "peripheral zone" includes areas that are within ~1.5 km from the present-day N and S shelf edges and ~2 km from the E shelf margin (Fig. 2.6). Wells HHD-1, LBL-1, RWP-2, EEZ-1, ESS-1, HMB-1, and RTR-1 are located in the zone. Given its position and that the subsurface Cayman Formation in these locations is comprised of dolostone, this zone is referred to as the peripheral dolostone zone (Fig. 2.6). These successions are dominated by LCD, with many being formed entirely of LCD-dominated dolostones (e.g., LBL-1, RWP-2, EEZ-1, FSR-1).

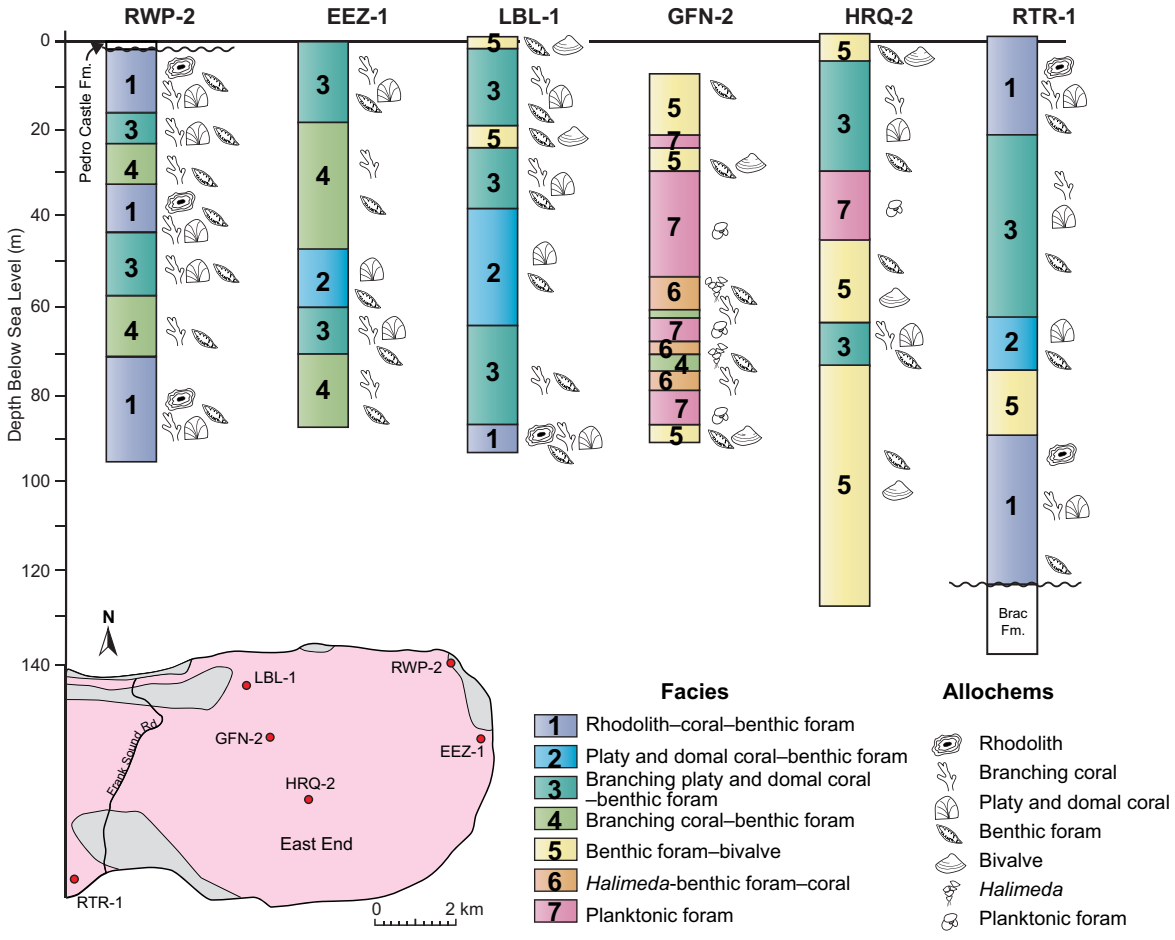

Fig. 2.3. Distribution of seven sedimentary facies in Cayman Formation based on this study, Der (2012) and Ren and Jones (2016).

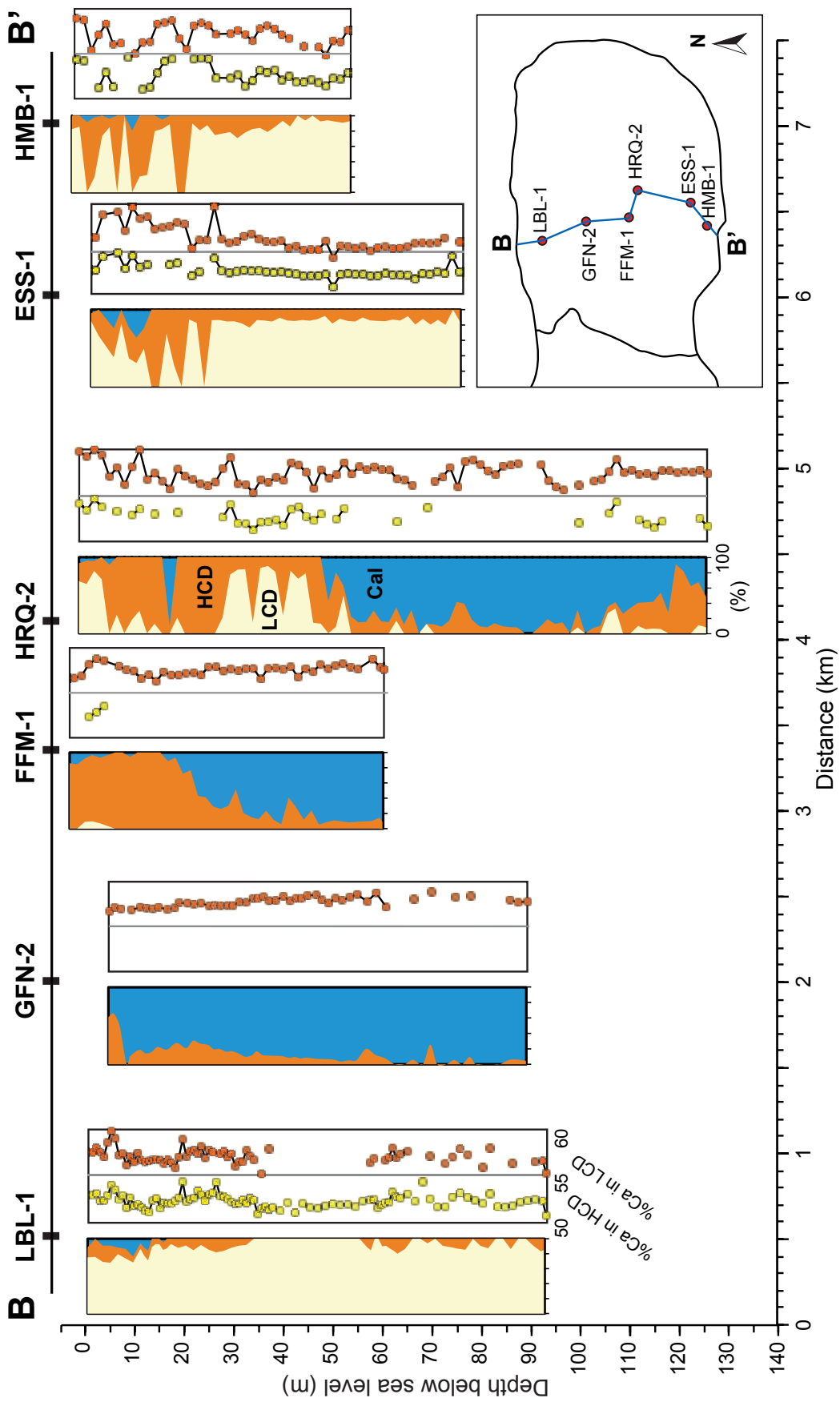

Fig. 2.4. Profile through successions in wells LBL-1, GFN-2, FFM-1, HRQ-2, ESS-1, and HMB-1 showing the spatial distribution of LCD, HCD, and calcite (Cal) in the Cayman Formation.

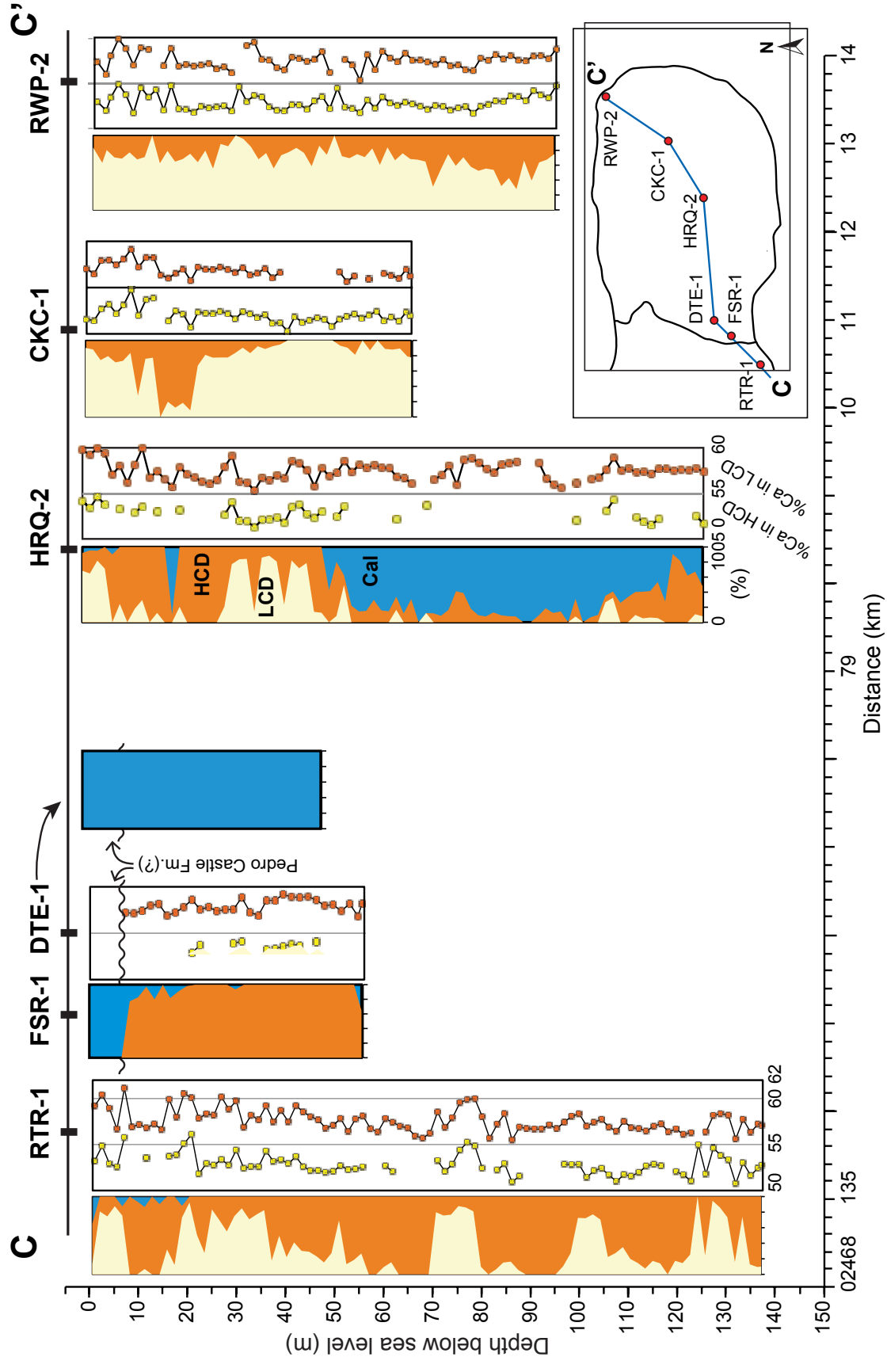

Fig. 2.5. Profile through successions in wells RTR-1, FSR-1, DTE-1, HRQ-2, CKC-1, and RWP-2 showing the spatial distribution of LCD, HCD, and calcite (Cal) in the Cayman Formation.

The “transitional zone”, located between the inner boundary of peripheral zone to ~2.7 km from the N and S shelf edges, and ~3 km from the E shelf edge, includes wells CKC-1, EEV-2, HRQ-3, and FSR-1 (Fig. 2.6). It is named the transitional dolostone zone because the Cayman Formation is the area is formed of LCD- and HCD-dominated dolostones (Fig. 2.6).

The “interior zone”, found in the innermost part of the island, is interior of the

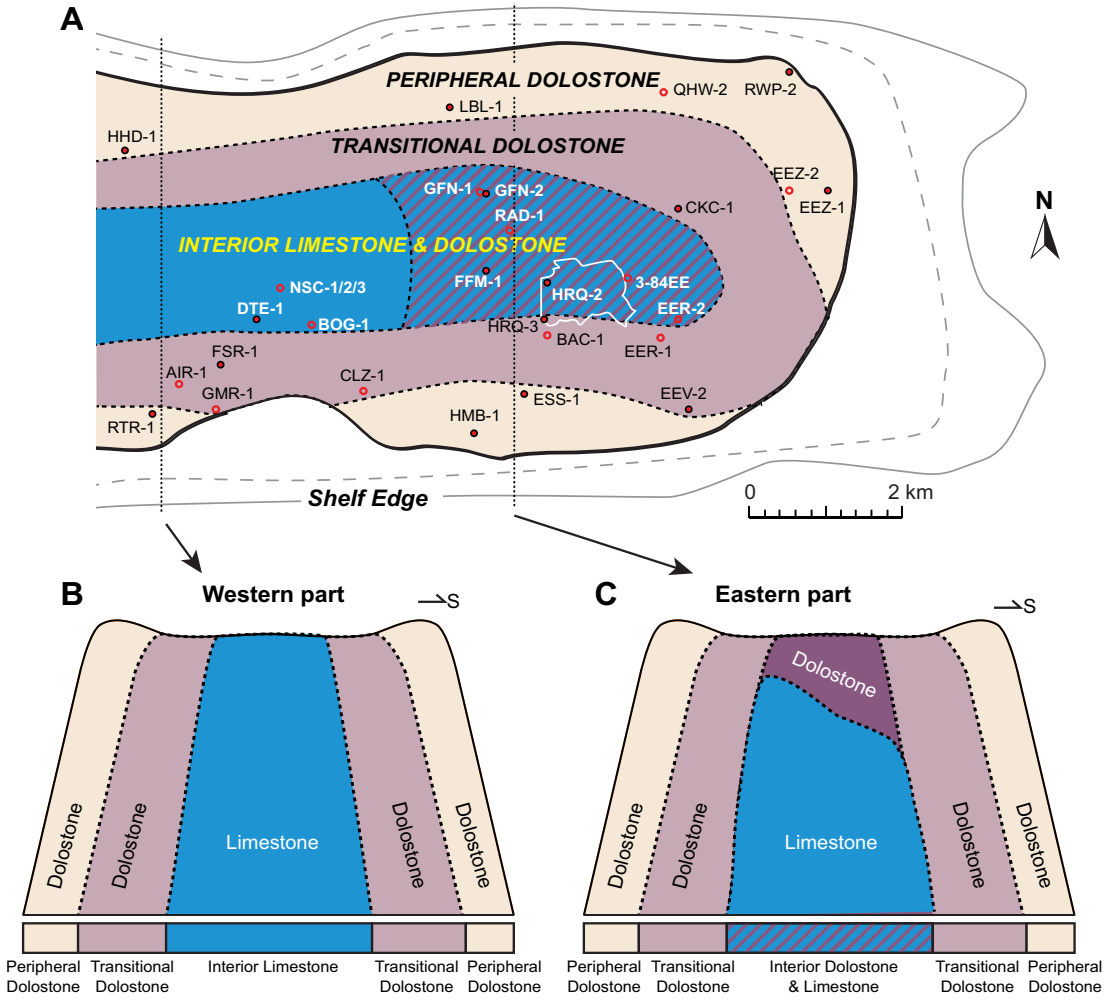

Fig. 2.6. Spatial distribution of peripheral dolostone, transitional dolostone, interior dolostone, and interior limestone in the Cayman Formation on the east end of Grand Cayman. (A) Geological map showing the four zones that are concentrically arranged. (B) A N-S profile indicating the distribution of peripheral dolostone, transitional dolostone and interior limestone in the western part of the east end of the island. (C) A N-S profile indicating the distribution of peripheral dolostone, transitional dolostone, interior dolostone and limestone in the eastern part of the east end of the island.

transitional zone and includes wells FFM-1, GFN-2, HRQ-2, HRQ-1, HRQ-4, HRQ-5, HRQ-6, HRQ-7, HRQ-8, and DTE-1 (Fig. 2.6). The Cayman Formation in this zone is comprised of limestones and calcian dolostones. The limestones, which are found in all of the wells in this area, are referred to as the interior limestones. In some wells, limestone forms the entire succession, whereas in other wells it is restricted to the deeper part of successions in other areas (Fig. 2.6). The boundary between these dolostones and limestones lies somewhere between wells CLZ-1 and HMB-1. Dolostones that lie on top of the limestone successions in the eastern interior (e.g., HRQ-2, FFM-1, GFN-2), formed largely of HCD, are referred to as the interior dolostones.

4.3. Distribution of calcite cements

The distribution of calcitic sediments and calcite cements in the Cayman Formation in the central part of the island is variable. The upper dolostone unit (~15 m thick), found on the eastern part of the island as in wells GFN-2, RWP-2 (Ren and Jones, 2016) and HRQ-3 (Fig. 2.7A-C), is characterized by calcite cement that fills cavities and pores. The calcite cement, dominated by blocky crystals (50-100 μm long), postdated pervasive dolomitization (Ren and Jones, 2016). The volume of calcite cement depends on the porosity and permeability of the host rock. In well GFN-2, for example, the calcite cement forms up to 40% of the porous calcareous dolostones. In contrast, the less permeable peripheral dolostones, like those in RWP-2, contain < 3% calcite cement.

In the interior wells, like GFN-2 and HRQ-2, the lower part of the Cayman Formation is formed of original limestones with only minor amounts of calcite cement (Fig. 2.7D-F). The depth to the upper boundary of this unit varies from ~55 m bsl in the HRQ wells to ~8 m bsl in GFN-2. In this unit, most of the aragonite skeletons were dissolved and resultant porosity is high (e.g., 50% in well GFN-2). Although the lower boundary of this unit is unknown, it continues to the base of well HRQ-2 at 125 m bsl.

4.4. Dolomite petrography

Dolostones in the Cayman Formation are petrographically heterogeneous and range from fabric retentive to fabric destructive (Figs. 2.8-2.10). Based on the preservation of precursor fabrics and the amount of dolomite cement, three textures are recognized.

Fabric retentive and pervasively cemented dolostones (Fig. 2.8), common in the peripheral dolostone zone, are typically light gray-brown and well indurated. Red algae, and foraminifera are well preserved and replaced by subhedral-anhedral dolomite crystals that are < 10 μm long. Limpid dolomite cements, forming up to 50% of the rock (commonly 20-25%), are characterized by tightly interlocking subhedral to euhedral crystals that are up to 100 μm long but typically 25-30 μm long (Fig. 2.8B, C). Individual crystals commonly have alternating LCD-HCD zones (each ~ 5 μm thick). Porosity, typically <10%, includes mainly inter- and intra-particle types and fossil moldic porosity is rare.

Fabric retentive to destructive and poorly cemented dolostones (Fig. 2.9A-D), common in the transitional and interior dolostones, are white and poorly indurated. The precursor carbonate fabrics are typically moderately to well preserved, being replaced by dolomite crystals that are < 10 μm long (Fig. 2.9A). Locally, however, some fabrics are poorly preserved (Fig. 2.9B, C). Widespread dissolution of the aragonitic components means that fossil-moldic porosity is common (Fig. 2.9B). Limpid dolomite is rare with only scattered euhedral-subhedral crystals (20-25 μm long) lining some cavities. Porosity is high (up to ~40%) and dominated by primary and fossil moldic porosity.

Dolomite in the interior limestone, which partly replaced some skeletal grains, consists of euhedral to subhedral crystals that are < 15 μm long (Fig. 2.9E, F). Dissolution, which is common, left scattered clusters of dolomite crystals in the chambers of some biofragments. There is no dolomite cement. Fossil moldic porosity dominates.

4.5. Dolomite stoichiometry

Dolostones in the Cayman Formation are composed of pure LCD (%LCD =100), pure

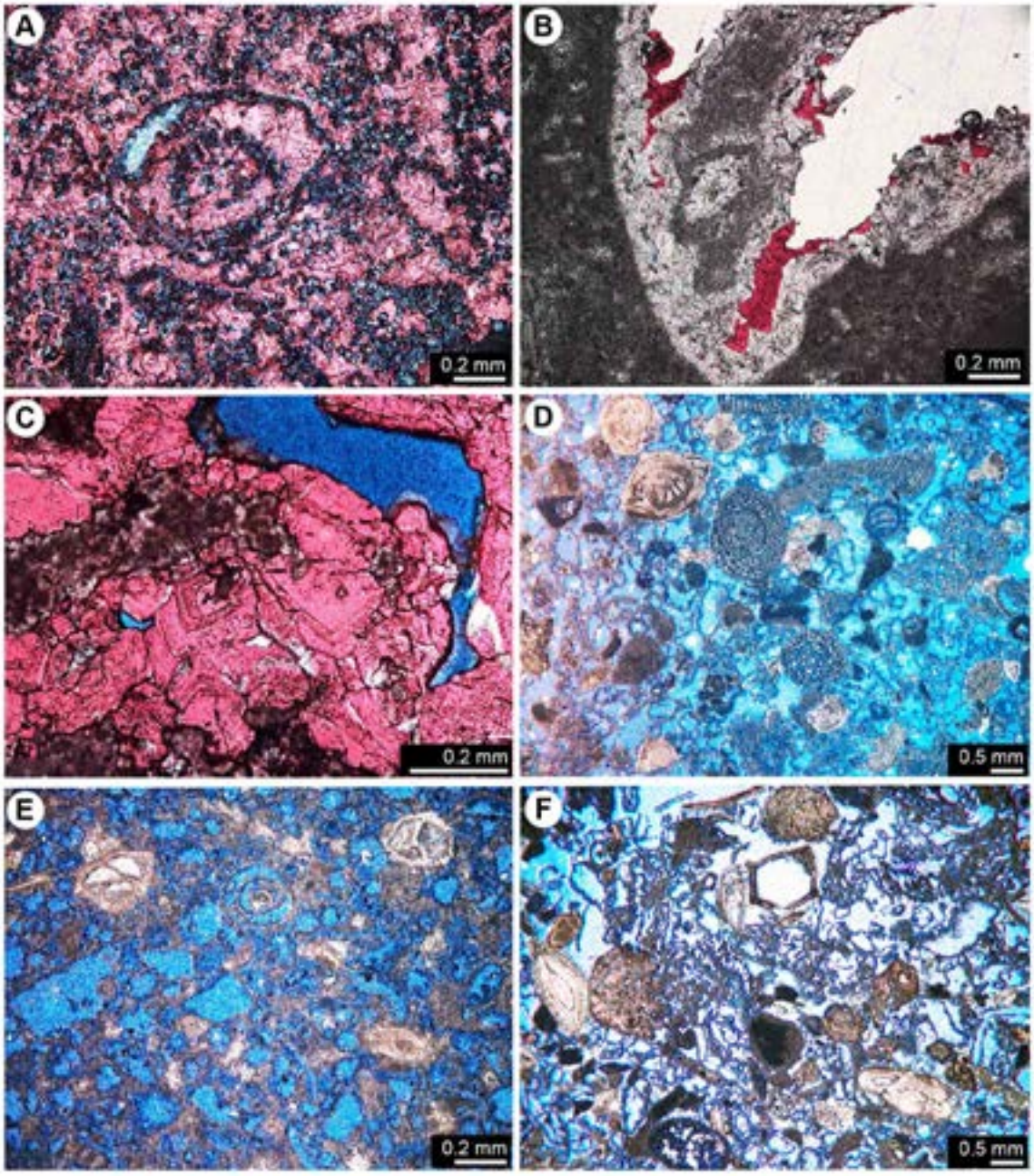

Fig. 2.7. Thin section photomicrographs illustrating the occurrence of calcite in Cayman Formation in the upper (A–C) and the lower calcite units (D–F). All depths are below ground surface. Thin sections are impregnated with blue epoxy to highlight porosity and stained with Alizarin Red S. (A) Blocky calcite cements completely filled the pores in dolostone. GFN-2, 9.6 m. (B) Pores in dolostone lined with limpid dolomite cement and partly filled with calcite (red) cement. RWP-2, 3.5 m. (C) Zoned blocky calcite cements in cavities in dolostone. HRQ-3, 3.4 m. (D) Porous benthic foraminifera limestone. GFN-2, 34.4 m. (E) Mudstone with planktonic forams. GFN-2, 59.1 m. (F) Limestone with a variety of fossils. GFN-2, 91.7 m.

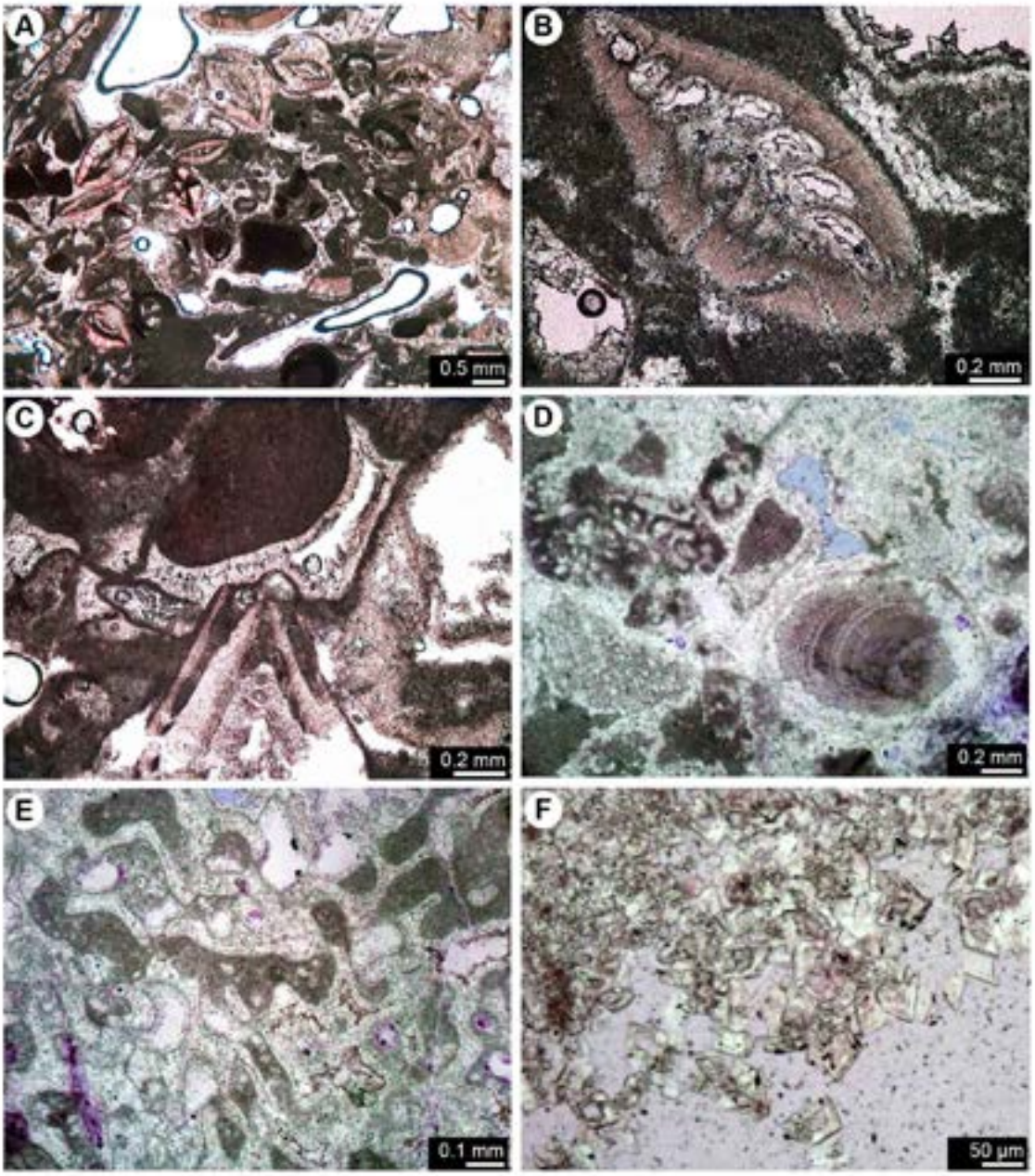

Fig. 2.8. Thin section photomicrographs of peripheral dolostones. All depths are below ground surface. (A) Fabric retentive dolostone with limpid dolomites lining the cavities. RWP-2, 94.6 m. (B) Benthic foraminifera with original fabrics well preserved in dolostone. Chamber of the foraminifera and the intra-particle pores are lined with limpid dolomite cement. RWP-2, 51.8 m. (C) Bladed dolomite cement encrusting grains in fabric retentive dolostone. RWP-2, 22.0 m. (D) Fabric retentive dolostone with a complete *Halimeda* plate, red algae fragments, and other grains. Tubules in the *Halimeda* plate and the intra-particle pores have been filled with dolomite cement. RTR-1, 116.6 m. (E) Dolostone with limpid dolomite filling cavities in a coral(?). RTR-1, 11.4 m. (F) Hollow dolomite crystals with leached cores – suggesting that the dolomite crystals originally had a HCD core. RTR-1, 130.3 m.

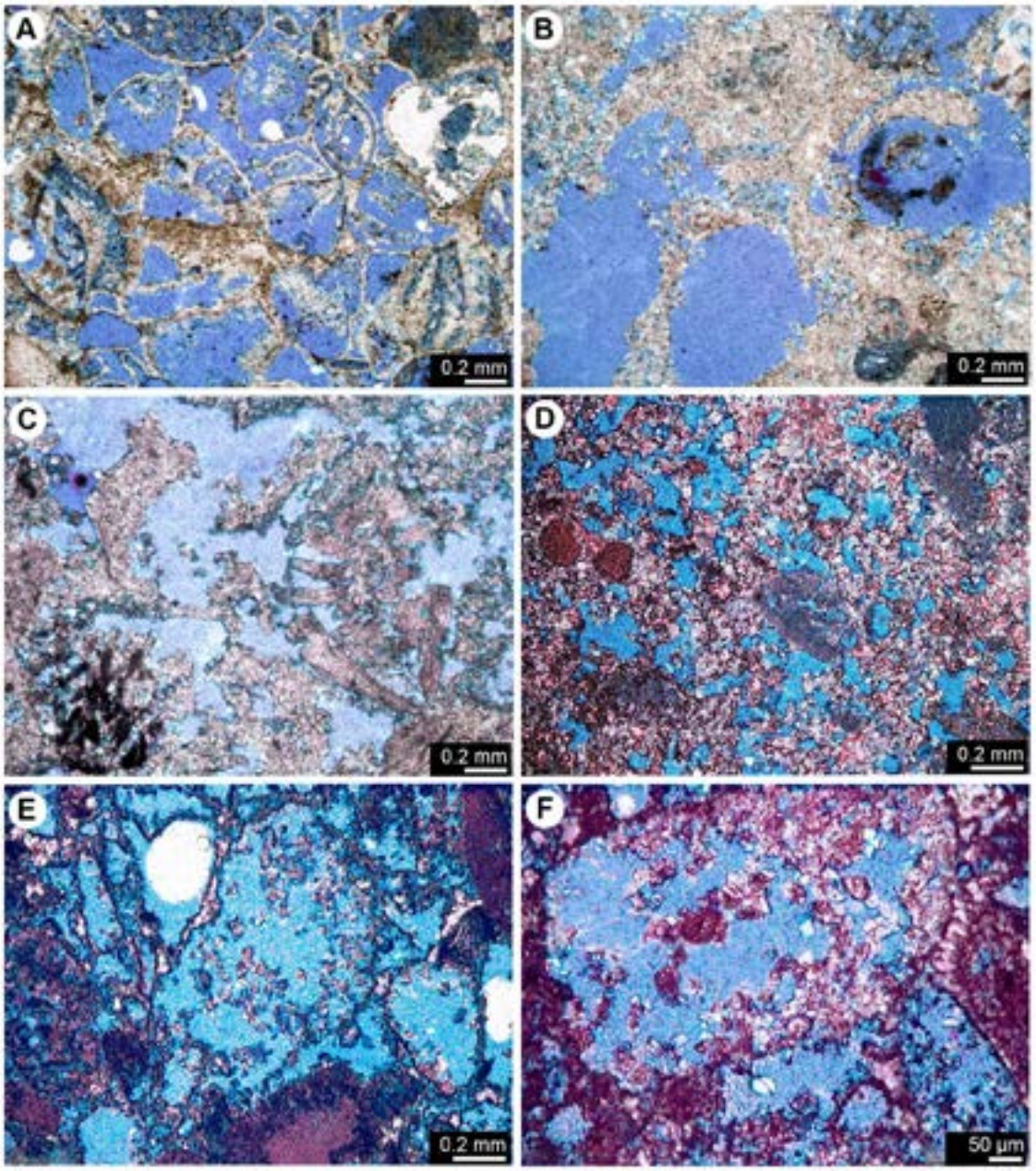

Fig. 2.9. Thin section photomicrographs of transitional dolostones (A–C), interior dolostone (D) and dolomites in interior limestone (E, F). All depths are below ground surface. Thin sections are impregnated with blue epoxy to highlight porosity and stained with Alizarin Red S. (A) Dolostone with original fabrics of precursor carbonate partly preserved. HRQ-3, 46.1 m. (B) Fabric destructive dolostone. Note molds formed by dissolution of foraminifera(?) in precursor carbonate. HRQ-3, 59.8 m. (C) Dolostone with original fabrics largely destroyed. HRQ-3, 79.6 m. (D) Fabric destructive dolostone with scattered limpid dolomite and blocky calcite cements. GFN-2, 2.6 m. (E, F) Dolomite crystals in chambers of foraminifera in dolomitic limestone. Dissolution and fossil moldic porosity are common. (E) GFN-2, 7.8 m; (F) GFN-2, 7.1 m.

HCD (%HCD=100), or mixed LCD and HCD. The distribution of LCD, HCD, and mixed LCD-HCD is variable at scales ranging from individual crystals (microns) to island scale (kilometres).

4.5.1. LCD-HCD – crystal scale

Dolomites in the peripheral dolostones are characterized by a variety of LCD-HCD patterns similar to those found in the Cayman Formation on the west part of Grand Cayman (cf., Jones and Luth, 2002). Dolomite crystals, up to 100 μm (typically 50 μm long),

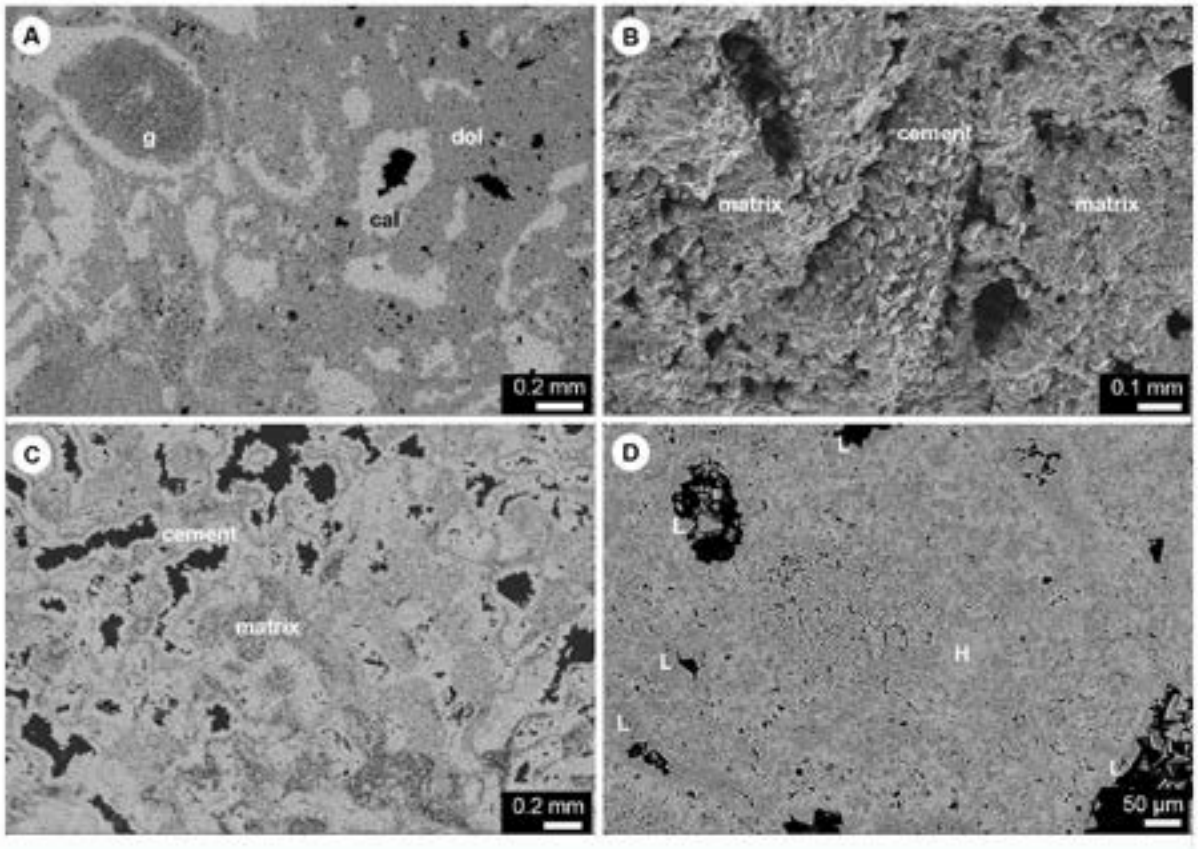

Fig. 2.10. SEM photomicrographs of dolostones from Cayman Formation. A, C, D are etched (in HCl for 12 s) and polished thin sections. B is fractured surface, unetched. All depths are below ground surface. (A) Calcite cement filling in cavities and coating the surface of a red algae fragment, g=grain, cal=calcite, dol=dolomite. EER-1, 2.7 m. (B) Dolomite cement encrusting surface of a tubular skeletal grain held in a dolomite matrix. HRQ-5, 4.2 m. (C) Dolomitized coral (?) with dolomite cement lining the cavities. HRQ-2, 11.8m. (D) Distribution of dark-gray LCD (L) and light-gray HCD (H) in dolostone. Note open pores lined with LCD. HRQ-2, 2.7m.

commonly have cores formed of HCD and cortices formed of LCD or alternating LCD and HCD zones. Pore-lining and pore-filling limpid dolomite crystals are formed of LCD or alternating LCD and HCD zones.

In the interior dolostone, most dolomite crystals (< 20 μm long with most 5-10 μm long) are formed entirely of HCD (Fig. 2.11). Euhedral to subhedral LCD pore-filling

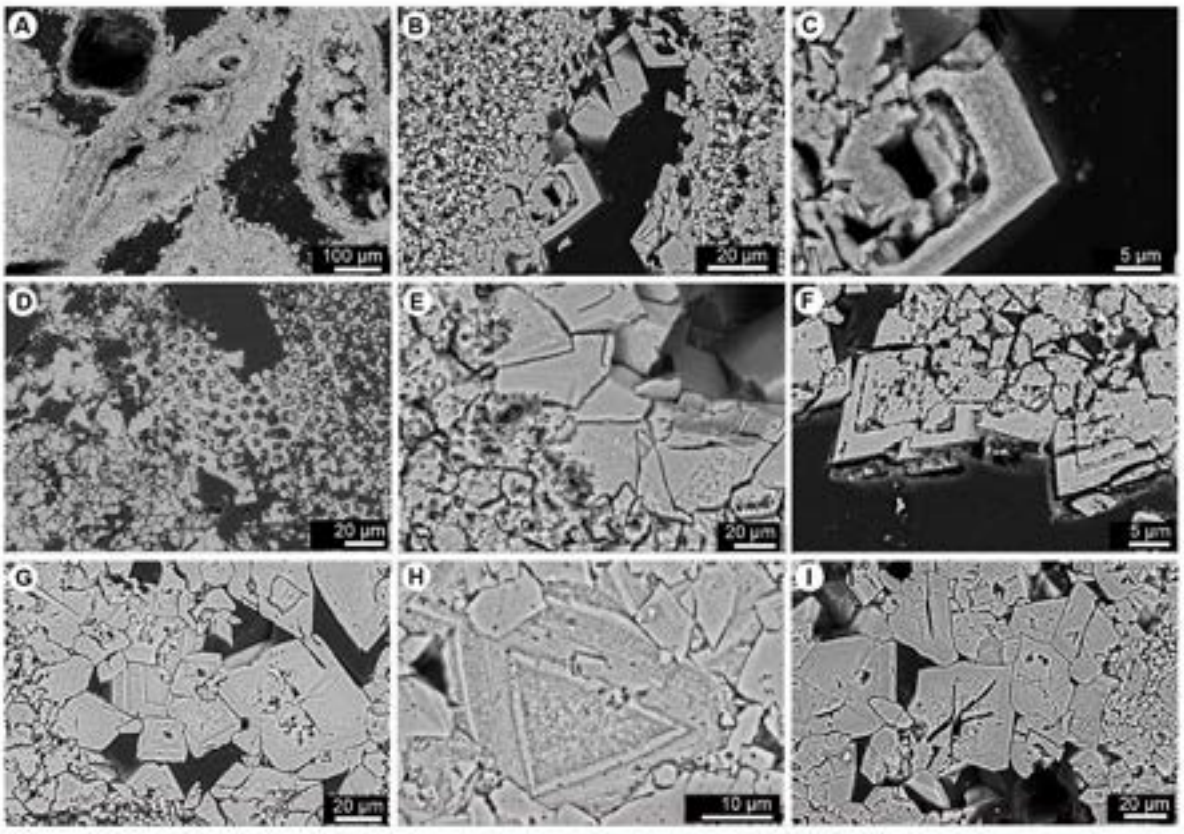

Fig. 2.11. SEM photomicrographs illustrating the compositional heterogeneity of dolomites from Cayman Formation. Polished thin sections, etched with HCl for 12 s. All from well HRQ-2. All depths are below ground surface. (A) Dolostone with dolomitized foraminifera, and dolomite cement in the pores. 42.3 m. (B) Enlarged view of etching in the matrix dolomites and the cement crystals in panel A. 42.3 m. (C) Enlarged view of cement crystal from panel B. Hollow dolomite crystal, formed by preferential dissolution of the core, partly refilled by dolomite cement. 42.3 m. (D) Preferential dissolution of matrix dolomites. 24.0 m. (E) Dolomite matrix crystals show extensive etching, and dolomite cements that overgrow on matrix crystals show clear zones. 8.8 m. (F) Dolomite crystals showing growth zones with HCD zones have been dissolved. 36.2 m. (G) Cement crystals showing growth zones, cortical boundaries, etch pits, and dissolution slots. 11.8 m. (H) Dolomite crystal showing clearly defined growth zones and cortical boundaries, 2.7 m. (I) Dolomite cement crystals with the core cut by dissolution slots. 21.0 m.

crystals (< 15 μm long) are locally present. Rare dolomite crystals have HCD cores encrusted by LCD cortices that are < 3 μm thick. The dolomite crystals are characterized by a variety of surface microstructures such as dissolution slots and etch pits (Fig. 2.11), like those documented by Jones (2013).

4.5.2. LCD-HCD – local scale

High Rock Quarry, located in the center of the eastern part of Grand Cayman, is ~1.3 km long E-W and ~1 km wide N-S (Fig. 2.1C, E). Analyses of samples from 8 closely spaced wells in this quarry show some stratigraphic and spatial patterns to the distribution of the LCD and HCD over distances of < 600 m (Fig. 2.12). In HRQ-5, for example, the dolostones that form the upper 70 m of the succession (Fig. 2.12) include (1) HCD dolostone from 41.5 to 70 m, (2) LCD dolostone from 26.3 to 41.5 m, (3) HCD dolostone from 17.1 to 26.3 m, and (4) LCD dolostone from 0 to 17.1 m.

Although the stacking patterns of the dolomite units, as defined by their LCD–HCD ratios, varies from well to well, some closely spaced wells such as HRQ-1, HRQ-2, HRQ-4, and HRQ-5, display similar mineralogical patterns (Fig. 2.12). This pattern, as illustrated in HRQ-5, is characterized by four alternating LCD-HCD units that start with a HCD unit at the bottom of the well and ends with a LCD unit near surface (Fig. 2.12). HRQ-4 and HRQ-5, which are only 140 m apart, are almost identical in terms of thicknesses, %Ca in LCD and HCD, and average %Ca (Fig. 2.12). In the calcian dolostones or dolomitic limestones, calcite is commonly found with HCD but is rarely associated with LCD.

4.5.3. LCD-HCD – island-wide scale

Most dolostones in the Cayman Formation are formed of LCD and HCD, typically with one type being dominant (Figs. 2.13-2.15). Samples formed of subequal amounts of LCD and HCD are rare. The compositions of the dolostones vary geographically between the peripheral dolostone, transitional dolostone, and interior dolostone/limestone zones (Figs. 2.13-2.15).

(1) Peripheral dolostones in HHD-1, LBL-1, RWP-2, EEZ-1, ESS-1, and HMB-1 are dominated by LCD except for RTR-1, where LCD-dominated dolostones forms only 50% of the succession (Figs. 2.13, 2.17A). LCD-dominated dolostones form all of the successions in LBL-1, RWP-2, and EEZ-1, 95% in ESS-1, 94% in HHD-1, 87% in HMB-1. Of the 421 peripheral dolostone samples in these 7 wells, 79% are LCD dominated with most containing 80-90 %LCD (Fig. 2.17A).

(2) Transitional dolostones in the CKC-1, HRQ-3, EEV-2, and FSR-1 generally

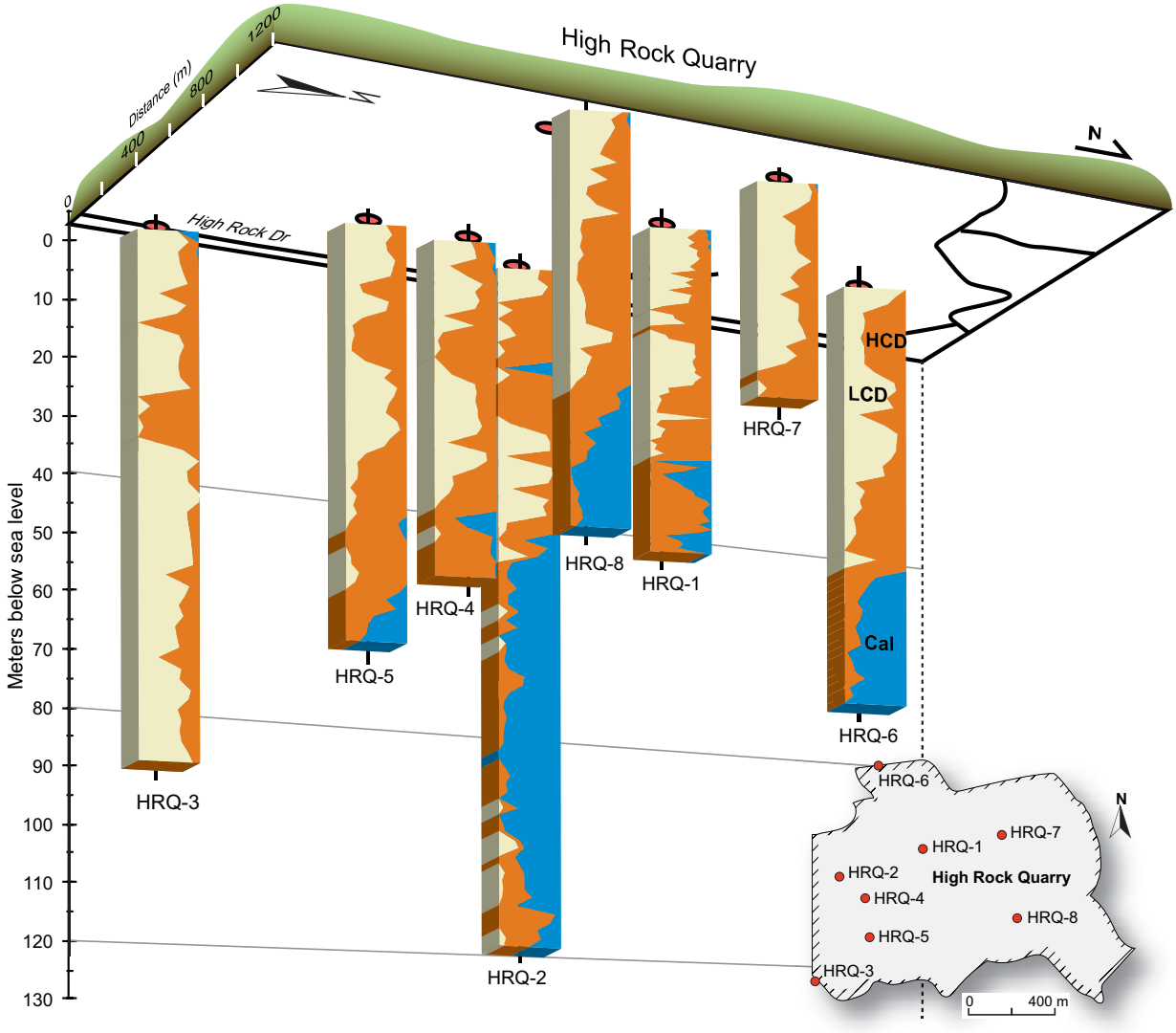

Fig. 2.12. Distribution of LCD (low calcium dolomite), HCD (high calcium dolomite), and Cal (calcite) in 8 wells in the Cayman Formation in High Rock Quarry (HRQ). Note similar patterns among the closely spaced wells.

contain LCD and HCD with the composition of the dolostones varying from well to well (Figs. 2.14, 2.17B). In the dolostone successions from CKC-1 and HRQ-3, the LCD-dominated dolostone forms 88% and 90% of the succession, respectively (Fig. 2.14). In

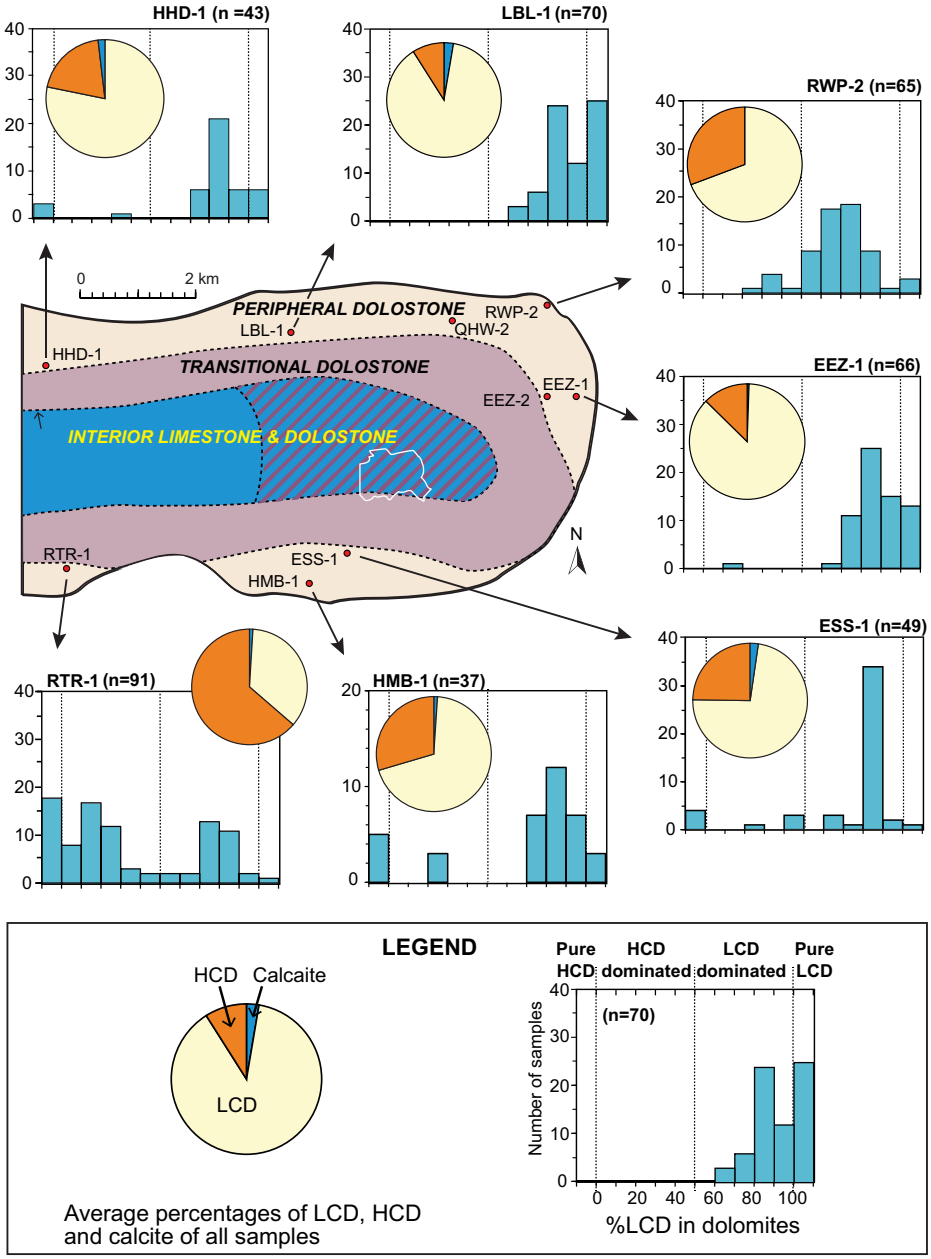

Fig. 2.13. Distribution of LCD, HCD, and calcite (Cal) in 7 wells in the peripheral dolostone zone. Pie charts showing the average compositions (%LCD, %HCD, and %calcite) of all samples in each well. Histograms illustrating the %LCD in dolomite samples in each well.

EEV-2 and FSR-1, which are closer to the southern coastline, the dolostone successions are formed entirely of HCD-dominated dolostones (Fig. 2.14). Of the 190 samples from these wells, 74% of the dolostones are LCD-dominated with most composed of 80-90%LCD (Fig. 2.17B).

(3) Interior dolostones, including those from FFM-1, GFN-2, HRQ-1, HRQ-2, HRQ-4, HRQ-5, HRQ-6, HRQ-7, and HRQ-8, differ from the peripheral and transitional dolostones because apart from HRQ-7, they all contain more HCD than LCD (Figs. 2.15, 2.17C). The average %HCD in dolostones from FFM-1 is 98.4%, whereas in the remaining wells it is 54.7-63.9% (Fig. 15). The average %HCD (42.0%) in the dolostones from HRQ-7 is misleading because that well is only 39.6 m deep and does not cover the full depth range of the other wells (Fig. 2.12). The average %HCD from 341 dolostone samples in these 9 wells is 42-98% (Fig. 2.15) and 65% of the 341 analyzed dolomite samples contain more HCD than LCD (Fig. 2.17C). Forty-five samples are formed of HCD alone.

(4) Interior limestones that contain some dolomite are dominated by HCD (Figs. 2.16, 2.17D). Of the 191 analyzed samples, dolomite was found in 186 of them with 93% of them

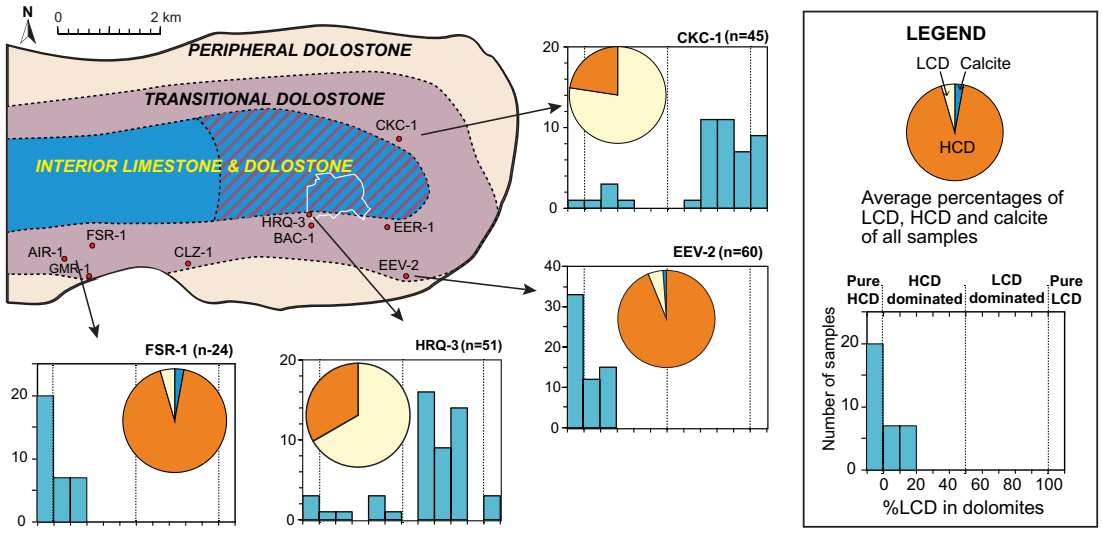

Fig. 2.14. Distribution of LCD, HCD, and calcite (Cal) in 4 wells located in the transitional dolostone zone. Pie charts showing the average compositions (%LCD, %HCD, and %calcite) of all samples in each well. Histograms illustrating the %LCD in dolomite samples in each well.

of pure LCD (Fig. 2.17D). LCD was found only in well HRQ-2 (Fig. 2.16).

At the island-wide scale, there is no readily apparent stratigraphic pattern to the distribution of the LCD and HCD (Figs. 2.4, 2.5). It seems, however, that the dolostones that overlie and/or underlie limestone successions are invariably dominated by HCD (Figs. 2.4, 2.5).

4.6. Oxygen and carbon isotopes

Dolomites from 206 samples in eight wells have $\delta^{18}O$ from 0.68‰ to 5.03‰ (average = 3.12 ± 1.02‰) and $\delta^{13}C$ ranging from 0.52 to 3.83‰ (average = 2.37 ± 0.84‰) (Fig. 2.18A). For dolomites in the calcian dolostones, the $\delta^{18}O$ ranges from 1.11‰ to 5.03‰ (average = 3.26 ± 0.94‰, n=182), and the $\delta^{13}C$ ranges from 0.52 to 3.83‰ (average= 2.50 ± 0.80‰, n=182). In contrast, the $\delta^{18}O$ values for dolomite in the dolomitic limestones range from 0.68‰ to 3.84‰ (average = 2.10 ± 1.03‰, n=24), and the $\delta^{13}C$ ranges from 0.64 to 2.15‰ (average= 1.42 ± 0.43‰, n=24).

The dolomites in the three geographically defined dolostone zones and the limestone

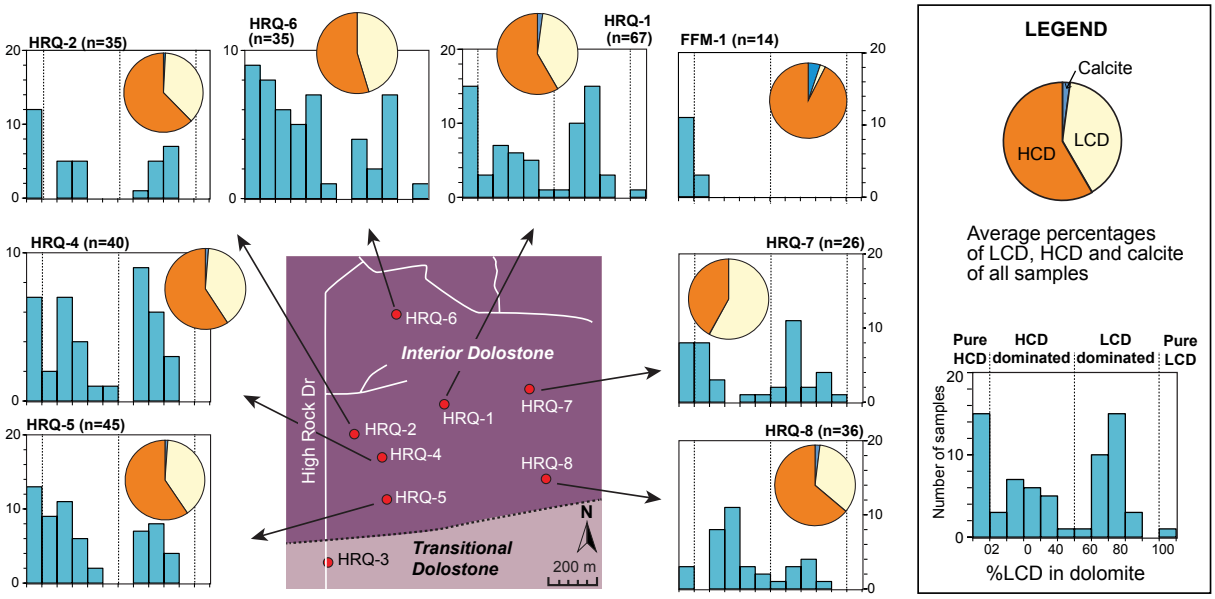

Fig. 2.15. Distribution of LCD, HCD, and calcite (Cal) in 8 wells in the interior dolostone zone. Pie charts showing the average compositions (%LCD, %HCD, and %calcite) of all samples in each well. Histograms illustrating the %LCD in dolomite samples in each well. See Fig. 2.6 for the distribution of the interior dolostone zone, and the locations of wells FFM-1 and GFN-2.

are characterized by isotopic compositions that become progressively less positive towards the interior of the island (Fig. 2.18A, B).

Peripheral dolostone – 105 dolomites from RWP-2, HMB-1, EEZ-1, and LBL-1 have high $\delta^{18}O$ (1.11 to 5.03‰, mean = 3.62 ± 0.85‰) and $\delta^{13}C$ (1.32 to 3.83‰, mean = 3.05 ± 0.47‰) values.

Transitional dolostone – 41 dolomites from HRQ-3 and CKC-1 are characterized by intermediate $\delta^{18}O$ (1.29 to 4.73‰, mean = 3.10 ± 0.88‰) and $\delta^{13}C$ (0.94 to 3.29‰, mean = 2.01 ± 0.44‰) values.

Interior dolostone – 36 dolomites from HRQ-1 (0 to 55 m) and HRQ-2 (0-54 m) have $\delta^{18}O$ values from 1.36 to 3.46‰ (mean = 2.37 ± 0.55‰), and $\delta^{13}C$ values from 0.52 to 2.33‰

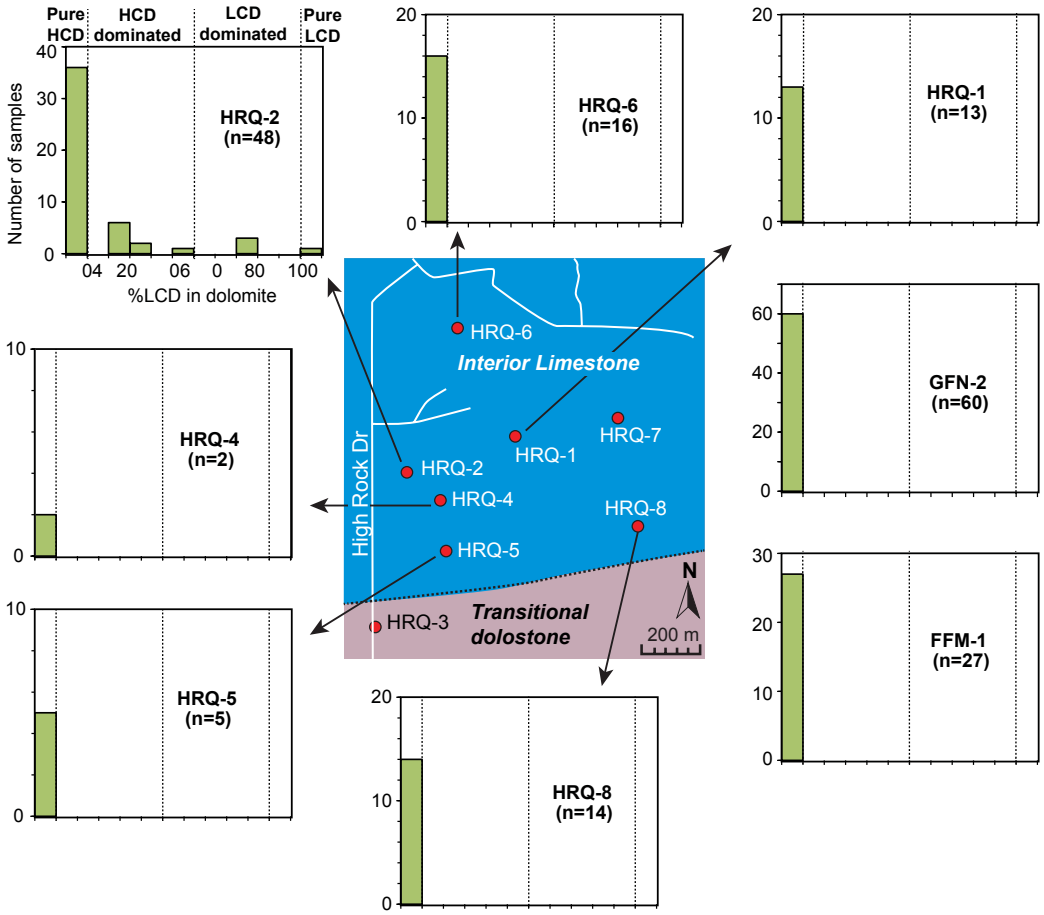

Fig. 2.16. Histograms illustrating the %LCD in dolomites in the limestone samples from each well in the interior limestone zone. See Fig. 2.6 for the distribution of the interior limestone zone, and the locations of wells FFM-1 and GFN-2.

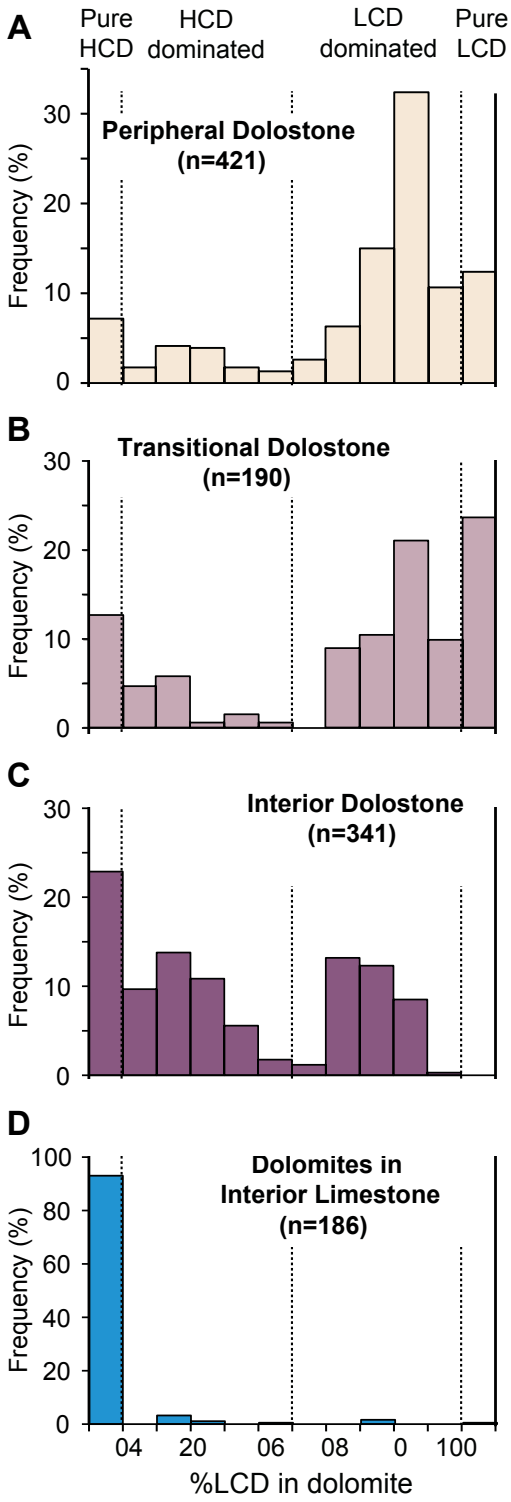

Fig. 2.17. Histograms of %LCD in all dolomites from (A) peripheral dolostone, (B) transitional dolostone, (C) interior dolostone, and (D) interior limestone. Note the increase in the frequency of the pure HCD and HCD dominated dolomites in the transitional dolostone zone relative to the interior dolostone zone.

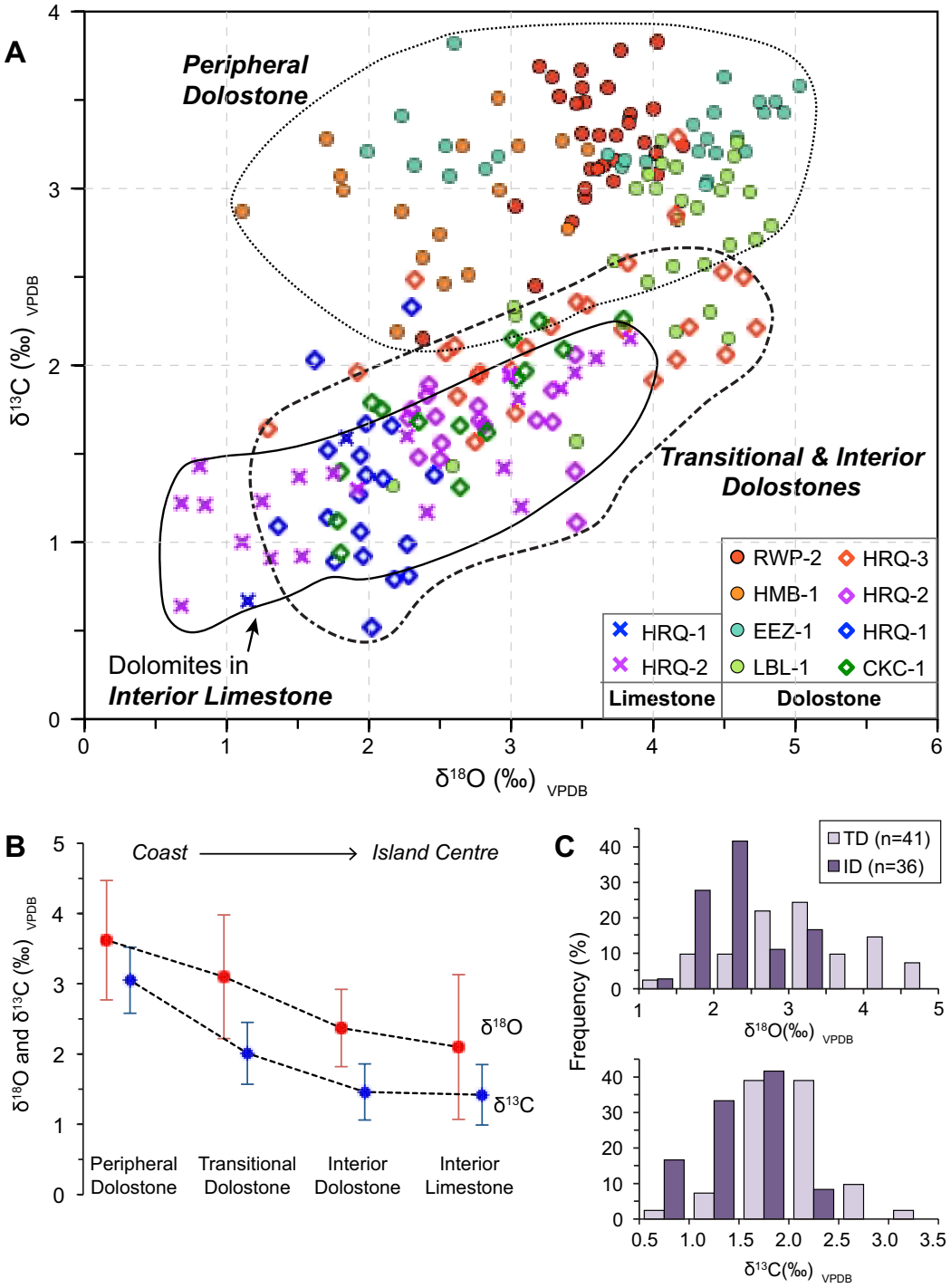

Fig. 2.18. Oxygen and carbon isotopes of dolomites in the Cayman Formation. (A) Cross-plots of $\delta^{18}O$ and $\delta^{13}C$ of dolomites from all dolomite samples grouped by the peripheral dolostone, transitional dolostone, interior dolostone, and interior limestone zones. (B) Distribution of the average $\delta^{18}O$ and $\delta^{13}C$ of dolomites from the peripheral dolostone, transitional dolostone, interior dolostone, and interior limestone zones (error bars represent ± 1σ). Note the decreasing trends of the isotopes from the periphery to the interior of the island. (C) Histograms of $\delta^{18}O$ and $\delta^{13}C$ of dolomites from transitional dolostone (TD) and interior dolostone (ID).

(mean = 1.46 ± 0.40‰). Although there is some overlap between the isotopes of interior and transitional dolostones, the former is generally lower than the latter (Fig. 2.18C).

Interior limestone – 24 dolomites in limestones from HRQ-1 (55-60 m) and HRQ-2 (54-127 m) have the lowest $\delta^{18}O$ (0.68 to 3.84‰, mean = 2.10 ± 1.03‰) and $\delta^{13}C$ (0.64 to 2.15 ‰, mean = 1.42 ± 0.43‰) values.

The oxygen and carbon isotopes from the peripheral dolostones display no apparent co-variation between the $\delta^{18}O$ and $\delta^{13}C$ values (Fig. 2.18A). In contrast, there is a positive co-variation between the two isotopes for dolomite in the transitional dolostones in CKC-1 (r^2=0.67) and in the interior dolostones and limestones from HRQ-2 (r^2=0.50) (Fig. 2.19).

Overall, the $\delta^{18}O$ and $\delta^{13}C$ values of the dolomites are poorly correlated with the average %Ca (Fig. 2.20A, B). For those dolomites formed almost entirely of LCD (%LCD > 90%) or HCD (%HCD > 90%), there is no obvious correlation between their $\delta^{18}O$ values and %Ca (Fig. 2.20C). The average $\delta^{18}O$ of 45 dolomite samples with LCD>90% (wells LBL-1, RWP-2, EEZ-1, CKC-1, HRQ-3, and HMB-1) is 2.97 ± 0.53‰; whereas the average $\delta^{18}O$ value for all 19 dolomite samples with HCD>90% (wells CKC-1, HRQ-1, HRQ-2, HRQ-3, and HMB-1) is 0.75‰ lower (2.22 ± 0.33‰; Fig. 2.20C).

In all of the wells, the $\delta^{18}O$ and $\delta^{13}C$ values of the dolomites increase with depth (Fig. 2.21). The rate of increase is commonly highest near the surface. In RWP-2, LBL-1, and HMB-1, for example, the increase in $\delta^{18}O$ from 10 to 20 m can be 1.0 to 1.5‰. Although

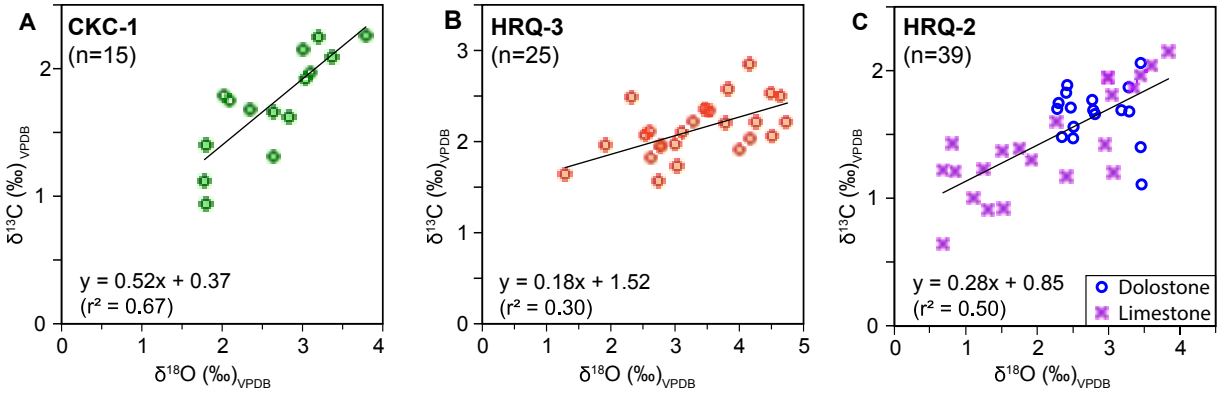

Fig. 2.19. Cross-plots of $\delta^{18}O$ and $\delta^{13}C$ of dolomites from wells (A) CKC-1, (B) HRQ-3, and (C) HRQ-2 showing the positive correlation between the isotopes.

apparent in each well, the rate of $\delta^{18}O$ increase with depth varies from well to well. For example, in the deeper part of the successions, the increases in $\delta^{18}O$ are higher in CKC-1, HMB-1, and HRQ-2 (increase ~ 1‰ in 30 m) than in the other wells (Fig. 2.21).

There is a good correlation between the $\delta^{18}O$ values of the dolomite and the associated calcite in well HRQ-2 (average $\Delta^{18}O_{dol\text{-}cal}$ = 1.75‰, n=24; Fig. 2.22A). Similarly, the $\delta^{13}C$

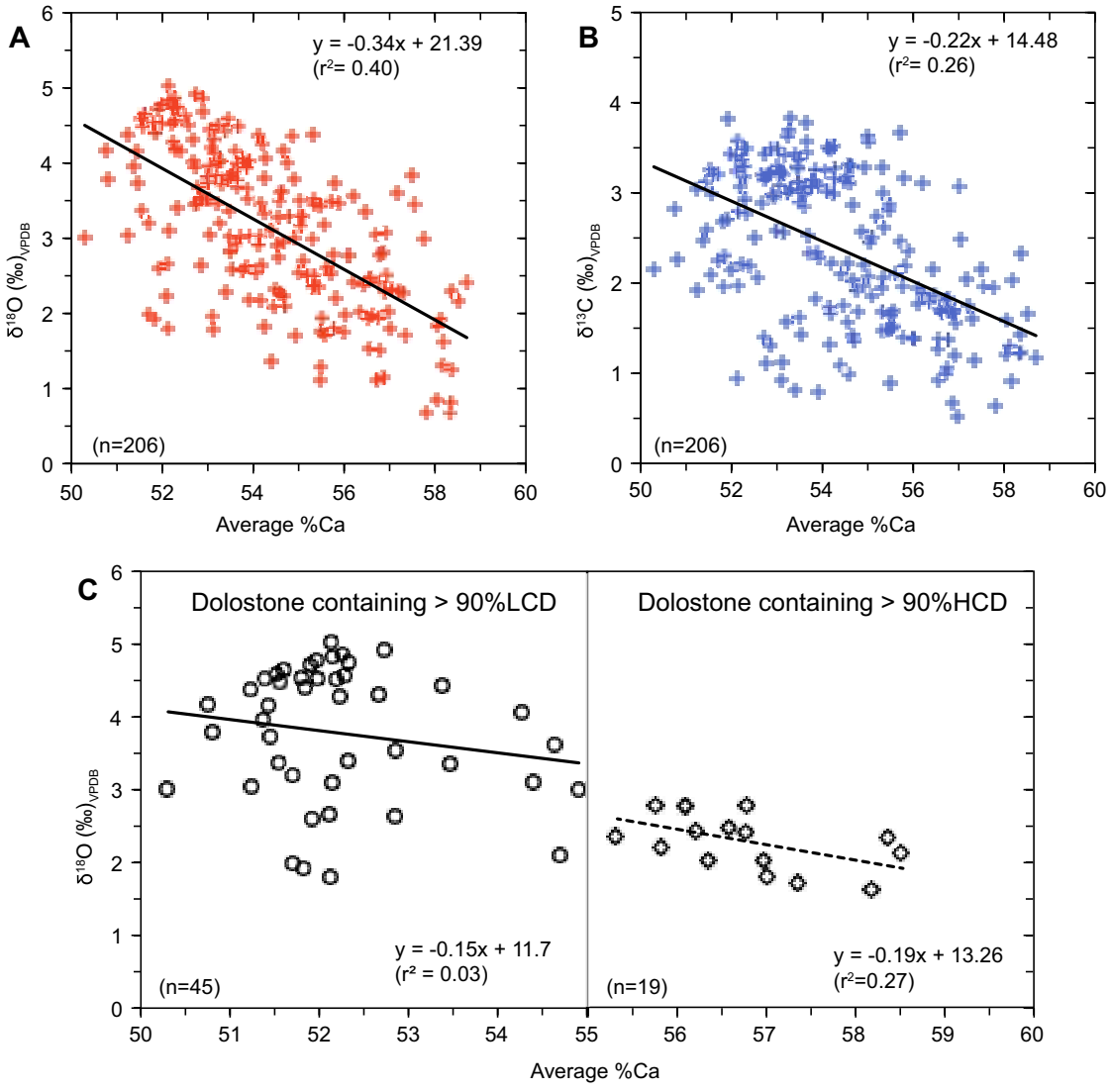

Fig. 2.20. Relationship between the stable isotopes and stoichiometry of the dolomite from Cayman Formation. (A) Comparison of $\delta^{18}O$ and average %Ca of dolomite. (B) Comparison of $\delta^{13}C$ and average %Ca of dolomite. (C) Comparison of $\delta^{18}O$ and average %Ca in dolostones with %LCD > 90%, and dolostones with %HCD > 90%.

values of the dolomite are ~ 0.60‰ higher than the coexisting calcite from the same well (Fig. 2.22B).

4.7. Strontium isotopes

Collectively, the $^{87}Sr/^{86}Sr$ ratios of the 100% dolomite samples, which range from 0.70888 to 0.70914 (average = 0.70902, n = 104), have a unimodal distribution with a mode of 0.70900-0.70902 (Fig. 2.23A). Nevertheless, the $^{87}Sr/^{86}Sr$ ratios vary from well to well. In the peripheral dolostones, an obvious bimodal distribution of the $^{87}Sr/^{86}Sr$ is apparent in well HMB-1 (modes at 0.70896-0.70898 and 0.70906-0.70908), whereas in RWP-2 and RTR-1 there is no bimodality (Fig. 2.23B-D). The transitional dolostones from CKC-1

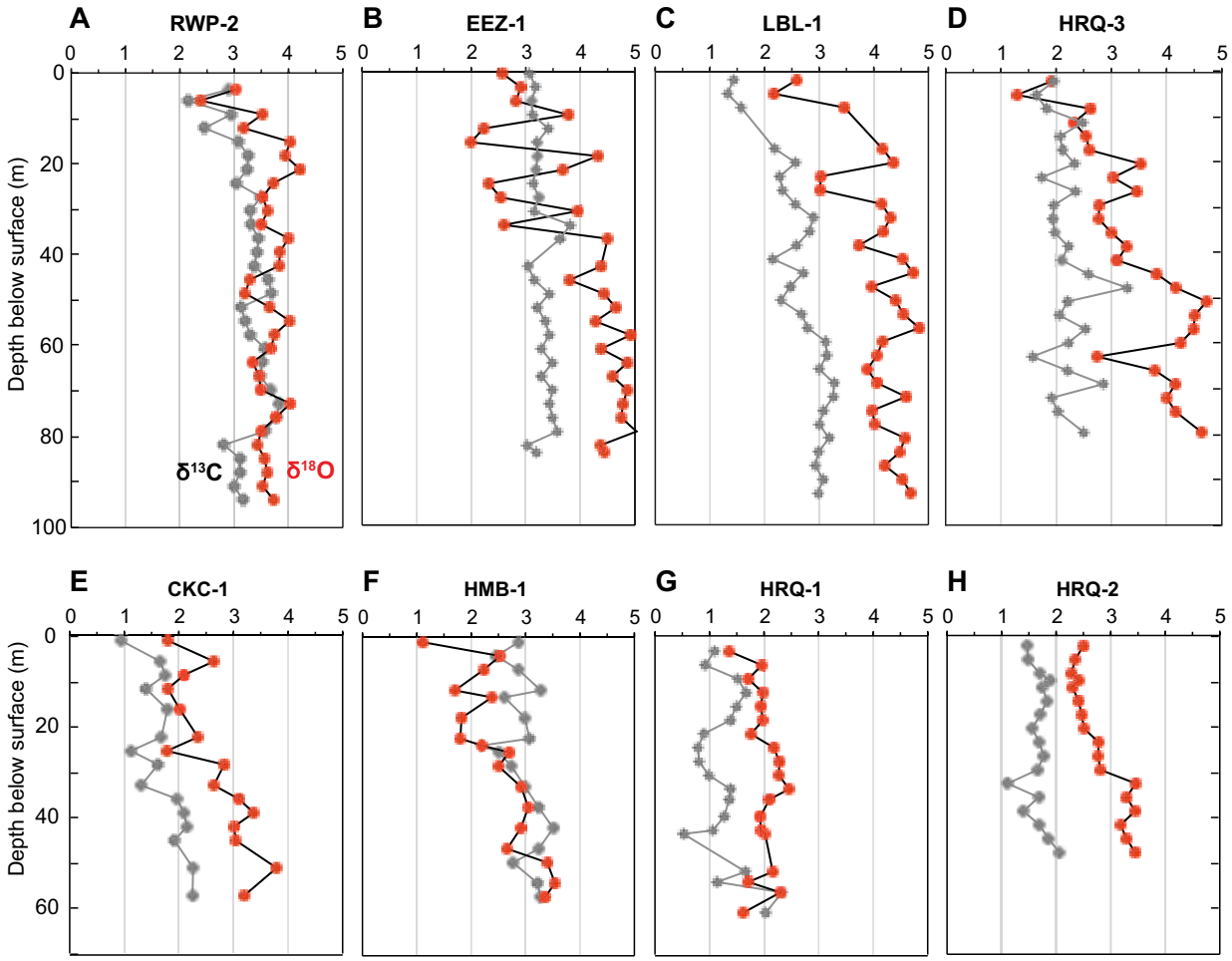

Fig. 2.21. Stratigraphic variations of $\delta^{18}O$ and $\delta^{13}C$ $(‰)_{VPDB}$ in dolostones from wells (A) RWP-2, (B) EEZ-1, (C) LBL-1, (D) HRQ-3, (E) CKC-1, (F) HMB-1, (G) HRQ-1, and (H) HRQ-2.

have a bimodal distribution of $^{87}Sr/^{86}Sr$ with the modes at 0.70900-0.70902 and 0.70908-0.70910 (Fig. 2.23E). In contrast, the interior dolostones from well FFM-1 have a unimodal distribution of $^{87}Sr/^{86}Sr$ with the mode at 0.70908-0.70910 (Fig. 2.23F).

There is no obvious correlation between the $^{87}Sr/^{86}Sr$ values and the %LCD or the average %Ca of the dolostones (Fig. 2.24).

Two pure limestone samples from GFN-2 have $^{87}Sr/^{86}Sr$ values of 0.70902 and 0.70915. The ratios from the 17 dolomitic limestones from FFM-1 and GFN-2 range from 0.70902 to 0.70912 (average=0.70904) (Fig. 2.23A).

4.8. Groundwater geochemistry and temperature

Today, the groundwater in the Cayman Formation on the east end of Grand Cayman includes the freshwater, saline, and brackish zones. A freshwater lens, centrally located on

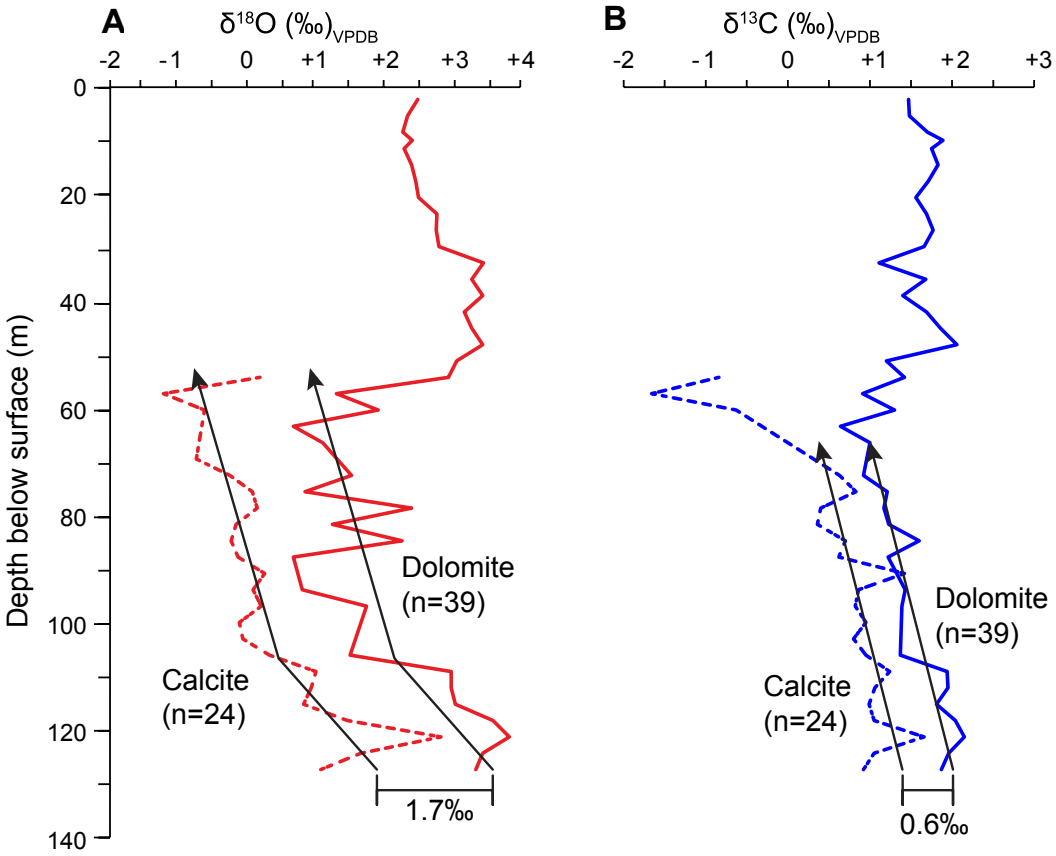

Fig. 2.22. Stratigraphic variations and correlations of (A) $\delta^{18}O$ and (B) $\delta^{13}C$ between coexisting dolomites and calcites from well HRQ-2. The arrows indicate the stratigraphic trends in the $\delta^{18}O$ and $\delta^{13}C$ values.

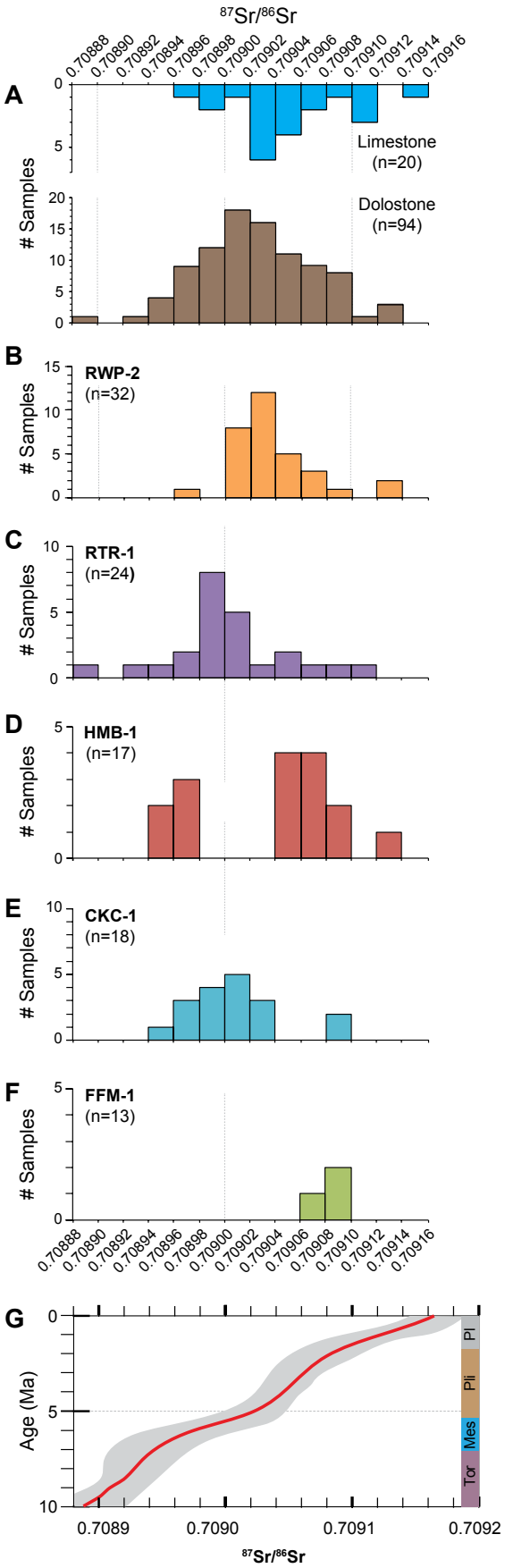

Fig. 2.23. Histograms of $^{87}Sr/^{86}Sr$ of dolostones and limestones from Cayman Formation. (A) All dolostones from wells illustrated in B-F, and (dolomitic) limestones from wells HRQ-2, FFM-1 and GFN-2. (B) Dolostones from well RWP-2. (C) Dolostones from well RTR-1. (D) Dolostones from well HMB-1. (E) Dolostones from well CKC-1. (F) Dolostones from well FFM-1. (G) Two phases of dolomitization derived from $^{87}Sr/^{86}Sr$ of dolostones from wells B-F. Seawater $^{87}Sr/^{86}Sr$ curve modified from McArthur et al. (2001).

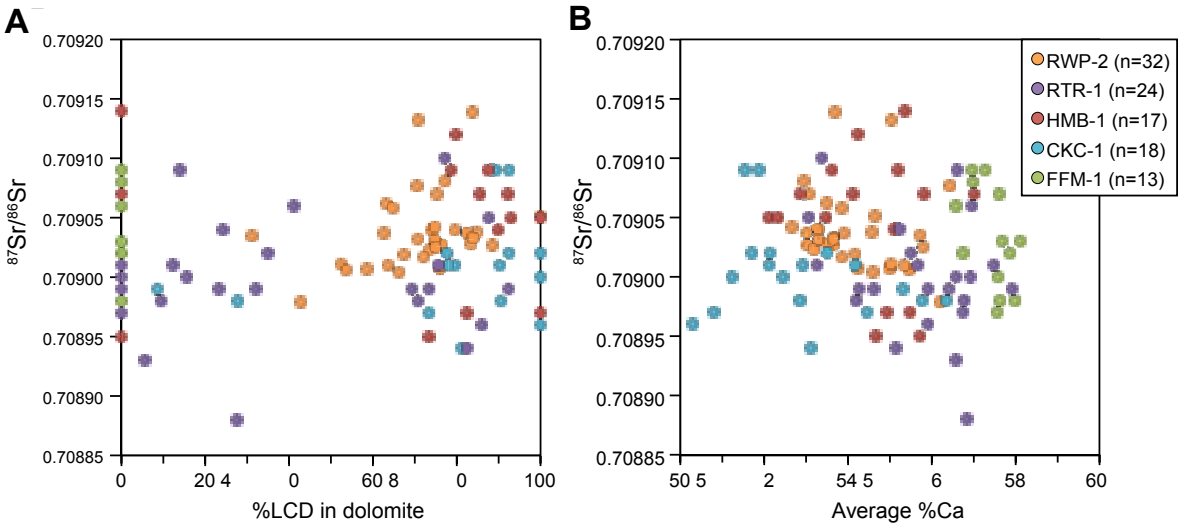

Fig. 2.24. Comparison of $^{87}Sr/^{86}Sr$ with (A) %LCD in dolomite, and (B) the average %Ca of dolomite.

the east end of Grand Cayman (e.g., Mather, 1971; Ng et al., 1992) (Fig. 2.1B), is < 20 m thick and separated from the underlying saline zone by a mixing zone that is ~20 m thick (Ng and Jones, 1995).

The water properties of the saline zone vary from location to location. Present-day seawater around Grand Cayman has an average Mg/Ca ratio of 5.4 (based on 3 samples collected from Spotts Bay) and contrasts with the ratios of groundwater from (1) RTR-1: 4.95

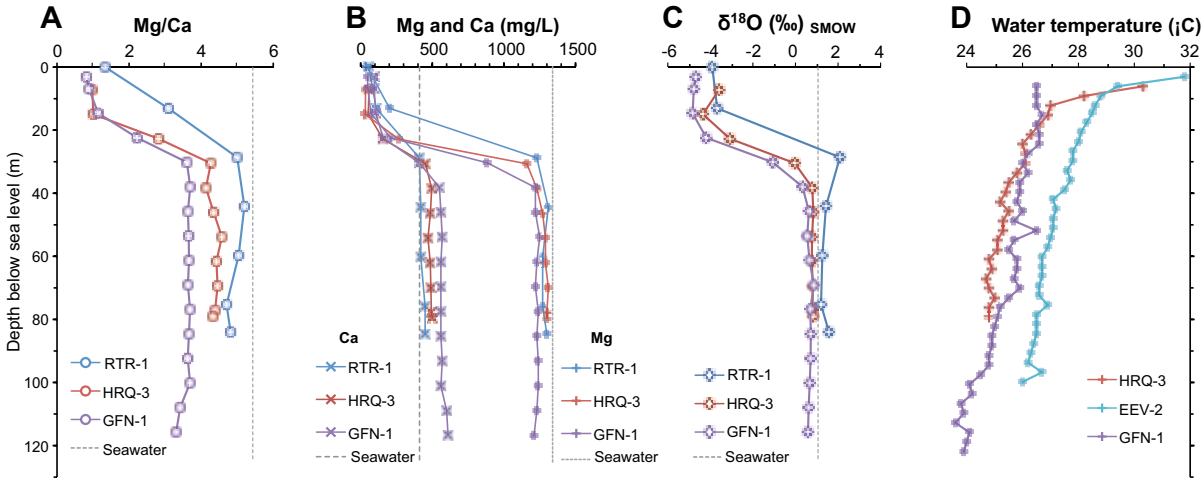

Fig. 2.25. Geochemistry (A-C) and temperature (D) of present-day pore water in Cayman Formation. (A) Molar Mg/Ca ratio. (B) The contents of Mg and Ca. (C) $\delta^{18}O$ (‰) $_{SMOW}$. (D) Temperature. Dashed lines in (A)-(C) represent the average values of 3 seawater samples collected in Spotts Bay (south coast).

± 0.20 (n=5), (2) HRQ-3: 4.38 ± 0.34 (n=7), and (3) GFN-1: 3.60 ± 0.13 (n=10) (Fig. 2.25A). Compared with seawater collected around the island, the lower Mg/Ca ratios of groundwater in these three wells are the result of a decrease in Mg and an increase in Ca (Fig. 2.25B).

The average $\delta^{18}O_{SMOW}$ of the saline water from RTR-1, HRQ-3, and GFN-1 are 1.51 ± 0.35‰ (n=12), 0.80 ± 0.03‰ (n=8), and 0.67 ± 0.08‰ (n=5), respectively (Fig. 2.25C). There is no correlation between the $\delta^{18}O$ of the water and the chloride concentration or the rock type in which it resides. The average $\delta^{18}O$ of three seawater samples collected in Spotts Bay is 1.06‰.

Groundwater temperature changes with depth and location (Fig. 2.25D). The rate of decrease with depth is variable, being about -2 °C /10m within ~10 m bsl and about -2.5 °C /100 m from ~10 m bsl to the base of GFN-1 at ~120 m bsl. The water temperature in HRQ-3 and GFN-1, located in the island interior, is 1.5 to 2.0 °C lower than that in EEV-2 at the same depth.

5. Interpretation of dolomitizing time and fluids

5.1. Time of dolomitization

Interpretation of the number of dolomitization phases and the exact timing of each phase is limited by the dating method employed. The error margin associated with $^{87}Sr/^{86}Sr$ dating is typically > 0.5 Ma and can be as high as 2 Ma if the data coincide with the plateaus on the $^{87}Sr/^{86}Sr$ curve (Jones and Luth, 2003b). The unimodal distribution of $^{87}Sr/^{86}Sr$ (0.70900-0.70902) from all the dolostones in the Cayman Formation on the east end of Grand Cayman (Fig. 2.23A) is similar to the unimodal histograms of Pleydell et al. (1990) and Jones and Luth (2003b) that had modes of 0.70900-0.70905 and 0.709025-0.709050, respectively. The large range in the $^{87}Sr/^{86}Sr$ values, however, means that two or even more phases of dolomitization may be included (Budd, 1997; Machel, 2000; Jones and Luth, 2003b).

For individual wells, the distribution of the $^{87}Sr/^{86}Sr$ values for the dolostones varies. The $^{87}Sr/^{86}Sr$ values of peripheral dolostones in RWP-2 and RTR-1 range from 0.70888-

0.70902 with a unimodal distribution (Fig. 2.23B, C), which may reflect the mixing of $^{87}Sr/^{86}Sr$ values from more than one dolomitizing phases. Despite that, the peripheral dolostones in HMB-1 and the transitional dolostones in CKC-1 show bimodality of the $^{87}Sr/^{86}Sr$ (Fig. 2.23D, E). The two modes in both wells are probably equivalent. When applying the $^{87}Sr/^{86}Sr$–time curve of seawater from McArthur et al. (2001), the two modes correspond to 5.5-7.5 Ma and 1.5-3 Ma, respectively (Fig. 2.23). These two dolomitizing phases are consistent with previously suggested phase I (late Miocene) and phase II (late Pliocene) dolomitization of the Cayman Formation on Cayman Islands (Jones and Luth, 2003b; Zhao and Jones, 2012). The unimodal distribution of $^{87}Sr/^{86}Sr$ from the interior dolostones in the upper 20 m of well FFM-1, with a narrow range of 0.70906 to 0.70910 may indicate phase II dolomitization alone (Fig. 2.23F).

Collectively, the available information suggests that phase I dolomitization was restricted to the coastal areas of the island, whereas phase II dolomitization extended into the center of the island. This model is consistent with Jones and Luth (2003b, their Fig. 15) who suggested that phase I produced a patchy distribution of dolostone throughout the Cayman Formation whereas phase II resulted in dolomitization of the remaining limestone.

The coexistence of LCD and HCD dolomites in Cayman Formation cannot be equated with the two phases of dolomitization because both LCD and HCD were probably generated during each phase. This is based on the fact that the $^{87}Sr/^{86}Sr$ ratio cannot be related to the %LCD or %Ca in the dolomite (Fig. 2.24) and many crystals that have three or more alternating LCD and HCD zones. It seems improbable that each zone would represent a different phase of dolomitization.

Some dolomite in the Cayman Formation was diagenetically modified after each episode of dolomitization. Since the last phase of dolomitization, for example, the rapid and dramatic glacioeustatic fluctuations in sea level and subaerial exposure led to the formation of hollow dolomite crystals (Ren and Jones, 2016) and the development of inside-out dolomite (Jones, 2007).

5.2. Properties of dolomitizing fluids

The Mg needed for dolomitizing the limestones in the Cayman Formation was most probably derived from seawater that surrounded Grand Cayman. Previous studies on dolomitization of the Cayman Formation on Grand Cayman and Cayman Brac concluded that seawater or slightly modified seawater mediated dolomitization (Pleydell et al., 1990; Jones and Luth, 2002; Zhao and Jones, 2012). The contrasts in the degree of dolomitization and the variations in the %Ca and HCD and LCD ratios of dolomites from the coast to the center of the island, however, may point to geographical variability in the composition of the dolomitizing fluids across the island.

5.2.1. Evidence from carbon isotopes

The $\delta^{13}C$ values of most dolomites from the Cayman Formation (+0.52 to +3.83‰, average = 2.37 ± 0.84‰, n=206) are typical of replacive island dolostones that are generally between +0.5‰ and +3.2‰ (cf., Budd, 1997). These carbon isotopic values, as suggested by Land (1992) and Budd (1997), were largely inherited from their precursor carbonates that contained marine carbon. The average $\delta^{13}C$ difference between the coexisting dolomite and calcite in the Cayman Formation ($\Delta^{13}C_{\text{dol-pres cal}}$) of about 0.6‰ (Fig. 2.22B) agrees with Land (1992) who argued that dolomite has < 1‰ difference in $\delta^{13}C$ from the precursor sediment. The true fractionation between the dolomites and their precursor carbonate ($\Delta^{13}C_{\text{dol-orig cal}}$) from Cayman Formation is probably < 0.6‰ because the present-day calcites that coexist with the dolomite have evolved through meteoric diagenesis after dolomitization and thus may have a lower $\delta^{13}C$ than their precursor carbonates.

Although the $\delta^{13}C$ in the dolomite may provide little information about the nature of the dolomitizing fluid that affected the Cayman Formation, some clues can still be determined by considering the spatial distribution of those values and by considering them together with the oxygen isotopes. In this respect, the following points are important:

(1) The $\delta^{13}C$ values are related to location, with the lower values (< 2‰) being mostly

from the central part of the island (dolomites in interior dolostone and limestone) and the higher values (>3‰) from the peripheral dolostones (Fig. 2.18A, B).

(2) Samples with a positive correlation between the $\delta^{18}O$ and $\delta^{13}C$ all came from the central part of the island (Fig. 2.19). This relationship is not apparent in the dolomite from the coastal areas. Covariation between the oxygen and carbon isotopes of carbonate is commonly regarded as an indicator of diagenetic alteration in the marine-meteoric mixing zone (e.g., Allan and Matthews, 1982). In this zone, both isotopes in the water increase with depth from typical meteoric values to marine values. The positive covariation between $\delta^{18}O$ and $\delta^{13}C$ evident in dolomites from the Yucatan Peninsula was attributed to a mixing zone origin (Ward and Halley, 1985). The positive $\delta^{13}C$ values, along with the covariation between $\delta^{13}C$ and $\delta^{18}O$ of the dolomites from the interior of Cayman Island indicate that they were probably precipitated in the lower part of the mixing zone.

Together, these points indicate that the dolomitizing fluids in the peripheral and interior parts of the island were different. Assuming that the dolomitizing fluid of the peripheral dolostones was seawater, the above points indicate that the parent fluid of the interior dolostone and limestone was probably a mixture of (modified) seawater and meteoric water.

5.2.2. Evidence from oxygen isotopes

Factors that determine the $\delta^{18}O$ value of dolomite include primarily reaction temperature and the $\delta^{18}O$ of the dolomitizing fluid (Land, 1985), dolomite stoichiometry (Aharon et al., 1987; Vahrenkamp et al., 1994; Gill et al., 1995; Zhao and Jones, 2012), dolomite precipitation rates (Vahrenkamp et al., 1994), and phosphoric acid fractionation (Aharon et al., 1977; Land and Moore, 1980). The role of non-stoichiometry on $\delta^{18}O$ values is evident in many Cenozoic dolostones. As yet, however, no agreement has been reached on the rate at which the $\delta^{18}O$ changes relative to the %Ca of the dolomite. Proposed values per 1% increase in the %Ca include -0.1‰ (the Bahamas; Vahrenkamp et al., 1994), -0.33‰ (St. Croix; Gill et al., 1995), -0.2‰ (Niue; Wheeler et al., 1999), -0.15‰ (Kita-daito-jima; Suzuki

et al., 2006), and -0.26‰ (Cayman Brac; Zhao and Jones, 2012). Budd (1997) suggested that the correction proposed by Vahrenkamp et al. (1994), of about -0.1‰, was probably the most realistic.

Data from the dolomites in the Cayman Formation examined in this study gives rise to the following values for the rate of change between $\delta^{18}O$ and %Ca:

(1) -0.34‰ – based on all dolomite samples, irrespective of their %Ca (Fig. 2.20A).

(2) -0.15‰ – based on dolomite samples with >90%LCD (Fig. 2.20C).

(3) -0.19‰ – based on dolomite samples with >90%HCD (Fig. 2.20D).

The low correlations between the $\delta^{18}O$ and average %Ca in the above three plots (r^2 = 0.40, 0.03, 0.60, respectively) indicate that factors (e.g., dolomitizing fluid, reaction rate) other than non-stoichiometry have affected the oxygen isotopes (cf., Vahrenkamp et al., 1994; Wheeler et al., 1999). The rate based on the plot of all dolomites (0.34‰) is much higher than those suggested for many other island dolostones. This higher $\delta^{18}O_{dol}$–%Ca rate can probably be attributed to the dolomitizing fluid rather than stoichiometry. As noted previously (Figs. 13-16), most HCD-dominated samples come from the island interior whereas LCD-dominated samples came from the periphery. The $\delta^{18}O$ values of the dolomitizing fluid probably varied in different areas and this would have affected the $\delta^{18}O$ of the dolomites and thus exaggerated the slope of the regression line between $\delta^{18}O$ and %Ca.

The stratigraphic trend of the oxygen isotopes also shows that dolomite stoichiometry had less influence than other factors. Dolostones in the upper part of many wells commonly have lower $\delta^{18}O$ values than those at the base (Fig. 2.21). In every well, the increase in $\delta^{18}O$ with depth (Fig. 2.21), which is independent of the %Ca, may indicate that (1) the influence of %Ca on the $\delta^{18}O$ is not as significant as previously suggested (e.g., Vahrenkamp et al., 1994; Zhao and Jones; 2012), (2) post-dolomitization diagenesis of the dolostones may have modified their isotopes, (3) dolostones at depth may have formed during sea-level lowstands when seawater was probably more enriched with ^{18}O than during the highstands (cf., Chappell and Shackleton, 1986), and/or (4) the dolomite pore-water temperature is lower at

depth than at the surface and there is a gradual decreasing of the temperature with depth.

Given that there are still uncertainties over the non-stoichiometric effect on dolomite $\delta^{18}O$ values, as well as the phosphoric acid fractionation factor (Land and Moore, 1980; Rosenbaum and Sheppard, 1986; Vahrenkamp et al., 1994; Zhao and Jones, 2012), the raw $\delta^{18}O$ data derived from the Cayman dolomites were not corrected for these two factors.

Equation (1), developed by Land (1985), can be used to estimate the $\delta^{18}O$ of the dolomitizing fluid:

$$\delta^{18}O_{dolomite} - \delta^{18}O_{water} = 1000 \ln\alpha_{(dolomite\text{-}water)} = 2.78*(10^6 T^{-2}) + 0.91 \quad (1)$$

The $\delta^{18}O_{dolomite}$ and $\delta^{18}O_{water}$ are in SMOW, and T is in Kelvin.

Herein, calculations of the paleo-temperature during dolomitization were based on (1) an average annual surface ocean water T around Cayman today of ~ 28 °C (capeweather.com), (2) the assumption that there was no significant difference in the sea surface T during phases I and II dolomitization (cf., O'Brien et al., 2014), (3) the average T gradient for groundwater was about -2.5 °C /100 m below 10 m bsl, and -2 °C /10 m from sea level to 10 m bsl, as it is today (Fig. 2.25D), (4) groundwater T, at any given depth, being ~ 1.5 °C lower in the interior than the periphery of the island (Fig. 2.25D), and (5) during phase I dolomitization, sea level rose from at least -40 m below to ~15 m above present sea level, and during Phase II dolomitization, sea level rose from -40 m to at least 12.5 m above present sea level (Jones and Luth, 2003b). Accordingly, dolomitization of the peripheral dolostones at 4 m asl to 94 m bsl interval involved fluid with T of 24-28 °C; the transitional dolostone at 3 m asl to 77 m bsl in wells HRQ-3 and CKC-1 at T of 22.5-26.5 °C; the interior dolostone at 3 m asl to 52 m bsl in HRQ-1 and HRQ-2 at T of 23.2-24.5 °C; and the interior limestone 52-124 m bsl in wells HRQ-1 and HRQ-2 at T of 21.5-24.5 °C. These temperatures were used to calculate the $\delta^{18}O$ of the dolomitizing fluids ($\delta^{18}O_{water}$) that mediated the four different types of dolomites (Fig. 2.26).

Peripheral dolostone – The calculated $\delta^{18}O_{water}$ is 1.3 to 3.9‰$_{SMOW}$ using a $\delta^{18}O_{dol}$ range of 3.62 ± 0.85‰$_{VPDB}$ and T range of 24-28 °C. The $\delta^{18}O_{water}$ calculated from the average

$\delta^{18}O_{dol}$ (3.62‰) and T (26 °C) is 2.6‰$_{SMOW}$.

Transitional dolostone – The $\delta^{18}O_{water}$ is 0.4 to 3.1‰$_{SMOW}$ using a $\delta^{18}O_{dol}$ range of 3.10 ± 0.88‰$_{VPDB}$ and T of 22.5-26.5 °C. The $\delta^{18}O_{water}$ calculated with the average $\delta^{18}O_{dol}$ (2.76‰) and T (24.5 °C) is 1.7‰$_{SMOW}$.

Interior dolostone – The $\delta^{18}O_{water}$ is 0.2 to 1.6‰$_{SMOW}$ using a $\delta^{18}O_{dol}$ range of 2.37 ± 0.55‰$_{VPDB}$ and T of 23.2-24.5 °C. The $\delta^{18}O_{water}$ calculated with the average $\delta^{18}O_{dol}$ (2.37‰) and T (23.9 °C) is 0.9‰$_{SMOW}$.

Interior limestone – The $\delta^{18}O_{water}$ is -0.97‰ to1.80‰$_{SMOW}$ using a $\delta^{18}O_{dol}$ range 2.10 ± 1.03‰$_{VPDB}$ and T of 21.5-24.5 °C. The $\delta^{18}O_{water}$ calculated with the average $\delta^{18}O$ (2.1‰) and T (23 °C) is 0.42‰$_{SMOW}$.

The highest $\delta^{18}O_{water}$ value (2.6‰$_{SMOW}$), associated with the peripheral dolostone, supports the notion that seawater mediated pervasive dolomitization in the peripheral part of the island given that the average $\delta^{18}O$ of seawater around Grand Cayman today is 1.06‰, and that seawater $\delta^{18}O$ values were probably 0.3-0.8‰ higher during the early Pliocene

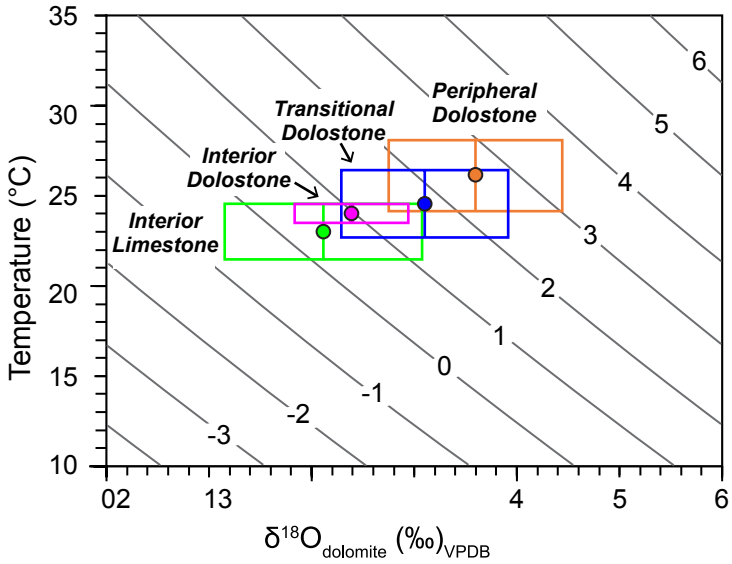

Fig. 2.26. Interpretation of $\delta^{18}O_{water}$ that mediated dolomitization of peripheral dolostones, transitional dolostones, interior dolostones, and dolomites in interior limestone in Cayman Formation. For each type of dolostone (dolomites), the box represent mean value ± 1σ, the midline represents the mean value of $\delta^{18}O_{dol}$, and the solid dot represents the calculated $\delta^{18}O_{water}$ using mean $\delta^{18}O_{dol}$ and temperature.

(Medina-Elizalde et al., 2008) and Pleistocene (Wheeler et al., 1999). The higher calculated $\delta^{18}O_{water}$ value is probably related to (1) the calculation method—the high $\delta^{18}O_{water}$ values were calculated using the high $\delta^{18}O_{dol}$ and T (Fig. 2.26), whereas in reality a large $\delta^{18}O_{dol}$ should be more likely produced at depth with a lower T (Fig. 2.21), (2) slight evaporation of the seawater, or (3) glacio-eustatic lowstands when seawater was enriched with ^{18}O (cf., Wheeler et al., 1999).

The lowest $\delta^{18}O_{dol}$ and calculated $\delta^{18}O_{water}$ of the dolomites in the interior limestone indicates that the dolomitizing fluid was more enriched with ^{18}O than seawater. The oxygen isotope composition of the dolomitizing fluid may have been derived from seawater, meteoric water, or from dissolution of the precursor carbonate. If the present-day $\delta^{18}O$ values of seawater around Grand Cayman ($1.06‰_{SMOW}$) and freshwater from the East End Lens ($-4.83‰_{SMOW}$; Ng, 1990) are utilized, the calculated $\delta^{18}O_{water}$ values of the fluid that mediated partial dolomitization of the limestones corresponds to a mixture of seawater with < 34% freshwater; and if the mean average of $\delta^{18}O_{water}$ (0.42‰) is used, a mixture of 11% freshwater with seawater is indicated. This degree of mixing suggests that dolomitization in the island interior may have taken place in the lower mixing to upper saline zone, which is probably the strongest circulation zone in the marine phreatic zone (cf., Kaufman, 1994; Whitaker et al., 2004).

Today, the $\delta^{18}O_{water}$ values of the saline groundwater from the interior wells are lower than those from the coastal wells (Fig. 2.25C). There is no correlation between the $\delta^{18}O_{water}$ and the chloride concentration or the rock type in which it resides. This indicates that the low $\delta^{18}O$ of saline water was not introduced by meteoric water or caused by water-rock reaction. It is difficult, however, to determine the $\delta^{18}O_{water}$ of saline groundwater when dolomitization of the central limestone took place. If the situation was like it is today, the $\delta^{18}O_{water}$ would have been ~ 0.85‰. If so, the fluid that mediated dolomitization may have been modified seawater with depleted ^{18}O rather than mixed seawater and meteoric water. The low $\delta^{18}O_{water}$ of the saline groundwater in the island interior may have been

generated by the dolomitization process itself because the heavy oxygen would have been preferentially consumed. At the island-wide scale, the $\delta^{18}O_{water}$ of the pore fluid was almost certainly continually evolving because of rock-water reaction along the flow path from shelf edge to center of the island. This may also explain the decreasing trend of $\delta^{18}O_{water}$ of the dolomitizing fluids that led to the formation of the peripheral dolostone, to the transitional dolostone, the interior dolostone and to dolomites in the interior dolostone (Fig. 2.26).

The differences in the $\delta^{18}O$ of coexisting dolomite and calcite ($\Delta^{18}O_{dol\text{-}cal} = \delta^{18}O_{dol} - \delta^{18}O_{pres\text{-}cal} = 1.75 \pm 0.65‰$; Fig. 2.22A) are far less than the fractionation $\Delta^{18}O_{dol\text{-}cal}$ that many authors have suggested (e.g., 3.8 ‰ of Land, 1991; 3‰ of Fouke, 1994; 3-5‰ of Budd, 1997). Limestones in the island interior have undergone various diagenetic modifications in meteoric settings since the last phase of pervasive dolomitization, which resulted in the reduced $\delta^{18}O_{pres\text{-}cal}$ values of the present-day calcium carbonate compared with the original sediments ($\delta^{18}O_{orig\text{-}cal}$) (Ren and Jones, 2016). If this is taken into consideration, the true $\Delta^{18}O_{dol\text{-}cal}$ between the dolomites and their precursor carbonate ($=\delta^{18}O_{dol} - \delta^{18}O_{orig\text{-}cal}$) would be lower than 1.75‰ and much lower than the theoretical value of 3-4‰. The low $\Delta^{18}O_{dol\text{-}cal}$ was caused, most likely, by the decreasing of $^{18}O_{dol}$. This supports the notion that the dolomites that coexist with calcite (dolomite in the interior island) were formed from fluids that were, relative to seawater, depleted with respect to ^{18}O.

Interpretations of the properties of the dolomitizing fluids based on the oxygen isotopes are consistent with those derived from the carbon isotopes. Together with variations in dolomite stoichiometry, the oxygen and carbon isotope data indicate that the (1) compositions of the dolomitizing fluids varied from the margin to the center of the island, (2) dolomitization in the peripheral areas was mediated by seawater that may have been slightly evaporated, (3) seawater gradually lost its ^{18}O as it migrated towards to the island center due to the water-rock reaction (i.e., dolomitization), (4) fluids that mediated dolomite formation in the interior limestones were probably a mixture of seawater that had been modified by dolomitization, and meteoric water, and (5) dissolution of the precursor carbonate may have

also influenced the isotopic compositions of the dolomites.

As Budd (1997) pointed out, isotopic values determined from bulk-rock samples must represent an average of numerous populations of dolomite. Thus, the interpretations provided here address the general conditions of dolomitization, but cannot be specific to each generation of dolomite.

6. Discussion

Dolostones in the Cayman Formation on Grand Cayman provide an opportunity for assessing the origin of thick dolostone successions. Island dolostones like these, found on many Caribbean islands and Pacific atolls (see Budd, 1997), have attributed to many different formational models (e.g., Tucker and Wright, 1990; their Fig. 8.31), including ocean current pumping (Saller, 1984; Wheeler et al., 1999), seepage reflux (Deffeyes, 1965; Ohde and Elderfield, 1992; Lucia and Major, 1994; Gill et al., 1995), tidal pumping (Carballo et al., 1987), and Kohout convection (Aharon et al., 1987; Machel, 2000). Most of these interpretations are based largely on the large-scale geometry of the dolostone bodies, stratigraphic relationships between the coeval dolostones and limestones, and the petrographic and geochemical attributes of the dolomite (e.g., Hardie, 1987; Wilson et al., 1990; Braithwaite, 1991; Budd, 1997; Warren, 2000).

Natural dolomite, like that in the Cayman Formation on the Cayman Islands, is a compositional series with variable Mg and Ca ratios (e.g., Jones and Luth, 2002). Although deemed “important” by Land (1985), these stoichiometric variations are usually not integrated into most dolomitization models. Dolostones of all ages are commonly Ca-rich with many containing two or more populations of dolomite with different %Ca. Three populations are present in the Miocene-Pliocene dolostones from Niue Island (Wheeler et al., 1999) and four populations have been identified in the dolostones from Kita-daito-jima (Suzuki et al., 2006). On the Cayman Islands, Oligocene-Pliocene dolostones are formed of LCD and/or HCD (Jones and Luth, 2002). Likewise, Ca-rich non-stoichiometric dolostones

with more than one population of dolomite are also common among ancient dolostones, including those from North America that were documented by Lumsden and Chimahusky (1980) and Sperber et al. (1984). Such examples suggest that heterogeneous dolomites are universal and have been present throughout geologic history. This is a critical issue because many other geochemical attributes (e.g., stable isotopes) are known to vary in accord with the %Ca of the dolomite (e.g., Vahrenkamp et al., 1991, 1994).

Many field (Lumsden and Chimahusky, 1980; Sass and Bein, 1988) and laboratory (Goldsmith and Graf, 1958; Katz and Matthews, 1977; Sibley et al., 1987, 1994; Sibley, 1990; Nordeng and Sibley, 1994; Kaczmarek and Sibley, 2011, 2014) studies have shown that dolomite stoichiometry is an important indicator of the chemical properties of their formative solutions. Folk and Land (1975) argued that the formation of (near)-stoichiometric dolomites is generally associated with solutions that have high salinities and high Mg/Ca ratios. Similarly, various experiments have also demonstrated that both the composition of the synthesized dolomite and the rate of replacement are highly dependent on the Mg/Ca in the formative solutions (e.g., Kaczmarek and Sibley, 2011).

On Grand Cayman, the overall trend of increasing volumes of HCD and decreasing volumes of LCD towards the island centre suggests that variations in dolomite stoichiometry were related to the landward migration of the seawater that mediated dolomitization (Fig. 2.27). With this model, there was a progressive loss of Mg and hence a decrease in the Mg/Ca ratio as the seawater moved inland. Accordingly, while seawater mediated LCD formation in the coastal areas, HCD was formed in the transitional zone, and dolomitization did not take place in the central part of the island. This pattern indicates that the chemical composition of the pore fluids was continually evolving along its flow path due to the rock-water interaction (Fig. 2.27). This is comparable with the present-day hydrochemistry whereby a progressive landward decrease in the Mg/Ca ratio of the saline water is evident (Fig. 2.22).

The lateral extent of dolomitization in the Cayman Formation on Grand Cayman was

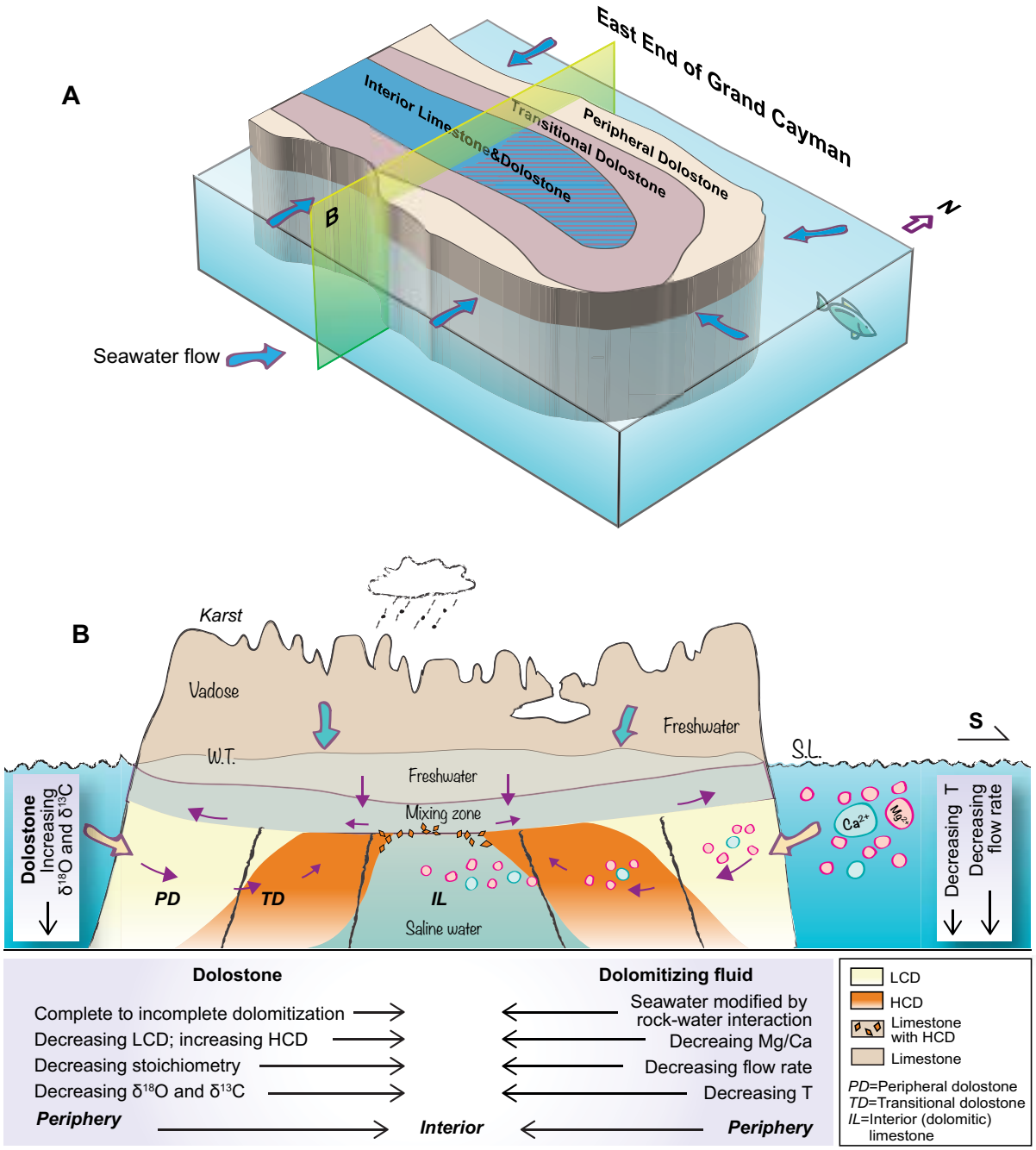

Fig. 2.27. Schematic diagram of the dolomitization model on Grand Cayman. (A) 3-D view of Cayman Formation on the east end of the island showing the concentric zones of dolostones and limestones which indicate that seawater flowed from all directions into the island during the dolomitization. (B) A N-S profile showing the spatial variations in many attributes of dolostones and a variety of dolomitizing conditions from the periphery to the interior of the island.

controlled largely by fluxes in the Mg supply. The fact that dolomitization was mediated by laterally derived seawater excludes the seepage reflux and thermal convection models as viable mechanisms for seawater circulation through the island. Sea level lowstands before each phase of dolomitization on Grand Cayman, meant that the island was subaerially exposed. Jones and Luth (2003b) argued that karst development during these lowstands led to increased porosity and permeability in the bedrock that would, during the next transgressive phase, have enhanced groundwater circulation throughout the island. The submixing-zone circulation model was proposed as the driving mechanism for dolomitization in Barbados (Machel et al., 1990) and the Bahamas (Vahrenkamp et al., 1991, 1994). Numerical simulation models for submixing-zone flow (Kaufman, 1994; Whitaker et al., 2004) also support this assessment.

Whitaker et al. (2004), using a model of carbonate island that was 4.5 km wide with a recharge of 0.5 m/year and a freshwater lens ~30 m thick (parameters akin to the eastern part of Grand Cayman), showed that the flow rate can be as high as 5×10^{-7} m/s in the coastal mixing zone. The flow and flux in the submixing-zone decreases landwards and downwards from the mixing zone (e.g., Kaufman, 1994; Whitaker et al., 2004). As illustrated in the model developed by Whitaker et al. (2004, their Fig. 10), the flow draws in seawater over a zone that extends to ~ 1 km offshore of their 4.5 km wide model island. The reduced flow rate and restricted flux of submixing-zone flow are probably important constraints on the supply of Mg to the island interior and may account for the lack of dolomitization in that part of the island. Moreover, dolomite cements and cavity-filling sediments that are common in the peripheral dolostones (Ren and Jones, 2016) may also have reduced pore connectivity and reduced groundwater circulation that, in turn, curtailed the Mg supply.

The fact that the different dolostone zones are concentrically arranged on Grand Cayman supports the notion that seawater flowed into the island from all directions during dolomitization (Fig. 2.27). The rate and volume of flow may have varied from coast to coast in accord with local factors such as permeability in the bedrock carbonates, precipitation,

climate, oceanographic currents, sea level fluctuations, platform geometry, and/or geography. Thus, the lateral extent of dolostone relative to the bordering coastline may indicate local variability in the lateral penetration of the dolomitizing fluids. On Grand Cayman, for example, the dolostones and the peripheral dolostone zone extend further inland from the northeast corner than from any other direction (Fig. 2.6). This suggests that the highest flux, and/or flow rate of seawater came from the northeast. This may be related to the permeability patterns in the bedrock, different topographic features, and/or a dominant paleowind direction from the northeast.

The dolomitization model developed for the dolostones on Grand Cayman may be applicable to Cenozoic dolostones found on other islands throughout the world. Like the Grand Cayman dolostones, the stoichiometric and geochemical attributes of the island dolostones can be used as indicators of the fluid flow directions and the source of Mg. Some caution must be used when applying this model to the interpretation of ancient dolostones, which may have experienced more than one phase of dolomitization/diagenetic modification with each phase involving a different source for the reactants and different flow patterns.

The non-stoichiometric signature of the dolostones from Grand Cayman, as with many Cenozoic dolostones, means that they are susceptible to further diagenetic modifications. When exposed to aggressive fluids such as meteoric water, the preferential dissolution of HCD can lead to the development of hollow dolomite crystals (James et al., 1993; Jones and Luth, 2003a; Swart et al., 2005), which may be further modified to inside-out dolomites (Jones, 2007). These processes could modify the quantity of dolostones as reservoir rocks by creating or occluding porosities. When buried, recrystallization of both dolomites is very likely to happen with time, resulting in an increase in the Mg/Ca ratio and cation ordering (McKenzie, 1981; Nordeng and Sibley, 1994; Malone et al., 1996; Machel, 1997; Kaczmarek and Sibley, 2014). Whether early meteoric or late burial diagenesis, modifications of dolomites can significantly change their geochemistry (e.g., Land, 1980; Land, 1985).

7. Conclusions

A network of wells drilled on the east end of Grand Cayman allowed assessment of the spatial variations in many aspects of the subsurface dolostones. Dolomites on the island are calcium-rich and composed of LCD and HCD. The geographic variations in the attributes of the dolostones, particularly with respect to the LCD and HCD and the oxygen and carbon values, provide a unique perspective on the origin of dolostone. Analysis of Cayman dolostones has led to the following conclusions:

The Miocene Cayman Formation is incompletely dolomitized with the peripheral zone being completely dolomitized whereas limestones are still present in the island interior.

Based on the distribution of LCD and HCD, the Cayman Formation is divided into the peripheral dolostone zone, the transitional dolostone zone, and the interior limestone/ dolostone zone. These concentrically arranged zones differ in their LCD/HCD compositions, petrographic attributes, and geochemical signatures.

Seawater provided the Mg needed for dolomitization of the Cayman Formation. Geographic variations in these dolostones reflect modifications of seawater chemistry caused by rock-water interaction as the dolomitizing fluids moved towards the island centre.

The Cayman Formation experienced two major phases of dolomitization as suggested by $^{87}Sr/^{86}Sr$ of the dolomites; the first during the late Miocene–early Pliocene, and the second during the late Pliocene. Dolomitization probably took place in the submixing zone where seawater was pumped into the island from all directions.

The Mg/Ca in the dolomites is an important proxy that could be applied in the interpreting the origin and the flow directions of dolomitizing fluid. As such it is a practical demonstration of the concept argued by Kaczmarek and Sibley (2011) on the basis of their experimental work.

The model developed from dolostones on Grand Cayman is probably applicable to island dolostones throughout the world.

References

Aharon, P., Kolodny, Y., Sass, E., 1977. Recent hot brine dolomitization in the "Solar Lake", Gulf of Elat, isotopic, chemical, and mineralogical study. Journal of Geology 85, 27-48.

Aharon, P., Socki, R.A., Chan, L., 1987. Dolomitization of atolls by sea water convection flow: test of a hypothesis at Niue, South Pacific. Journal of Geology 95, 187-203.

Blake, D.F., Peacor, D.R., Wilkinson, B.H., 1982. The sequence and mechanism of low-temperature dolomite formation: calcian dolomites in a Pennsylvanian echinoderm. Journal of Sedimentary Research 52, 59-70.

Blanchon, P., Jones, B., 1995. Marine-planation terraces on the shelf around Grand Cayman: a result of stepped Holocene sea-level rise. Journal of Coastal Research 11, 1-33.

Braithwaite, C.J.R., 1991. Dolomites, a review of origins, geometry and textures. Earth and Environmental Science Transactions of the Royal Society of Edinburgh 82, 99-112.

Budd, D.A., 1997. Cenozoic dolomites of carbonate islands: their attributes and origin. Earth-Science Reviews 42, 1-47.

Carballo, J.D., Land, L.S., Miser, D.E., 1987. Holocene dolomitization of supratidal sediments by active tidal pumping, Sugarloaf Key, Florida. Journal of Sedimentary Petrology 57, 153-165.

Chai, L., Navrotsky, A., Reeder, R.J., 1995. Energetics of calcium-rich dolomite. Geochimica et Cosmochimica Acta 59, 939-944.

Chappell, J., Shackleton, N.J., 1986. Oxygen isotopes and sea level. Nature 324, 137-140.

Dawans, J.M., Swart, P.K., 1988. Textural and geochemical alternations in Late Cenozoic Bahamian dolomites. Sedimentology 35, 385-403.

Deffeyes, K.S., 1965. Dolomitization of recent and Plio-Pleistocene sediments by marine evaporite waters on Bonaire Netherlands Antilles. In: Pray, L.C., Murray, R.C. (Eds.), Dolomitization and Limestone Diagenesis. SEPM Special Publication 13, pp. 71-88.

Der, A., 2012. Deposition and sea level fluctuation during Miocene times, Grand Cayman, British West Indies. Unpublished M.Sc. thesis, University of Alberta, 101 pp.

Drits, V.A., McCarty, D.K., Sakharov, B., Milliken, K.L., 2005. New insight into structural and compositional variability in some ancient excess-Ca dolomite. Canadian Mineralogist 43, 1255-1290.

Folk, R.L., Land, L.S., 1975. Mg/Ca ratio and salinity: two controls over crystallization of dolomite. American Association of Petroleum Geologists Bulletin 59, 60-68.

Folkman, Y., 1969. Diagenetic dedolomitization in the Albian-Cenomanian Yagur Dolomite on Mount Carmel (northern Israel). Journal of Sedimentary Research 39, 380-385.

Fouke, B.W., 1994. Deposition, diagenesis and dolomitization of Neogene Seroe Domi Formation coral reef limestones on Curaqao, Netherlands Antilles. Natuurwetenschappelijke Studiekring voor het Caraibisch Gebied, Amsterdam, 182 pp.

Gill, I.P., Moore Jr, C.H., Aharon, P., 1995. Evaporitic mixed-water dolomitization on St. Croix, U.S.V.I.. Journal of Sedimentary Research 65, 591-604.

Glover, E.D., Sippel, R.F., 1967. Synthesis of magnesium calcites. Geochimica et Cosmochimica Acta 31, 603-613.

Goldsmith, J.R., Graf, D.L., 1958. Relation between lattice constants and composition of the Ca-My carbonates. American Mineralogist 43, 84-101.

Gregg, J.M., Bish, D.L., Kaczmarek, S.E., Machel, H.G., 2015. Mineralogy, nucleation and growth of dolomite in the laboratory and sedimentary environment: A review. Sedimentology 62, 1749-1769.

Hardie, L.A., 1987. Dolomitization: a critical view of some current views. Journal of Sedimentary Research 57, 166-183.

James, N.P., Bone, Y., Kyser, T.K., 1993. Shallow burial dolomitization and dedolomitization of Mid-Cenozoic, cool-water, calcitic, deep-self limestones, southern Australia. Journal of Sedimentary Research 63, 528-538.

Jones, B., 1989. Syntaxial overgrowths on dolomite crystals in the Bluff Formation, Grand Cayman, British West Indies. Journal of Sedimentary Petrology 59, 839-847.

Jones, B., 2005. Dolomite crystal architecture: genetic implications for the origin of the

Tertiary dolostones of the Cayman Islands. Journal of Sedimentary Research 75, 177-189.

Jones, B., 2007. Inside-out dolomite. Journal of Sedimentary Research 77, 539-551.

Jones, B., 2013. Microarchitecture of dolomite crystals as revealed by subtle variations in solubility: Implications for dolomitization. Sedimentary Geology 288, 66-80.

Jones, B., Hunter, I.G., 1994. Messinian (late Miocene) karst on Grand Cayman, British West Indies; an example of an erosional sequence boundary. Journal of Sedimentary Research 64, 531-541.

Jones, B., Hunter, I., Kyser, K., 1994a. Revised stratigraphic nomenclature for Tertiary strata of the Cayman Islands, British West Indies. Caribbean Journal of Science 30, 53-68.

Jones, B., Hunter, I.G., Kyser, T.K., 1994b. Stratigraphy of the Bluff Formation (Miocene-Pliocene) and the newly defined Brac Formation (Oligocene), Cayman Brac, British West Indies. Caribbean Journal of Science 30, 30-51.

Jones, B., Luth, R.W., 2002. Dolostones from Grand Cayman, British West Indies. Journal of Sedimentary Research 72, 559-569.

Jones, B., Luth, R.W., 2003a. Petrography of finely crystalline Cenozoic dolostones as revealed by backscatter electron imaging: Case study of the Cayman Formation (Miocene), Grand Cayman, British West Indies. Journal of Sedimentary Research 73, 1022-1035.

Jones, B., Luth, R.W., 2003b. Temporal evolution of Tertiary dolostones on Grand Cayman as determined by $^{87}Sr/^{86}Sr$. Journal of Sedimentary Research 73, 187-205.

Jones, B., Luth, R.W., MacNeil, A.J., 2001. Powder X-ray diffraction analysis of homogeneous and heterogeneous sedimentary dolostones. Journal of Sedimentary Research 71, 790-799.

Kaczmarek, S.E., Sibley, D.F., 2011. On the evolution of dolomite stoichiometry and cation order during high-temperature synthesis experiments: an alternative model for the geochemical evolution of natural dolomites. Sedimentary Geology 240, 30-40.

Kaczmarek, S.E., Sibley, D.F., 2014. Direct physical evidence of dolomite recrystallization. Sedimentology 61, 1862-1882.

Katz, A., Matthews, A., 1977. The dolomitization of $CaCO_3$: an experimental study at 252-295 °C. Geochimica et Cosmochimica Acta 41, 297-308.

Kaufman, J., 1994. Numerical models of fluid flow in carbonate platforms: implications for dolomitization. Journal of Sedimentary Research 64, 128-139.

Land, L.S., 1985. The origin of massive dolomite. Journal of Geological Education 33, 112-125.

Land, L.S., 1991. Dolomitization of the Hope Gate Formation (north Jamaica) by seawater: reassessment of mixing-zone dolomite. In: Taylor, H.P., O'Neil, J.R., Kaplan, I.R. (Eds.), Stable Isotope Geochemistry: A Tribute to Samuel Epstein. Geochemical Society, Special Publication 3, pp. 121-130.

Land, L.S. 1992. The dolomite problem: stable and radiogenic isotope clues. In: Clauer, N., Chaudhuri, S. (Eds.), Isotopic Signatures and Sedimentary Records. Springer, Berlin, Heidelberg, pp. 49-68.

Land, L.S., Moore, C.H., 1980. Lithification, micritization and syndepositional diagenesis of biolithites on the Jamaican island slope. Journal of Sedimentary Research 50, 357-369.

Liang, T., Jones, B., 2014. Deciphering the impact of sea-level changes and tectonic movement on erosional sequence boundaries in carbonate successions: A case study from Tertiary strata on Grand Cayman and Cayman Brac, British West Indies. Sedimentary Geology 305, 17-34.

Lucia, F.J., Major, R.P., 1994. Porosity evolution through hypersaline reflux dolomitization. In: Purser, B.H., Tucker, M.E., Zenger, D.L. (Eds.), Dolomites: A Volume in Honour of Dolomieu. International Association of Sedimentologists Special Publication 21, pp. 325-341.

Lumsden, D.N., Chimahusky, J.S., 1980. Relationship between dolomite nonstoichiometry and carbonate facies parameters. In: Zenger, D.H., Dunham, J.B., Ethington, R.L. (Eds.),

Concepts and Models of Dolomitization. SEPM Special Publication 28, pp.123-137.

Machel, H.G., 1997. Recrystallization versus neomorphism, and the concept of 'significant recrystallization' in dolomite research. Sedimentary Geology 113, 161-168.

Machel, H.G., 2000. Dolomite formation in Caribbean Islands: driven by plate tectonics?! Journal of Sedimentary Research 70, 977-984.

Machel, H.G., 2004. Concepts and models of dolomitization: a critical reappraisal. In: Braithwaite, C.J.R., Rizzi, G., Darke, G. (Eds.), The Geometry and Petrogenesis of Dolomite Hydrocarbon Reservoirs. Geological Society of London Special Publication 235, pp. 7-63.

Machel, H.G., Mountjoy, E.W., Humphrey, J.D., Quinn, T.M., 1990. Coastal mixing zone dolomite, forward modeling, and massive dolomitization of platform-margin carbonates: discussion and reply. Journal of Sedimentary Research 60, 1008-1016.

MacNeil, A., Jones, B., 2003. Dolomitization of the Pedro Castle Formation (Pliocene), Cayman Brac, British West Indies. Sedimentary Geology 162, 219-238.

Malone, M.J., Baker, P.A., Burns, S.J., 1996. Recrystallization of dolomite: an experimental study from 50-200 °C. Geochimica et Cosmochimica Acta 60, 2189-2207.

Mather, J.D., 1971. A preliminary survey of the groundwater resources of the Cayman Islands with recommendations for their development. Institute of Geological Sciences, London, 91 pp.

McArthur, J.M., Howarth, R.J., Bailey, T.R., 2001. Strontium isotope stratigraphy: LOWESS Version 3: best fit to the marine Sr-isotope curve for 0–509 Ma and accompanying look-up table for deriving numerical age. Journal of Geology 109, 155–170.

McKenzie, J.A., 1981. Holocene dolomitization of calcium carbonate sediments from the coastal sabkhas of Abu Dhabi, U.A.E.: a stable isotope study. Journal of Geology 89, 185-198.

Medina-Elizalde, M., Lea, D.W., Fantle, M.S., 2008. Implications of seawater Mg/Ca variability for Plio-Pleistocene tropical climate reconstruction. Earth and Planetary

Science Letters 269, 585-595.

Ng, K.C., 1990. Diagenesis of the Oligocene-Miocene Bluff Formation of the Cayman Islands - A petrographic and hydrogeochemical approach. Unpublished PhD thesis, University of Alberta, 344 pp.

Ng, K.C., Jones, B., 1995. Hydrogeochemistry of Grand Cayman, British West Indies: implications for carbonate diagenetic studies. Journal of Hydrology 164, 193-216.

Ng, K.C., Jones, B., Beswick, R., 1992. Hydrogeology of Grand Cayman, British West Indies: a karstic dolostone aquifer. Journal of Hydrology 134, 273-295.

Nordeng, S.H., Sibley, D.F., 1994. Dolomite stoichiometry and Ostwald's step rule. Geochimica et Cosmochimica Acta 58, 191-196.

O'Brien, C.L., Foster, G.L., Martinez-Boti, M.A., Abell, R., Rae, J.W.B., Pancost, R.D., 2014. High sea surface temperatures in tropical warm pools during the Pliocene. Nature Geoscience 7, 606-611.

Ohde, S., Elderfield, H., 1992. Strontium isotope stratigraphy of Kita-daito-jima Atoll, North Philippine Sea: implications for Neogene sea-level change and tectonic history. Earth and Planetary Science Letters 113, 473-486.

Pleydell, S.M., Jones, B., Longstaffe, F.J., Baadsgaard, H., 1990. Dolomitization of the Oligocene-Miocene Bluff Formation on Grand Cayman, British West Indies. Canadian Journal of Earth Sciences 27, 1098-1110.

Reeder, R.J., 1981. Electron optical investigation of sedimentary dolomites. Contributions to Mineralogy and Petrology 76, 148-157.

Reeder, R.J. 1991. An overview of zoning in carbonate minerals. In: Barker, C.E., Burruss, R.C., Kopp, O.C., Machel, H.G., Marshall, D.J., Wright, P., Colbum, H.Y. (Eds.), Luminescence Microscopy and Spectroscopy: Qualitative and Quantitative Applications. SEPM Special Publication 25, pp. 77-82.

Ren, M., Jones, B., 2016. Diagenesis in limestone-dolostone successions after 1 million years of rapid sea-level fluctuations: A case study from Grand Cayman, British West Indies.

Sedimentary Geology 342, 15-30.

Roberts, H.H., 1994. Reefs and lagoons of Grand Cayman. In: Brunt, M.A., Davies, J.E. (Eds.), The Cayman Islands: Natural History and Biogeography. Springer, Netherlands, pp. 75-104.

Rosenbaum, J., Sheppard, S.M.F., 1986. An isotopic study of siderites, dolomites and ankerites at high temperatures. Geochimica et Cosmochimica Acta 50, 1147-1150.

Saller, A.H., 1984. Petrologic and geochemical constraints on the origin of subsurface dolomite, Enewetak Atoll: an example of dolomitization by normal seawater. Geology 12, 217-220.

Sass, E., Bein, A., 1988. Dolomites and salinity: a comparative geochemical study. In: Shukla, V., Baker, P.A. (Eds.), Sedimentology and Geochemistry of Dolostones. SEPM Special Publication 43, pp. 223-233.

Schmidt, V., 1965. Facies, diagenesis, and related reservoir properties in the Gigas Beds (Upper Jurassic), northwester Germany. In: Prey, L.C., Murray, R.C. (Eds.), Dolomitization and Limestone Diagenesis. SEPM Special Publication 13, pp. 124-169.

Searl, A., 1994. Discontinuous solid solution in Ca-rich dolomites: the evidence and implications for the interpretation of dolomite petrographic and geochemical data. In: Purser, B.H., Tucker, M.E., Zenger, D.L. (Eds.), Dolomites: A Volume in Honour of Dolomieu. International Association of Sedimentologists Special Publication 21, pp. 361-376.

Sibley, D.F., 1990. Unstable to stable transformations during dolomitization. Journal of Geology 98, 739-748.

Sibley, D.F., Dedoes, R.E., Bartlett, T.R., 1987. Kinetics of dolomitization. Geology 15, 1112-1114.

Sibley, D.F., Nordeng, S.H., Borkowski, M.L., 1994. Dolomitization kinetics of hydrothermal bombs and natural settings. Journal of Sedimentary Research 64, 630-637.

Sperber, C.M., Wilkinson, B.H., Peacor, D.R., 1984. Rock composition, dolomite

stoichiometry, and rock/water reactions in dolomitic carbonate rocks. Journal of Geology 92, 609-622.

Suzuki, Y., Iryu, Y., Inagaki, S., Yamada, T., Aizawa, S., Budd, D.A., 2006. Origin of atoll dolomites distinguished by geochemistry and crystal chemistry: Kita-daito-jima, northern Philippine Sea. Sedimentary Geology 183, 181-202.

Swart, P.K., Cantrell, D.L., Westphal, H., Handford, C.R., Kendall, C.G., 2005. Origin of dolomite in the Arab-D reservoir from the Ghawar Field, Saudi Arabia: evidence from petrographic and geochemical constraints. Journal of Sedimentary Research 75, 476-491.

Tucker, M.E., Wright, V.P. 1990. Carbonate Sedimentology. Blackwell Scientific Publications, Oxford, 482 pp.

Vahrenkamp, V.C., Swart, P.K., Purser, B., Tucker, M., Zenger, D., 1994. Late Cenozoic dolomites of the Bahamas: metastable analogues for the genesis of ancient platform dolomites. In: Purser, B.H.,Tucker, M.E., Zenger, D.L. (Eds.), Dolomites: A Volume in Honour of Dolomieu. International Association of Sedimentologists Special Publication 21, 133-153.

Vahrenkamp, V.C., Swart, P.K., Ruiz, J., 1991. Episodic dolomitization of late Cenozoic carbonates in the Bahamas: evidence from strontium isotopes. Journal of Sedimentary Research 61, 1002-1014.

Ward, W.C., Halley, R.B., 1985. Dolomitization in a mixing zone of near-seawater composition, late Pleistocene, northeastern Yucatan Peninsula. Journal of Sedimentary Research 55, 407-420.

Warren, J., 2000. Dolomite: occurrence, evolution and economically important associations. Earth-Science Reviews 52, 1-81.

Wheeler, C.W., Aharon, P., Ferrell, R.E., 1999. Successions of Late Cenozoic platform dolomites distinguished by texture, geochemistry, and crystal chemistry: Niue, South Pacific. Journal of Sedimentary Research 69, 239-255.

Whitaker, F.F., Smart, P.L., Jones, G.D., 2004. Dolomitization: from conceptual to numerical models. In: Braithwaite, C.J.R., Rizzi, G., Darke, G. (Eds.), The Geometry and Petrogenesis of Dolomite Hydrocarbon Reservoirs. Geological Society of London Special Publication 235, pp. 99-139.

Wilson, E.N., Hardie, L.A., Phillips, O.M., 1990. Dolomitization front geometry, fluid flow patterns, and the origin of massive dolomite: the Triassic Latemar buildup, northern Italy. American Journal of Science 290, 741-796.

Zhao, H., Jones, B., 2012. Origin of “island dolostones”: A case study from the Cayman Formation (Miocene), Cayman Brac, British West Indies. Sedimentary Geology 243-244, 191-206.

CHAPTER THREE

DIAGENESIS IN LIMESTONE-DOLOSTONE SUCCESSIONS OF THE CAYMAN FORMATION[1]

1. Introduction

Before burial, most marine carbonate sequences have undergone significant shallow marine and meteoric diagenetic changes. In younger rocks like those found in Holocene successions (Land and Goreau, 1970; Ginsberg et al., 1971; Schroeder, 1972; James et al., 1976; Buchbinder and Friedman, 1980; Lighty, 1985; Budd and Land, 1990) and Pliocene–Pleistocene successions (Steinen and Matthews, 1973; Buchbinder and Friedman, 1980; Aissaoui et al., 1986; Quinn and Matthews, 1990; Beach, 1995; Melim, 1996; Braithwaite and Camoin, 2011), diagenetic features have been linked to the rapid and high-amplitude changes in sea level that have been ongoing since the Pleistocene. Given that the positions of sea level, the water table, and the vadose zone are intimately linked (e.g., Longman, 1980; Quinn, 1991), the diagenetic fabrics in these rocks should reflect the changes caused by sea-level fluctuations. Accordingly, many sequences of diagenetic fabrics have been linked to sea-level oscillations (e.g., Aissaoui et al., 1986; Hardie et al., 1986; Quinn, 1991; Beach, 1995; Sherman et al., 1999) and models have been developed to show how diagenetic patterns develop in response to high-frequency glacio-eustatic sea-level cycles (Matthews and Frohlich, 1987; Whitaker et al., 1997). Such observations and models have been fundamental to the development of early diagenetic histories for carbonate successions of all ages. They are, however, predicated on the assumption the carbonate successions will contain a diagenetic record that fully reflects every diagenetic regime that it has experienced. But this is not always the case, as has been shown in studies from carbonate platforms such

---

1 This chapter was published as: Ren, M., Jones, B., 2016. Diagenesis in limestone-dolostone successions after 1 million years of rapid sea-level fluctuations: A case study from Grand Cayman, British West Indies. Sedimentary Geology 342, 15-30.

as Moruroa (Braithwaite and Camoin, 2011) and Bermuda (Vollbrecht and Meischner, 1996).

Isolated carbonates islands such as Grand Cayman, which are surrounded by deep oceanic waters, are highly sensitive to sea-level fluctuations. On the east end of Grand Cayman (Fig. 3.1), the carbonate bedrock is formed largely of the Miocene Cayman Formation (Fig. 3.2), which encompasses sediments that were deposited on an isolated bank (Jones and Hunter, 1989; Jones et al., 1994b). There, the central part of the island is formed largely of limestones whereas the bedrock in the coastal areas is formed entirely of dolostone (e.g., Jones et al., 1994b; Der, 2012). The fact that dolomitization took place prior to the

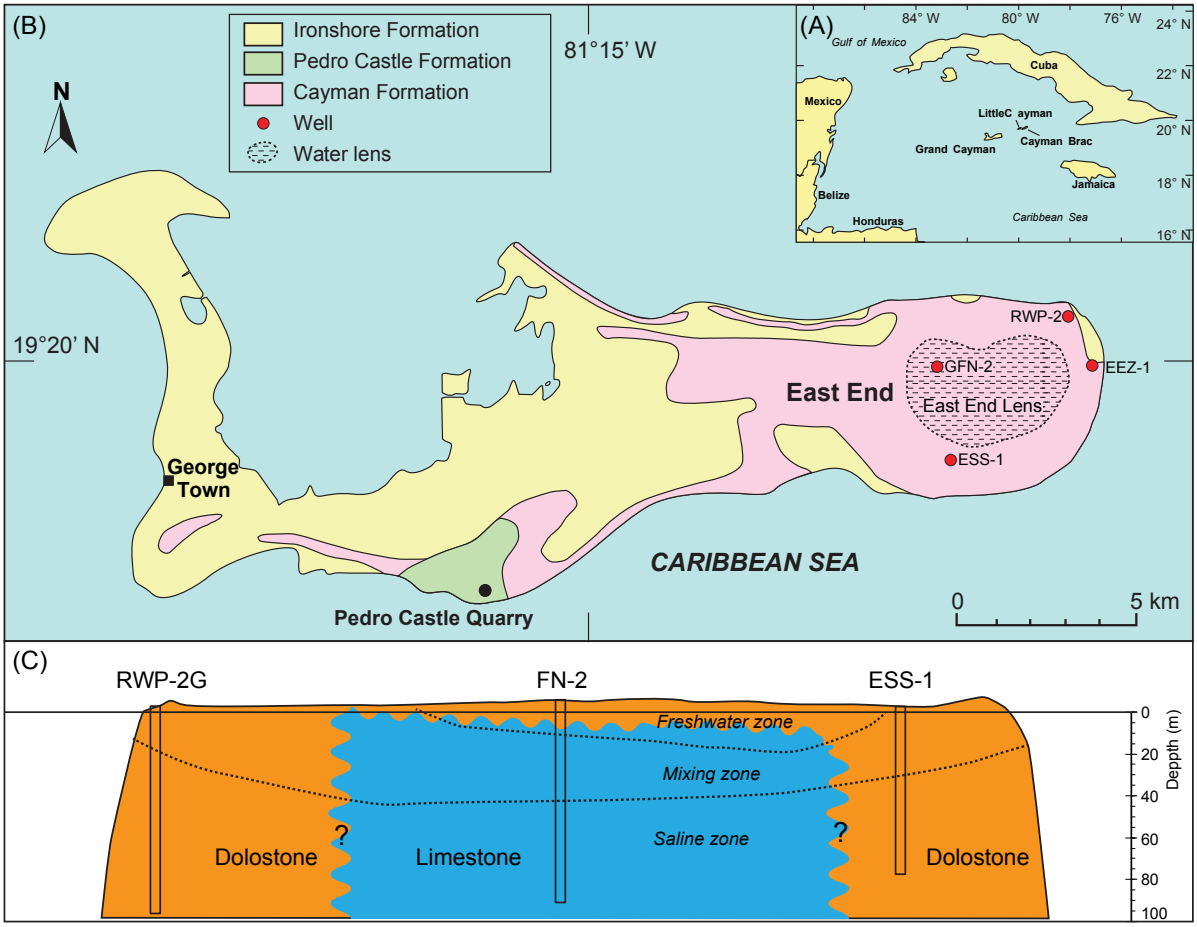

Fig. 3.1. Geological and hydrological settings of Grand Cayman. (A) Location of Grand Cayman. (B) Geological map of Grand Cayman (modified from Jones et al., 1994a) showing distribution of Cayman Formation, location of well GFN-2, and approximate distribution of East End Lens (EEL). Distribution of EEL modified from Ng et al. (1992). (C) Schematic diagrams illustrating the present hydrological zones, and the peripheral dolostone–interior limestone distribution pattern evident from wells RWP-2, GFN-2 and ESS-1.

onset of the rapid high amplitude glacio-eustatic changes in sea level that started about 1 million years ago further complicates the diagenetic history of the succession. This situation also contrasts sharply with other areas in the world (e.g., Bermuda, Enewetak) where diagenesis triggered by eustatic changes in sea level acted on relatively young Holocene limestones that had not been previously dolomitized.

This study focuses on one cored well (GFN-2, 92.2 m deep) that was drilled in the limestone succession in the centre of the island, and two wells (RWP-2, 94.6 m deep; and ESS-1, 77.4 m deep) that penetrated the dolostone successions in the coastal areas (Fig. 3.1B, C). Over the last 1 Ma, sea level has fluctuated from about -140 to +20 m relative to modern sea level (Fig. 3.3), as has been shown in numerous studies (e.g., Siddall et al., 2003; Liseicki and Raymo, 2005; Miller et al., 2005; Naish and Wilson, 2009; Rohling et al., 2014). For the cored wells on the east end of Grand Cayman, this sea-level curve suggests that sea level was below or close to the base of GFN-2 on at least 11 occasions and close to

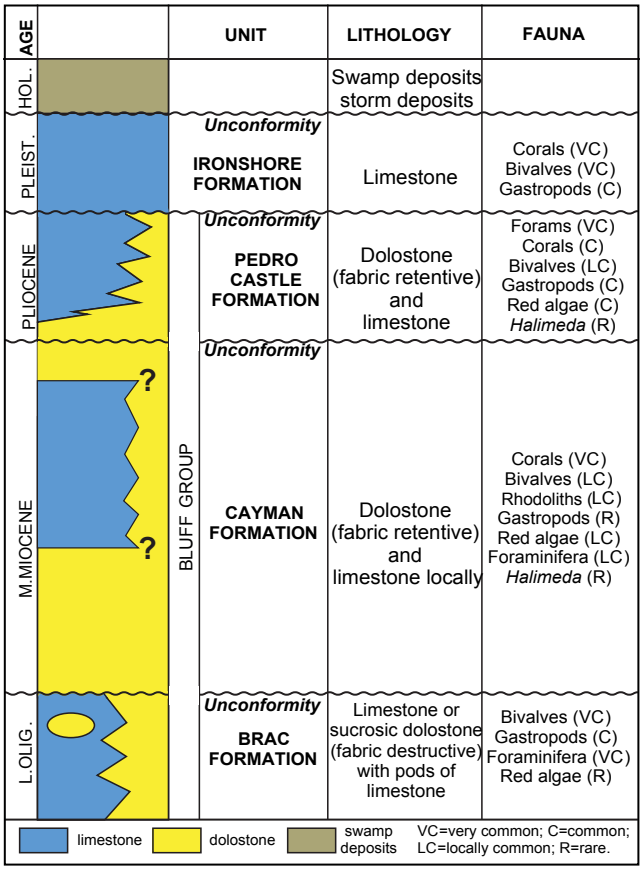

Fig. 3.2. Stratigraphic succession on Grand Cayman (modified from Jones et al., 1994a).

or above the top of GFN-2 during 11 periods (Fig. 3.3). Such fluctuations also meant that the hydrological zones on the island were constantly moving up and down through the bedrock of the island. Thus, from a theoretical perspective, the diagenetic history of the limestones and dolostones in GFN-2, RWP-2, and ESS-1 should be complex and reflect the ever-changing diagenetic regimes that they have experienced. In particular, it might be expected that these rocks should contain a clear record of the progressive change in the hydrological zones caused by the transgression that has taken place over the last 20 kyr as sea level has risen since the lowstand during the Last Glacial Maximum that was ~120 m below present-day sea level (e.g., Peltier and Fairbanks, 2006; Clark et al., 2009). Accordingly, the rocks in the three cored wells on Grand Cayman were examined to determine if (1) the diagenetic fabrics reflect the numerous transgressive–regressive cycles (Fig. 3.3) that have affected these rocks over the last 1 million years, (2) the limestones and dolostones responded differently to these sea-level oscillations, and (3) they provide any record of the rapid transgression that has passed through the rocks over the last 16,000 years. Although based on Grand Cayman, the results of this study have implications for carbonate successions of all ages because it

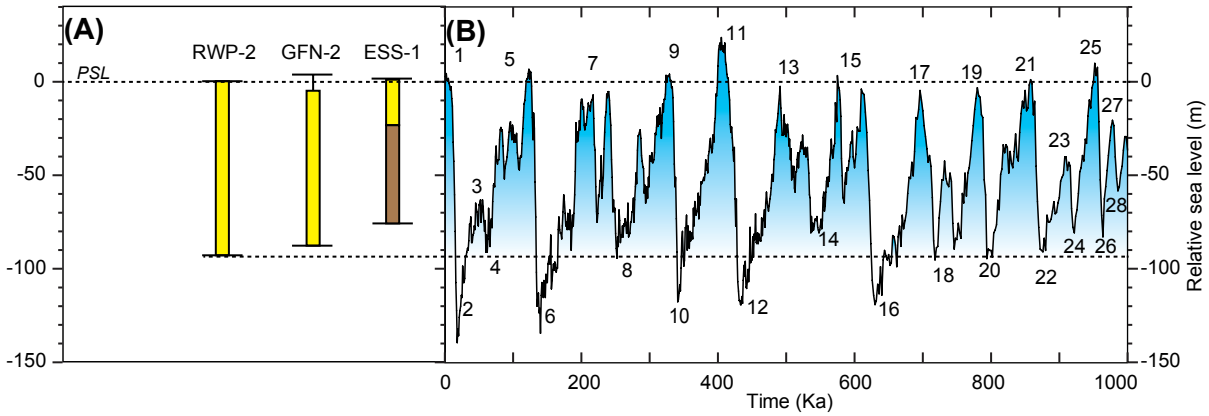

Fig. 3.3. Comparison of cored wells on Grand Cayman and sea-level curve for last 1 Ma. (A) Extent of cores from the Cayman Formation in wells RWP-2, GFN-2, and ESS-1. See Figure 1B for location of wells. PSL = present sea level. (B) Sea-level curve for last 1 Ma based on δ18O record of benthic foraminifera from Lisiecki and Raymo (2005) and equations from Spratt and Lisiecki (2015). Note repeated highstands, highlighted by blue shading, that placed all or most of the sequences in wells RWP-2, GFN-2, and ESS-1 under water and various lowstands when all of the cored sequences in wells RWP-2, GFN-2, and ESS-1 would have been above sea level.

questions the premise that carbonate rocks will always contain evidence of all the diagenetic zones in which they have been placed throughout their evolution.

2. Geological and hydrological settings

The Cayman Islands (Grand Cayman, Cayman Brac, and Little Cayman) are located on separate fault blocks that are part of the Cayman Ridge (Matley, 1926) (Fig. 3.1A). Grand Cayman, the largest island, has a low-lying interior that is generally < 3 m above sea level (asl) with a peripheral rim that rises up to 13.5 m asl around the eastern margin of the island (e.g., Jones et al., 1994a; Jones and Hunter, 1994b; Liang and Jones, 2014). The island has been tectonically stable over the last 500 kyr (Vézina et al., 1999) and probably over the past 5 Ma (Blanchon and Jones, 1995).

The surface to shallow subsurface carbonate succession on the Cayman Islands belongs to the Bluff Group that Jones et al. (1994a) divided into the Brac Formation (Oligocene), Cayman Formation (Miocene), and Pedro Castle Formation (Pliocene). The Bluff Group is unconformably overlain by the Pleistocene Ironshore Formation (Fig. 3.2). All of these formations are bounded by unconformities that formed during sea-level lowstands (Jones et al., 1994a).

The Cayman Formation crops out at the surface over most of the eastern part of Grand Cayman (Fig. 3.1B, C). In this area, the formation around the periphery of the islands is formed entirely of dolostones whereas the interior is formed largely of limestones that contain varying amounts of dolomite (Fig. 3.1C). This pattern is supported by the analysis of all available outcrops and samples from 43 wells that have been drilled over the last 15 years (e.g., Jones et al., 1994b; Der, 2012). For the purposes of this study, attention is focused on (1) well GFN-2 from the interior of the island because it is the only well in that area that was fully cored to a depth of 92.2 m, (2) well RWP-2, located on the northeast corner of the island, 4.5 km ENE of GFN-2 at 068.5°, that was cored to a depth of 94.6 m, and (3) well ESS-1, located 4.1 km south of GFN-2, that was drilled, partly cored, and sampled by well

cuttings to a depth of 77.4 m (Fig. 3.1B). The successions in wells RWP-2, GFN-1, and ESS-1 clearly illustrate the lateral and vertical distribution of the dolostones and limestones (Fig. 3.1C) that are herein considered to be part of the Cayman Formation because there is no evidence of any stratigraphic boundary that would place them in different formations. Furthermore, there is no evidence of folding or faulting of the strata between these areas. On the basis of the stratigraphy and $^{87}Sr/^{86}Sr$ ratios, the dolomitization that probably took place during the late Miocene (Budd, 1997; Jones and Luth, 2003; Zhao and Jones, 2012), Pliocene (Pleydell et al., 1990), and possibly during the Pliocene to early Pleistocene (Budd, 1997; Jones and Luth, 2003; Zhao and Jones, 2012) was mediated by seawater. Critically, this means that the limestone core and peripheral dolostone scheme has been in place for at least the last 1 million years. Irrespective of the exact timing of the dolomitization, it is readily apparent that it took place before the onset of large, rapid sea-level oscillations that have taken place over the last 1 million years.

Three main unconfined freshwater lenses are housed in the Cayman Formation on Grand Cayman, namely the East End, North Side, and Lower Valley lenses (e.g., Mather, 1971; Ng et al., 1992). The irregular configurations of the lenses have been attributed to the attitude and orientation of the joint and fissure systems (Ng et al., 1992). Generally less than 20 m thick, these lens are capped by water tables that are generally < 0.5 m asl (Ng et al., 1992). A thick mixing zone (> 20 m) has developed between the freshwater and saline water zones in response to the tide-generated hydrodynamic dispersion (Ng and Jones, 1995).

Fig. 3.4. Stratigraphic variations in the Cayman Formation in well GFN-2. (A) Distribution of sedimentary facies and facies associations (FA-I, II, III). (B) Distribution of diagenetic zones DZ-I, II, and III. (C) Composition of samples as determined by thin section analyses. (D) Tested porosity and permeability (K_{90}). (E) Distribution of calcite, LCD, and HCD as determined by XRD analyses. (F) Average %Ca of dolomite. (G) $\delta^{18}O$ and $\delta^{13}C$ of calcite and dolomite. (H) Distribution of groundwater zones as defined by chloride concentrations. PSL = present sea level.

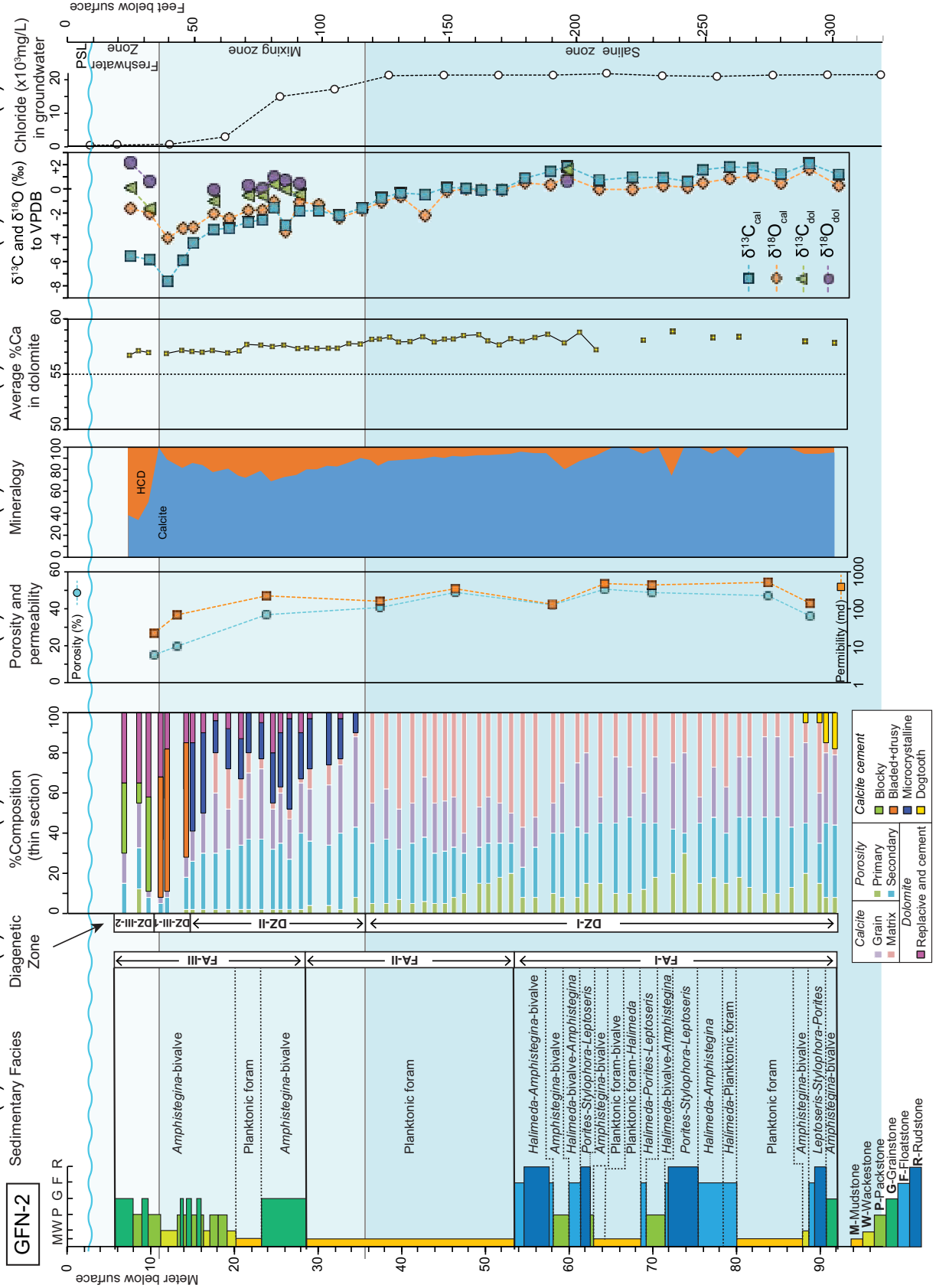
GFN-2
(A) Sedimentary Facies
(B) Diagenetic Zone
(C) %Composition (thin section)
(D) Porosity and permeability
(E) Mineralogy
(F) Average %Ca in dolomite
(G) δ13C and δ18O (‰) to VPDB
(H) Chloride (x10³mg/L) in groundwater
Meter below surface
Feet below surface
MWPGFR
Amphistegina-bivalve
Planktonic foram
Halimeda-Amphistegina-bivalve
Halimeda-bivalve-Amphistegina
Poorites-Stylophora-Leptoseris
Planktonic foram-bivalve
Planktonic foram-Halimeda
Halimeda-Porites-Leptoseris
Halimeda-bivalve-Amphistegina
Halimeda-Amphistegina
Halimeda-Planktonic foram
Leptoseris-Stylophora-Porites
FA-III
FA-II
FA-I
DZ-III-1
DZ-III-2
DZ-II
DZ-I
HCD
Calcite
Porosity (%)
Permibility (md)
PSL
Freshwater Zone
Mixing zone
Saline zone
δ13Ccal
δ18Ocal
δ13Cdol
δ18Odol
M-Mudstone
W-Wackestone
P-Packstone
G-Grainstone
F-Floatstone
R-Rudstone
Calcite
Grain
Matrix
Porosity
Primary
Secondary
Dolomite
Replacive and cement
Calcite cement
Blocky
Bladed+drusy
Microcrystalline
Dogtooth

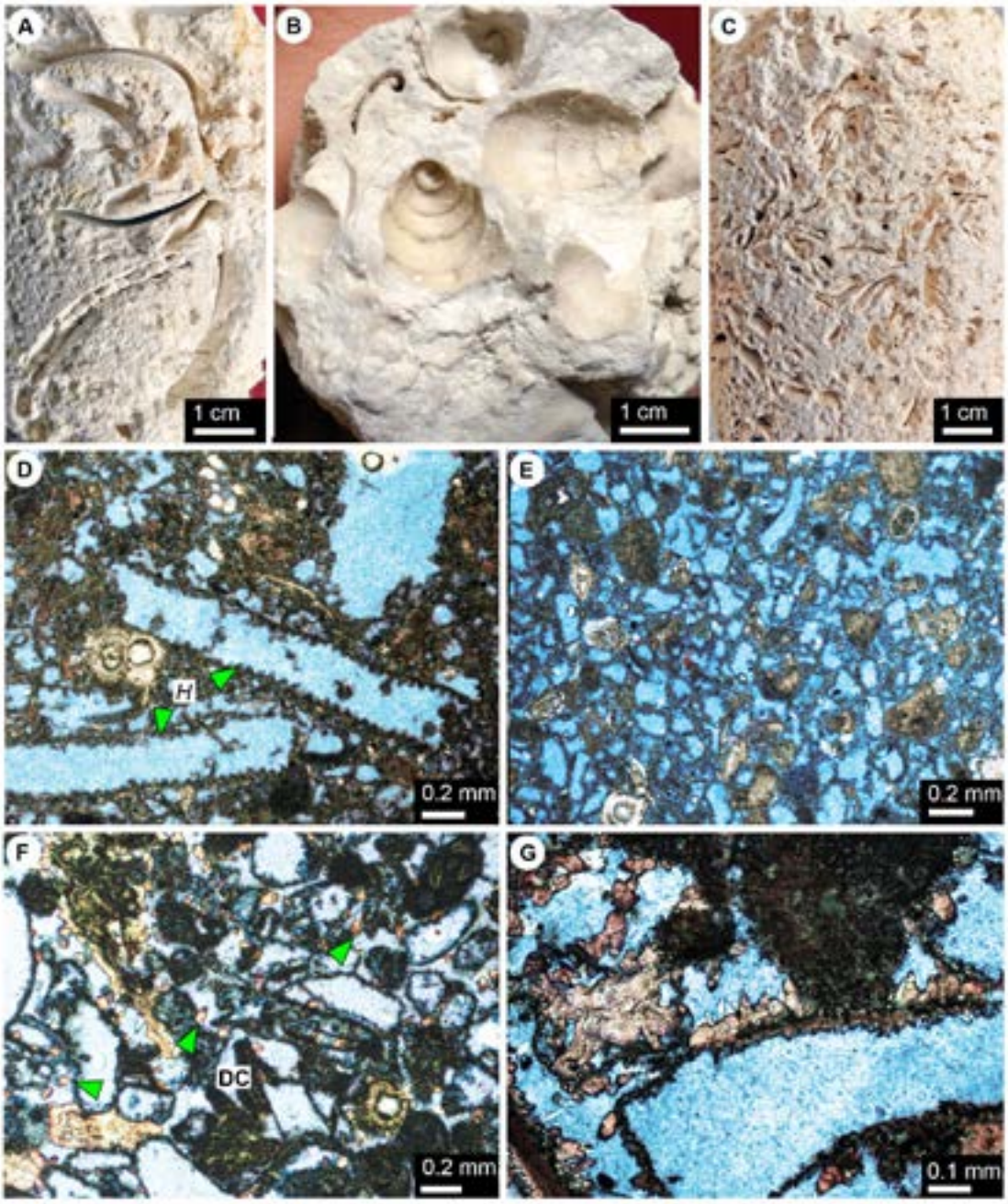

Fig. 3.5. Core photographs (A–C) and thin section photomicrographs (D–G) illustrating diagenetic features in DZ-I in well GFN-2. All depths below top well, which is 3 m asl. Thin section images in panels D and E from unstained thin section; panels F and G from thin section stained with Alizarin Red S. (A) Molds of articulated (bottom) and disarticulated (top) bivalves shells (71.2 m). (B) Molds of gastropods (73.0 m). (C) Molds of *Halimeda* plates (H) (57.3 m). (D) Molds of *Halimeda* plates and planktonic foraminifera (75.6 m). (E) Partial dissolution of planktonic foraminifera (83.4 m). (F) Scattered dogtooth calcite (DC) in porous limestone (90.7m). (G) Dogtooth calcite encasing and partly filling leached skeletal molds (91.7 m).

3. Methods

This paper is based largely on the analysis of three wells (ESS-1, GFN-2, RWP-2) drilled on the eastern part of Grand Cayman (Fig. 3.1B). They were selected from 43 wells that have been drilled in this area because they are the deepest wells in the areas of interest, and GFN-2 and RWP-2 were completely cored and ESS-1 was partly cored with cuttings collected from the part that was not cored.

Well GFN-2 was cored to a depth of 92.2 m with an average core recovery rate of 63%. This well is located 6 m east of GFN-1, which was an exploratory well drilled to 121.9 m in 2011 but not cored. Wells RWP-2 and ESS-1 are located in the coastal areas of the island (Fig. 3.1B). Drilling of RWP-2 (in 1993) yielded continuous cores to a depth of 94.1 m below present sea level (bsl) with an average core recovery rate 97%. Well ESS-1, located 4.1 km south of GFN-2, was cored to 25 m bsl with average core recovery 88%, and sampled by well cuttings to a depth of 77.4 m (Fig. 3.1B). Sixteen groundwater samples from GFN-1 were collected from surface to the base of the wells for chemical analysis. Present-day hydrological zones are defined following the scheme of Ng et al. (1992). Thus, the freshwater zone, mixing zone, and saline zone are divided by 600 mg/L and 19,000 mg/L chloride contents, respectively. The distribution of the groundwater zones in well RWP-2 is based on 7 groundwater samples from well EEZ-1 (~2 km SSE of RWP-2 and ~350 m from the coast) that is the nearest well to RWP-2 from which water samples are available (Fig. 3.1B).

For GFN-2, whole core porosity and permeability (K_{max}, K_{90}, K_{vert}) were measured from 10 core pieces (5 cm in diameter, 13 to 22 cm long). For RWP-2, porosities were acquired from 59 core plugs. These analyses were performed by Core Laboratories Ltd., Calgary, Alberta, Canada.

The mineral compositions of whole-rock powders for 59 samples from GFN-2, 62 samples from RWP-2, and 49 samples from ESS-1 were analyzed by X-ray diffraction analysis (XRD) following the procedure of Jones et al. (2001). The results allow

determination of the mol % of $CaCO_3$ in the dolomite (%Ca), and the percentages of calcite, high calcium dolomite (HCD, %Ca > 55%), and low calcium dolomite (LCD, %Ca < 55%) of the samples. The accuracies for these analyses are ± 10% for the proportion of each population of dolomite and ± 0.5% for the %Ca of each population (Jones et al., 2001).

Microscopic components and diagenetic features are based on the analysis of 59 thin sections from GFN-2 and 41 thin sections from RWP-2. All thin sections from GFN-2 were impregnated with blue epoxy in order to highlight the porosity, and stained with Alizarin

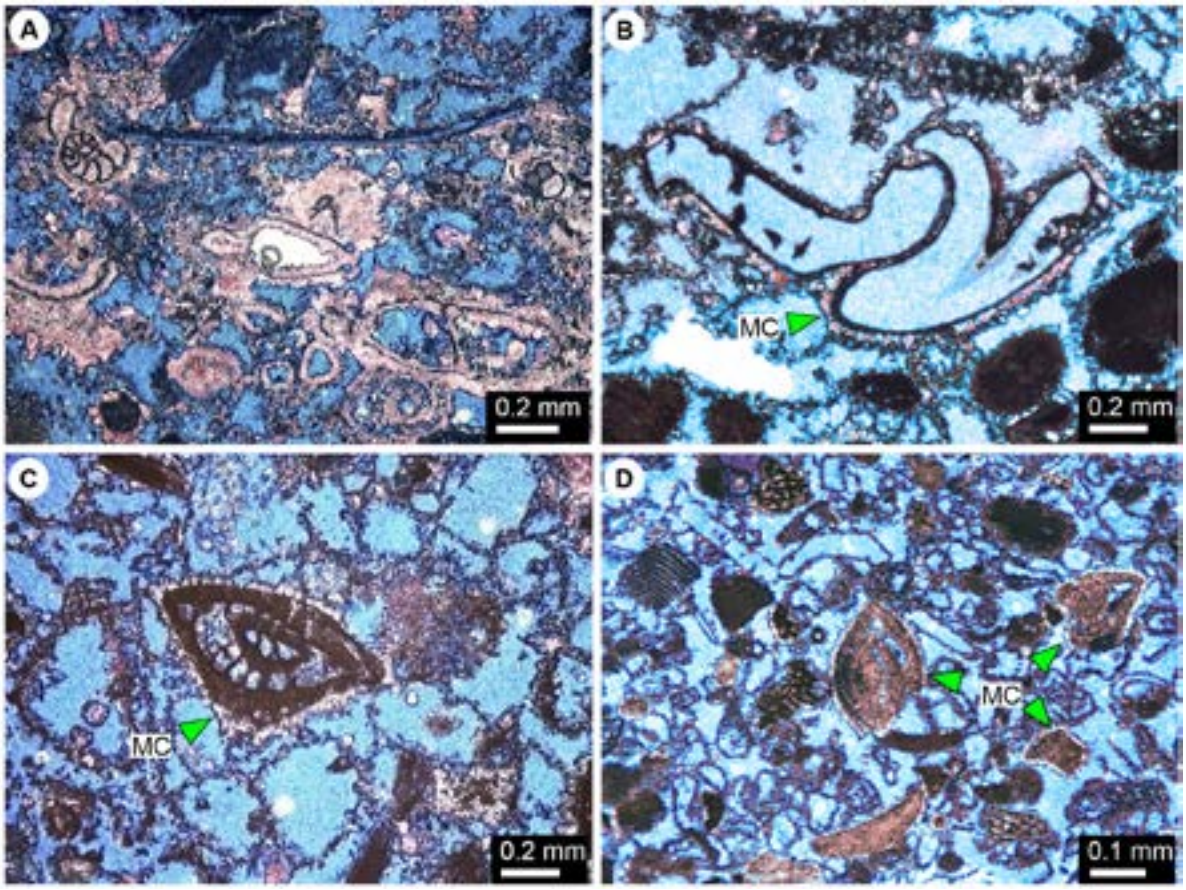

Fig. 3.6. Thin section photomicrographs showing diagenetic features in DZ-II in well GFN-2. All depths below top well, which is 3 m asl. Thin sections stained with Alizarin Red S. (A) Microcrystalline calcite cement lining walls of foraminifera and shells (14.9 m). (B) Micrite envelope encrusted by microcrystalline calcite cements (MC) (26.5 m). (C) High secondary porosity in grainstone due to dissolution of allochems. Note microcrystalline calcite (MC) encrusting the benthic foraminifera (26.5 m). (D) High porosity due to extensive dissolution of allochems. Note minor amounts of microcrystalline calcite cement (MC) around some of grains (34.4 m).

Red S to allow discrimination of the calcite and dolomite. Thin sections from RWP-2 were stained with Alizarin Red S.

Carbon and oxygen stable isotope analyses were obtained for 35 samples from GFN-2 that contained various amount of calcite and dolomite. Isotope analyses for dolomite were obtained for 31 samples from RWP-2. These analyses were performed by Isotope Tracer Technologies Inc. (Waterloo, Canada) using a DELTA^{Plus} XL Isotope Ratio Mass Spectrometer (IRMS) that is coupled with a ConFlo III interface and EA1110 Elemental

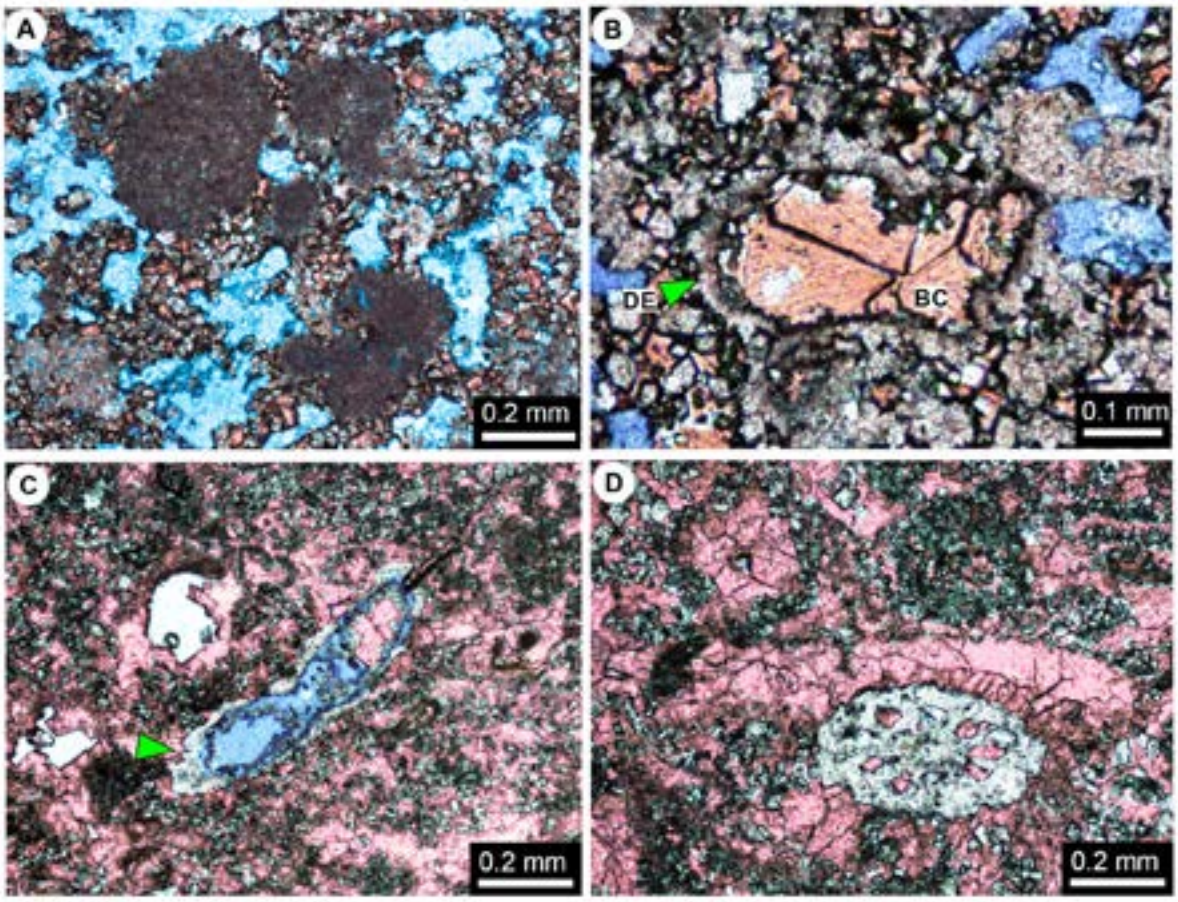

Fig. 3.7. Thin section microphotographs showing micritization (A) and dolomitization (B-D) in DZ-III in well GFN-2. All depths are from the surface of the well, which is 3 m asl. Stained with Alizarin Red S. (A) Completely micritized grains in calcitic dolostone (8.5 m). (B) Dolomite cement (DE) lining fossil mold and overlain by blocky calcite (BC) that filled the void (8.5 m). (C) Dolomite cement (arrow) around secondary pore formed by leaching of a skeletal grain or peloid (9.6 m). (D) Fabric-selective dolomitization of a skeletal allochem, and scattered dolomite crystals. Intercrystal pores completely occluded by blocky calcite cement (9.6 m).

Analyzer. All results are reported against the Vienna Peedee Belemnite (VPDB). Standards were run before, during, and after analysis of the samples in order to maintain accuracy. The error margin for the $\delta^{18}O$ and $\delta^{13}C$ is ± 0.1‰.

4. Results

4.1. Well GFN-2

4.1.1. Sedimentary facies

The Cayman Formation in well GFN-2 contains a diverse array of facies that are herein grouped into facies associations FA-I, FA-II, and FA-III (Fig. 3.4).

FA-I, in the lower part of the core (53 to 92.2 m), is formed mainly of skeletal rudstones and floatstones that contain domal (mainly *Leptoseris*) and branching (*Stylophora*, *Porites*) corals, green algae (mainly *Halimeda*), red algae, bivalves, gastropods, and benthic foraminifera (mostly *Amphistegina*). Mudstones with planktonic foraminifera occur at two intervals (63.0 to 68.7 m, and 80.0 to 88.0 m; Fig. 3.4). In general, both mudstone intervals transition upwards into coralline rudstones or floatstones through *Halimeda*-dominated facies or *Amphistegina*-dominated facies (Fig. 3.4).

FA-II, in the middle part of the succession (29 to 53 m), is formed largely of mudstone that contains planktonic foraminifera (mainly *Globigerinoides*?, *Globorotalia*?) and peloids formed by micritization of skeletal grains that are similar in size to the planktonic foraminifera.

FA-III, from the upper part of the formation (6 to 29 m) is formed largely of grainstones (Fig. 3.4). It is differentiated from the underlying FA-II by the presence of numerous benthic foraminifera (mainly *Amphistegina*), numerous micritized grains, scattered bivalve fragments, and scattered coral fragments (mainly small-diameter *Stylophora*).

4.1.2. Mineralogy

Apart from the upper part of the succession (6 to ~9 m), which consists of calcareous

dolostone (10% < %calcite < 50%), the Cayman Formation in GFN-2 is formed of limestone (< 10% dolomite) and dolomitic limestone (10–50% dolomite). On average, the rocks

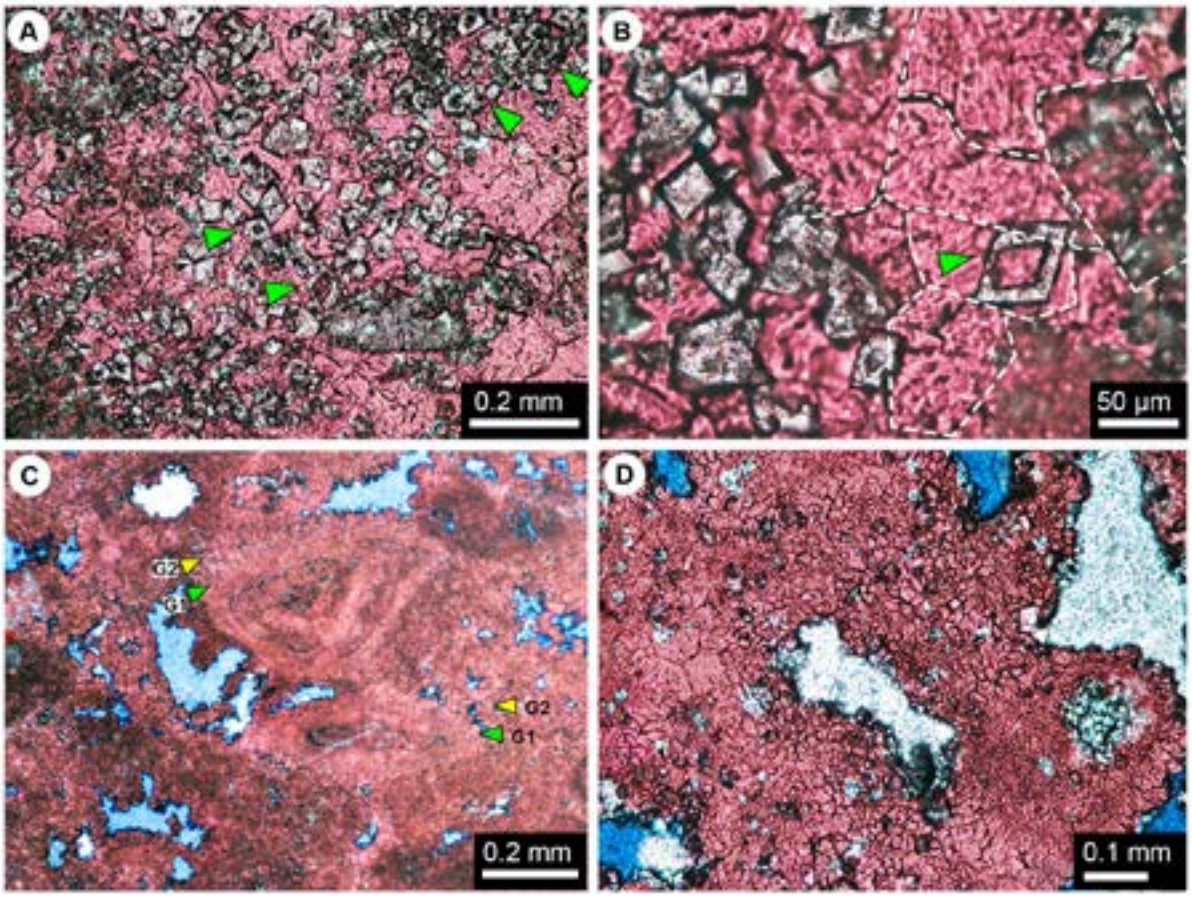

Fig. 3.8. Thin section microphotographs showing dissolution in dolomites (A–B) and various calcite cements in DZ-III in well GFN-2. Stained with Alizarin Red S. (A) Dolomite and hollow dolomite crystals in calcite cement (9.6 m). (B) Dolomite and hollow dolomite crystal (9.6 m) held in calcite cement. Dashed white lines indicate boundaries between large calcite crystals. (C) Two generations of calcite cements: first generation isopachous bladed cement encrusting foraminifera and second generation of drusy calcite partly filling pores (11.1 m). (D) Drusy calcite cement around grains (14.2 m).

Fig. 3.9. Stratigraphic variations in the Cayman Formation in well RWP-2. (A) Detailed sedimentary facies and one facies association (FA-IV). (B) Diagenetic zones DZ-IV, V, and VI as determined by thin section analyses. (C) Composition of samples and diagenetic zones (DZ-IV, V, VI) as determined by thin section analyses. (D) Porosity. (E) Distribution of LCD, and HCD based on XRD analyses. (F) Average %Ca of dolomite. (G) $\delta^{18}O$ and $\delta^{13}C$ of dolomite. (H) Distribution of groundwater zones based primarily on chloride concentration from EEZ-1 located on northeastern periphery of the island. PSL = present sea level.

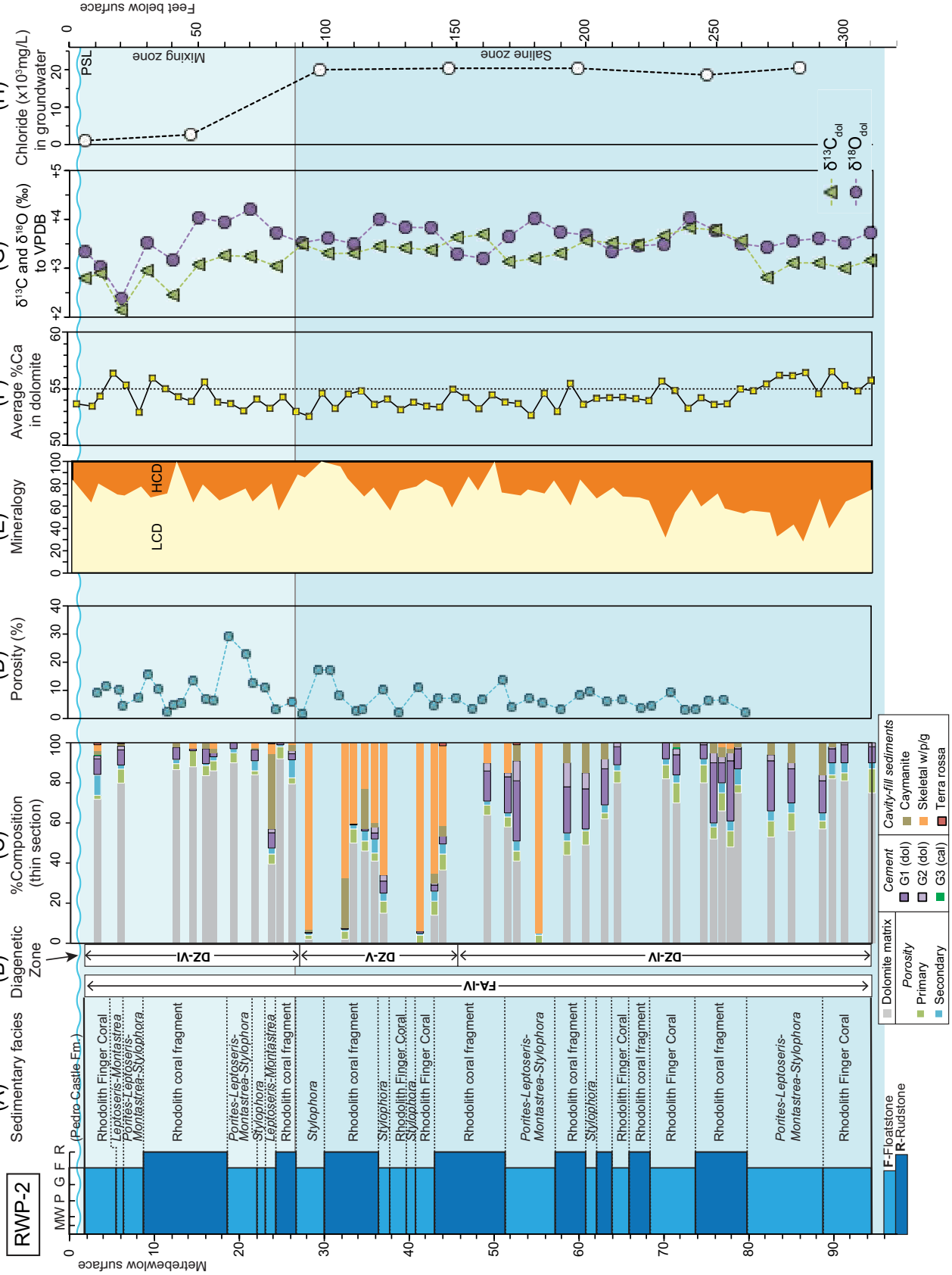
RWP-2
(A) Sedimentary facies
(B) Diagenetic Zone
(C) %Composition (thin section)
(D) Porosity (%)
(E) Mineralogy
(F) Average %Ca in dolomite
(G) δ13C and δ18O (‰) to VPDB
(H) Chloride (x10³mg/L) in groundwater
Meters below surface
Feet below surface
MW P G F R
(Pedro Castle Fm.)
Rhodolith Finger Coral
Leptoseris-Montastrea
Porites-Leptoseris-Montastrea-Stylophora
Rhodolith coral fragment
Stylophora
Rhodolith Finger Coral
FA-IV
DZ-VI
DZ-V
DZ-IV
HCD
LCD
PSL
Mixing zone
Saline zone
δ13Cdol
δ18Odol
F-Floatstone
R-Rudstone
Dolomite matrix
Porosity
Primary
Secondary
Cement
G1 (dol)
G2 (dol)
G3 (cal)
Cavity-fill sediments
Caymanite
Skeletal w/p/g
Terra rossa

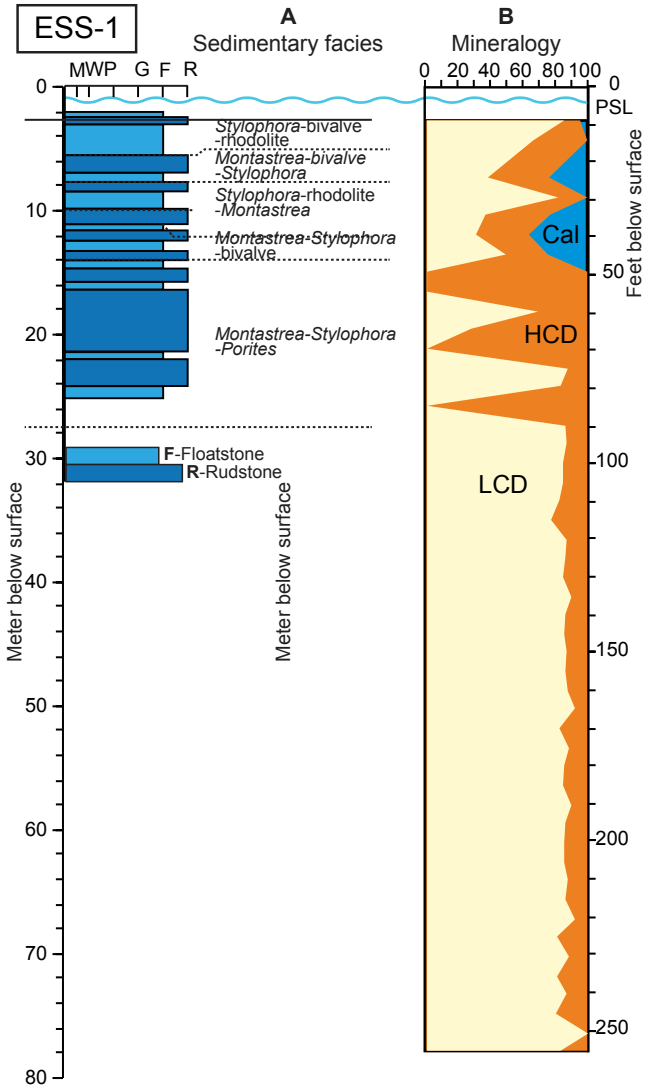

Fig. 3.10. Stratigraphic variations in the Cayman Formation in well ESS-1. (A) Sedimentary facies. (B) Distribution of LCD, HCD, and calcite (CAL) as determined by XRD analyses. PSL = present sea level.

are 85–90% calcite, which includes the grains, matrix, and cements (Fig. 3.4). All of the dolomite is nonstoichiometric with 56.7 to 58.9%Ca and an average of 57.78%Ca.

4.1.3. Porosity and permeability

Porosity in GFN-2 (Fig. 3.4) ranges from 15.0 to 50.6% (mean = 43.9 ± 5.7%, n = 10), whereas permeability (K_{max}) ranges from 21.8 to 520.0 mD (mean = 306.13 ± 161.35 mD, n = 10). In nine out of the ten samples, K_{max} is greater than $K_{vertical}$. Porosity and permeability (K_{max}) are positively correlated (Fig. 3.4). The lowest porosities (<20%) and permeabilities

(<70 mD) are found in the upper part of the succession (6–14.5 m), whereas samples with higher porosity (>35%) and permeability (>130 mD) came from the middle and lower part of the succession (14.5–92.2 m).

4.1.4. Diagenetic zones

The Cayman Formation in GFN-2 is characterized by a wide array of diagenetic features, including micritization, dolomitization, five types of calcite cement, limpid dolomite, and dissolution. The succession is divided into diagenetic zones DZ-I, DZ-II, and DZ-III based on the types and distribution of these diagenetic fabrics (Fig. 3.4). There is no obvious correlation between the diagenetic zones and the facies associations.

DZ-I, from 92.2 m (base of well) to 35.5 m, is characterized by poorly cemented limestones with high porosities (Figs. 3.4, 3.5). The upper boundary is defined by the appearance of thin isopachous rims of microcrystalline calcite cement around the allochems (Fig. 3.4). Dissolution is common throughout this interval with almost complete leaching of aragonitic allochems such as the bivalves, gastropods, and corals (Fig. 3.5). Foraminifera were dissolved to varying degrees (Fig. 3.5E). Most red algae, however, are well preserved. Calcite cement is rare, being restricted to scattered dogtooth crystals in the basal part of the succession below 88 m (Fig. 3.5F, G). Limestones in this part of the succession have porosities of 36.1 to 50.6% and K_{max} of 132 to 560 mD (Fig. 3.4).

DZ-II, from 14.5 to 35.5 m, is characterized by limestones that are partly cemented by microcrystalline calcite, have intermediate porosities, and extensive dissolution features (Figs. 3.4, 3.6). The upper boundary at 14.5 m marks the disappearance of microcrystalline calcite cement and a significant increase in the diversity of diagenetic features (Fig. 3.4). Microcrystalline calcite cement is ubiquitous throughout this interval. There is a notable increase in the thickness of the isopachous rims around the allochems from ~5 μm at the base to 30 μm at the top (Fig. 3.6). This is accompanied by a gradual increase in the amount of cement, from <15% at the base to ~50% at the top. Pervasive micritization, like that in DZ-I, and leaching of skeletal grains is ubiquitous in DZ-II. One sample from 24.1 m had a

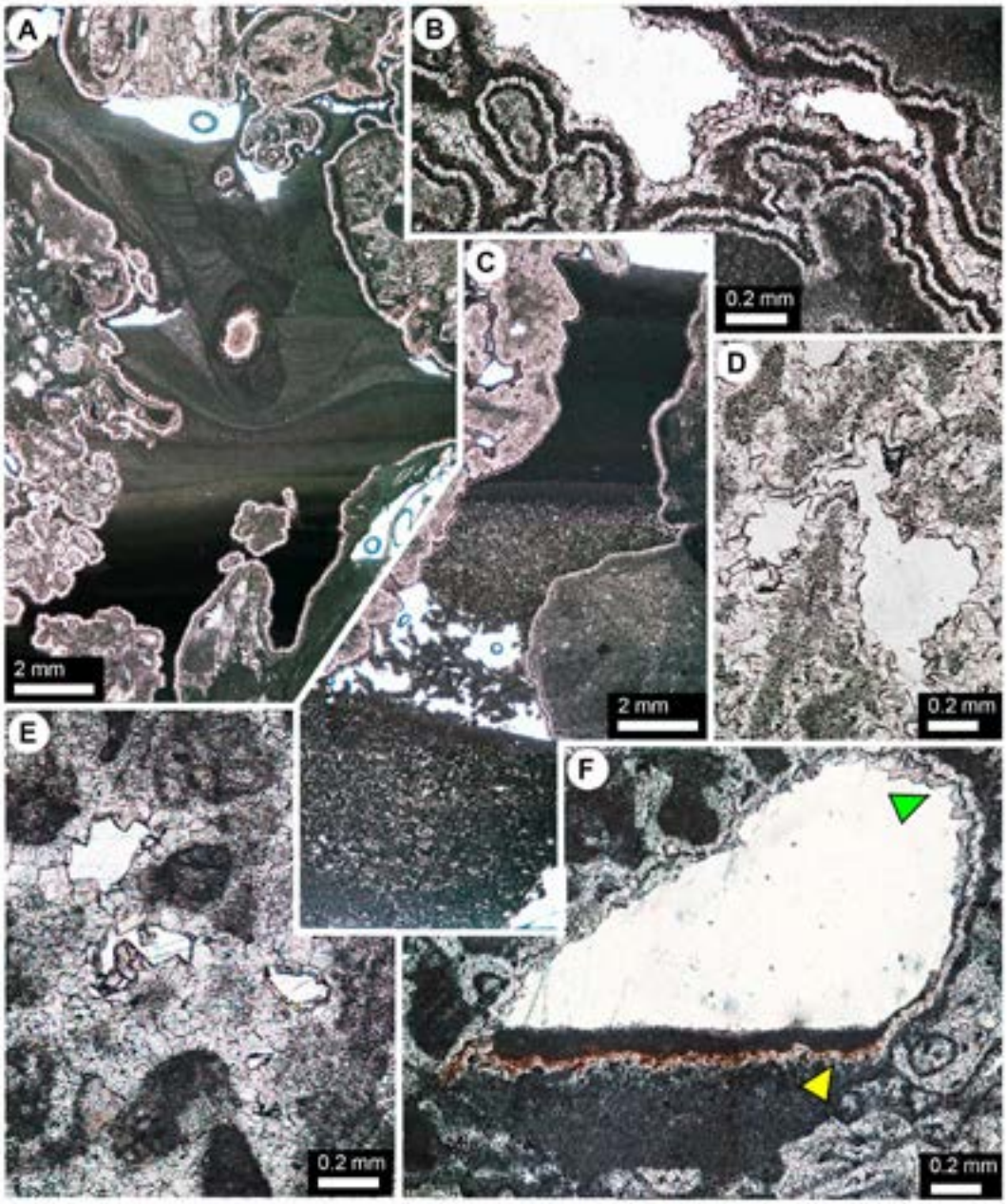

Fig. 3.11. Thin section microphotographs showing diagenetic zones in well RWP-2. All depths are from the surface of the well, which is 0.5 m asl. (A) Interparticle cavity lined with dolomite cement and then filled with two generations of caymanite (26.4 m). (B) Dolomite cement with multiple generations of dark and limpid dolomite (type G1c) (35.2 m). (C) Cavity filled with peloidal pack-grainstone and caymanite (29.9 m). (D) Dolomite cements with multiple zones of limpid dolomite (Type G1b) (78.3 m). (E) Blocky dolomite (G2) overlying the first generation of dolomite cement (G1a) (16.6 m). (F) Two generations of internal sediments that are separated by a layer of dolomite cement (G1a, yellow arrow) (52.8 m). Note two generations of dolomite cement hanging from the roof of the cavity (green arrow).

porosity of 36.8% and K_{max} of 224 mD.

DZ-III, from 6.0 to 14.5 m, is formed of dolostones/dolomitic limestones that have low porosities (Fig. 3.4). It is separated from DZ-II by its higher diversity of diagenetic features and its lower porosity (15.0–19.7%) and permeability (K_{max}, 21.8–68.7 mD). Rocks in this section are characterized by the following:

- Numerous skeletal grains that are now represented only by micrite envelopes or were transformed into peloids by pervasive micritization (Fig. 3.7A).
- Dolomite is present as (a) limpid crystals, commonly ~ 50 μm long, on peloidal and skeletal substrates (Fig. 3.7B, C), and (b) crystals, 20–50 μm long, that fill pores (commonly interparticle); some crystals are clear whereas others have dirty cores and clear rims (Fig. 3.7).
- Hollow dolomite crystals that are commonly filled with blocky calcite cement (Fig. 3.8A, B).
- Calcite cements that include (a) bladed crystals in the lower part (DZ-III-1; 10.4–14.5 m), that formed isopachous rims 30 to 100 μm thick around grains and the chamber walls of skeletal grains (Fig. 3.8C), (b) drusy crystals, which typically overlies the bladed calcite, formed of crystals that increase in size from 5 to 50 μm towards the centre of the pores (Fig. 3.8C, D), and (c) blocky crystals, 50 to 300 μm long (Figs. 3.7, 3.8A, B), which was the last cement precipitated and commonly fills many of the cavities in the upper part of the interval (DZ-III-2; 6.5–10.4 m). Most pores in DZ-III are completely occluded by these three cements.

4.1.5. Stable isotopes

The $\delta^{18}O$ of the calcite ranges from -4.06 to +1.63‰ (mean = -0.87 ± 1.45‰, n = 35), and the $\delta^{13}C$ ranges from -7.63 to +2.10‰ (mean = -1.08 ± 2.57‰, n = 35). Overall, the $\delta^{18}O$ and $\delta^{13}C$ of the calcite are highly correlated ($\delta^{13}C \approx 1.6\ \delta^{18}O + 0.31$, $r^2 = 0.82$) (Fig. 3.4). Both isotopic values vary between the diagenetic zones: (1) the average $\delta^{18}O$ increases from -2.73‰ (DZ-I) to -2.02‰ (DZ-II) and +0.13‰ (DZ-III), and (2) the average $\delta^{13}C$ values

from -6.23‰ (DZ-I) to -2.57‰ (DZ-II), and +0.77‰ (DZ-III).

Dolostones from upper part of the succession (6.5-27.6 m) have $\delta^{18}O$ from -0.08 to +2.16‰ (+0.64 ± 0.66‰, n = 9), and $\delta^{13}C$ from -1.63 to +1.59‰ (-0.25 ± 0.91‰, n = 9) (Fig. 3.4).

4.2. Wells RWP-2 and ESS-1

The depositional and diagenetic features in the Cayman Formation in well RWP-2 (Fig. 3.9) are based on Willson (1998) and analyses done in this study. The succession in well ESS-1 is essentially the same as that in RWP-2 (Fig. 3.10). Most of the following description is, however, based on the succession in well RWP-2 because it was completely cored to a depth of 94.6 m with a 98% recovery rate.

4.2.1. Sedimentary facies

The Cayman Formation in well RWP-2 is characterized by the coral-rhodolith floatstone–rudstone facies association (FA-IV) that includes the (1) *Stylophora* floatstone facies, (2) rhodolith branching coral floatstone facies, (3) rhodolith coral fragment rudstone–grainstone facies, (4) *Porites-Leptoseris-Montastrea-Stylophora* floatstone facies, and (5) *Leptoseris-Montastrea* floatstone facies (Fig. 3.9). There is no systematic pattern to the vertical stacking of these facies (Fig. 3.9). Cores from the upper 25 m of well ESS-1 reveals similar lithologies that dominated by skeletal grains derived from *Porites*, *Stylophora*, *Montastrea*, and rhodololiths (Fig. 3.10).

4.2.2. Mineralogy

The Cayman Formation in well RWP-2 is formed entirely of dolostone (Fig. 3.9). The same is true for well ESS-1 (Fig. 3.10) apart from minor amounts of calcite (<35%) in the upper 14 m of the well. Most of the dolostones (58 of 63 samples from RWP-2, and 43/50 of ESS-1) contain more LCD (average %LCD = 72.3% from RWP-2, and 83.6% from ESS-1) than HCD. HCD-dominated dolostones are restricted to the bottom part of RWP-2 (84–90

m), and the upper part of ESS-1 (10–20 m). All dolomite is nonstoichiometric with 54.4%Ca (RWP-2) and 53.2%Ca (ESS-1).

4.2.3. Porosity

Fossil moldic, interparticle, and fracture porosities dominate in RWP-2 and ESS-1. Porosity in the dolostones from well RWP-2 ranges from 1.7 to 29.2% with an average of 8.0 ± 5.4% (n = 50) (Fig. 3.9). Apart from two samples that have porosities of 29.2% (19 m) and 22.9% (21 m), the porosities are less than 10% (Fig. 3.9).

4.2.4. Diagenetic zones

The Cayman Formation in well RWP-2 is formed of finely crystalline dolostones that are characterized by low porosity, a complex array of limpid dolomite cements, and various types of cavity-filling sediments. This includes caymanite, which is a multicolored (white, red, black), cavity-filling sediment (mudstone to grainstone) with laminae that dip at angles up to 60° (Jones, 1992).

The original limestones in the succession in RWP-2 were completely replaced by fabric-retentive dolostones that are composed of anhedral to subhedral crystals < 50 μm long. Three generations of cement are present:

- Generation 1 (G1), common throughout the succession, is formed of subhedral to euhedral dolomite crystals, 30–100 μm (average ~50 μm) long, that form isopachous rims around the cavities and between the allochems. These crystals are divided into unzoned (G1a), zoned with 2–5 layers of clear dolomite (G1b, Fig. 3.11D), and dolomite with a limpid dolomite core encased by a thin dark-colored, inclusion-rich zone (Jones 1984), that is then overlain by a zone of clear dolomite (G1c, Fig. 3.11B, F). The latter two zones are, in some examples, repeated.
- Generation 2 (G2), which commonly overlies G1, is formed of subhedral drusy to blocky crystals, 100–120 um long (Fig. 3.11E).
- Generation 3 (G3), found in only one sample at a depth of 3.5 m, is formed of calcite

cement that overlies the dolomite cement.

Internal sediments that filled many of the cavities in the Cayman Formation in RWP-2 (Fig. 3.11A, C, F) include caymanite, skeletal wacke/pack/grainstones, and terra rossa. These cavity-filling sediments are characterized by various sedimentary structures such as graded laminae in the caymanite and typically have low porosity. The complex relationships between the cavity-filling sediments and cements include (1) sediments that filled cavities with no cement, (2) sediments that filled cavities that were lined with dolomite cements (mostly G1, Fig. 3.11A, C), and (3) dolomite cements (G1) that postdated the cavity fills (Fig. 3.11F).

Dolostones in the Cayman Formation in well RWP-2 are divided into diagenetic zones DZ-IV to DZ-VI (Fig. 3.9).

DZ-IV (45.8–94.6 m) is characterized by dolostones with low porosity (average 5.2 ± 2.8%) with G1 cements throughout. The upper boundary at 45.8 m, is defined by a significant increase in the amount of cavity-filling sediments. Dolostones in this part of the succession contain 5–17% dolomite cements (types G1b and G1c). The cavity-filling sediments are formed largely of caymanite with lesser amounts of skeletal wacke/pack/grainstones above 55 m and minor terra rossa at 52.8 m.

DZ-V (27.0–45.8 m), is characterized by dolostones with cavities of various sizes that have been filled with internal sediments (Fig. 3.9). The boundary between DZ-V and DZ-VI, placed at 27 m, marks a significant decrease in the cavity fills. The internal sediments are formed mostly of skeletal wacke/pack/grainstones. In some cavities, two or more types of internal sediment are stacked on top of each other; for example, caymanite on top of peloidal packstone (Fig. 3.11C). Dolomite cements (type G1c) form < 3% of the rock. The average porosity (7.6 ± 5.2%) is higher than that in DZ-IV.

DZ-VI (0–27.0 m) consists of dolostones that are cemented primarily by type G1a cement, which forms ~6% of the rock. Calcite cement (G3) was found only in the uppermost sample at 3.5 m. Small amounts of terra rossa (0.5–1%) are present in the cavities at the top

(3.5 m) and bottom (24.4 m). Porosities in this zone range from 2.4 to 29.2%.

4.2.5. Stable isotopes

The $\delta^{18}O$ value from 31 dolomite samples from well RWP-2 range from 2.38 to 4.21‰ (average 3.59 ± 0.36‰), and the $\delta^{13}C$ from 2.15 to 3.83‰ (average 3.26 ± 0.37‰) (Figs. 3.9, 3.12). There is no correlation between (1) the oxygen and carbon isotopes, and (2) the isotopic values and the %Ca.

5. Interpretation

5.1. Depositional environment

There are significant differences in the sedimentary facies in the Cayman Formation found on the island periphery and interior as illustrated by comparing wells RWP-2 and ESS-1 with well GFN-2. Comparison of GFN-2 and RWP-2, for example, highlights the abundance of corals and rhodoliths in RWP-2 (Fig. 3.9) as opposed to the dominance of skeletal grains and rare corals in GFN-2 (Fig. 3.4). Given that there is no evidence of folding or faulting of the strata between these two localities, these contrasts must reflect original facies.

Numerous corals and photosynthetic algae in RWP-2 and ESS-1 indicate that the depositional environments around the edge of the island were characterized by normal marine conditions with open circulation between the bank edge and open ocean, probably within the photic zone. Corals from these areas are characterized by their variable morphologies (branching, domal, platy) that can be linked to a depositional spectrum that varied from high energy and low sedimentation settings to low energy and high sedimentation settings, as suggested by Willson (1998). The numerous rhodoliths found in these areas probably originated under relatively high-energy conditions. The recurring coral- and rhodolith-dominated facies found on the peripheral parts of the island (wells RWP-2 and ESS-1), indicate deposition on a bank edge to inner bank setting (Willson, 1998). This is consistent

with the conclusion of Jones and Hunter (1994a).

In well GFN-2, FA-I, FA-II, and FA-III record progressive changes in the depositional conditions in the island interior through time. FA-I, in the lower part of the well, includes the *Leptoseris-Stylophora-Porites* floatstone/rudstone facies that is similar to the *Stylophora-Porites* and *Stylophora* associations described by Hunter (1994), and the branching coral-*Amphistigina* facies of Der (2012). Dominated by fragile branching corals, this facies represents coral thickets that grew on a sandy seafloor under moderate to low energy conditions with high sedimentation rates in water 10 to 30 m deep (Hunter, 1994; Der, 2012). The *Halimeda*-dominated facies and mudstone facies found in parts of FA-I probably formed under lower energy conditions.

FA-II (29-53 m), formed largely of mudstones with planktonic foraminifera, records deposition in a quite-water setting. *Globigerinoides*, the dominant species, is a shallow-

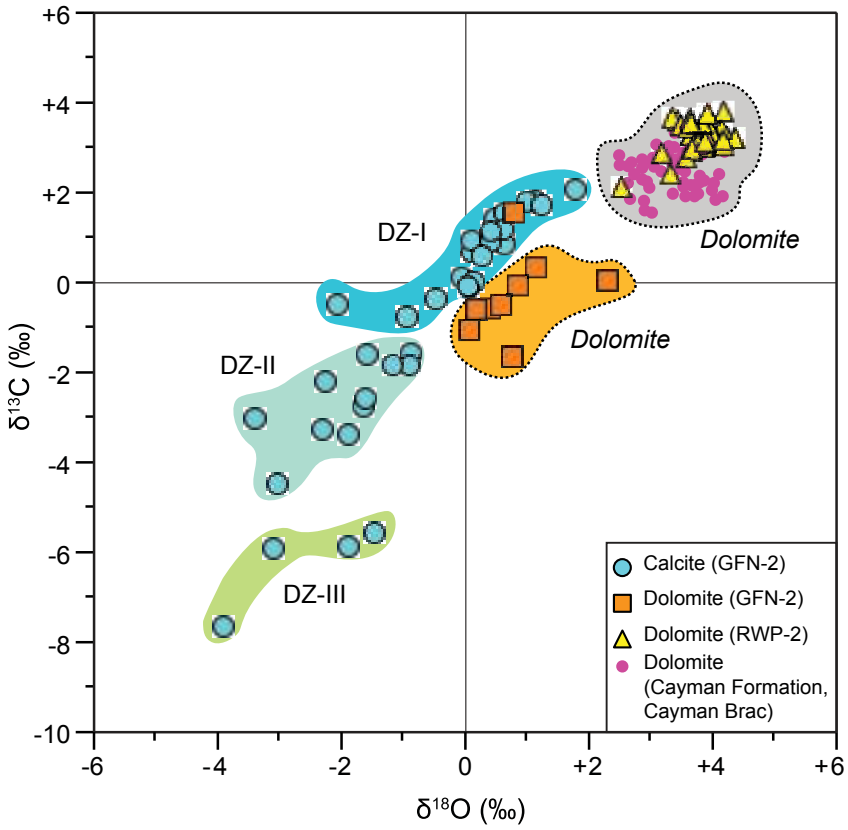

Fig. 3.12. Oxygen and carbon isotopes of calcite and dolomite from well GFN-2 and dolomite samples from well RWP-2. Dolomite isotopes from Cayman Formation on Cayman Brac (Zhao and Jones, 2012) are shown as a comparison.

water planktonic foraminifera that has inhabited the euphotic zone in waters 10–50 m deep since the Oligocene (Gupta, 2003). As such, FA-II probably developed while low energy conditions prevailed, possibly in deeper water than that associated with FA-I.

FA-III (6 to 29 m), with its *Amphistigina* and bivalve dominated wackestone to grainstone facies, has been found in other wells on the eastern part of Grand Cayman (Der, 2012). These facies probably developed under low- to high-energy conditions in water that was 10 to 20 m deep.

5.2. Diagenesis

Dolostones and limestones in the Cayman Formation have undergone extensive diagenetic modifications since the original sediments were deposited during the early to middle Miocene, with one of the main results being significant difference in the extent of dolomitization in different parts of the island. This is clearly evident on the eastern part of Grand Cayman where the Cayman Formation in GFN-2 consists largely of limestone (generally < 15% dolomite), whereas the successions in RWP-2 and ESS-1 are formed entirely of dolostone (Figs. 3.4, 3.9). For the purposes of this paper, the diagenetic history is considered relative to the pervasive dolomitization that affected the Cayman Formation. Based on stratigraphic relationships and the $^{87}Sr/^{86}Sr$ ratios, pervasive dolomitization on Grand Cayman has been attributed to either one phase, 2–5 Ma (Pleydell et al., 1990) or two phases, 6–8 Ma and 1.9–2.2 Ma (Jones and Luth, 2003). For Cayman Brac, two phases of dolomitization from 6–8 Ma and 1–5 Ma were proposed by Zhao and Jones (2012). Irrespective of the details, all of these studies argued that pervasive dolomitization had finished before 1 Ma. Critically, this means that the basic architecture of a peripheral dolostone and central limestone core for the Cayman Formation has been in place for at least 1 million years. Accordingly, the diagenetic history of the Cayman Formation on the eastern part of Grand Cayman can be divided into the pre- and post-dolomitization phases.

5.2.1. Pre-dolomitization diagenesis and dolomitization

In GFN-2, pre-dolomitization diagenesis included extensive micritization of various allochems that took place on sea floor shortly after sediment deposition. This led to the formation of micrite envelopes around many allochems and the transformation of others to peloids. Textural evidence indicates that micritization took place before the onset of allochem dissolution.

Later processes, evident in well RWP-2, included (1) the development of fossil-moldic porosity as the aragonitic skeletons (e.g., corals) were dissolved, (2) the filling of cavities by internal sediments and cements, and (3) lithification. Cavity-filling sediments in RWP-2 include caymanite and skeletal wacke/pack/grainstones, which have been attributed to various marine and terrestrial processes (Jones, 1992). The fact that these cavity-filling sediments are pervasively dolomitized and have similar stable and radiogenic isotope signatures to the surrounding dolostone bedrock indicates that they were emplaced before dolomitization took place (Pleydell et al., 1990; Jones, 1992). These cavity-filling sediments and cements, which led to a significant reduction in porosity in RWP-2, are absent from the succession in GFN-2.

By the time pervasive dolomitization had ceased, there was a significant difference between the Cayman Formation found in the interior and the peripheral parts of the island. The peripheral succession was pervasively dolomitized, contained cavities that were largely filled by internal sediments and cements, and had low porosity. In contrast, the Cayman Formation in the interior of the island was formed largely of limestone, lacked cavity filling sediments and cements, and was highly porous. This stark contrast set the stage for post-dolomitization diagenesis.

5.2.2. Post-dolomitization diagenesis

Post-dolomitization diagenesis in well GFN-2, included dissolution and precipitation of calcite cements. In the upper part of the well (DZ-III, 6.5–14.5 m), the negative stable

isotope values ($\delta^{18}O_{cal}$ = -2.73 ± 1.12‰, $\delta^{13}C_{cal}$ = -6.23 ± 0.95‰; Fig 12) and pervasive calcite cementation point to diagenesis in the meteoric-phreatic zone. Reduction in the proportion of the heavier isotopes in the calcite relative to the original sediments points to alteration by isotopically light freshwater (Fig. 3.12). Occlusion of pores by drusy, blocky, and isopachous calcite cements implies precipitation in the phreatic zone where pores were filled by freshwater. The absence of vadose cements in this interval may reflect (1) vadose waters that were unsaturated with respect to calcite/aragonite and/or physical-chemical conditions in the pores and cavities that were unfavorable for precipitation, (2) water that flowed through the vadose zone in GFN-2 area so rapidly that precipitation did not take place, (3) vadose waters that did not flow through the rocks in the area where GFN-2 was drilled (cf., Thorstenson et al., 1972; Braithwaite and Camoin, 2011), and/or (4) removal by erosion of the rocks that originally contained evidence of vadose diagenesis.

In the middle part of GFN-2 (DZ-II and upper DZ-I, 14.5–60 m), carbon and oxygen isotopes gradually shift to positive values towards the base of the interval ($\delta^{18}O_{cal}$ from -3.18‰ to +0.99‰, $\delta^{13}C_{cal}$ from -4.45‰ to +1.85‰) (Figs. 3.4, 3.12). This may reflect either (1) diagenesis in a mixing zone where varying mixtures of freshwater and saline

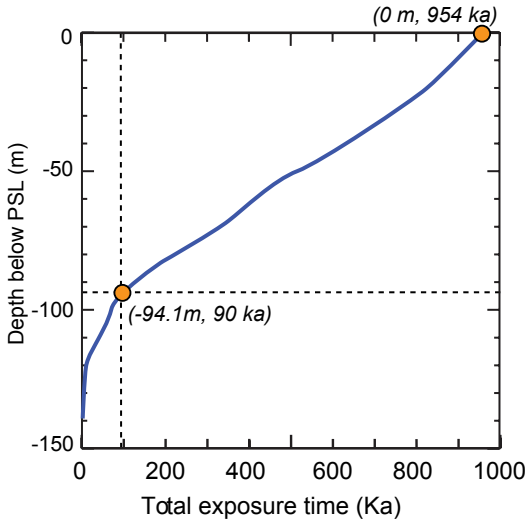

Fig. 3.13. Cumulative time of exposure of Cayman Formation at different depth over the last 1myr. Sea level data based on $\delta^{18}O$ record of benthic foraminifera from Lisiecki and Raymo (2005) and equations from Spratt and Lisiecki (2015).

water produced gradual changes in the isotopic compositions of pore fluid with depth, or (2) an artifact of sampling with the analyzed samples including both the cements that were precipitated from isotopically lighter freshwater and the skeletal grains and matrix that formed from isotopically heavier marine waters. If the second possibility is applicable, then the whole-rock isotope values would be negatively correlated with the amount of cement in the samples. This is not true for the lower part of this interval (36.5–60.0 m) where both isotopes increase with depth even though calcite cement in this interval is absent. Thus, this middle interval of GFN-2, 45.5 m thick, probably represents a paleo-mixing zone.

Positive isotope values ($\delta^{18}O_{cal}$ = +0.57 ± 0.53‰, $\delta^{13}C_{cal}$ = +1.35 ± 0.49‰), and extensive dissolution of skeletal grains characterizes the lower part of the succession (lower DZ-I, 60–92.2 m) (Figs. 3.4, 3.5). This may indicate that the diagenetic fabric and isotopes in this interval resulted from modification by meteoric and saline phreatic diagenesis. According to the sea-level curve for the last 1 myr (Fig. 3.3), sea level has dropped below the base of GFN-2 at least five times. During those periods, the succession would have been subaerially exposed and pervasive dissolution of skeletal grains may have been mediated by meteoric diagenesis, particularly in the vadose zone. Positive carbon and oxygen isotopes of the limestone suggest saline water modification of the sediments when they were submerged in the saline water zone after meteoric dissolution had taken place. The basal part of this interval, below ~90 m, includes some dogtooth calcite cement that may be related to submarine diagenesis, as has been suggested for similar cements found on Grand Bahamas Bank (Melim et al., 1995) and Mururoa (Braithwaite and Camoin, 2011).

6. Discussion

The Miocene strata of the Cayman Formation in the interior and coastal parts of Grand Cayman contrast sharply in terms of their facies, mineralogy, porosity, permeability, diagenetic fabrics, and geochemical signatures. Spatial variability in diagenesis like this is evident in many carbonate platforms worldwide. Submarine cements are, for example,

largely restricted to marginal facies and the degree of marine cementation commonly decreases from the peripheral to the central parts of a platform (James et al., 1976; Lighty, 1985; Aissaoui et al., 1986; Marshall, 1986; Vollbrecht, 1990). On the eastern part of Grand Cayman, pervasive dolomitization was restricted to coastal areas where the large volumes of seawater needed for such diagenesis could be pumped through the rocks (cf., James et al., 1976; Marshall, 1986). Early diagenesis, including cavity formation, filling of cavities with internal sediments and dolomitization, significantly reduced the porosity and permeability in the strata in these coastal regions. Although seawater still percolated through those dolostones during post-dolomitization times, the reduced porosity and permeability resulting from the earlier diagenesis decreased flow rates and curtailed diagenetic activity. Dolomitization of the coastal strata before 1 Ma was critical to the subsequent evolution of the strata on Grand Cayman because it (1) produces dolostones that were less susceptible to meteoric diagenesis, and (2) it reduced porosity and hence impeded the flow of waters through the rocks.

The sea-level curve for the last 1 myr shows 16 highstand-lowstand cycles of various magnitudes that are characterized by rapid transgressions, short-lived highstands, and slow regressions (Fig. 3.3). Collectively, this means that the rocks in the basal parts (at ~ 94 m bsl) of wells RWP-2, GFN-2, and ESS-1 on Grand Cayman have experienced longer cumulative times of exposure to meteoric water than the rocks higher in the succession (Fig. 3.13). There is an almost linear relationship between the cumulative length of exposure time over the last 1 myr and the depth below present-day sea level. For example, relative to present-day sea level, strata in the Cayman Formation in wells RWP-2, GFN-2, and ESS-1 at 0 m, -50 m, and -94 m have, over the last 1 myr, been subaerially exposed for cumulative periods of ~ 950,000 years, 520,000 years, and 90,000 years, respectively (Fig. 3.13). Thus, it might be reasonable to expect that there should be some trends in the type and/or degree of diagenetic change that could be matched with the linear trend between depth and cumulative exposure time (Fig. 3.13). There are, however, no obvious correlations between any aspect

of the diagenesis with either the repeated highstand-lowstand cycles or cumulative exposure time. In the upper part of GFN-2 (6.5–14.5 m), the sequence of calcite cements is simple with the limestones containing no more than two types of cement. Although those pores with two types of calcite cement may have evolved during different highstands, it is impossible to date those cements and they cannot, therefore, be linked to specific sea-level highstands. Nevertheless, precipitation of these cements would have reduced the porosity/permeability and possibly affect fluid circulation during later times (cf., Braithwaite and Camoin, 2011). Similarly, there is no pattern to the distribution of the dissolution features. In GFN-2, for example, the degree of dissolution is consistent throughout the entire succession. This, however, may simply be the reflection of two factors. First, there was a relatively even distribution of the solubility-prone components throughout the succession. Second, all of these components may have been dissolved when they were first exposed to meteoric diagenesis during the first regressive cycle. This is plausible, especially if exposure to the atmosphere occurred during a time when there was a humid paleoclimate with high rainfall that allowed large volumes of freshwater to be flushed through the strata (cf., Whitaker et

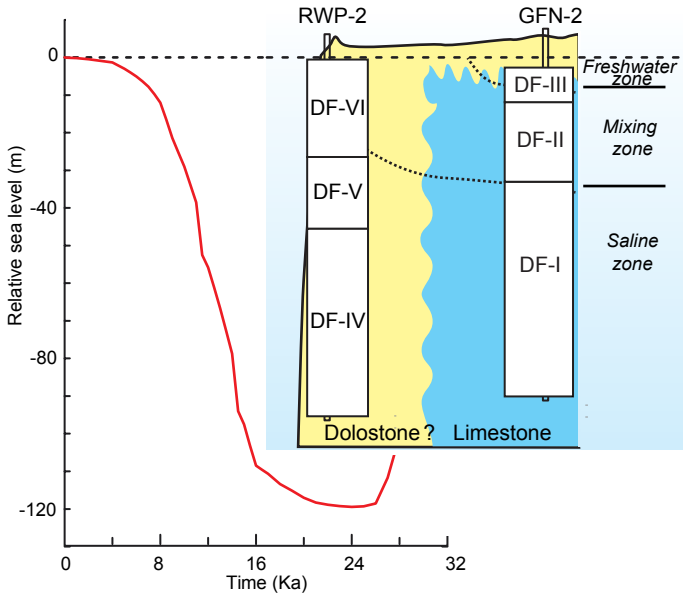

Fig. 3.14. Correlation of the diagenetic zones of GFN-2 and RWP-2 and the present-day groundwater distribution on Grand Cayman with the last sea level transgression. Sea-level curve modified from Peltier and Fairbanks (2006).

al., 2006; Li and Jones, 2013). Once the solubility-prone components were dissolved, no further dissolution would take place even if the diagenetic conditions were suitable for such diagenesis. In the shallow part of the succession, diagenetic alteration dominated, with the surface zone being case-hardened by pervasive calcite cement. This offers a stark contrast to the poorly cemented limestones in the deep part of the succession. Similar diagenetic patterns have been found in Mururoa (Aissaoui et al., 1986), the Bahamas (Beach, 1995; Melim, 1996), Florida (Melim, 1996), and on Enewetak Atoll (Quinn, 1991).

The contrast in the amount of calcite cement between the coast and interior of Grand Cayman can probably be attributed to contrasts in the hydrological regimes associated with the establishment of freshwater lenses during sea-level highstands over the past 1 myr. Today, the East End water lens on Grand Cayman is centrally located (e.g., Mather, 1971; Ng et al., 1992) and does not extend into the dolostones of the coastal areas (Fig. 3.1B). Meteoric calcite cement in the Cayman Formation in the interior part of the island is (1) stratigraphically controlled and restricted to particular depth intervals, (2) found in thin, dense, more or less stratiform horizons, and (3) increases towards the center of the island. This pattern is similar to that on Mururoa Atoll (Aissaoui et al., 1986). On Grand Cayman, these cementation patterns probably developed in response to the positions of the hydrological zones that fluctuated in concert with changes in sea level (cf., Whitaker et al., 1997; Melim et al., 2002).

It seems probable that freshwater lens developed during lowstands when sea levels were ~90 m bsl. This is supported by many modern examples of freshwater lenses that have developed beneath thick vadose zones on small islands like Grand Cayman, Cayman Brac (~40 m thick vadose zone; Mather, 1971; Ng et al., 1992) and Niue (30-70 m thick vadose zone; Jacobson and Hill, 1980; Wheeler and Aharon, 1997). It has also been shown that during the last sea-level lowstand, when the water table was 120 m bsl, bank-wide phreatic lenses developed across the Grand Bahamas Bank and Cat Island (Beach, 1995). Determining the exact extent of the freshwater lens on Grand Cayman during those

lowstands is difficult because the size and distribution of the lens is controlled by many factors, including topography, climate, geological structure, and platform size (e.g., Cant and Weech, 1986; Budd and Vacher, 1991; Beach, 1995; Vollbrecht and Meischner, 1996; Vacher, 1997). Irrespective, as sea level rose and fell during the transgressive-regressive cycles, the freshwater lens and its associated hydrological zones would have moved vertically through the strata in the upper part of the Cayman Formation. With such a scenario, it might be expected that these strata would contain substantial amounts of calcite cement and that the porosity would have been largely occluded. Most of the transgressive-regressive cycles over the last 1 myr were of short duration (Fig. 3.3) and it therefore seems probable that the situation was so dynamic that the hydrological zones were never established long enough to allow pervasive calcite cementation (cf., Steinen, 1974; Quinn, 1991). Alternatively, even if the freshwater lens were established, the water may have been chemically inactive and calcite precipitation impossible (cf., Melim, 1996; Melim et al., 2002).

Analysis of the diagenetic features in the Cayman Formation in wells GFN-2 has shown that there is no clear correlation between the different diagenetic features and the different diagenetic environments that the rock may have experienced over the last 1 myr. It is possible, however, that this simply reflects issues associated with the evolution of these rocks over an extended period of time. This notion, however, can be tested by considering the diagenesis that has taken place in the upper part of the Cayman Formation since the last transgression that started ~20 kyr ago (Fig. 3.14) when sea level was 120 m bsl. During this progressive rise in sea level, the Cayman Formation must have been subject to ever-changing hydrological regimes. Despite this, none of the diagenetic features in the Cayman Formation can be directly linked to any of the groundwater zones or hydrological conditions that existed during this transgressive phase (Fig. 3.14). Thus, it is readily apparent that this last dramatic transgression has left little or no record on the limestones and dolostones of the Cayman Formation on Grand Cayman.

7. Conclusions

The sediments that now form the Cayman Formation (Miocene) on Grand Cayman accumulated on a carbonate bank. Before the high-frequency, high-amplitude glacio-eustatic changes in sea levels that started ~1 Ma, the peripheral part of the island had been subject to marine diagenesis and dolomitization. Since then, oscillations in sea level have repeatedly placed the limestones and dolostones of the Cayman Formation into contrasting marine and meteoric diagenetic environments. The main conclusions reached in this study are:

- On the east end of Grand Cayman, partial dolomitization of the Cayman Formation, more than 1 million years ago, meant that limestones in the central part of the island were encircled by dolostones in coastal areas.
- Over the last 1 myr, limestones found in the interior of the island have undergone more diagenetic changes than the dolostones found in the coastal regions.
- Dissolution features and high secondary porosities evident in middle to lower parts of the limestone succession reflect diagenetic activity in vadose and/or phreatic zones that took place during sea-level lowstands.
- Pervasive meteoric cements are restricted to upper part of the limestone succession even though the entire succession has been repeatedly placed in the meteoric phreatic zone as sea level has oscillated.
- Dissolution features, which are relatively consistent throughout the limestone succession in the interior of the island cannot be correlated with the cumulative exposure time over the last 1 myr and cannot be specifically matched to any of the numerous transgressive-regressive cycles that have affected the succession.
- The different generations of calcite cement, evident in some parts of the succession, cannot be matched with the multiple cycles of sea-level fluctuations that have passed through the succession.
- The Cayman Formation does not seem to include any diagenetic fabrics that can be attributed to the last transgression that has affect the upper succession over the last

16,000 years.

The diagenetic fabrics evident in the limestones and dolostones of the Cayman Formation do not reflect the ever-fluctuating positions of the diagenetic zones that accompanied the frequent changes in sea level over the last 1 million years. This is due largely to the fact that diagenesis was controlled by numerous intrinsic and extrinsic factors that were not directly linked to sea level. The results obtained from this study parallel many of the conclusions that have been obtained from the study of young carbonate successions found on other islands in the Caribbean Sea and Pacific Ocean.

References

Aissaoui, D.M., Buigues, D., Purser, B.H., 1986. Model of reef diagenesis: Mururoa atoll, French Polynesia. In: Schroeder, J.H., Purser, B.H. (Eds.), Reef Diagenesis. Springer-Verlag, Berlin, Heidelberg, pp. 27-52.

Beach, D.K., 1995. Controls and effects of subaerial exposure on cementation and development of secondary porosity in the subsurface of Great Bahama Bank. In: Budd, D.A., Saller, A.H., Harris, P.M. (Eds.), Unconformities and Porosity in Carbonate Strata. Association of American Petroleum Geologists, Memoir 63, pp. 1-33.

Blanchon, P., Jones, B., 1995. Marine-planation terraces on the shelf around Grand Cayman: A result of stepped Holocene sea-level rise. Journal of Coastal Research 11, 1-33.

Braithwaite, C.J.R., Camoin, G.F., 2011. Diagenesis and sea-level change: lessons from Moruroa, French Polynesia. Sedimentology 58, 259-284.

Buchbinder, L.G., Friedman, G.M., 1980. Vadose, phreatic, and marine diagenesis of Pleistocene-Holocene carbonates in a borehole; Mediterranean coast of Israel. Journal of Sedimentary Research 50, 395-407.

Budd, D.A., 1997. Cenozoic dolomites of carbonate islands: Their attributes and origin. Earth-Science Reviews 42, 1-47.

Budd, D.A., Land, L.S., 1990. Geochemical imprint of meteoric diagenesis in Holocene ooid sands, Schooner Cays, Bahamas; correlation of calcite cement geochemistry with extant groundwaters. Journal of Sedimentary Research 60, 361-378.

Budd, D.A., Vacher, H.L., 1991. Predicting the thickness of fresh-water lenses in carbonate paleo-islands. Journal of Sedimentary Research 61, 43-53.

Cant, R.V., Weech, P.S., 1986. A review of the factors affecting the development of Ghyben-Hertzberg lenses in the Bahamas. Journal of Hydrology 84, 333-343.

Clark, P.U., Dyke, A.S., Shakun, J.D., Carlson, A.E., Clark, J., Wohlfarth, B., Mitrovica, J.X., Hostetler, S.W., McCabe, A.M., 2009. The last glacial maximum. Science 325, 710-714.

Der, A., 2012. Depositon and sea level fluctuation during Miocene times, Grand Cayman,

British West Indies. Unpublished M.Sc. thesis, University of Alberta, 101 pp.

Ginsberg, R.N., Marszalek, D.S., Schneidermann, N., 1971. Ultrastructure of carbonate cements in a Holocene algal reef of Bermuda. Journal of Sedimentary Research 41, 472-482.

Gupta, B.K.S., 2003. Modern Foraminifera. Springer, Netherlands, 371 pp.

Hardie, L.A., Bosellini, A., Goldhammer, R.K., 1986. Repeated subaerial exposure of subtidal carbonate platforms, Triassic, northern Italy: Evidence for high frequency sea level oscillations on a 104 year scale. Paleoceanography 1, 447-457.

Hunter, I.G., 1994. Modern and ancient coral associations of the Cayman Islands. Unpublished Ph.D. thesis, University of Alberta, 345 pp.

Jacobson, G., Hill, P.J., 1980. Hydrogeology of a raised coral atoll–Niue Island, South Pacific Ocean. BMR Journal of Australian Geology and Geophysics 5, 271-278.

James, N.P., Ginsburg, R.N., Marszalek, D.S., Choquette, P.W., 1976. Facies and fabric specificity of early subsea cements in shallow Belize (British Honduras) reefs. Journal of Sedimentary Research 46, 523-544.

Jones, B., 1992. Caymanite, a cavity-filling deposit in the Oligocene Miocene Bluff Formation of the Cayman Islands. Canadian Journal of Earth Sciences 29, 720-736.

Jones, B., Hunter, I.G., 1989. The Oligocene-Miocene Bluff Formation on Grand Cayman. Caribbean Journal of Science 25, 71-85.

Jones, B., Hunter, I.G., 1994a. Evolution of an isolated carbonate bank during Oligocene, Miocene and Pliocene times, Cayman Brac, British West Indies. Facies 30, 25-50.

Jones, B., Hunter, I.G., 1994b. Messinian (late Miocene) karst on Grand Cayman, British West Indies; an example of an erosional sequence boundary. Journal of Sedimentary Research 64, 531-541.

Jones, B., Luth, R.W., 2003. Temporal evolution of tertiary dolostones on Grand Cayman as determined by $^{87}Sr/^{86}Sr$. Journal of Sedimentary Research 73, 187-205.

Jones, B., Hunter, I., Kyser, K., 1994a. Revised Stratigraphic nomenclature for Tertiary strata

of the Cayman Islands, British West Indies. Caribbean Journal of Science 30, 53-68.

Jones, B., Hunter, I., Kyser, T., 1994b. Stratigraphy of the Bluff Formation (Miocene-Pliocene) and the newly defined Brac Formation (Oligocene), Cayman Brac, British West Indies. Caribbean Journal of Science 30, 30-51.

Jones, B., Luth, R.W., MacNeil, A.J., 2001. Powder X-ray diffraction analysis of homogeneous and heterogeneous sedimentary dolostones. Journal of Sedimentary Research 71, 790-799.

Land, L.S., Goreau, T.F., 1970. Submarine lithification of Jamaican reefs. Journal of Sedimentary Research 40, 457-462.

Li, R., Jones, B., 2013. Heterogeneous diagenetic patterns in the Pleistocene Ironshore Formation of Grand Cayman, British West Indies. Sedimentary Geology 294, 251-265.

Liang, T., Jones, B., 2014. Deciphering the impact of sea-level changes and tectonic movement on erosional sequence boundaries in carbonate successions: A case study from Tertiary strata on Grand Cayman and Cayman Brac, British West Indies. Sedimentary Geology 305, 17-34.

Lighty, R.G., 1985. Preservation of internal reef porosity and diagenetic sealing of submerged early Holocene barrier reef, southeast Florida shelf. In: Schneidermann, N., Harris, P.M. (Eds.), Carbonate Cements. Society of Economic Paleontologists and Mineralogists Special Publication 36, pp. 123-151.

Lisiecki, L.E., Raymo, M.E., 2005. A Pliocene-Pleistocene stack of 57 globally distributed benthic $\delta^{18}O$ records. Paleoceanography 20, 1-17. Doi:10.1029/2004PA001071.

Longman, M.W., 1980. Carbonate diagenetic textures from nearsurface diagenetic environments. American Association for Petroleum Geologists, Bulletin 64, 461-487.

Marshall, J.F., 1986. Regional distribution of submarine cements within an epicontinental reef system: central Great Barrier Reef, Australia. In: Schroeder, J.H., Purser, B.H. (Eds.), Reef Diagenesis. Springer-Verlag, Berlin, Heidelberg, pp. 8-26.

Mather, J.D., 1971. A preliminary survey of the groundwater resources of the Cayman Islands

with recommendations for their development. Institute of Geological Sciences, London, 91 pp.

Matley, C.A., 1926. The geology of the Cayman Islands, British West Indies, and their relations to the Bartlett Trough. Quarterly Journal of the Geological Society of London 82, 352-387.

Matthews, R.K., Frohlich, C., 1987. Forward modeling of bank-margin carbonate diagenesis. Geology 15, 673-676.

Melim, L.A., 1996. Limitations on lowstand meteoric diagenesis in the Pliocene-Pleistocene of Florida and Great Bahama Bank: Implications for eustatic sea-level models. Geology 24, 893-896.

Melim, L.A., Swart, P.K., Maliva, R.G., 1995. Meteoric-like fabrics forming in marine waters: Implications for the use of petrography to identify diagenetic environments. Geology 23, 755-758.

Melim, L.A., Westphal, H., Swart, P.K., Eberli, G.P., Munnecke, A., 2002. Questioning carbonate diagenetic paradigms: evidence from the Neogene of the Bahamas. Marine Geology 185, 27-53.

Miller, K.G., Kominz, M.A., Browning, J.V., Wright, J.D., Mountain, G.S., Katz, M.E., Sugarman, P.J., Cramer, B.S., Christie-Blick, N., Pekar, S.F., 2005. The Phanerozoic record of global sea-level change. Science 310, 1293-1298.

Naish, T.R., Wilson, G.S., 2009. Constraints on the amplitude of Mid-Pliocene (3.6-2.4 Ma) eustatic sea-level fluctuations from the New Zealand shallow-marine sediment record. Philosophical Transactions of the Royal Society of London A 367, 169-187.

Ng, K.C., Jones, B., 1995. Hydrogeochemistry of Grand Cayman, British West Indies: implications for carbonate diagenetic studies. Journal of Hydrology 164, 193-216.

Ng, K.C., Jones, B., Beswick, R., 1992. Hydrogeology of Grand Cayman, British West Indies; a karstic dolostone aquifer. Journal of Hydrology 134, 273-295.

Peltier, W.R., Fairbanks, R.G., 2006. Global glacial ice volume and Last Glacial Maximum duration from an extended Barbados sea level record. Quaternary Science Reviews 25,

3322-3337.

Pleydell, S.M., Jones, B., Longstaffe, F.J., Baadsgaard, H., 1990. Dolomitization of the Oligocene-Miocene Bluff Formation on Grand Cayman, British West Indies. Canadian Journal of Earth Sciences 27, 1098-1110.

Quinn, T.M., 1991. Meteoric diagenesis of Plio-Pleistocene limestones at Enewetak atoll. Journal of Sedimentary Research 61, 681-703.

Quinn, T.M., Matthews, R.K., 1990. Post-Miocene diagenetic and eustatic history of Enewetak Atoll: Model and data comparison. Geology 18, 942-945.

Rohling, E.J., Foster, G.L., Grant, K.M., Marino, G., Roberts, A.P., Tamisiea, M.E., Williams, F., 2014. Sea-level and deep-sea-temperature variability over the past 5.3 million years. Nature 508, 477-482.

Schroeder, J.H., 1972. Fabrics and sequences of submarine carbonate cements in Holocene Bermuda cup reefs. Geologische Rundschau 61, 708-730.

Sherman, C.E., Fletcher, C.H., Rubin, K.H., 1999. Marine and meteoric diagenesis of Pleistocene carbonates from a nearshore submarine terrace, Oahu, Hawaii. Journal of Sedimentary Research 69, 1083-1097.

Siddall, M., Rohling, E.J., Almoogi-Labin, A., Hemleben, Ch., Meischner, D., Schmelzer, I., Smeed, D.A., 2003. Sea-level fluctuations during the last glacial cycle. Nature 423, 853-858.

Spratt, R.M., Lisiecki, L.E., 2016. A Late Pleistocene sea level stack. Climate of the Past 12, 1079-1092.

Steinen, R.P., 1974. Phreatic and vadose diagenetic modification of Pleistocene limestone: petrographic observations from subsurface of Barbados, West Indies. American Association of Petroleum Geologists, Bulletin 58, 1008-1024.

Steinen, R.P., Matthews, R.K., 1973. Phreatic vs. vadose diagenesis: stratigraphy and mineralogy of a cored borehole on Barbados, W.I. Journal of Sedimentary Research 43, 1012-1020.

Thorstenson, D.C., Mackenzie, F.T., Ristvet, B.L., 1972. Experimental vadose and phreatic cementation of skeletal carbonate sand. Journal of Sedimentary Research 42, 162-167.

Vacher, L.H.L., 1997. Introduction: varieties of carbonate islands and a historical perspective. In: Vacher, H.L., Quinn, T.M. (Eds.), Geology and Hydrogeology of Carbonate Islands. Elsevier Science, pp. 1-34.

Vézina, J., Jones, B., Ford, D., 1999. Sea-level highstands over the last 500,000 years: Evidence from the Ironshore formation on Grand Cayman, British West Indies. Journal of Sedimentary Research 69, 317-327.

Vollbrecht, R., 1990. Marine and meteoric diagenesis of submarine Pleistocene carbonates from the Bermuda Carbonate Platform. Carbonates and Evaporites 5, 13-96.

Vollbrecht, R., Meischner, D., 1996. Diagenesis in coastal carbonates related to Pleistocene sea level, Bermuda Platform. Journal of Sedimentary Research 66, 243-258.

Wheeler, C., Aharon, P. 1997. Chapter 17 Geology and hydrogeology of Niue. In: Vacher, H.L., Quinn, T.M. (Eds.), Geology and Hydrogeology of Carbonate Islands. Elsevier Science, Amsterdam, Netherlands, pp. 537-564.

Whitaker, F., Smart, P., Hague, Y., Waltham, D., Bosence, D., 1997. Coupled two-dimensional diagenetic and sedimentological modeling of carbonate platform evolution. Geology 25, 175-178.

Whitaker, F.F., Paterson, R.J., Johnston, V.E., 2006. Meteoric diagenesis during sea-level lowstands: Evidence from modern hydrochemical studies on northern Guam. Journal of Geochemical Exploration 89, 420-423.

Willson, E.A., 1998. Depositional and diagenetic features of the Middle Miocene Cayman Formation, Roger's Wreck Point, Grand Cayman, British West Indies. Unpublished M.Sc. thesis, University of Alberta, 103 pp.

Zhao, H., Jones, B., 2012. Origin of "island dolostones": A case study from the Cayman Formation (Miocene), Cayman Brac, British West Indies. Sedimentary Geology 24, 191-206.

CHAPTER FOUR

CENOZOIC ISLAND DOLOSTONES WORLDWIDE AND THE APPLICABILITY OF THE CAYMAN DOLOMITIZATION MODEL[1]

1. Introduction

The origin of dolostone has long been a matter of debate because the processes and conditions that lead to dolomitization are still poorly understood. Budd (1997) suggested that "island dolomites", which are Cenozoic dolostone successions found on isolated oceanic islands, atolls, or platforms throughout the world, offer ideal natural laboratories for resolving the dolomite problem. As noted by Budd (1997), the advantages in studying these dolostones is that they are relatively young, have not been buried, and the conditions under which dolomitization took place can be reasonably inferred from the present-day conditions. Accordingly, these Cenozoic island dolostones, which are commonly over 100 m thick (e.g., Little Bahama Bank, Cayman Islands), provide an opportunity for resolving some of the issues that are inherent to the dolomite problem.

Previous studies, including those by Land (1973, 1991), Saller (1984), Aharon et al. (1987), Dawans and Swart (1988), and Swart and Melim (2000), have described many aspects of island dolomites in an effort to develop models that would explain the process of dolomitization. Much of this work focused on stratigraphic variations because most of these island dolostones have been characterized on the basis of information from a single well or isolated surface outcrops. Thus, little attention has been paid to geographic variations in the dolostones and this aspect has generally not been factored into any of the dolomitization models that have been proposed for the formation of island dolostones (e.g., Braithwaite, 1991). Ren and Jones (2017), based on the investigation of Miocene dolostones from the subsurface of Grand Cayman, demonstrated that there are clearly defined geographic

---

1 This chapter is submitted as: Ren M., Jones B., [submitted]. New insights into Cenozoic island dolostones: geometries, and spatial variations. Sedimentary Geology.

variations in many aspects of the dolostones (e.g., dolomite stoichiometry, stable isotope compositions) that are commonly evident over distances of less than 2 km.

The fact that many Cenozoic island dolostones share petrographic and geochemical attributes in common suggests that they have probably developed under similar conditions and possibly are unified under a common dolomitization model. Previous studies that have used the same principle to develop such dolomitization models have been based largely on stratigraphic (i.e., time) variations in the dolostone successions and have taken little consideration of the issue of geographic variations. The model proposed by Ren and Jones (2017), if valid, means that dolomitization models for pervasively dolomitized successions that are based solely on samples that came from one well or outcrop through that succession are open to question.

This study re-evaluates island dolostones worldwide from the perspective of the Cayman model that takes into account geographic variations in the dolomite petrography, stoichiometry and stable isotopic geochemistry. It demonstrates that the Cayman model is applicable to many Cenozoic island dolostone successions, particularly those where dolomitization was mediated by seawater. This work clearly shows that the geographic locations of dolostone samples relative to the coast should be carefully evaluated when developing a model to interpret the origin of these dolostone bodies.

2. Database

Cenozoic island dolomites have been found on many islands in the Caribbean Sea (e.g., Cayman Islands, Jamaica, Curacao, Bonaire, St. Croix, Barbados, Yucatan), the Atlantic Ocean (the Bahamas), the Pacific Ocean (e.g., Enewetak Atoll, Niue Island, Cook Islands, Mururoa Atoll, Funafuti, Midway), the Philippine Sea (Kita-daito-jima), and the South China Sea (Xisha Islands) (Table 4.1; Fig. 4.1; see also Budd, 1997, his Table 2). These islands range in size from tens of square kilometers (e.g., Cayman Brac) to over a hundred thousand square kilometers (e.g., the Great Bahama Bank), with most being small (< 2000 km2) or

Table 4.1. Cenozoic island dolostones and dolomitic limestones.

Island	Formation/ Dolomite strata	#Wells/ outcrops or area	Approx. distance from samples to island edge (km)	Age	References
Group A - Extensive dolostone bodies below/on island, pervasive dolomitization					
(A1: Dolostones from >1 well/location, island-wide variations demonstrated)					
Grand Cayman	Cayman Fm.	21	0-4	E.–M. Mio.	Jones (1989); Ng (1990); Pleydell and Jones (1991); Jones and Luth (2002, 2003a, b); Ren and Jones (2016, 2017)
Cayman Brac	Cayman Fm.	4	0-1	E.–M. Mio.	Zhao and Jones (2012, 2013a, b)
Little Bahamas Bank	Lower & Upper Dolomite	4	0-20	M. Mio.–Plio.	Vahrenkamp and Swart (1991, 1994)
Mururoa	--	5	0-4	Plio.	Chevalier (1973); Aissaoui et al. (1986)
Kita-daito-jima	Daito Fm.	77	0-2	Plio.	Suzuki et al. (2006); Ohde and Elderfield, 1992
(A2: island-wide variations unknown)					
San Salvador	--	1	<1	L. Mio.–Plio.	Supko (1977); Swart et al. (1987); Dawans and Swart (1988);
Kita-daito-jima	--	1	~2	L. Mio.–Plio.	Schlanger (1963); Berner (1965); Suzuki et al. (2006)
Funafuti	--	--	--	--	Schlanger (1963); Berner (1965);
Xisha Islands	Xuande Fm. / Huangliu Fm.	Xichen-1, Xike-1	<1	M.–L. Mio.	Wei et al. (2006, 2008); Wang et al. (2016)
Group B - Localized or restricted distribution of dolostones/dolomites, pervasive-partial dolomitization					
Bonaire	Seroe Domi Fm.	NW	0-2	Plio.	Deffeyes (1965); Bandoian and Murray (1974); Sibley (1980, 1982); Lucia and Major (1994)
Caracao	Seroe Domi Fm.	SW	0-1	Mio.–Pleist.	Fouke (1994)
Great Bahama Bank	--	Unda	-15 (slope)	E.–M. Mio.	Beach (1993, 1995); Swart and Melim (2000); Melim

Table 4.1. Continued.

					and Swart (2002)
Cayman Brac	Brac Fm.	5	0-1	Olig.	Zhao and Jones (2012a)
Cayman Islands	Pedro Castle Fm.	16	0-2	Plio.	MacNeil (2002); Jones and Luth (2002); MacNeil and Jones (2003)
Niue	--	Fonakula	<1	M.–L. Mio.	Rodgers et al. (1982); Aharon et al. (1987)
Niue	Upper Dolomite	DH4	~3	Plio.	Wheeler et al. (1999)
Group C - Localized or restricted distribution of dolomites, partial dolomitization					
Jamaica	Hope Gate Fm.	N coast	0-3	L.Plio.–E.Pleist.	Land (1973, 1991, 1994)
Yucatan	--	K274	~2	L. Pleist.	Ward and Halley (1984)
Enewetak	--	F-1	<1	Eocene	Schlanger (1963); Bener (1965); Saller (1984)
Midway	--	Reef Hole	<1	--	Ladd et al. (1970)
Niue	Lower Dolomite	DH4	~3	L. Mio.	Wheeler et al. (1999)
Aitutaki	--	Hole 2	<1	Pleist.	Hein et al. (1992)
Barbados	--	Golden Grove	<2	L. Pleist.	Humphrey (1988, 2000); Humphrey and Radjef (1991); Machel et al. (1994, 2000)
St. Croix	--	Krause Lagoon	0-2	Plio.	Gill et al. (1995)

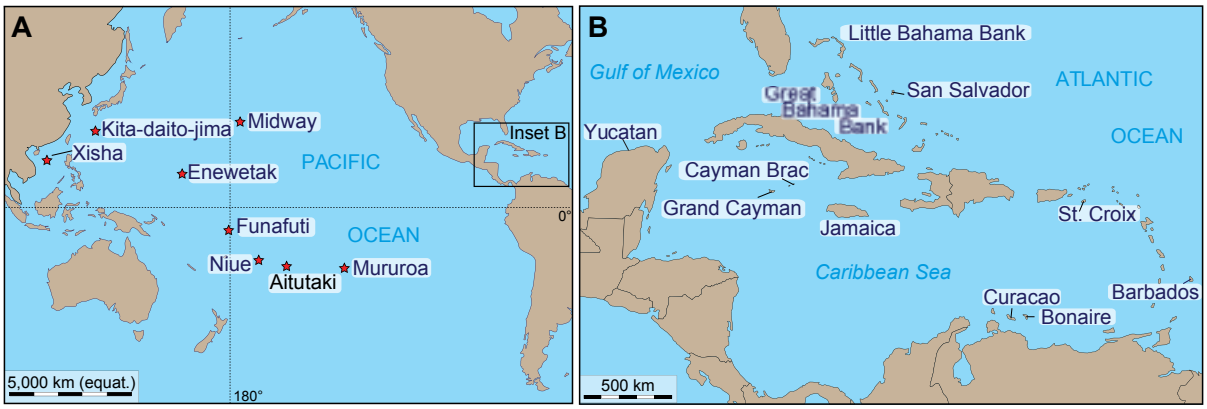

Fig. 4.1. Location of islands with Cenozoic island dolostones.

very small islands (< 100 km^2) if the classification system of Vacher (1997) is used. Island widths range from ~2 km (e.g., Kita-daito-jima, Cayman Brac) to over 100 km (the Great Bahama Bank). Most studies on island dolomites have been focused on shallow samples collected from outcrops and cores to depths of ~100 m, although deep drillings have revealed Cenozoic dolomites to up to 300 m below sea level on some Pacific atolls (e.g., Funafuti, Midway), to ~600 m on the Great Bahama Bank, and to a depth of 1400 m on Enewetak (e.g., Ladd et al, 1970; Saller, 1984; Swart and Melim, 2000).

The data available from these island dolomite successions is highly variable in all respects. For this study, preference is given to thick successions of dolostones that are geographically widespread and have been well characterized stratigraphically, petrographically, and geochemically. These include, for example, the surface to subsurface dolomites found on Grand Cayman, Cayman Brac, the Little Bahama Bank, Kita-daito-jima, and Mururoa. Less emphasis is placed on geographically restricted dolostones that display little lateral variation at a kilometer scale.

This study is based on data from three major resources (Table 4.1). Data for the Cayman Islands comes from the same database that was used by Pleydell et al. (1990), Jones and Luth (2001, 2002, 2003a, b), MacNeil and Jones (2003), Zhao and Jones (2012, 2013a, b), and Ren and Jones (2016, 2017). Most of the data for the other islands comes from the tables, appendices, and reports that have documented those successions. Where datasets were not supplied, data was extracted from the figures used in the papers. Although errors do

arise with respect to the last group of data, they are estimated to be < 5%. Errors arising from different analytical techniques and laboratories are inevitable with this approach, but careful evaluation of these data before use means that the errors are minimal.

3. Extent of dolomitization

The extent of dolomitization in island dolomites is highly variable. For the purpose of this study, island dolostones are divided into three groups based primarily on the extent of dolomitization and the availability of dolomite data (Table 4.1). Group A includes those islands with thick, geographically widespread dolostone bodies that provide evidence of pervasive dolomitization. In this group, patterns of lateral variations in the dolomite properties is demonstrated for those islands with sufficient data (A1), whereas this variability is unknown in other samples (A2). Group B includes islands where dolomitization was not pervasive and the lithologies include dolostones, dolomitic limestone, and limestone. Group C includes islands where the dolomitization was highly localized and did not fully replace the original limestones. In general, those islands with pervasively dolomitized successions (Group A) are less common than those with localized dolomitization. When the island carbonates are partially dolomitized, the dolostones are more common in the coastal areas than in the center of the island. Budd (1997) pointed out that "… partial dolomitization should be focused towards the periphery of an island, atoll or platform, and also extensive massive dolomites could occur below older limestones". This situation is well illustrated by the Cayman Formation on the eastern part of Grand Cayman (Ren and Jones, 2017) and on The Great Bahama Bank (Beach, 1993, 1995) where limestone and dolomite at the margins grade into limestone in the bank interior.

There is no uniform stratigraphic relationship between the extent of dolomitization and the age of the formations. On some islands, the older, deeper parts of the succession are less dolomitized than the younger, overlying strata. Examples of this architecture include, for example, Cayman Brac where the partly dolomitized Brac Formation (Oligocene) is overlain

by the pervasively dolomitized Cayman Formation; Niue where the partly dolomitized Lower Dolomites (Late Miocene) are overlain by the pervasively dolomitized Upper Dolomite (Pliocene) (Wheeler et al., 1999); and Xisha Islands where the absence of dolomite in the Lower Miocene Xisha Formation contrasts with the pervasively dolomitized successions in the overlying Middle Miocene Xuande Formation and Upper Miocene Yongle Formation (Wei et al., 2006).

4. Diagenetic fabrics

Cenozoic island dolostones are commonly fabric-retentive with evidence of the original depositional fabrics clearly visible (e.g., Sibley, 1982). On island-wide scales, diagenetic fabrics commonly range from fabric-retentive to fabric-destructive (e.g., Vahrenkamp and Swart, 1994; Ren and Jones, 2017). The dolostone fabrics have been classified in different ways. Budd (1997), for example, divided island dolostones into mimetic, non-mimetic but texture preserving, and non-mimetic and texture destroying. In contrast, dolostones on the Bahamas Bank (Dawans and Swart, 1984; Vahrenkamp and Swart, 1994), Niue (Wheeler et al., 1999) and Kita-daito-jima (Suzuki et al., 2006) have been

---

Fig. 4.2. Dolomite stoichiometry, and stable isotopes of island dolostones throughout the world (see Fig. 4.1 for locations). CB: Cayman Brac, GC(W): Grand Cayman (west), GC(E): Grand Cayman (east). PD: Peripheral Dolostone, TD: Transitional Dolostone, ID: Interior Dolostone, IL: Interior Dolomitic Limestone. GB1, WC, GB2, SC, Clino, Unda, DH4, and Fonuakula are wells on the islands. Data source: Cayman Formation, Cayman Islands (Jones and Luth, 2002; Zhao and Jones, 2012a; Ren and Jones, 2017); Mururoa (Aissaoui et al. 1986); Daito Formation, Kita-daito-jima (Suzuki et al., 2006); Little Bahama Bank (Vahrenkamp and Swart, 1994); San Salvador (Supko, 1977); Kita-daito-jima (Mio.) (Suzuki et al., 2006); Xuande Formation, Xisha (Wei et al., 2006); Bonaire (1) (Sibley, 1980); Bonaire (2) (Lucia and Major, 1994); Curacao and Curacao Dol II (Fouke, 1994); Pedro Castle Formation, Cayman Brac (MacNeil, 2002; MacNeil and Jones, 2003); Great Bahama Bank (Swart and Melim, 2000); Aitutaki (Hein et al., 1992); Niue Upper Dolomite (DH4) (Wheeler et al., 1999); Niue Upper Dolomite (Fonuakula) (Aharon et al., 1987); Jamaica (Land, 1973, 1991); Enewetak (Saller, 1984); Niue Lower Dolomite (Wheeler et al., 1999); Yucatan (Ward and Halley, 1984), Barbados (Humphrey, 1988; Machel, 1994), St. Croix (Gill et al., 1995).

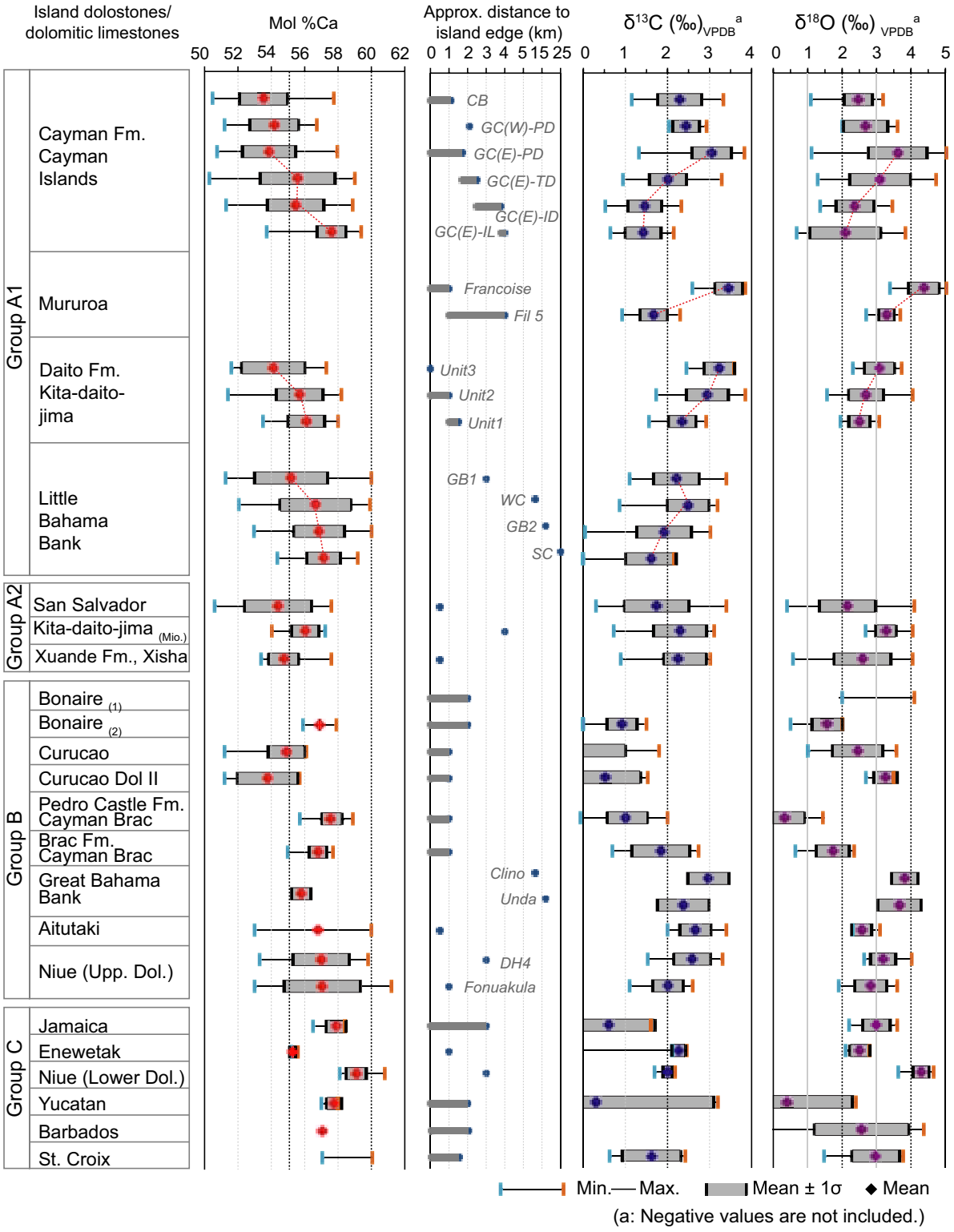
Island dolostones/ dolomitic limestones
Mol %Ca
Approx. distance to island edge (km)
δ13C (‰)VPDB a
δ18O (‰) VPDB a
Group A1
Cayman Fm. Cayman Islands
Mururoa
Daito Fm. Kita-daito-jima
Little Bahama Bank
Group A2
San Salvador
Kita-daito-jima (Mio.)
Xuande Fm., Xisha
Group B
Bonaire (1)
Bonaire (2)
Curucao
Curucao Dol II
Pedro Castle Fm. Cayman Brac
Brac Fm. Cayman Brac
Great Bahama Bank
Aitutaki
Niue (Upp. Dol.)
Group C
Jamaica
Enewetak
Niue (Lower Dol.)
Yucatan
Barbados
St. Croix
CB
GC(W)-PD
GC(E)-PD
GC(E)-TD
GC(E)-ID
GC(E)-IL
Francoise
Fil 5
Unit3
Unit2
Unit1
GB1
WC
GB2
SC
Clino
Unda
DH4
Fonuakula
Min.— Max.
Mean ± 1σ
◆ Mean
(a: Negative values are not included.)

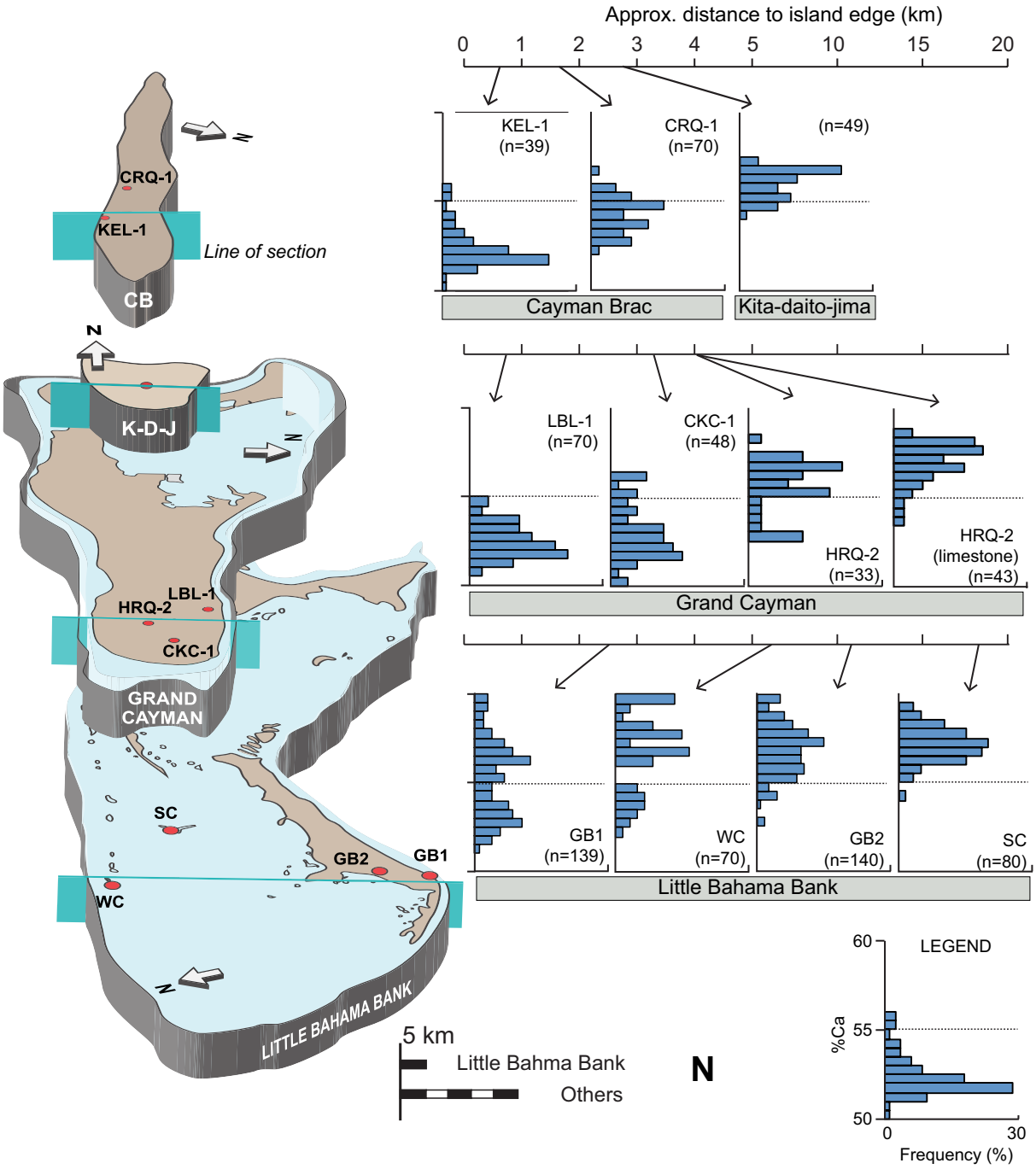

Fig. 4.3. Geometry and size of the dolostone bodies and landward decrease in the dolomite stoichiometry in island dolostones from Cayman Brac (CB, Miocene Cayman Formation), Kita-daito-jima (K-D-J, Pliocene Daito Formation), Grand Cayman (Miocene Cayman Formation), and Little Bahama Bank (Miocene-Pliocene) along line of section indicated on island. Data source: Cayman Brac (Zhao and Jones, 2012a), Kita-daito-jima (Suzuki et al., 2006), Grand Cayman (Ren and Jones, 2017), and Little Bahama Bank (Vahrenkamp and Swart, 1994).

classified as crystalline mimetic (CM), crystalline microsucrosic (CMS), crystalline non-mimetic (CNM), and microsucrosic (MS) dolomites.

Geographic variations in fabrics of the dolostones are apparent in the sequences on many group A1 dolostone islands (Table 4.1) including Little Bahama Bank, Mururoa, Niue, and Grand Cayman. In the pervasively dolomitized bodies, dolostones from the coastal areas tend to have better preserved depositional fabrics than the dolostones from the interior of the island. In the Cayman Formation on the east end of Grand Cayman, for example, there is a gradual change from fabric retentive fabrics in the coastal areas to fabric destructive fabrics in the interior of the island (Ren and Jones, 2017). Similar transitions are also apparent in the Cayman Formation on the western part of Grand Cayman (Jones and Luth, 2002). In contrast, only fabric-retentive dolostones are evident in the Cayman Formation on Cayman Brac, which is only ~3 km wide (Zhao and Jones, 2012a). On the Little Bahama Bank, crystalline mimetic dolomites are more common near the bank margins and there is a gradual change to microsucrosic dolostone inland (Vahrenkamp and Swart, 1994). On some islands, there is also a landward decrease in the amount of dolomite cement. This is well illustrated on Mururoa (Aissaoui et al., 1986) where void-lining dolomite cement or overgrowths on replacive dolomites (Type 2 dolomite in Aissaoui et al., 1986), is best developed in the hard-crystalline dolostones found around the coast of the island.

In other dolostone bodies (groups A2, B, and C; Table 4.1) where geographic variation in the dolostone petrography is unknown, their diagenetic fabrics seem to be related to their geographic and stratigraphic locations. Examples of fabric retentive dolostones include those in the (1) Pliocene dolostones from the coastal area of San Salvador (Dawans and Swart, 1988), (2) Pleistocene dolostones from Hole 2 drilled in the coastal area of Aitutaki (Hein et al., 1992), (3) Upper Miocene dolostones from Xisha Islands (Wei et al., 2008, their Fig. 5; Wang et al., 2016, their Figs. 4, 5), (4) dolostones in the Seroe Domi Formation (Pliocene) on Bonaire and Curacao (Sibley, 1980; Fouke, 1994), (5) Upper Dolomites (Pliocene) from Niue (Wheeler et al., 1999), and (6) Pedro Castle Formation (Pliocene) from the Cayman Islands

(MacNeil and Jones, 2003). These samples demonstrate that fabric-retentive dolostones are commonly found in the shallow coastal areas of a pervasively dolomitized island-wide successions. Dolostones with fabric destructive fabrics are found in the interior of the islands, including those from a well drilled in the interior of Kita-daito-jima (Suzuki et al., 2006), in the incompletely dolomitized limestones in the Oligocene dolomites from the Brac Formation on Cayman Brac (Zhao and Jones, 2012), in the Lower Dolomites (Miocene) on Niue (Wheeler et al., 1999), in the deep part of the succession on Enewetak (1250 m below surface; Saller et al., 1984), and the Miocene dolostones on San Salvador (110 m below surface; Dawans and Swart, 1988). In all cases, these fabric-destructive dolostone samples are overlain by dolostones that are characterized by fabric retentive fabrics (i.e., Pliocene dolomites above Miocene dolomites from Kita-daito-jima, Upper Dolomite above the Lower Dolomite from Niue, Cayman Formation above Brac Formation from Cayman Islands, and Pliocene dolomites above Miocene dolomites from San Salvador, respectively). In general, the distribution of these fabric-destructive dolostone samples seem to suggest that the original depositional fabrics evident in the deeper and/or interior dolostones on the islands are less well preserved than in the overlying younger, coastal dolostones.

In most Cenozoic island dolostones, the dolomite crystals are generally up to ~2 mm long (Budd, 1997). In the Caymanian and Bahamian dolostones, crystal size is correlated, to some extent, with the diagenetic fabrics (cf., Dawans and Swart, 1988; Vahrenkamp and Swart, 1994; Zhao and Jones, 2012). Thus, the fabric destructive dolostones tend to be formed of larger crystals (100–200 μm in the crystalline non-mimetic Bahamian dolostones; 50–1500 μm in the dolostones of the Brac Formation from Cayman Brac) than in the fabric retentive dolostones (10–60 μm of the crystalline mimetic and microsucrosic Bahamian dolomites; 10–20 μm of the dolostones of Cayman Formation from Cayman Brac).

5. Stoichiometry

Cenozoic dolomite always contain excess calcium with molar %$CaCO_3$ (hereafter

refer to %Ca) >50% (Figs. 4.2, 4.3). Based on the %Ca, many of the island dolostones are composed of more than one population of dolomite (e.g., Vahrenkamp and Swart, 1994; Jones et al., 2001), with each group being characterized by different crystal microstructures (e.g., Jones, 2013). This includes, for example, two populations (LCD: low calcium dolomite, %Ca <55%; HCD: high calcium dolomite, %Ca >55%) in the dolostones of the Cayman Islands (Jones et al., 2001), three populations in the dolostones from Niue (Wheeler et al., 1999), and four populations in the dolostones from Kita-daito-jima (Suzuki et al., 2006).

5.1. Variations in stoichiometry in extensively dolomitized bodies

Lateral variations in dolomite stoichiometry are observed in the large dolostone bodies. Dolomites from the Cayman Formation (Miocene) on Grand Cayman, the Pliocene–Miocene dolostones on Little Bahama Bank, and the Pliocene dolostones on Kita-daito-jima (Figs. 4.2, 4.3). can be divided into several zones with each being characterized by dolostones with different %Ca.

5.1.1. Cayman Formation (Miocene), Grand Cayman

Based on the LCD-HCD compositions of the dolostones, the Cayman Formation on the east end of Grand Cayman is divided concentrically into the peripheral dolostone, transitional dolostone, interior dolostone, and interior dolomitic limestone zones (Ren and Jones, 2017). In the peripheral zone, the dolostones are formed largely of LCD (average 71%) with an average %Ca of 53.9%. Inland, the average %LCD in the dolostones progressive decreases to 38% and the average %Ca increases to 55.5% (Table 4.2; Figs. 4.2, 4.3). These variations take place over a distance of less than 4 km. In the interior, dolomite in the interior dolomitic limestones is entirely of HCD with an average %Ca 57.6%.

The lateral variations in the dolomite stoichiometry are also evident on the western part of Grand Cayman. There, the dolostones in the Cayman Formation in wells STW, SHT-2, SHT-3, and SHT-5, drilled at the Sewerage Works site <2.0 km from the west coast

Table 4.2. Dolomite stoichiometry, stable isotopes, and interpreted (equivalent) geographic zones of dolostones and dolomitic limestones from the Brac Formation, Cayman Formation, Pedro Castle Formation, and Ironshore Formation on Grand Cayman and Cayman Brac. (PD = peripheral dolostone, TD = transitional dolostone, ID/L = interior dolostone / dolomitic limestone)

Formation	Location (Extent of dolomitization)	Geographic Zone (Equivalent)	% LCD> HCD samples	%LCD range (mean ± 1σ)	%Ca range (mean ± 1σ)	$\delta^{18}O$ (‰) range (mean ± 1σ)	$\delta^{13}C$ (‰) range (mean ± 1σ)	#Well/ XRD	#Well/ Isotopes
Ironshore	Cayman Islands (Rare (<12%) dolomite in Unit A only)								
Pedro Castle	Cayman Brac (Partially dolomitized)	= ID/L?	-- --	-- --	55.85–58.95 (57.67 ± 0.61)	-1.82–1.41 (0.23 ± 0.70)	-0.22–2.02 (1.07 ± 0.55)	3/33	3/33
Cayman	Eastern Grand Cayman (>50% formation dolomitized, complete dolomitized in peripheral and partially in the center)	Peripheral Dolostone	79.3	0-100 (71 ± 30)	50.75–57.96 (53.86 ± 1.66)	1.11–5.03 (3.62 ± 0.85)	1.32–3.83 (3.05 ± 0.47)	7/421	4/105
		Transitional Dolostone	74.2	0-100 (39 ± 38)	50.29–59.01 (55.58 ± 2.25)	1.29–4.73 (3.10 ± 0.88)	0.94–3.29 (2.01 ± 0.44)	4/190	2/41
		Interior Dolostone	36.0	0-100 (38 ± 32)	51.29–58.88 (55.46 ± 1.73)	1.36–3.46 (2.37 ± 0.55)	0.52–2.33 (1.46 ± 0.40)	8/341	2/36
		Interior Dolomitic Limestone	2.2	0–100 (2.7 ± 13)	53.72–59.39 (57.6 ± 0.86)	0.68–3.84 (2.10 ± 1.03)	0.64–2.15 (1.42 ± 0.43)	8/186	2/24
	Western peripheral GC (Completely dolomitized)	=PD-TD?	75.0	0-100 (60 ± 28)	51.20–56.73 (54.18 ± 1.47)	2.00–3.61 (2.68 ± 0.65)	2.03–2.93 (2.44 ± 0.32)	4/84	4/11
	Cayman Brac (Completely dolomitized)	=PD?	92.3	0–100 (73 ± 21)	50.48–57.75 (53.53 ± 1.45)	1.09–3.19 (2.47 ± 0.41)	1.15–3.33 (2.29 ± 0.52)	4/207	4/53
Brac	Cayman Brac (Partially dolomitized)	(Dolomitic limestone) = ID/L?	0	0-36.7 (2 ± 7.9)	54.98–57.70 (56.79 ± 0.52)	2.0–3.6 (2.8 ± 0.4)	1.5–2.9 (2.4 ± 0.4)	2/32	1/19
		(Dolostone) =ID?	0	0-32 (3 ± 9)	55.0–57.7 (56.6 ± 0.5)	0.64–2.35 (1.73 ± 0.48)	0.69–2.74 (1.84 ± 0.69)	5/41	5/41

(Jones and Luth, 2002; their Fig. 1) are dominated by LCD (average %Ca= 54%, average %LCD=73%, with 93% samples being LCD dominated; Table 4.2). These dolostones are equivalent to the peripheral dolostones on the east end of the island.

5.1.2. Daito Formation (Pliocene), Kita-daito-jima

Dolostones from the Pliocene Daito Formation on Kita-daito-jima have been divided into three laterally arranged units (Unit 3, 2, and 1), from the coast to the island interior (Suzuki et al., 2006). The average %Ca varies from 54% in the coastal area (Unit 3) to 55% in the transitional zone (Unit 2), to 56% in the interior island (Unit 1) (Figs. 4.2, 4.3). The only well in the interior of the island, drilled into Late Miocene to Pliocene (0–100 m below ground surface), shows that the limestones have been completely dolomitized and have a high average %Ca (56%).

5.1.3. Miocene–Pliocene dolostones, Little Bahama Bank

The Miocene–Pliocene dolostones on Little Bahama Bank are formed of dolostones with 51–60 %Ca (Vahrenkamp and Swart, 1994). On a N-S profile that includes four wells, the average %Ca in the dolostones progressively increases landward from ~55% in the coastal well (GB1, ~ 3 km from coastline) to ~56.6% (WC) to ~56.9% (GB2) and ~57% in an interior well (SC, ~25 km from coastline) (Figs. 4.2, 4.3).

5.2. Stoichiometry of dolostones from small islands or localized dolostone bodies

Dolostones collected from small areas (generally < 1 km perpendicular to shelf edge) or from a single well on an island may not show any obvious geographic trends in stoichiometry and it therefore becomes difficult to relate them to the dolostones from larger islands. In these situations, scale is critical with the distance from the shoreline being the most important.

5.2.1. Cayman Formation (Miocene), Cayman Brac

The Cayman Formation on Cayman Brac has been completely dolomitized (Jones et

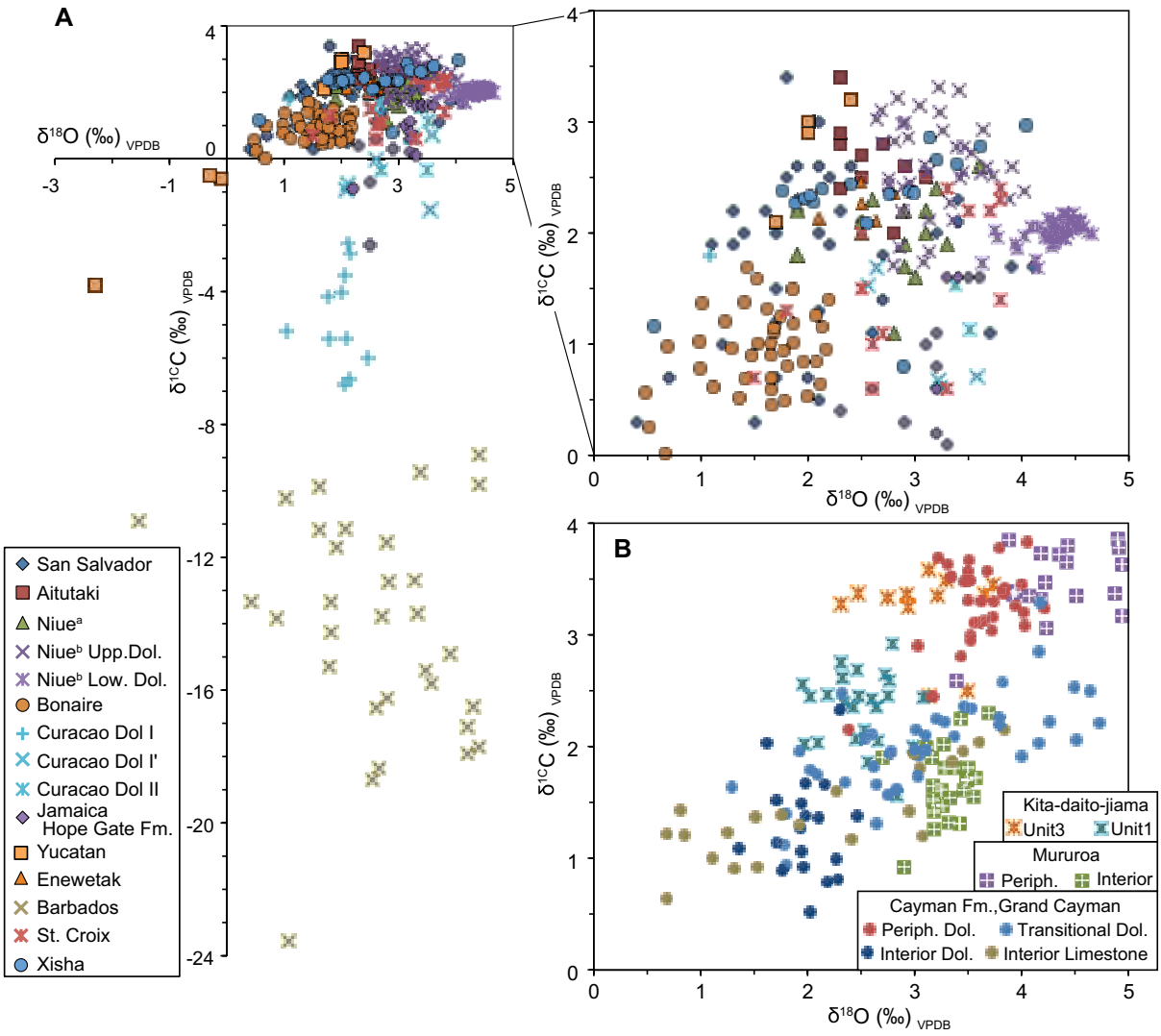

Fig. 4.4. Oxygen and Carbon isotopes of (A) the island dolostones, and (B) dolostones from Grand Cayman (Cayman Formation), Daito Formation (Kita-daito-jima), and Mururoa (Pliocene), grouped by their geographic locations. Note geographic trends and overlaps in the isotope values of the formations from the three islands highlighted in panel B. Shaded areas in (A) represent the isotopic ranges from the three islands in (B). Data source: San Salvador (Supko, 1977), Aitutaki (Hein et al., 1992), Niue[a] (Aharon et al., 1987), Niue[b] Upper Dol. (Wheeler et al., 1999), Niueb Lower Dolomite (Wheeler et al., 1999), Bonaire (Lucia and Major, 1994), Curacao Dol I, I', II (Fouke, 1994), Jamaica Hope Gate Formation (Land, 1973, 1991), Yucatan (Ward and Halley, 1984), Enewetak (Saller, 1984), Barbados (Humphrey, 1988; Machel, 1994), St. Croix (Gill et al., 1995), Xisha (Wei et al., 2008); and Daito Formation, Kita-daito-jima (Suzuki et al., 2006), Mururoa (Aissaoui et al. 1986), Cayman Formation, Grand Cayman (Ren and Jones, 2017).

al, 1994; Zhao and Jones, 2012a). Dolostones from four wells drilled at various locations on this island are formed largely of LCD (up to 92.3% of the dolostones have LCD > HCD, overall average %LCD=73%) and an average of 53.5 ± 1.5 %Ca (n=207) (Zhao and Jones, 2012b) (Figs. 4.2, 4.3). There is no obvious difference in the %Ca between the dolostones in these four wells. In terms of their stoichiometry, all of the dolostones in the Cayman Formation on Cayman Brac are comparable to the peripheral dolostones on Grand Cayman.

5.2.2. A coastal dolostone succession (Upper Miocene–Pliocene), San Salvador

Dolostones from a well drilled on the coast of the San Salvador Island have an average 54.4 ± 2.0 %Ca (50.6–57.6 %Ca, n=38) (Supko, 1977) and are therefore akin, in terms of their stoichiometry, to the dolostones from the peripheral zone in the Cayman Formation on Grand Cayman (Fig. 4.2).

5.2.3. Upper Miocene dolostones, Xisha Islands

In South China Sea, the Middle to Upper Miocene dolostones from Chenhang Island (Xisha Islands) have an average %Ca of 54.8 ± 0.9% (53.7–54.5%, n=19) (Wei et al., 2006). In terms of their stoichiometry, they are similar to the dolostones from the peripheral dolostone found on Grand Cayman, Little Bahama Bank, and Kita-daito-jima.

5.3. Stoichiometry of dolomites in partially dolomitized samples

On many islands, the carbonate sequences are only partially dolomitized. Almost without exception, the dolomite in the incompletely dolomitized samples contain high %Ca (mostly >55%), irrespective of their positions relative to the coast of the island. Specific examples include those in the Brac Formation and Pedro Castle Formation on Cayman Brac, the Cayman Formation in the interior of Grand Cayman, the Hope Gate Formation on north Jamaica, dolostones from the slope of the Great Bahama Bank, and dolostones from subsurface of the Yucatan Peninsula (Fig. 4.2). A negative correlation between the percent dolomite and the %Ca is evident in some samples from the Great Bahama Bank (Swart and

Melim, 2000).

5.3.1. Brac Formation (Oligocene), Cayman Brac

Dolostones in the Brac Formation from Cayman Brac all have more HCD than LCD with 98% of all samples being formed of HCD alone. The average %Ca in these dolostones is 56.8 ± 0.5% (55.0–57.7%, n=32) (Zhao and Jones, 2012b).

5.3.2. Pleistocene dolomites, northeastern coastal Yucatan

On the Yucatan Peninsula, well K274 that was drilled near the coast, includes dolomitic limestones that contain 20–50% dolomite (replacive and cement). The bulk dolomite %Ca ranges from 57–58%, and the dolomite cements have 57–62%Ca (Ward and Halley, 1984).

5.3.3. Dolomite from the slope, Great Bahama Bank

Two deep wells (Clino and Unda) drilled on the western edge of the Great Bahama Bank revealed partial dolomitization of the limestones, ranging from <15% dolomite in Clino to <50% dolomite in Unda (Swart and Melim, 2000; Melim et al., 2002). The dolomite in the dolomitic limestones from both wells is calcium-rich and ranges from 54.2–58.2 %Ca. Swart and Melim (2000) also noted that dolomite stoichiometry increased as the dolomite content increased, although there is a wide range of scatter in the data.

5.3.4. Hope Gate Formation (Pleistocene), north Jamaica

On north Jamaica, the limestones of the Hope Gate Formation have been partly dolomitized with the percentage of dolomite ranging from 45–90% (mean=68 ± 19%, n=13). The dolomite has 57.9 ± 0.6 %Ca (56.5–58.4 %Ca; Land, 1991). There is no relationship between the percent dolomite and the dolomite %Ca.

5.3.5. Miocene and Pliocene dolomites, Niue

A Pliocene succession on west Niue (well Fonuakula) contains 81–100% (mean=89%,

n=16) dolomite (Aharon et al., 1987). These dolostones have an average %Ca of 57.0 ± 2.3% (53.0–61.3%) (Aharon et al., 1987; their Table 1). A Miocene succession on southwest of the island (well DH4) includes limestone with <30% dolomite (Wheeler et al., 1999). The average %Ca of these dolostones is ~59.0 ± 0.5% (58.1–60.6%) (Wheeler et al., 1999; their Fig. 7).

5.3.6. Seroe Domi Formation (Pliocene), Bonaire and Curacao

On the Leeward Antilles, the Seroe Domi Formation contains limestones that have been variably dolomitized. On Bonaire, the formation shows stratiform dolostones with a high %Ca (mean=56.9 %Ca, range from 55.9–57.9 %Ca; Lucia and Major, 1994, their Fig. 13). On Curacao, the Seroe Domi Formation comprises three types of dolomite (I, I', II) that have 55.3 %Ca, 55.0 %Ca, and 53.8 %Ca, respectively (overall 54.9 Ca%) (Fouke, 1994).

5.3.7. Others

Other examples include dolomites from a deep Enewetak succession (3–98% dolomite, Eocene) have an average of 55.3%Ca (n=5) (Saller, 1984), and eight dolostones from Golden Grove on Barbados that have an average of 57%Ca (Humphrey, 1988).

6. Stable isotopes

Most of the island dolostones have positive stable isotope values with $\delta^{13}C$ ranging from 0–4 ‰, and $\delta^{18}O$ from 0–5 ‰ (Table 4.1; Figs. 4.2, 4.4). Exceptions are those with negative $\delta^{13}C$ values like those found in the Seroe Domi Formation (e.g., Fouke, 1994) and the Golden Grove dolostones on Barbados (e.g., Humphrey, 1988; Machel and Burton, 1994). The oxygen and carbon isotopes, like dolomite stoichiometry, typically exhibit geographic variations.

6.1. Variations in stable isotopes in extensively dolomitized bodies

In the geographically widespread dolostones, the heavier oxygen and carbon isotope values generally decrease towards the centers of the islands. This systematic variation is

evident in the dolostones from the Cayman Formation (Grand Cayman), the Pleistocene dolostone on Kita-daito-jima, the Miocene–Pliocene dolostones on the Little Bahama Bank, and the Pliocene dolostones on Mururoa (Figs. 4.2, 4.4).

6.1.1. Cayman Formation (Miocene), Grand Cayman

The average $\delta^{18}O$ values of the dolostones from the peripheral, transitional, and interior dolostone zones are 3.62 ± 0.85‰, 3.10 ± 0.88‰, and 2.37 ± 0.55‰, respectively (Ren and Jones, 2017; Table 4.2). Likewise, the average $\delta^{13}C$ from the dolostones from these three zones are 3.05 ± 0.47‰, 2.01 ± 0.44‰, 1.46 ± 0.40‰, respectively. Dolostones from the interior limestones have even lower $\delta^{18}O$ (2.10 ± 1.03‰) and $\delta^{13}C$ values (1.42 ± 0.43‰) than the pure dolostones from the coastal zones.

6.1.2. Daito Formation (Pliocene), Kita-daito-jima

From the periphery to the island to the interior (Unit 3, 2, and 1, respectively), the average $\delta^{18}O$ ranges from 3.09 ± 0.44‰ (2.31–3.73‰), to 2.69 ± 0.51‰ (1.56–4.05‰), to 2.50 ± 0.31‰ (1.95–3.08‰) (Suzuki et al., 2006). Similarly, the average $\delta^{13}C$ ranges from 3.23 ± 0.36‰ (range 2.45–3.58‰), to 2.95 ± 0.50‰ (range 1.73–3.85‰), to 2.35 ± 0.32‰ (1.56–2.92‰), respectively (Figs. 4.2, 4.4). These values illustrate the progressive landward changes in the stable isotopes.

6.1.3. Miocene–Pliocene dolostones, Little Bahama Bank

On Little Bahama Bank, dolostones from wells GB1, WC, GB2, and SC (in order of increasing distance from bank edge) have $\delta^{13}C$ values of 2.21 ± 0.54‰ (1.10–3.40‰), 2.49 ± 0.49‰ (0.86–3.19‰), 1.92 ± 0.65‰ (0.04–3.02‰), and 1.61 ± 0.60‰ (0–2.16‰), respectively (Vahrenkamp and Swart, 1994). The landward reduction in the $\delta^{13}C$ is readily apparent (Fig. 4.2). Although the $\delta^{18}O$ values of these dolostones were not reported separately for each well, they may follow the same trend as the $\delta^{13}C$.

6.1.4. Pliocene dolostones, Mururoa

On Mururoa, the peripheral dolostones are characterized by higher $\delta^{18}O$ values (mean=4.38 ± 0.45‰, range 3.39–5.03‰) than the interior dolostones (mean=3.29 ± 0.22‰, range 2.70–3.69‰; Figs. 4.2, 4.4). This is also true for the $\delta^{13}C$ values, which have an average of 3.45 ± 0.33‰ (range 2.59–3.85‰) in the peripheral dolostones contrasted to the average of 1.67 ± 0.32‰ (0.92–2.30‰) in the interior dolostones (Aissaoui et al., 1988).

6.2. Stable isotopes of dolostones from small islands or localized dolostone bodies

Dolostones from small or localized dolostone bodies (groups A2 and B) show no particular relationship between the locations of the samples and the dolomite %Ca (Fig. 4.2). This may be scale-related and reflect the fact that on smaller islands with localized dolostone bodies there is little or no lateral variation in the stable isotopes. The dolostones from Cayman Formation on Cayman Brac, for example, have equivalent stoichiometry with the peripheral dolostones on Grand Cayman, but have dissimilar oxygen and carbon isotopes values (Table 4.2). The average $\delta^{18}O$ (2.47 ± 0.41‰) of these dolostones is similar with the interior dolostone whereas the $\delta^{13}C$ (2.29 ± 0.52‰) is comparable to the transitional dolostones on Grand Cayman. Despite this, comparison of the isotopes from different dolostone bodies show that for most island dolostones, those dolostone samples with high or low $\delta^{18}O$ have correspondingly high or low $\delta^{13}C$ values (Fig. 4.2).

6.3. Stable isotopes of dolomite in partially dolomitized samples

The $\delta^{18}O$ and $\delta^{13}C$ of dolomite from the partly dolomitized limestones vary from island to island and from formation to formation. Within the same dolostone body, the partial dolomitized limestones typically have lower $\delta^{18}O$ and $\delta^{13}C$ values than samples formed entirely of dolomite, as demonstrated by the Cayman Formation from Grand Cayman and the Brac Formation from Cayman Brac (Zhao and Jones, 2012b) (Fig. 4.2). No particular $\delta^{18}O$ and $\delta^{13}C$ values or ranges can be assigned to the incompletely dolomitized samples and they show no obvious correlations with the percentage of dolomite in the sample. Despite

the pattern in the Caymanian dolostones, available data from other partial dolomitized bodies shows that partial dolomitization does not necessarily translate into low $\delta^{18}O$ and $\delta^{13}C$ values, as is shown by the Hope Gate Formation from north Jamaica and the Lower Dolomites from Niue. Both of the examples are from the peripheral areas of islands and have isotopic values that are comparable with the peripheral dolomites on Grand Cayman.

7. Case study: comparisons between the Cenozoic dolostones, Grand Cayman and Cayman Brac

The exposed carbonate succession on the Cayman Islands comprises the Brac Formation (Oligocene, ~33 m thick), the Cayman Formation (Early–Middle Miocene, ~100–140 m thick), and the Pedro Castle Formation (Pliocene, ~15–20 m thick), which collectively belong to the Bluff Group. The Ironshore Formation (Pleistocene) unconformable overlies the Bluff Group. The distribution and attributes of dolostones in this succession varies from formation to formation and from island to island. As such, these dolostones provide a unique opportunity for comparison of dolostones that are of different ages and come from islands of different sizes, different morphologies, and different tectonic backgrounds.

7.1. Extent of dolostones

Most of the dolostones on Grand Cayman and Cayman Brac are found in the Cayman Formation, Brac Formation, and Pedro Castle Formation (e.g., Jones, 1994). Only minor amounts of dolomite (<12%) have been found in the oldest part of the Ironshore Formation (Unit A) on Grand Cayman (Li and Jones, 2013). With respect to the dolostones in the older formations, the following points are important:

- On both islands, the Cayman Formation is the most extensively dolomitized part of the succession. Based on available data, about 75% of the formation on Grand Cayman and all of the formation on Cayman Brac have been dolomitized (Ren and Jones, 2017).
- On Cayman Brac, the Brac Formation is incompletely dolomitized. On the north

coast, dolomite is absent apart from scattered rhombs and small pods near the upper boundary (e.g., Jones, 1994). In contrast, on the south coast it is formed of coarsely crystalline dolostones that contains isolated pods of limestone (e.g., Jones, 1994; Zhao and Jones, 2012b). On Grand Cayman the Brac Formation, which is only found in the deepest wells, is also incompletely dolomitized. Based on available data, less than half of the limestones in the Brac Formation have been dolomitized.

- The Pedro Castle Formation on Grand Cayman and Cayman Brac has been variably dolomitized (Jones, 1994; MacNeil and Jones, 2003). On Cayman Brac, the formation is characterized by a basal dolostones that grade upwards into dolomitic limestone and then limestone. Collectively, dolostones form less than half of the formation. It should be noted that the Pedro Castle Formation itself is less extensive than the Cayman Formation and Brac Formation, being restricted to the western parts

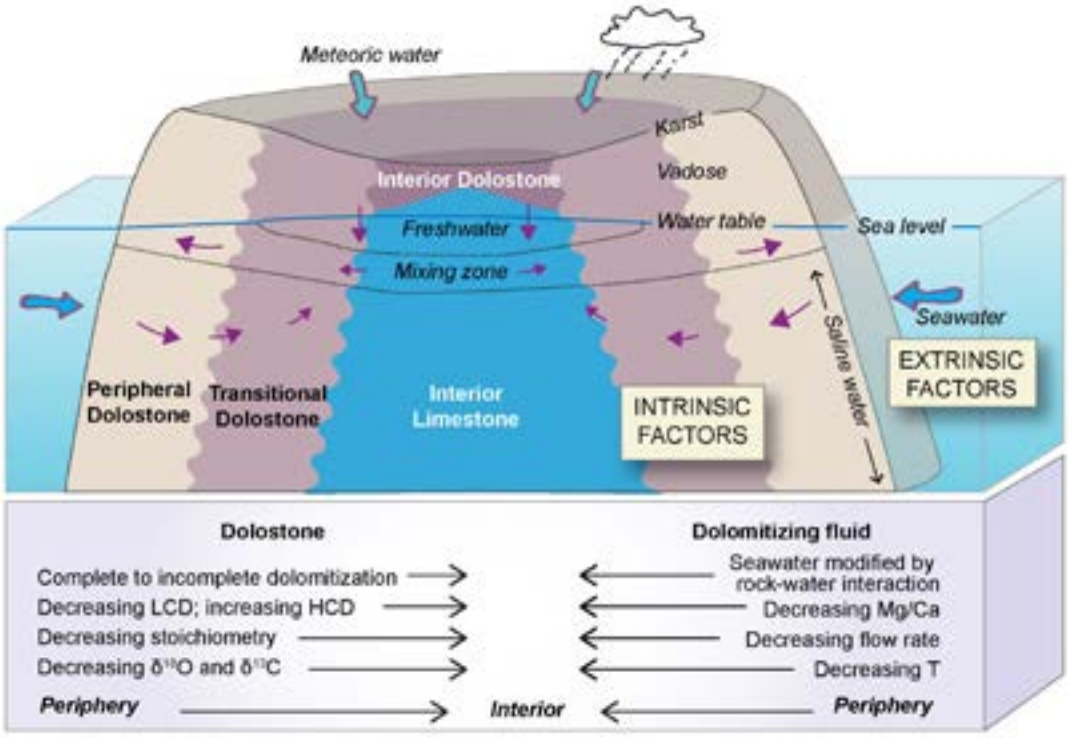

Fig. 4.5. Dolomitization model showing the lateral variations in various attributes of island dolostones that are affected by intrinsic and extrinsic factors (after Ren and Jones, 2017). See text for discussion.

of Grand Cayman and Cayman Brac.

7.2. Petrography

In general, the depositional textures of the original limestones are well preserved in the dolostones of the Cayman Formation and Pedro Castle Formation. In contrast, fabric-destructive dolomitization characterizes the Brac Formation (Zhao and Jones, 2012b). Most of the dolostones in the Cayman Formation and Pedro Castle Formation are formed of finely crystalline dolomite, whereas the dolostones in the Brac Formation are formed of crystals that are up to 1.5 mm long.

7.3. Stoichiometry of the dolomites

Dolostones from the Bluff Group consist of LCD and HCD that occur in varying ratios.

- On the eastern end of Grand Cayman, dolostones in the Cayman Formation range from LCD-dominated dolostones, with low average %Ca in the coastal regions to HCD-dominated dolostones with high average %Ca in the interior of the island (Table 4.3). In contrast, on Cayman Brac, all of the dolostones in the Cayman Formation are dominated by LCD and are therefore equivalent to the peripheral dolostones on Grand Cayman.
- On Grand Cayman, dolostones in the Pedro Castle Formation are formed largely of LCD with an average %Ca <55%. In contrast, on Cayman Brac, the dolostones in the Pedro Castle Formation are formed largely of HCD with an average %Ca >55% (MacNeil and Jones, 2003).
- The Brac Formation is composed of HCD-dominated dolostones with average %Ca 56.8 ± 0.5% in the pure dolostones and 56.6 ± 0.5% in the partially dolomitized limestones (Table 4.2).

7.4. Stable isotopes

There is no readily identifiable pattern of the oxygen and carbon isotope values in

the dolostones from the three formations in the Bluff Group (Table 4.2). In the Cayman Formation, the isotope values vary by location: (1) dolostones from the interior part of the eastern part of Grand Cayman are depleted with respect to the heavy isotopes, and (2) the $\delta^{18}O$ and $\delta^{13}C$ values of dolostones from the peripheral area of western part of Grand Cayman and Cayman Brac are lower than those from the peripheral dolostones on the eastern end of Grand Cayman (Table 4.2). Dolomite from partially dolomitized samples from the Pedro Castle Formation and Brac Formation, have $\delta^{18}O$ and $\delta^{13}C$ values that are similar to those obtained from the dolomites in the dolomitic limestones in the interior of Grand Cayman (Table 4.2). In the Brac Formation, the average $\delta^{18}O$ and $\delta^{13}C$ of dolomite in the pure dolostones are 1.1‰ and 0.6‰ higher than the dolomite that came from the partly dolomitized limestones (Table 4.2).

7.5. Time of dolomitizing

Based on $^{87}Sr/^{86}Sr$ dating and stratigraphy, the carbonate successions on the Cayman Islands appear to have experienced multiple episodes of dolomitization since the Oligocene (Jones and Luth, 2002, 2003b; MacNeil and Jones, 2003; Zhao and Jones, 2012a, 2013; Ren and Jones, 2017).

Fig. 4.6. Schematic diagram showing geographic zones on various islands based primarily on the dolomite stoichiometry including (A-C) a full range of zones (or part of them in smaller sized islands) on pervasively dolomitized islands, and (D) incomplete zones on partially dolomitized islands. (A) Cayman Formation includes PD (Peripheral dolostone), TD (Transitional dolostone), ID (Interior dolostone), and IL (Interior (dolomitic) limestone) on Grand Cayman, and PD only on Cayman Brac defined by the LCD-HCD compositions and %Ca. (B) Possible zones in the Daito Formation, Kita-daito-jima, and Miocene-Pliocene dolostones on the Little Bahama Bank, based on zones recognized in the Cayman model. Note the difference in the lateral extending of each zones between these islands and Grand Cayman. (C) Single successions on San Salvador (Pliocene) and Kita-daito-jima (Miocene) that are equivalent to the zones in the Cayman model. (D) Less extensive, partial dolomitization in the Pedro Castle Formation, the Brac Formation, and the Hope Gate Formation contain zones that are equivalent to the interior dolostone/dolomitic limestones zone of the Cayman model. Size of arrows indicating seawater flow directions indicate differences in dolomitization potential.

EXTENSIVE DOLOMITIZATION, FULL RANGE OF DOLOSTONE ZONES (LARGE ISLANDS)

A Islands with >1 well, include dolomite %Ca and HCD-LCD data

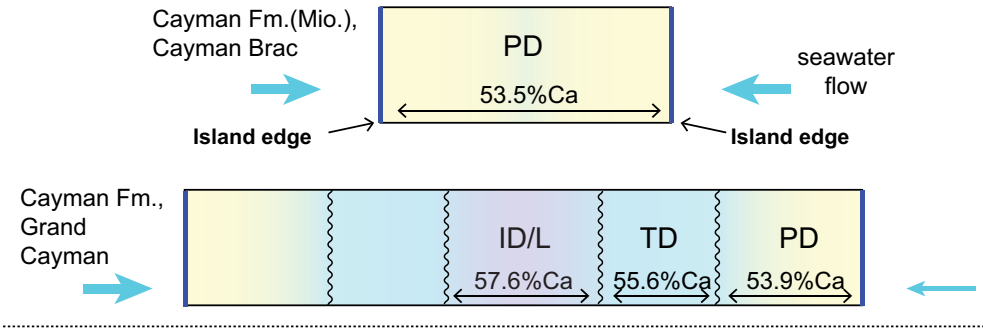

B Islands with >1 well/outcrop locality, include dolomite %Ca data

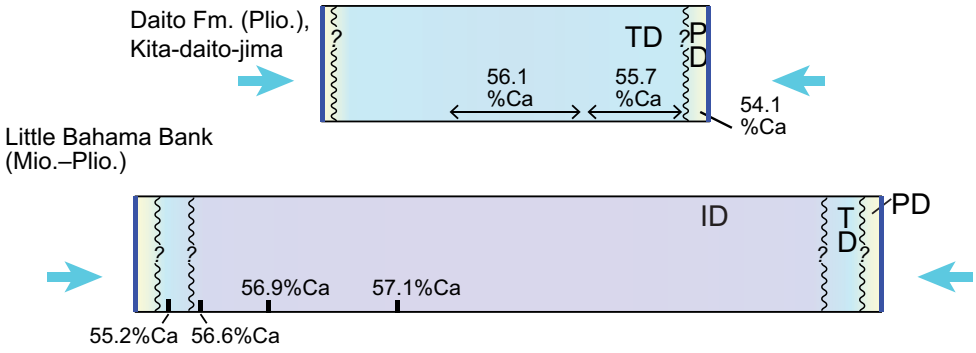

C Islands with 1 well, include dolomite %Ca data

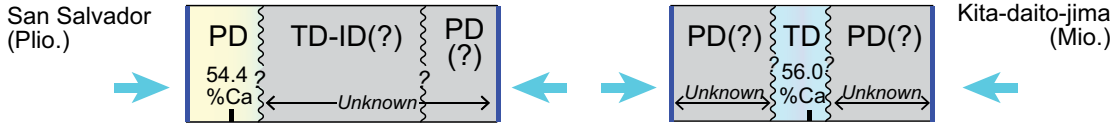

RESTRICTED DOLOMITIZATION, PD AND TD ZONES ABSENT

D

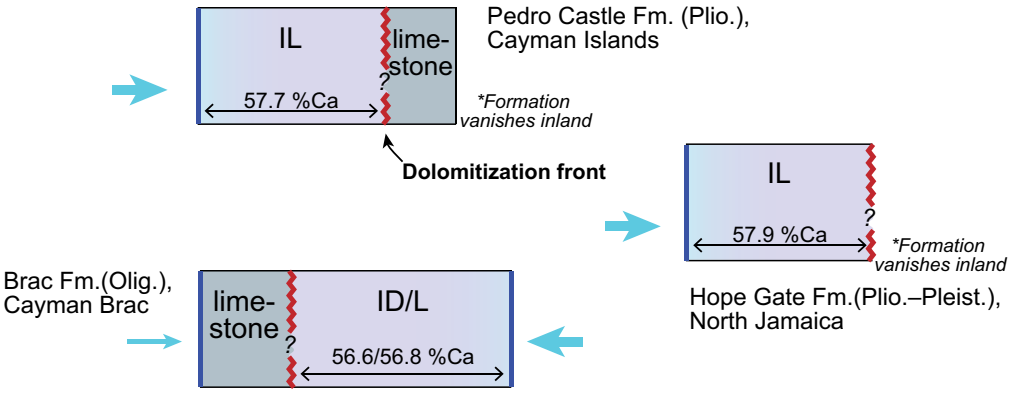

- The Brac Formation was affected by Late Miocene (6–8 Ma) dolomitization (Zhao and Jones, 2012a).
- Dating the dolomitization events that have affected the Cayman Formation has proven difficult because of the error margins that are associated with the dating techniques. Although generally attributed to two major phases of dolomitization, the timing of those events is open to debate. Proposed dates include Late Miocene (8.0–6.0 Ma) and Late Pliocene (2.2–1.9 Ma) (Jones and Luth, 2003b), Late Miocene (8–6 Ma) and Pliocene to Late Pleistocene (5–1 Ma) (Zhao and Jones, 2012a, b), and Late Miocene (7.5–5.5 Ma) and Late Pliocene–Early Pleistocene (3–1.5 Ma) (Ren and Jones, 2017). A third phase in Middle Pleistocene may have a local effect on the formation (Jones and Luth, 2003b).
- Dolomitization of the Pedro Castle Formation occurred during Late Pliocene according to Jones and Luth (2003b), and some time between 4.4 Ma and 1.2 Ma ago according to MacNeil and Jones (2003).
- The minor amounts of dolomite in Unit A of the Ironshore Formation must have formed after the deposition of that unit, which took place ~0.4 Ma according to Vézina et al. (1999).

8. Discussion

Studies of Cenozoic island dolostones have produced many important insights into the dolomitization process in Cenozoic seas (cf., Budd, 1997) with the development of many different dolomitization models (e.g., Kohout, 1967; Land, 1973, 1985; Saller, 1984). Given that most of these studies have been based on a limited number of vertical successions, emphasis has been placed on stratigraphic variations in the petrographic and geochemical attributes of the dolostones. Thus, the proposed interpretations for the origin of the dolostones have relied largely on stratigraphic variations with little or no attention being given to the geographic variations. Ren and Jones (2017), based on the investigation

of subsurface dolostones from Grand Cayman, demonstrated that the lateral variation in the stoichiometric and geochemical attributes of the dolostones from the coast to the center of a carbonate island are significant and must be incorporated into any model that is used to explain island dolomitization. On Grand Cayman, for example, readily apparent differences in many aspects of the dolostones, which are evident over distances of 1–2 km, include differences in the (1) composition of the dolomite populations, (2) average %Ca of the dolostones, (3) $\delta^{18}O$ and $\delta^{13}C$ values, and (4) preservation of sedimentary fabrics and the content of dolomite cement (Fig. 4.5).

Lateral variations in dolomite stoichiometry and geochemistry originate from the dolomitization process, which is controlled by many different intrinsic and extrinsic factors (Ren and Jones, 2017). The Cayman model reflects the notion that after seawater enters the island at the coastline, its chemical composition is constantly modified as it flows inland and the dolomitization processes proceed (Fig. 4.5). Dolomite precipitation is essentially driven by disequilibrium with the precursor carbonates in a calcium carbonate–groundwater system and theoretically, the attributes of the precipitated dolomite have the tendency to re-equilibrate with the on-site conditions. Meanwhile, the on-site conditions can be greatly influenced by the precipitation of dolomites and transmitted to the next landward site as seawater migrates landwards. If the rate of Mg and ^{18}O consumption during dolomitization is higher than the rate of supply of seawater, then the high Mg/Ca ratio and ^{18}O content of the dolomitizing fluid at the edge of an island cannot be maintained as seawater flows landwards. Eventually, this results in a negative feedback mechanism between the attributes of the dolostones and the parent fluid. Dolomite stoichiometry and stable isotopes, for example, are controlled largely by the chemical composition of the fluids (e.g., Folk and Land, 1975; Ward and Halley, 1985; Hardier, 1987; Kaczmarek and Sibley, 2011) and precipitation of dolomite can cause a change in the properties of the fluid and thereby reduce its capability for dolomitization. This mechanism may be further enhanced by lateral variations in some of the environmental conditions, including for example, a landward decrease in flow

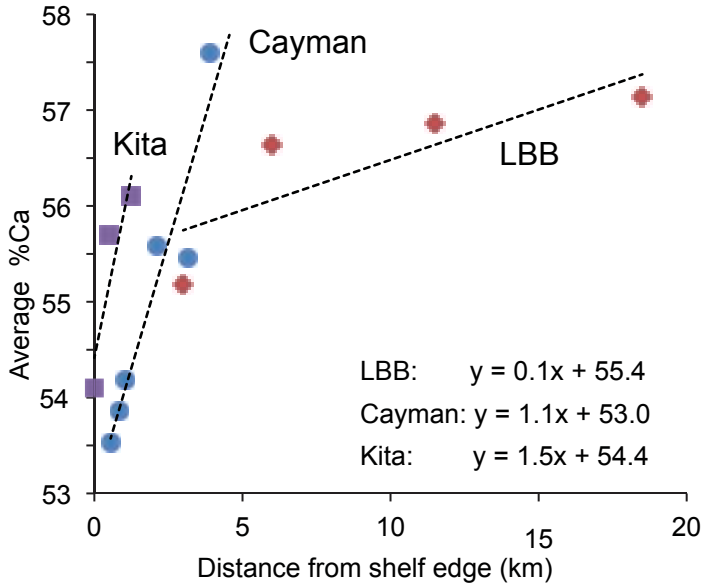

Fig. 4.7. Increases of the average %Ca in dolomites with distance from the edge of the Little Bahama Bank (Miocene-Pliocene), Grand Cayman (Cayman Formation), and Kita-daito-jima (Daito Formation).

rate and possibly, a decrease in groundwater temperature. This negative feedback in the dolomitization system may eventually lead to a situation where dolomitization is no longer possible. Depending on where that limit is, the original limestones in the interior of the island will not be dolomitized. This is the situation, for example, in the Cayman Formation on the eastern part of Grand Cayman (Ren and Jones, 2017).

The possibility that the lateral variations in the extent of dolomitization as well as variations in the dolostone geochemical attributes in the Cenozoic dolostones reflect post-dolomitization diagenetic modifications, recrystallization, or inheritance from precursor carbonates is not supported by available evidence. There is no clear petrographic evidence that post-dolomitization diagenesis has had any significant impact on island dolostones. Although the metastable HCD may be altered to LCD with time (cf., Jones, 2007), there is little evidence that this has taken place in the dolostones on the Cayman Islands. If this had taken place, then there would have been a high probability that the HCD in the Oligocene Brac Formation would have been converted to LCD. Mazzullo (1992) and Machel (1997) argued that recrystallization will lead to increased stoichiometry, increased

crystal size, depletion of ^{18}O, decreased Sr and Na concentrations, and homogenization of primary cathodoluminescent crystal zonations. In the Brac Formation on Cayman Brac, the high calcium content (>55%), lack of correlation between %Ca and diagenetic fabrics, no evidence of depletion of ^{18}O and Sr, and the zoned dolomite crystals (Zhao and Jones, 2012b) indicates that these dolostones have not been recrystallized. Likewise, the dolostones in the younger Cayman Formation and Pedro Castle Formation show no evidence of recrystallization.

The Cayman dolomitization model, which takes into account lateral variations, can be applied to the geographically extensive Cenozoic dolostones that are found on Cayman Brac, the Little Bahama Bank, Kita-daito-jima, and Mururoa (Fig. 4.6). These examples are characterized by geographic variations in the dolomite geochemical attributes on a kilometer-scale. Dolostones on the Little Bahama Bank and Mururoa are characterized by systematic changes in dolomite stoichiometry and chemical compositions landward from the coastal areas. Although the general patterns of these changes are geochemically akin to those on Grand Cayman, they are not exactly the same. On Cayman Brac, for example, which is only 150 km from Grand Cayman and has a similar geological setting, the Cayman Formation has been pervasively dolomitized and there is no limestone in the interior of the island. Moreover, all the dolostones in the Cayman Formation on Cayman Brac are formed largely of LCD (average >75%) and have a low average %Ca (average <54%) and are akin to peripheral dolostones on Grand Cayman (Fig. 4.6A). The differences between these islands reflects their relative scale because the width (N-S) of Cayman Brac, which is about half that of Grand Cayman, is comparable to the width of peripheral dolostone zone on Grand Cayman. For the Little Bahama Bank and Kita-daito-jima, the lateral extension of individual dolostone zones also differs from those on the Cayman Islands. In both cases, relative to Grand Cayman, the peripheral zones are narrower and the transitional or interior dolostone zones are wider (Fig. 4.6B). The situation on San Salvador, Kita-daito-jima (Miocene), and Xisha Islands is more difficult to assess because each island is represented by only one

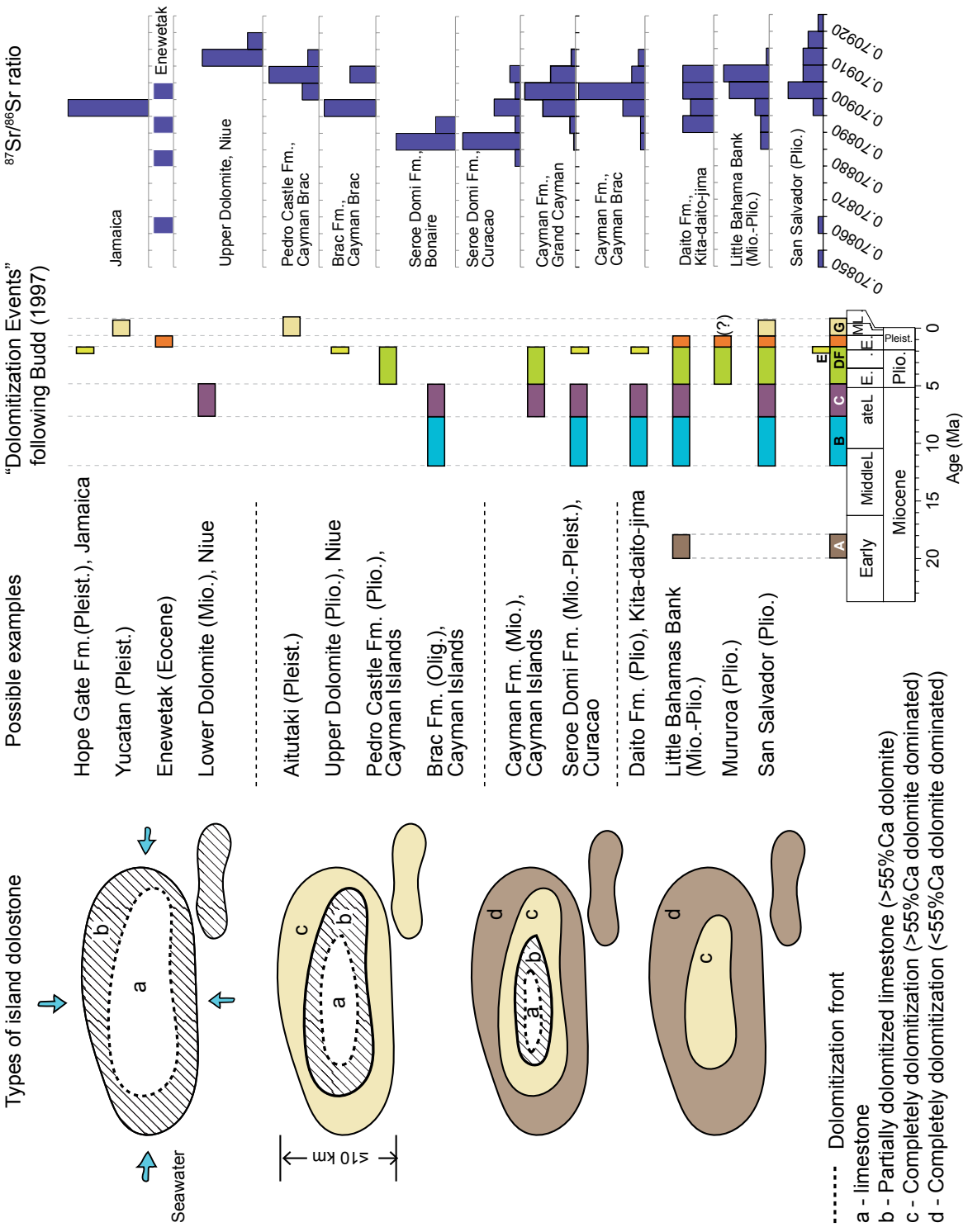

Fig. 4.8. Cenozoic island carbonate successions showing variation in development stages in terms of the landward extending of the dolomites and the lateral distribution pattern of the dolomite attributes relative to the dolomitization events (as defined by Budd, 1997), and the $^{87}Sr/^{86}Sr$ ratios of the dolostones (dolomitic limestones).

succession. Nevertheless, if those successions are considered relative to their geographic position (peripheral or interior), they do show dolomite stoichiometric properties that are consistent with the Cayman model (Fig. 4.6C).

The Cayman dolomitization model has the potential of explaining many of the Cenozoic island dolostones found on islands throughout the world including those less extensive, partially dolomitized carbonate bodies as in the Brac Formation, Pedro Castle Formation, and Hope Gate Formation (Fig. 4.6D). Unlike the extensive dolostone bodies (Fig. 4.6A–C), these formations do not include the peripheral and transitional zones. In terms of dolomite stoichiometry, dolomites in partially dolomitized island carbonates, despite being located near the coast, resemble dolomites in the interior dolomitic limestone zone of the Cayman model as they both contain more calcium than pure dolomites. This underpins, as demonstrated in the Cayman model, that while laterally approaching the dolomitization front inland, dolomite content and stoichiometry decrease (see also Budd et al., 2006; Budd and Mathias, 2015). The dolomite properties, particularly stoichiometry, as shown in the Cayman model, reflect the geographic locations of the samples relative to the island edge as well as to the dolomitization front.

The Cayman model is a general model that cannot be precisely quantified. This, however, is probably a reflection of the fact that it is impossible to generate a single model that will precisely predict the variances in the stratigraphic and geographic attributes of pervasively dolomitized successions on oceanic islands. Such problems arise for reasons that are inherent to the dolomitization process itself and reflect geographic differences in the nature of the dolomitizing fluids. This is clearly demonstrated by the following considerations.

- On any given island, the pattern of dolomitization is not geographically symmetrical. On Grand Cayman, for example, the lateral extent of dolomitization is greater on the northeast corner than elsewhere (Ren and Jones, 2017). This is the area where the dolomitizing fluids were able to penetrate the greatest distance inland. Similarly, in

Pliocene strata on Kita-daito-jima, the lateral extent on dolomitization is greater on the east coast than on the west coast.

- The lateral extent of the different dolostone zones, like those evident on Grand Cayman, varies from island to island. For example, the gradient of dolomite stoichiometry with distance from the island edge (lateral changes in the average %Ca of dolomites per km, %Ca/km) is variable from island to island. The gradient on Grand Cayman (1.5%Ca/km) is greater than that on Kita-daito-jima (1.1%Ca/km; Figs. 4.3, 4.7). On the Little Bahama Bank, which seems to be an "enlarged" version of the Grand Cayman model, the lateral stoichiometric gradient is only 0.1%Ca/km (Figs. 4.3, 4.7).
- Dolostones from the same zone, with similar stoichiometry, can have different stable isotopes. The isotopic values of the dolostones from the Cayman Formation on Cayman Brac, for example, are lower than those from peripheral dolostone zone on Grand Cayman (~1‰ difference in average values).

These variations in the dolomitization patterns from island to island illustrate the dynamic nature of the dolomitization model and the fact that dolomitization is influenced by many intrinsic factors. Theoretically, dolomitization can take place once the extrinsic factors have created suitable conditions, including: (1) an efficient seawater circulation mechanism where seawater can be transported into the island from all directions, (2) a fluid with geochemical properties (e.g., Mg/Ca, pCO_2, temperature) that favor dolomitization, and (3) stability over a period of time that will allow the dolomitization process to take place. Once these conditions are established, intrinsic factors then become important. Such factors include the extent of the water-rock interaction, development of a freshwater lens, porosity and permeability in the bedrock and their evolution during dolomitization and diagenesis (e.g., Banner and Hanson, 1990). Collectively, these factors affect the flux and geochemistry of the dolomitizing fluid that, in turn, control the mass supply of the reactants and reaction kinetics. Given this multitude of variables, it is not surprising that the dolostones that

develop on different islands will deviate from the theoretical model. It is also important to note that the geographic variations evident in the island dolostones are consistent with numerical modeling and the conclusions obtained from high-temperature dolomite synthesis experiments (Wilson et al., 1990; Kaufman, 1994; Whitaker et al., 2004; Sibley, 1990; Kaczmarek and Sibley, 2011).

The universality of the Cayman model for the development of island dolostones does not preclude the possibility of other dolomitization models being operative on some islands. Downward and seaward flow of dolomitizing fluid, such as that associated with the reflux dolomitization model (e.g., Krause Lagoon, St. Croix; Gill et al., 1995), can also produce geographic variations in dolomitization; but those patterns will differ from those generated with the Cayman model. Nevertheless, most examples of Cenozoic island dolostones and particularly those pervasively dolostone bodies are compatible with the Cayman model. In terms of the hydrological mechanisms for dolomitization, dolostones of Cayman Formation are probably associated with the sub-mixing zone entrainment (Ren and Jones, 2017), as with many other Caribbean and Pacific islands (e.g., Vahrenkamp and Swart, 1994, Wheeler et al., 1999; Suzuki et al., 2006). Other hydrological mechanisms that can pump seawater inland laterally, such as some thermal convections (e.g., Kohout 1967; Saller, 1984; Simms, 1984), may lead to similar geographic variation patterns as demonstrated in the Cayman model.

The geographic variability in dolomite stoichiometry and stable isotopes means that it is dangerous to characterize dolomitization of an entire island based on limited samples from a single geographic locality. If samples are available from many different localities on an island, then their geographic location relative to the coastline and to each other must be taken into account.

The variability evident between Cenozoic dolostones from different oceanic islands has been a major problem in developing models that explain the dolomitization processes. In scope, Cenozoic island dolostone bodies range from limestones that have only been partly dolomitized with the dolomite typically being HCD, to the pervasively dolomitized

successions that are characterized by organized geographic zones that parallel the coastlines (Fig. 4.8). These variations, however, may simply reflect the development stage of the dolomitization and how far the dolomitizing fluids have migrated from the coastlines.

The similarities in petrography, stoichiometry, and geochemistry between island dolostones throughout the Caribbean Sea and Pacific Ocean has led to the suggestion that they may have developed during Caribbean-wide or even world-wide dolomitization events (e.g., Sibley, 1980; Pleydell et al., 1990; Vahrenkamp et al., 1991; Budd, 1997; Jones and Luth, 2003b). Most of the pervasively dolomitized successions, which are typically at shallow depths with many being directly under the present-day island surface, seem to have experienced multiple phases of dolomitization during the Late Miocene to Pliocene (dolomitization events C and/or D of Budd, 1997; Fig. 4.8). Although there are few common features to the geographically localized dolostone successions, most of them seem to be younger (Pleistocene and later), older (Eocene), or deeper (typically >100 m burial) than the pervasively dolomitized successions. Also, most of these localized dolostone successions seem to have experienced only one phase of dolomitization. Pervasive dolomitization such as in the Miocene-Pliocene dolostones from the Bahamas and Miocene dolostones on Cayman Islands may have benefited from longer duration of dolomitization, higher efficiency of seawater circulation, together with favorable atmospheric and seawater compositions including for example, the increased seawater Mg/Ca ratio during late Cenozoic.

9. Conclusions

Many Cenozoic island dolostone bodies worldwide demonstrate similar geographic variability in various dolomite attributes that are akin to those embodied in the Cayman dolomitization model. A review of these island dolostone examples from the viewpoint of geographic variation patterns has led to the following important conclusions.

- Pervasive dolomitized successions typically have a full range of peripheral to transitional to interior dolostone zones. Dolomitization was initiated at the periphery

of the island and then extended toward the island center. This produced systematic landward variations in the dolomite stoichiometry, stable isotopes, and dolomite texture.

- An incomplete range of dolostone zones is illustrated on many Cenozoic carbonate islands. Pervasive dolomitization of a small island may have peripheral dolostone zone only. Less extensive, partially dolomitized carbonate on an island is typically equivalent to the dolomitic limestone zone of the Cayman model.
- The lateral variability within dolostone bodies originates from dolomitization. Laterally derived seawater gradually changes its chemical compositions along flow path as it migrates inland. Accompanied factors include lateral changes in environmental conditions, such as the rate and flux of the groundwater flow.
- Theoretically, a geographically concentrated zonation pattern in dolostone attributes can be applied to the Cenozoic island dolostones where laterally derived seawater was the parent dolomitizing fluid. Individual island dolostone bodies deviate from the theoretical model due a variety of intrinsic factors.

References

Aharon, P., Socki, R.A., Chan, L., 1987. Dolomitization of atolls by sea water convection flow: Test of a hypothesis at Niue, South Pacific. Journal of Geology 95, 187-203.

Aissaoui, D.M., Buigues, D., Purser, B.H., 1986. Model of reef diagenesis: Mururoa Atoll, French Polynesia. In: Schroeder, J.H., Purser, B.H. (Eds.), Reef Diagenesis. Springer-Verlag, Berlin, Heidelberg, pp. 27-52.

Bandoian, C.A., Murray, R.C., 1974. Pliocene-Pleistocene carbonate rocks of Bonaire, Netherlands Antilles. Geological Society of America Bulletin 85, 1243-1252.

Banner, J.L., Hanson, G.N., 1990. Calculation of simultaneous isotopic and trace element variations during water-rock interaction with applications to carbonate diagenesis. Geochimica et Cosmochimica Acta 54, 3123-3137.

Beach, D.K., 1993. Submarine cementation of subsurface Pliocene carbonates from the interior of Great Bahama Bank. Journal of Sedimentary Research 63, 1059-1069.

Beach, D.K., 1995. Controls and effects of subaerial exposure on cementation and development of secondary porosity in the subsurface of Great Bahama Bank. In: Budd, D.A., Saller, A.H., Harris, P.M. (Eds.), Unconformities and Porosity in Carbonate Strata. American Association of Petroleum Geologists Memoir 63, pp. 1-33.

Berner, R.A., 1965. Dolomitization of the Mid-Pacific Atolls. Science 147, 1297-1299.

Braithwaite, C.J.R., 1991. Dolomites, a review of origins, geometry and textures. Earth and Environmental Science Transactions of the Royal Society of Edinburgh 82, 99-112.

Budd, D.A., 1997. Cenozoic dolomites of carbonate islands: their attributes and origin. Earth-Science Reviews 42, 1-47.

Budd, D.A., Mathias, W.D., 2015. Formation of lateral patterns in rock properties by dolomitization: evidence from a Miocene reaction front (Bonaire, Netherlands Antilles). Journal of Sedimentary Research 85, 1082-1101.

Budd, D.A., Pranter, M.J., Reza, Z.A., 2006. Lateral periodic variations in the petrophysical and geochemical properties of dolomite. Geology 34, 373-376.

Chevalier, J., 1973. Geomorphology and geology of coral reefs in French Polynesia. In: Jones, O.A., Endean, R. (Eds.), Biology and Geology of Coral Reefs. Academic Press, pp. 113-141.

Dawans, J.M., Swart, P.K., 1988. Textural and geochemical alternations in Late Cenozoic Bahamian dolomites. Sedimentology 35, 385-403.

Deffeyes, K.S., 1965. Dolomitization of recent and Plio-Pleistocene sediments by marine evaporite waters on Bonaire Netherlands Antilles. In: Pray, L.C., Murray, R.C. (Eds.), Dolomitization and Limestone Diagenesis. SEPM Special Publication 13, pp. 71-88.

Folk, R.L., Land, L.S., 1975. Mg/Ca ratio and salinity: two controls over crystallization of dolomite. American Association of Petroleum Geologists Bulletin 59, 60-68.

Fouke, B.W., 1994. Deposition, diagenesis and dolomitization of Neogene Seroe Domi Formation coral reef limestones on Curacao, Netherlands Antilles. Natuurwetenschappelijke Studiekring voor het Caraibisch Gebied, Amsterdam, 182 pp.

Gill, I.P., Moore Jr, C.H., Aharon, P., 1995. Evaporitic mixed-water dolomitization on St. Croix, U.S.V.I.. Journal of Sedimentary Research 65, 591-604.

Hardie, L.A., 1987. Dolomitization: a critical view of some current views. Journal of Sedimentary Research 57, 166-183.

Hein, J.R., Gray, S.C., Richmond, B.M., White, L.D., 1992. Dolomitization of Quaternary reef limestone, Aitutaki, Cook Islands. Sedimentology 39, 645-661.

Humphrey, J.D., 1988. Late Pleistocene mixing zone dolomitization, southeastern Barbados, West Indies. Sedimentology 35, 327-348.

Humphrey, J.D., 2000. New geochemical support for mixing-zone dolomitization at Golden Grove, Barbados. Journal of Sedimentary Research 70, 1160-1170.

Humphrey, J.D., Radjef, E.M., 1991. Dolomite stoichiometric variability resulting from changing aquifer conditions, Barbados, West Indies. Sedimentary Geology 71, 129-136.

Jones, B., 1989. Syntaxial overgrowths on dolomite crystals in the Bluff Formation, Grand Cayman, British West Indies. Journal of Sedimentary Petrology 59, 839-847.

Jones, B. 1994. Geology of the Cayman Islands. In: Brunt, M.A., Davies, J.E. (Eds.), The Cayman Islands: Natural History and Biogeography. Kluwer Academic Publishers, Dordrecht, Netherlands, pp. 13-49.

Jones, B., 2007. Inside-out dolomite. Journal of Sedimentary Research 77, 539-551.

Jones, B., 2013. Microarchitecture of dolomite crystals as revealed by subtle variations in solubility: Implications for dolomitization. Sedimentary Geology 288, 66-80.

Jones, B., Luth, R.W., 2002. Dolostones from Grand Cayman, British West Indies. Journal of Sedimentary Research 72, 559-569.

Jones, B., Luth, R.W., 2003a. Petrography of finely crystalline Cenozoic dolostones as revealed by backscatter electron imaging: Case study of the Cayman Formation (Miocene), Grand Cayman, British West Indies. Journal of Sedimentary Research 73, 1022-1035.

Jones, B., Luth, R.W., 2003b. Temporal evolution of Tertiary dolostones on Grand Cayman as determined by $^{87}Sr/^{86}Sr$. Journal of Sedimentary Research 73, 187-205.

Jones, B., Luth, R.W., MacNeil, A.J., 2001. Powder X-ray diffraction analysis of homogeneous and heterogeneous sedimentary dolostones. Journal of Sedimentary Research 71, 790-799.

Kaczmarek, S.E., Sibley, D.F., 2011. On the evolution of dolomite stoichiometry and cation order during high-temperature synthesis experiments: An alternative model for the geochemical evolution of natural dolomites. Sedimentary Geology 240, 30-40.

Kaufman, J., 1994. Numerical models of fluid flow in carbonate platforms: Implications for dolomitization. Journal of Sedimentary Research 64, 128-139.

Kohout, F., 1967. Ground-water flow and the geothermal regime of the Floridian Plateau. Transactions—Gulf Coast Association of Geological Societies 17, 339-354.

Ladd, H.S., Tracey, J.I., Gross, M.G., 1970. Deep drilling on Midway Atoll. Geological Survey Professional Paper 680-A. United States Government Printing Office, Washington, 22 pp.

Land, L.S., 1973. Holocene meteoric dolomitization of Pleistocene limestones, North Jamaica. Sedimentology 20, 411-424.

Land, L.S., 1985. The origin of massive dolomite. Journal of Geological Education 33, 112-125.

Land, L.S., 1991. Dolomitization of the Hope Gate Formation (north Jamaica) by seawater: reassessment of mixing-zone dolomite. In: Taylor, H.P., O'Neil, J.R., Kaplan, I.R. (Eds.), Stable Isotope Geochemistry: A Tribute to Samuel Epstein. Geochemical Society Special Publication 3, pp. 121-130.

Land, L.S. 1992. The dolomite problem: stable and radiogenic isotope clues. In: Clauer, N., Chaudhuri, S. (Eds.), Isotopic signatures and sedimentary records. Springer, Berlin, Heidelberg, pp. 49-68.

Li, R., Jones, B., 2013. Heterogeneous diagenetic patterns in the Pleistocene Ironshore Formation of Grand Cayman, British West Indies. Sedimentary Geology 294, 251-265.

Lucia, F.J., Major, R.P., 1994. Porosity evolution through hypersaline reflux dolomitization. In: Purser, B.H., Tucker, M.E., Zenger, D.L. (Eds.), Dolomites: A Volume in Honour of Dolomieu. International Association of Sedimentologists Special Publication 21, pp. 325-341.

Machel, H.G., 1997. Recrystallization versus neomorphism, and the concept of 'significant recrystallization' in dolomite research. Sedimentary Geology 113, 161-168.

Machel, H.G., 2000. Dolomite formation in Caribbean Islands: driven by plate tectonics?! Journal of Sedimentary Research 70, 977-984.

Machel, H.G., Burton, E.A., 1994. Golden Grove dolomite, Barbados; origin from modified seawater. Journal of Sedimentary Research 64, 741-751.

MacNeil, A., 2002. Sedimentology, diagenesis, and dolomitization of the Pedro Castle Formation on Cayman Brac, British West Indies. Unpublished M.Sc. thesis, University of Alberta, 128 pp.

MacNeil, A., Jones, B., 2003. Dolomitization of the Pedro Castle Formation (Pliocene),

Cayman Brac, British West Indies. Sedimentary Geology 162, 219-238.

Mazzullo, S., 1992. Geochemical and neomorphic alteration of dolomite: A review. Carbonates and Evaporites 7, 21-37.

Ng, K.C., 1990. Diagenesis of the Oligocene-Miocene Bluff Formation of the Cayman Islands - A petrographic and hydrogeochemical approach. Unpublished PhD thesis, University of Alberta, 344 pp.

Ohde, S., Elderfield, H., 1992. Strontium isotope stratigraphy of Kita-daito-jima Atoll, North Philippine Sea: Implications for Neogene sea-level change and tectonic history. Earth and Planetary Science Letters 113, 473-486.

Pleydell, S.M., Jones, B., Longstaffe, F.J., Baadsgaard, H., 1990. Dolomitization of the Oligocene-Miocene Bluff Formation on Grand Cayman, British West Indies. Canadian Journal of Earth Sciences 27, 1098-1110.

Ren, M., Jones, B., 2016. Diagenesis in limestone-dolostone successions after 1 million years of rapid sea-level fluctuations: A case study from Grand Cayman, British West Indies. Sedimentary Geology 342, 15-30.

Ren, M., Jones, B., 2017. Spatial variations in the stoichiometry and geochemistry of Miocene dolomite from Grand Cayman: Implications for the origin of island dolostone. Sedimentary Geology 348, 69-93.

Rodgers, K.A., Easton, A.J., Downes, C.J., 1982. The chemistry of carbonate rocks of Niue Island, South Pacific. Journal of Geology 90, 645-662.

Saller, A.H., 1984. Petrologic and geochemical constraints on the origin of subsurface dolomite, Enewetak Atoll: an example of dolomitization by normal seawater. Geology 12, 217-220.

Schlanger, S.O., Graf, D.L., Goldsmith, J.R., Macdonald, G.A., Sackett, W.M., Potratz, H.A., 1963. Subsurface geology of Eniwetok atoll. Geological Survey Professional Paper 260-BB: 991-1066.

Sibley, D.F., 1980. Climatic control of dolomitization, Seroe Domi Formation (Pliocene),

Bonaire, NA. In: Zenger, D.H., Dunham, J.B., Ethington, R.L. (Eds.), Concepts and Models of Dolomitization. SEPM Special Publication 28, pp. 247-258.

Sibley, D.F., 1982. The origin of common dolomite fabrics: Clues from the Pliocene. Journal of Sedimentary Research 52, 1087-1100.

Sibley, D.F., 1990. Unstable to stable transformations during dolomitization. Journal of Geology 98, 739-748.

Sibley, D.F., Dedoes, R.E., Bartlett, T.R., 1987. Kinetics of dolomitization. Geology 15, 1112-1114.

Sibley, D.F., Nordeng, S.H., Borkowski, M.L., 1994. Dolomitization kinetics of hydrothermal bombs and natural settings. Journal of Sedimentary Research 64, 630-637.

Simms, M., 1984. Dolomitization by groundwater-flow system in carbonate platforms. Transactions—Gulf Coast Association of Geological Societies 34, 411-420.

Supko, P.R., 1977. Subsurface dolomites, San Salvador, Bahamas. Journal of Sedimentary Research 47, 1063-1077.

Suzuki, Y., Iryu, Y., Inagaki, S., Yamada, T., Aizawa, S., Budd, D.A., 2006. Origin of atoll dolomites distinguished by geochemistry and crystal chemistry: Kita-daito-jima, northern Philippine Sea. Sedimentary Geology 183, 181-202.

Swart, P.K., Melim, L.A., 2000. The origin of dolomites in Tertiary sediments from the margin of Great Bahama Bank. Journal of Sedimentary Research 70, 738-748.

Swart, P.K., Ruiz, J., Holmes, C.W., 1987. Use of strontium isotopes to constrain the timing and mode of dolomitization of Upper Cenozoic sediments in a core from San Salvador, Bahamas. Geology 15, 262-265.

Vacher, L.H.L., 1997. Introduction: varieties of carbonate islands and a historical perspective. In: Vacher, H.L., Quinn, T.M. (Eds.), Geology and Hydrogeology of Carbonate Islands. Elsevier, Amsterdam, pp. 1-34.

Vahrenkamp, V.C., Swart, P.K., Purser, B., Tucker, M., Zenger, D., 1994. Late Cenozoic dolomites of the Bahamas: metastable analogues for the genesis of ancient platform

dolomites. In: Purser, B.H.,Tucker, M.E., Zenger, D.L. (Eds.), Dolomites: A Volume in Honour of Dolomieu. International Association of Sedimentologists Special Publication 21, pp. 133-153.

Vahrenkamp, V.C., Swart, P.K., Ruiz, J., 1991. Episodic dolomitization of late Cenozoic carbonates in the Bahamas: evidence from strontium isotopes. Journal of Sedimentary Research 61, 1002-1014.

Vézina, J., Jones, B., Ford, D., 1999. Sea-level highstands over the last 500,000 years: Evidence from the Ironshore Formation on Grand Cayman, British West Indies. Journal of Sedimentary Research 69, 317–327.

Wang, Z., Shi, Z., Zhang, D., Huang, K., You, L., Duan, X., Li, S., 2015. Microscopic features and genesis for Miocene to Pliocene dolomite in well Xike-1, Xisha Islands. Earth Science-Journal of China University of Geosciences 40, 633-644. [in Chinese]

Ward, W.C., Halley, R.B., 1985. Dolomitization in a mixing zone of near-seawater composition, Late Pleistocene, northeastern Yucatan Peninsula. Journal of Sedimentary Research 55, 407-420.

Wei, X., Jia, C., Meng, W., 2008. Dolomitization characteristics of carbonate rock in Xisha Islands and its formation: A case study of well Xichen-1. Journal of Jilin University (Earth Science Edition) 38, 217-224. [in Chinese]

Wei, X., Zhu, Y., Xu, H., Zhao, G., Li, Y., 2006. Discussion on Neogene dolostone forming condition in Xisha Islands: Evidences from isotope C and O and fluid inclosures. Acta Petrologica Sinica 22, 2394-2404. [in Chinese]

Wheeler, C.W., Aharon, P., Ferrell, R.E., 1999. Successions of Late Cenozoic platform dolomites distinguished by texture, geochemistry, and crystal chemistry: Niue, South Pacific. Journal of Sedimentary Research 69, 239-255.

Whitaker, F.F., Smart, P.L., Jones, G.D., 2004. Dolomitization: from conceptual to numerical models. In: Braithwaite, C.J.R., Rizzi, G., Darke, G. (Eds.), The Geometry and Petrogenesis of Dolomite Hydrocarbon Reservoirs. Geological Society of London

Special Publication 235, pp. 99-139.

Wilson, E.N., Hardie, L.A., Phillips, O.M., 1990. Dolomitization front geometry, fluid flow patterns, and the origin of massive dolomite: the Triassic Latemar buildup, northern Italy. American Journal of Science 290, 741-796.

Zhao, H., Jones, B., 2012a. Origin of "island dolostones": A case study from the Cayman Formation (Miocene), Cayman Brac, British West Indies. Sedimentary Geology 243-244, 191-206.

Zhao, H., Jones, B., 2012b. Genesis of fabric-destructive dolostones: A case study of the Brac Formation (Oligocene), Cayman Brac, British West Indies. Sedimentary Geology 267-268, 36-54.

Zhao, H., Jones, B., 2013. Distribution and interpretation of rare earth elements and yttrium in Cenozoic dolostones and limestones on Cayman Brac, British West Indies. Sedimentary Geology 284-285, 26-38.

CHAPTER FIVE

CONCLUSIONS

Ever since its deposition during the Early-Middle Miocene, the Cayman Formation on Grand Cayman has undergone a variety of diagenetic modifications, including extensive dolomitization. The diagenetic patterns in the Cayman Formation show significant spatial variabilities in many aspects of the dolostone and limestone on an island-wide scale. The geometry of the dolostone bodies and the spatial variations in the petrography and geochemistry of the dolostones provide significant insight into the dolomite problem, and the early-stage diageneses and evolution of island carbonates.

(1) The limestones and dolostones in the Cayman Formation have experienced various diagenetic processes, including micritization, calcite cementation, dolomitization (replacive and cement), and dissolution of aragonite, calcite, and some of the dolomite. These diagenetic changes, which involved meteoric water and seawater, took place in a variety of vadose to shallow saline water settings. The diagenetic environment and conditions were primarily affected by sea level fluctuations.

(2) Dolomitization significantly modified the precursor carbonates in their mineral compositions, preservation of depositional fabrics, and porosity and permeability. This also played a key role in establishing the diagenetic stability of the rocks and the diagenesis that postdated dolomitization.

(3) Despite completely dolomitized in the peripheral areas of the island, dolomitization was less common in the interior of the island where limestone and/or dolomitic limestone are still present. A peripheral dolostone – interior limestone pattern characterizes the Cayman Formation.

(4) The Cayman Formation can be divided into three concentrically arranged zones, relative to the coastline, that are based primarily on the distribution of LCD and HCD including:

- the peripheral dolostone zone (0-1.5 km inland),

- the transitional dolostone (1.5-2.7 km inland), and
- the interior dolostone and interior limestone zones (2.7 km to island center).

(5) Variations in the petrography, stoichiometry and stable isotopes of the dolostones (dolomitic limestones) are evident from the peripheral to the interior zones.

- The petrography of dolostones and dolomitic limestones of the Cayman Formation vary from fabric retentive dolostones in the peripheral zone to fabric destructive dolomitic limestone that is dominant in the interior of the island. The volume of dolomite cements decreases toward the center of the island.
- The percentage of LCD decreases towards the center of the island, ranging from an average of 79 %LCD in the peripheral dolostones, to 74% in the transitional dolostones, to 35% in the interior dolostones, to < 3% in the interior dolomitic limestones. Thus, the dolomites become more calcium-rich towards the center of the island.
- The $\delta^{18}O$ and $\delta^{13}C$ values of the dolomites in the Cayman Formation decrease inland. The mean $\delta^{18}O$ values of the dolomites from the peripheral dolostone, transitional dolostone, interior dolostone and interior dolomitic limestone are 3.62 ± 0.85‰ (n = 105), 3.10 ± 0.88‰ (n = 41), 2.37 ± 0.55‰ (n = 36), and 2.10 ± 1.03‰ (n = 24) respectively. The mean $\delta^{13}C$ values of the dolomites from the four zones are 3.05 ± 0.47‰ (n = 105), 2.01 ± 0.44‰ (n = 41), 1.46 ± 0.40‰ (n = 36), and 1.42 ± 0.43‰ (n = 24), respectively.

(6) Seawater provided the Mg that was needed for dolomitization, which probably took place in the submixing zone where seawater was pumped into the island from all directions. Slight mixing of seawater with meteoric water may have been responsible for the dolomitization in the interior areas.

(7) A Cayman model is built to show the significance of gradual transition and variations in dolomite properties from the coast to the center of the island while seawater immigrates inland. Unlike the previous dolomitization models, the Cayman model

emphasizes both the dolostones and the dolomitization process, and essentially reflects feedback between dolostones and dolomitizing fluid while approaching a dolomite-water equilibrium.

(8) The Cayman Formation experienced two major phases of dolomitization as suggested by $^{87}Sr/^{86}Sr$ of the dolomites: the first during the late Miocene–early Pliocene, and the second during the late Pleistocene.

Post-dolomitization diagenesis is evident in the Cayman Formation. The diagenetic patterns reflect rapid sea-level changes and the spatial distribution pattern of the limestone-dolostone.

(1) Diageneses following dolomitization of the Cayman Formation were associated with glacio-eustasy over the last 1 Ma. The diagenetic patterns preserved in the formation, however, do not exactly match or reflect all the sea-level oscillation cycles.

(2) Comparisons between the coastal dolostone successions (RWP-2 and ESS-1) and the inland limestone succession (GFN-1) illustrate the higher diagenetic stability of the dolostone relative to limestone when subjected to meteoric diagenetic environment.

(3) Overall, the limestone succession is characterized by extensive dissolution and high porosities. This suggests the predominance of destructive effect on the limestone (i.e., remove carbonate components) by meteoric water while the rock was subjected to periodic subaerial exposure during repeated glacio-eustatic oscillations.

(4) The contrast between the "tight" cap rock (highly cemented dolomitic limestone and limestone by calcite) and the "soft" lower limestone (barely cemented) is probably associated with the lower rates of sea-level change during highstands. The generations of calcite cement cannot be directly correlated to the cycles of sea-level oscillation.

The Cayman dolomitization model, which essentially reflects the lateral variations in the dolomitizing conditions and dolostone properties in a dolostone body, can be applied to many Cenozoic island dolostones including almost all known thick, laterally extensive dolostone bodies such as the Miocene-Pliocene dolostones on Little Bahama Bank and

Miocene-Pliocene dolostones on Kita-daito-jima.

(1) Theoretically, a geographically concentric zonation pattern in dolostone attributes can be applied to any Cenozoic island dolostones where laterally derived seawater was the parent dolomitizing fluid.

(2) Individual island dolostone bodies deviate from the Cayman model in the geographical asymmetry of the dolostone zones on individual islands, the lateral extent of zones between different islands, and the oxygen and carbon isotopic values in the same zones on different islands. The model was controlled by a variety of extrinsic and intrinsic factors.

(3) The lateral variability within the dolostone bodies originates from dolomitization. Geographic variations in these dolostones essentially reflect the fact that laterally derived seawater gradually changes its chemical compositions along flow path as it migrates inland and that environmental conditions such as the rate and flux of the groundwater flow change inland.

(4) Dolomitization is a dynamic system in which negative feedbacks between dolomites and geochemistry of dolomitizing fluid (and perhaps other dolomitizing conditions) continue until equilibrium is attained.

The dolomite problem has long been a puzzle. Although it has been widely acknowledged that dolomite can be formed in a variety of settings, the requirements and most favorable conditions for the genesis of a large extensive dolostone body are the key of the problem. The Cenozoic island dolostones, particularly those large-sized (km^2 in area, over 100 m in thickness) spatially extensive island dolostone bodies such as those on the Cayman Formation on Grand Cayman, are ideal for addressing the problem. The demonstration that the Cayman model is applicable to many Cenozoic island dolostones suggests that most island dolostones may originate from similar geological and hydrological conditions under similar dolomitization mechanisms. A favorable hydrological condition is the prerequisite for dolomitization and the length of time that it can be maintained (to overcome the kinetic constraints for dolomitization) is probably the key to the size and lateral extent of a dolostone

body.

Dolomite is an important component of the earth's geological history. Its formation can be closely connected to the geochemical and/or biogeological conditions of the Earth's hydrosphere, atmosphere, lithosphere, and/or biosphere. The origin of dolostone from Cayman Formation on Grand Cayman was associated with the seawater chemistry and the eustasy in the past 11 Ma, yet this dolostone is only a small segment of the entire dolostone volumes on the earth. The overall spatial and temporal distributions and properties of these dolomites can perhaps provide significant implications for the seawater chemistry and paleoclimate on geological time scale or even the evolution of the earth.

REFERENCES

Aharon, P., Kolodny, Y., Sass, E., 1977. Recent hot brine dolomitization in the "Solar Lake", Gulf of Elat, isotopic, chemical, and mineralogical study. Journal of Geology 85, 27-48.

Aharon, P., Socki, R.A., Chan, L., 1987. Dolomitization of atolls by sea water convection flow: test of a hypothesis at Niue, South Pacific. Journal of Geology 95, 187-203.

Aissaoui, D.M., Buigues, D., Purser, B.H., 1986. Model of reef diagenesis: Mururoa Atoll, French Polynesia. In: Schroeder, J.H., Purser, B.H. (Eds.), Reef Diagenesis. Springer-Verlag, Berlin, Heidelberg, pp. 27-52.

Azmy, K., Lavoie, D., Wang, Z., Brand, U., Al-Aasm, I., Jackson, S., Girard, I., 2013. Magnesium-isotope and REE compositions of Lower Ordovician carbonates from eastern Laurentia: implications for the origin of dolomites and limestones. Chemical Geology 356, 64-75.

Bandoian, C.A., Murray, R.C., 1974. Pliocene-Pleistocene carbonate rocks of Bonaire, Netherlands Antilles. Geological Society of America Bulletin 85, 1243-1252.

Banner, J.L., Hanson, G.N., 1990. Calculation of simultaneous isotopic and trace element variations during water-rock interaction with applications to carbonate diagenesis. Geochimica et Cosmochimica Acta 54, 3123-3137.

Beach, D.K., 1993. Submarine cementation of subsurface Pliocene carbonates from the interior of Great Bahama Bank. Journal of Sedimentary Research 63, 1059-1069.

Beach, D.K., 1995. Controls and effects of subaerial exposure on cementation and development of secondary porosity in the subsurface of Great Bahama Bank. In: Budd, D.A., Saller, A.H., Harris, P.M. (Eds.), Unconformities and Porosity in Carbonate Strata. Association of American Petroleum Geologists, Memoir 63, pp. 1-33.

Berner, R.A., 1965. Dolomitization of the Mid-Pacific Atolls. Science 147, 1297-1299.

Blake, D.F., Peacor, D.R., Wilkinson, B.H., 1982. The sequence and mechanism of low-temperature dolomite formation: calcian dolomites in a Pennsylvanian echinoderm. Journal of Sedimentary Research 52, 59-70.

Blanchon, P., Jones, B., 1995. Marine-planation terraces on the shelf around Grand Cayman: A result of stepped Holocene sea-level rise. Journal of Coastal Research 11, 1-33.

Braithwaite, C.J.R., 1991. Dolomites, a review of origins, geometry and textures. Earth and Environmental Science Transactions of the Royal Society of Edinburgh 82, 99-112.

Braithwaite, C.J.R., Camoin, G.F., 2011. Diagenesis and sea-level change: lessons from Moruroa, French Polynesia. Sedimentology 58, 259-284.

Buchbinder, L.G., Friedman, G.M., 1980. Vadose, phreatic, and marine diagenesis of Pleistocene-Holocene carbonates in a borehole; Mediterranean coast of Israel. Journal of Sedimentary Research 50, 395-407.

Budd, D.A., 1997. Cenozoic dolomites of carbonate islands: their attributes and origin. Earth-Science Reviews 42, 1-47.

Budd, D.A., Land, L.S., 1990. Geochemical imprint of meteoric diagenesis in Holocene ooid sands, Schooner Cays, Bahamas; correlation of calcite cement geochemistry with extant groundwaters. Journal of Sedimentary Research 60, 361-378.

Budd, D.A., Mathias, W.D., 2015. Formation of lateral patterns in rock properties by dolomitization: evidence from a Miocene reaction front (Bonaire, Netherlands Antilles). Journal of Sedimentary Research 85, 1082-1101.

Budd, D.A., Pranter, M.J., Reza, Z.A., 2006. Lateral periodic variations in the petrophysical and geochemical properties of dolomite. Geology 34, 373-376.

Budd, D.A., Vacher, H.L., 1991. Predicting the thickness of fresh-water lenses in carbonate paleo-islands. Journal of Sedimentary Research 61, 43-53.

Burns, S.J., Mckenzie, J.A., Vasconcelos, C., 2000. Dolomite formation and biogeochemical cycles in the Phanerozoic. Sedimentology 47, 49-61.

Cant, R.V., Weech, P.S., 1986. A review of the factors affecting the development of Ghyben-Hertzberg lenses in the Bahamas. Journal of Hydrology 84, 333-343.

Carballo, J.D., Land, L.S., Miser, D.E., 1987. Holocene dolomitization of supratidal sediments by active tidal pumping, Sugarloaf Key, Florida. Journal of Sedimentary

Petrology 57, 153-165.

Chai, L., Navrotsky, A., Reeder, R.J., 1995. Energetics of calcium-rich dolomite. Geochimica et Cosmochimica Acta 59, 939-944.

Chappell, J., Shackleton, N.J., 1986. Oxygen isotopes and sea level. Nature 324, 137-140.

Chevalier, J., 1973. Geomorphology and geology of coral reefs in French Polynesia. In: Jones, O.A., Endean, R. (Eds.), Biology and Geology of Coral Reefs. Academic Press, pp. 113-141.

Clark, P.U., Dyke, A.S., Shakun, J.D., Carlson, A.E., Clark, J., Wohlfarth, B., Mitrovica, J.X., Hostetler, S.W., McCabe, A.M., 2009. The last glacial maximum. Science 325, 710-714.

Dawans, J.M., Swart, P.K., 1988. Textural and geochemical alternations in Late Cenozoic Bahamian dolomites. Sedimentology 35, 385-403.

Deffeyes, K.S., 1965. Dolomitization of recent and Plio-Pleistocene sediments by marine evaporite waters on Bonaire Netherlands Antilles. In: Pray, L.C., Murray, R.C. (Eds.), Dolomitization and Limestone Diagenesis. SEPM Special Publication 13, pp. 71-88.

Der, A., 2012. Deposition and sea level fluctuation during Miocene times, Grand Cayman, British West Indies. Unpublished M.Sc. thesis, University of Alberta, 101 pp.

Drits, V.A., McCarty, D.K., Sakharov, B., Milliken, K.L., 2005. New insight into structural and compositional variability in some ancient excess-Ca dolomite. Canadian Mineralogist 43, 1255-1290.

Emery, K., Milliman, J., 1980. Shallow-water limestones from slope off Grand Cayman Island. The Journal of Geology 88, 483-488.

Fairbridge, R.W., 1957. The dolomite question. In: Le Blanc R.J., Breeding. J.G. (Eds.) Regional Aspects of Carbonate Deposition. Society of Economic Paleontologists and Mineralogists Special Publication 5, pp. 125-178.

Folk, R.L., Land, L.S., 1975. Mg/Ca ratio and salinity: two controls over crystallization of dolomite. American Association of Petroleum Geologists Bulletin 59, 60-68.

Folkman, Y., 1969. Diagenetic dedolomitization in the Albian-Cenomanian Yagur Dolomite

on Mount Carmel (northern Israel). Journal of Sedimentary Research 39, 380-385.

Fouke, B.W., 1994. Deposition, diagenesis and dolomitization of Neogene Seroe Domi Formation coral reef limestones on Curacao, Netherlands Antilles. Natuurwetenschappelijke Studiekring voor het Caraibisch Gebied, Amsterdam, 182 pp.

Gill, I.P., Moore Jr, C.H., Aharon, P., 1995. Evaporitic mixed-water dolomitization on St. Croix, U.S.V.I.. Journal of Sedimentary Research 65, 591-604.

Ginsberg, R.N., Marszalek, D.S., Schneidermann, N., 1971. Ultrastructure of carbonate cements in a Holocene algal reef of Bermuda. Journal of Sedimentary Research 41, 472-482.

Glover, E.D., Sippel, R.F., 1967. Synthesis of magnesium calcites. Geochimica et Cosmochimica Acta 31, 603-613.

Goldsmith, J.R., Graf, D.L., 1958. Relation between lattice constants and composition of the Ca-My carbonates. American Mineralogist 43, 84-101.

Gregg, J.M., Bish, D.L., Kaczmarek, S.E., Machel, H.G., 2015. Mineralogy, nucleation and growth of dolomite in the laboratory and sedimentary environment: A review. Sedimentology 62, 1749-1769.

Gupta, B.K.S., 2003. Modern Foraminifera. Springer, Netherlands, 371 pp.

Hardie, L.A., 1987. Dolomitization: a critical view of some current views. Journal of Sedimentary Research 57, 166-183.

Hardie, L.A., Bosellini, A., Goldhammer, R.K., 1986. Repeated subaerial exposure of subtidal carbonate platforms, Triassic, northern Italy: Evidence for high frequency sea level oscillations on a 104 year scale. Paleoceanography 1, 447-457.

Hayman, N.W., Grindlay, N.R., Perfit, M.R., Mann, P., Leroy, S., de Lépinay, B.M., 2011. Oceanic core complex development at the ultraslow spreading Mid-Cayman Spreading Center. Geochemistry, Geophysics, Geosystems 12, 1-21.

Hein, J.R., Gray, S.C., Richmond, B.M., White, L.D., 1992. Dolomitization of Quaternary reef limestone, Aitutaki, Cook Islands. Sedimentology 39, 645-661.

Humphrey, J.D., 1988. Late Pleistocene mixing zone dolomitization, southeastern Barbados, West Indies. Sedimentology 35, 327-348.

Humphrey, J.D., 2000. New geochemical support for mixing-zone dolomitization at Golden Grove, Barbados. Journal of Sedimentary Research 70, 1160-1170.

Humphrey, J.D., Radjef, E.M., 1991. Dolomite stoichiometric variability resulting from changing aquifer conditions, Barbados, West Indies. Sedimentary Geology 71, 129-136.

Hunter, I.G., 1994. Modern and ancient coral associations of the Cayman Islands. Unpublished Ph.D. thesis, University of Alberta, 345 pp.

Jacobson, G., Hill, P.J., 1980. Hydrogeology of a raised coral atoll–Niue Island, South Pacific Ocean. BMR Journal of Australian Geology and Geophysics 5, 271-278.

James, N.P., Bone, Y., Kyser, T.K., 1993. Shallow burial dolomitization and dedolomitization of Mid-Cenozoic, cool-water, calcitic, deep-self limestones, southern Australia. Journal of Sedimentary Research 63, 528-538.

James, N.P., Ginsburg, R.N., Marszalek, D.S., Choquette, P.W., 1976. Facies and fabric specificity of early subsea cements in shallow Belize (British Honduras) reefs. Journal of Sedimentary Research 46, 523-544.

Jones, B., 1989. Syntaxial overgrowths on dolomite crystals in the Bluff Formation, Grand Cayman, British West Indies. Journal of Sedimentary Petrology 59, 839-847.

Jones, B., 1992. Caymanite, a cavity-filling deposit in the Oligocene Miocene Bluff Formation of the Cayman Islands. Canadian Journal of Earth Sciences 29, 720-736.

Jones, B., 1994. Geology of the Cayman Islands. In: Brunt, M.A., Davies, J.E. (Eds.), The Cayman Islands: Natural History and Biogeography. Kluwer Academic Publishers, Dordrecht, Netherlands, pp. 13-49.

Jones, B., 2005. Dolomite crystal architecture: genetic implications for the origin of the Tertiary dolostones of the Cayman Islands. Journal of Sedimentary Research 75, 177-189.

Jones, B., 2007. Inside-out dolomite. Journal of Sedimentary Research 77, 539-551.

Jones, B., 2013. Microarchitecture of dolomite crystals as revealed by subtle variations in solubility: Implications for dolomitization. Sedimentary Geology 288, 66-80.

Jones, B., Hunter, I.G., 1989. The Oligocene-Miocene Bluff Formation on Grand Cayman. Caribbean Journal of Science 25, 71-85.

Jones, B., Hunter, I.G., 1994a. Evolution of an isolated carbonate bank during Oligocene, Miocene and Pliocene times, Cayman Brac, British West Indies. Facies 30, 25-50.

Jones, B., Hunter, I.G., 1994b. Messinian (late Miocene) karst on Grand Cayman, British West Indies; an example of an erosional sequence boundary. Journal of Sedimentary Research 64, 531-541.

Jones, B., Hunter, I.G., Kyser, T.K., 1994a. Revised Stratigraphic nomenclature for Tertiary strata of the Cayman Islands, British West Indies. Caribbean Journal of Science 30, 53-68.

Jones, B., Hunter, I.G., Kyser, T.K., 1994b. Stratigraphy of the Bluff Formation (Miocene-Pliocene) and the newly defined Brac Formation (Oligocene), Cayman Brac, British West Indies. Caribbean Journal of Science 30, 30-51.

Jones, B., Luth, R.W., 2002. Dolostones from Grand Cayman, British West Indies. Journal of Sedimentary Research 72, 559-569.

Jones, B., Luth, R.W., 2003a. Petrography of finely crystalline Cenozoic dolostones as revealed by backscatter electron imaging: Case study of the Cayman Formation (Miocene), Grand Cayman, British West Indies. Journal of Sedimentary Research 73, 1022-1035.

Jones, B., Luth, R.W., 2003b. Temporal evolution of Tertiary dolostones on Grand Cayman as determined by $^{87}Sr/^{86}Sr$. Journal of Sedimentary Research 73, 187-205.

Jones, B., Luth, R.W., MacNeil, A.J., 2001. Powder X-ray diffraction analysis of homogeneous and heterogeneous sedimentary dolostones. Journal of Sedimentary Research 71, 790-799.

Kaczmarek, S.E., Sibley, D.F., 2011. On the evolution of dolomite stoichiometry and cation

order during high-temperature synthesis experiments: An alternative model for the geochemical evolution of natural dolomites. Sedimentary Geology 240, 30-40.

Kaczmarek, S.E., Sibley, D.F., 2014. Direct physical evidence of dolomite recrystallization. Sedimentology 61, 1862–1882.

Katz, A., Matthews, A., 1977. The dolomitization of $CaCO_3$: an experimental study at 252-295 °C. Geochimica et Cosmochimica Acta 41, 297-308.

Kaufman, J., 1994. Numerical models of fluid flow in carbonate platforms: implications for dolomitization. Journal of Sedimentary Research 64, 128-139.

Kohout, F., 1967. Ground-water flow and the geothermal regime of the Floridian Plateau. Transactions—Gulf Coast Association of Geological Societies 17, 339-354.

Ladd, H.S., Tracey, J.I., Gross, M.G., 1970. Deep drilling on Midway Atoll. Geological Survey Professional Paper 680-A. United States Government Printing Office, Washington, 22 pp.

Land, L.S. 1992. The dolomite problem: stable and radiogenic isotope clues. In: Clauer, N., Chaudhuri, S. (Eds.), Isotopic signatures and sedimentary records. Springer, Berlin, Heidelberg, pp. 49-68.

Land, L.S., 1973. Holocene meteoric dolomitization of Pleistocene limestones, North Jamaica. Sedimentology 20, 411-424.

Land, L.S., 1985. The origin of massive dolomite. Journal of Geological Education 33, 112-125.

Land, L.S., 1991. Dolomitization of the Hope Gate Formation (north Jamaica) by seawater: reassessment of mixing-zone dolomite. In: Taylor, H.P., O'Neil, J.R., Kaplan, I.R. (Eds.), Stable Isotope Geochemistry: A Tribute to Samuel Epstein. Geochemical Society, Special Publication 3, pp. 121-130.

Land, L.S., Goreau, T.F., 1970. Submarine lithification of Jamaican reefs. Journal of Sedimentary Research 40, 457-462.

Land, L.S., Moore, C.H., 1980. Lithification, micritization and syndepositional diagenesis of

biolithites on the Jamaican island slope. Journal of Sedimentary Research 50, 357-369.

Leroy, S., Mauffret, A., Patriat, P., Mercier de Lépinay, B., 2000. An alternative interpretation of the Cayman trough evolution from a reidentification of magnetic anomalies. Geophysical Journal International 141(3), 539-557.

Li, R., Jones, B., 2013. Heterogeneous diagenetic patterns in the Pleistocene Ironshore Formation of Grand Cayman, British West Indies. Sedimentary Geology 294, 251-265.

Liang, T., Jones, B., 2014. Deciphering the impact of sea-level changes and tectonic movement on erosional sequence boundaries in carbonate successions: A case study from Tertiary strata on Grand Cayman and Cayman Brac, British West Indies. Sedimentary Geology 305, 17-34.

Lighty, R.G., 1985. Preservation of internal reef porosity and diagenetic sealing of submerged early Holocene barrier reef, southeast Florida shelf. In: Schneidermann, N., Harris, P.M. (Eds.), Carbonate Cements. Society of Economic Paleontologists and Mineralogists Special Publication 36, pp. 123-151.

Lisiecki, L.E., Raymo, M.E., 2005. A Pliocene-Pleistocene stack of 57 globally distributed benthic $d^{18}O$ records. Paleoceanography 20, 1-17. Doi:10.1029/2004PA001071.

Longman, M.W., 1980. Carbonate diagenetic textures from nearsurface diagenetic environments. American Association for Petroleum Geologists, Bulletin 64, 461-487.

Lucia, F.J., Major, R.P., 1994. Porosity evolution through hypersaline reflux dolomitization. In: Purser, B.H., Tucker, M.E., Zenger, D.L. (Eds.), Dolomites: A Volume in Honour of Dolomieu. International Association of Sedimentologists Special Publication 21, pp. 325-341.

Lumsden, D.N., Chimahusky, J.S., 1980. Relationship between dolomite nonstoichiometry and carbonate facies parameters. In: Zenger, D.H., Dunham, J.B., Ethington, R.L. (Eds.), Concepts and Models of Dolomitization. SEPM Special Publication 28, pp.123-137.

Machel, H.G., 1997. Recrystallization versus neomorphism, and the concept of ‘significant recrystallization’ in dolomite research. Sedimentary Geology 113, 161-168.

Machel, H.G., 2000. Dolomite formation in Caribbean Islands: driven by plate tectonics?! Journal of Sedimentary Research 70, 977-984.

Machel, H.G., 2004. Concepts and models of dolomitization: a critical reappraisal. In: Braithwaite, C.J.R., Rizzi, G., Darke, G. (Eds.), The Geometry and Petrogenesis of Dolomite Hydrocarbon Reservoirs. Geological Society of London Special Publication 235, pp. 7-63.

Machel, H.G., Burton, E.A., 1994. Golden Grove dolomite, Barbados: origin from modified seawater. Journal of Sedimentary Research 64, 741-751.

Machel, H.G., Mountjoy, E.W., Humphrey, J.D., Quinn, T.M., 1990. Coastal mixing zone dolomite, forward modeling, and massive dolomitization of platform-margin carbonates: discussion and reply. Journal of Sedimentary Research 60, 1008-1016.

MacNeil, A., 2001. Sedimentology, Diagenesis and Dolomitization of the Pedro Castle Formation on Cayman Brac, BWI. Master Thesis, Unversity of Alberta, 128 pp.

MacNeil, A., Jones, B., 2003. Dolomitization of the Pedro Castle Formation (Pliocene), Cayman Brac, British West Indies. Sedimentary Geology 162, 219-238.

Malone, M.J., Baker, P.A., Burns, S.J., 1996. Recrystallization of dolomite: an experimental study from 50-200°C. Geochimica et Cosmochimica Acta 60, 2189-2207.

Marshall, J.F., 1986. Regional distribution of submarine cements within an epicontinental reef system: central Great Barrier Reef, Australia. In: Schroeder, J.H., Purser, B.H. (Eds.), Reef Diagenesis. Springer-Verlag, Berlin, Heidelberg, pp. 8-26.

Mather, J.D., 1971. A preliminary survey of the groundwater resources of the Cayman Islands with recommendations for their development. Institute of Geological Sciences, London, 91 pp.

Mather, J.D., 1971. A preliminary survey of the groundwater resources of the Cayman Islands with recommendations for their development. Institute of Geological Sciences, London, 91 pp.

Matley, C.A., 1926. The geology of the Cayman Islands, British West Indies, and their

relations to the Bartlett Trough. Quarterly Journal of the Geological Society of London 82, 352-387.

Matthews, R.K., Frohlich, C., 1987. Forward modeling of bank-margin carbonate diagenesis. Geology 15, 673-676.

Mazzullo, S. J., 2000. Organogenic dolomitization in peritidal to deep-sea sediments. Journal of Sedimentary Research 70, 10-23.

Mazzullo, S., 1992. Geochemical and neomorphic alteration of dolomite: A review. Carbonates and Evaporites 7, 21-37.

McArthur, J.M., Howarth, R.J., Bailey, T.R., 2001. Strontium isotope stratigraphy: LOWESS Version 3: best fit to the marine Sr-isotope curve for 0–509 Ma and accompanying look-up table for deriving numerical age. Journal of Geology 109, 155–170.

Mckenzie, J. A., Vasconcelos, C., 2009. Dolomite Mountains and the origin of the dolomite rock of which they mainly consist: historical developments and new perspectives. Sedimentology 56, 205–219.

McKenzie, J.A., 1981. Holocene dolomitization of calcium carbonate sediments from the coastal sabkhas of Abu Dhabi, U.A.E.: a stable isotope study. Journal of Geology 89, 185-198.

Medina-Elizalde, M., Lea, D.W., Fantle, M.S., 2008. Implications of seawater Mg/Ca variability for Plio-Pleistocene tropical climate reconstruction. Earth and Planetary Science Letters 269, 585-595.

Melim, L.A., 1996. Limitations on lowstand meteoric diagenesis in the Pliocene-Pleistocene of Florida and Great Bahama Bank: Implications for eustatic sea-level models. Geology 24, 893-896.

Melim, L.A., Swart, P.K., Maliva, R.G., 1995. Meteoric-like fabrics forming in marine waters: Implications for the use of petrography to identify diagenetic environments. Geology 23, 755-758.

Melim, L.A., Westphal, H., Swart, P.K., Eberli, G.P., Munnecke, A., 2002. Questioning

carbonate diagenetic paradigms: evidence from the Neogene of the Bahamas. Marine Geology 185, 27-53.

Miller, K.G., Kominz, M.A., Browning, J.V., Wright, J.D., Mountain, G.S., Katz, M.E., Sugarman, P.J., Cramer, B.S., Christie-Blick, N., Pekar, S.F., 2005. The Phanerozoic record of global sea-level change. Science 310, 1293-1298.

Naish, T.R., Wilson, G.S., 2009. Constraints on the amplitude of Mid-Pliocene (3.6-2.4 Ma) eustatic sea-level fluctuations from the New Zealand shallow-marine sediment record. Philosophical Transactions of the Royal Society of London A 367, 169-187.

Ng, K.C., 1990. Diagenesis of the Oligcene-Miocene Bluff Formation of the Cayman Islands - A petrographic and hydrogeochemical approach. Unpublished PhD thesis, University of Alberta, 344 pp.

Ng, K.C., Jones, B., 1995. Hydrogeochemistry of Grand Cayman, British West Indies: implications for carbonate diagenetic studies. Journal of Hydrology 164, 193-216.

Ng, K.C., Jones, B., Beswick, R., 1992. Hydrogeology of Grand Cayman, British West Indies: a karstic dolostone aquifer. Journal of Hydrology 134, 273-295.

Nordeng, S.H., Sibley, D.F., 1994. Dolomite stoichiometry and Ostwald's step rule. Geochimica et Cosmochimica Acta 58, 191-196.

O'Brien, C.L., Foster, G.L., Martinez-Boti, M.A., Abell, R., Rae, J.W.B., Pancost, R.D., 2014. High sea surface temperatures in tropical warm pools during the Pliocene. Nature Geoscience 7, 606-611.

Ohde, S., Elderfield, H., 1992. Strontium isotope stratigraphy of Kita-daito-jima Atoll, North Philippine Sea: implications for Neogene sea-level change and tectonic history. Earth and Planetary Science Letters 113, 473-486.

Peltier, W.R., Fairbanks, R.G., 2006. Global glacial ice volume and Last Glacial Maximum duration from an extended Barbados sea level record. Quaternary Science Reviews 25, 3322-3337.

Perfit, M.R., Heezen, B.C., 1978. The geology and evolution of the Cayman Trench.

Geological Society of America Bulletin 89, 1155-1174.

Pleydell, S.M., Jones, B., Longstaffe, F.J., Baadsgaard, H., 1990. Dolomitization of the Oligocene-Miocene Bluff Formation on Grand Cayman, British West Indies. Canadian Journal of Earth Sciences 27, 1098-1110.

Quinn, T.M., 1991. Meteoric diagenesis of Plio-Pleistocene limestones at Enewetak Atoll. Journal of Sedimentary Research 61, 681-703.

Quinn, T.M., Matthews, R.K., 1990. Post-Miocene diagenetic and eustatic history of Enewetak Atoll: Model and data comparison. Geology 18, 942-945.

Reeder, R.J. 1991. An overview of zoning in carbonate minerals. In: Barker, C.E., Burruss, R.C., Kopp, O.C., Machel, H.G., Marshall, D.J., Wright, P., Colbum, H.Y. (Eds.), Luminescence Microscopy and Spectroscopy: Qualitative and Quantitative Applications. SEPM Special Publication 25, pp. 77-82.

Reeder, R.J., 1981. Electron optical investigation of sedimentary dolomites. Contributions to Mineralogy and Petrology 76, 148-157.

Ren, M., Jones, B., 2016. Diagenesis in limestone-dolostone successions after 1 million years of rapid sea-level fluctuations: A case study from Grand Cayman, British West Indies. Sedimentary Geology 342, 15-30.

Ren, M., Jones, B., 2017. Spatial variations in the stoichiometry and geochemistry of Miocene dolomite from Grand Cayman: Implications for the origin of island dolostone. Sedimentary Geology 348, 69-93.

Roberts, H.H., 1994. Reefs and lagoons of Grand Cayman. In: Brunt, M.A., Davies, J.E. (Eds.), The Cayman Islands: Natural History and Biogeography. Springer, Netherlands, pp. 75-104.

Roberts, J.A., Kenward, P.A., Fowle, D.A., Goldstein, R.H., González, L.A., Moore, D.S., 2013. Surface chemistry allows for abiotic precipitation of dolomite at low temperature. Proceedings of the National Academy of Sciences 110, 14540-14545.

Rodgers, K.A., Easton, A.J., Downes, C.J., 1982. The chemistry of carbonate rocks of Niue

Island, South Pacific. Journal of Geology 90, 645-662.

Rohling, E.J., Foster, G.L., Grant, K.M., Marino, G., Roberts, A.P., Tamisiea, M.E., Williams, F., 2014. Sea-level and deep-sea-temperature variability over the past 5.3 million years. Nature 508, 477-482.

Rosenbaum, J., Sheppard, S.M.F., 1986. An isotopic study of siderites, dolomites and ankerites at high temperatures. Geochimica et Cosmochimica Acta 50, 1147-1150.

Saller, A.H., 1984. Petrologic and geochemical constraints on the origin of subsurface dolomite, Enewetak Atoll: an example of dolomitization by normal seawater. Geology 12, 217-220.

Sass, E., Bein, A., 1988. Dolomites and salinity: a comparative geochemical study. In: Shukla, V., Baker, P.A. (Eds.), Sedimentology and Geochemistry of Dolostones. SEPM Special Publication 43, pp. 223-233.

Schlanger, S.O., Graf, D.L., Goldsmith, J.R., Macdonald, G.A., Sackett, W.M., Potratz, H.A., 1963. Subsurface geology of Eniwetok atoll. Geological Survey Professional Paper 260-BB: 991-1066.

Schmidt, V., 1965. Facies, diagenesis, and related reservoir properties in the Gigas Beds (Upper Jurassic), northwester Germany. In: Prey, L.C., Murray, R.C. (Eds.), Dolomitization and Limestone Diagenesis. SEPM Special Publication 13, pp. 124-169.

Schroeder, J.H., 1972. Fabrics and sequences of submarine carbonate cements in Holocene Bermuda cup reefs. Geologische Rundschau 61, 708-730.

Searl, A., 1994. Discontinuous solid solution in Ca-rich dolomites: the evidence and implications for the interpretation of dolomite petrographic and geochemical data. In: Purser, B.H., Tucker, M.E., Zenger, D.L. (Eds.), Dolomites: A Volume in Honour of Dolomieu. International Association of Sedimentologists Special Publication 21, pp. 361-376.

Sherman, C.E., Fletcher, C.H., Rubin, K.H., 1999. Marine and meteoric diagenesis of Pleistocene carbonates from a nearshore submarine terrace, Oahu, Hawaii. Journal of

Sedimentary Research 69, 1083-1097.

Sibley, D.F., 1980. Climatic control of dolomitization, Seroe Domi Formation (Pliocene), Bonaire, NA. In: Zenger, D.H., Dunham, J.B., Ethington, R.L. (Eds.), Concepts and Models of Dolomitization. SEPM Special Publication 28, pp. 247-258.

Sibley, D.F., 1982. The origin of common dolomite fabrics: Clues from the Pliocene. Journal of Sedimentary Research 52, 1087-1100.

Sibley, D.F., 1990. Unstable to stable transformations during dolomitization. Journal of Geology 98, 739-748.

Sibley, D.F., Dedoes, R.E., Bartlett, T.R., 1987. Kinetics of dolomitization. Geology 15, 1112-1114.

Sibley, D.F., Nordeng, S.H., Borkowski, M.L., 1994. Dolomitization kinetics of hydrothermal bombs and natural settings. Journal of Sedimentary Research 64, 630-637.

Siddall, M., Rohling, E.J., Almoogi-Labin, A., Hemleben, Ch., Meischner, D., Schmelzer, I., Smeed, D.A., 2003. Sea-level fluctuations during the last glacial cycle. Nature 423, 853-858.

Simms, M., 1984. Dolomitization by groundwater-flow system in carbonate platforms. Transactions—Gulf Coast Association of Geological Societies 34, 411-420.

Sperber, C.M., Wilkinson, B.H., Peacor, D.R., 1984. Rock composition, dolomite stoichiometry, and rock/water reactions in dolomitic carbonate rocks. Journal of Geology 92, 609-622.

Spratt, R.M., Lisiecki, L.E., 2016. A Late Pleistocene sea level stack. Climate of the Past 12, 1079-1092.

Steinen, R.P., 1974. Phreatic and vadose diagenetic modification of Pleistocene limestone: petrographic observations from subsurface of Barbados, West Indies. American Association of Petroleum Geologists, Bulletin 58, 1008-1024.

Steinen, R.P., Matthews, R.K., 1973. Phreatic vs. vadose diagenesis: stratigraphy and mineralogy of a cored borehole on Barbados, W.I. Journal of Sedimentary Research 43,

1012-1020.

Supko, P.R., 1977. Subsurface dolomites, San Salvador, Bahamas. Journal of Sedimentary Research 47, 1063-1077.

Suzuki, Y., Iryu, Y., Inagaki, S., Yamada, T., Aizawa, S., Budd, D.A., 2006. Origin of atoll dolomites distinguished by geochemistry and crystal chemistry: Kita-daito-jima, northern Philippine Sea. Sedimentary Geology 183, 181-202.

Swart, P.K., Cantrell, D.L., Westphal, H., Handford, C.R., Kendall, C.G., 2005. Origin of dolomite in the Arab-D reservoir from the Ghawar Field, Saudi Arabia: evidence from petrographic and geochemical constraints. Journal of Sedimentary Research 75, 476-491.

Swart, P.K., Melim, L.A., 2000. The origin of dolomites in Tertiary sediments from the margin of Great Bahama Bank. Journal of Sedimentary Research 70, 738-748.

Swart, P.K., Ruiz, J., Holmes, C.W., 1987. Use of strontium isotopes to constrain the timing and mode of dolomitization of Upper Cenozoic sediments in a core from San Salvador, Bahamas. Geology 15, 262-265.

Thorstenson, D.C., Mackenzie, F.T., Ristvet, B.L., 1972. Experimental vadose and phreatic cementation of skeletal carbonate sand. Journal of Sedimentary Research 42, 162-167.

Tucker, M.E., Wright, V.P. 1990. Carbonate Sedimentology. Blackwell Scientific Publications, Oxford, 482 pp.

Uzelman, B.C., 2009. Sedimentology, diagenesis, and dolomitization of the Brac Formation (Lower Oligocene), Cayman Brac, British West Indies. Master Thesis, University of Alberta, 120 pp.

Vacher, L.H.L., 1997. Introduction: varieties of carbonate islands and a historical perspective. In: Vacher, H.L., Quinn, T.M. (Eds.), Geology and Hydrogeology of Carbonate Islands. Elsevier Science, pp. 1-34.

Vahrenkamp, V.C., Swart, P.K., Purser, B., Tucker, M., Zenger, D., 1994. Late Cenozoic dolomites of the Bahamas: metastable analogues for the genesis of ancient platform

dolomites. In: Purser, B.H.,Tucker, M.E., Zenger, D.L. (Eds.), Dolomites: A Volume in Honour of Dolomieu. International Association of Sedimentologists Special Publication 21, pp. 133-153.

Vahrenkamp, V.C., Swart, P.K., Ruiz, J., 1991. Episodic dolomitization of late Cenozoic carbonates in the Bahamas: evidence from strontium isotopes. Journal of Sedimentary Research 61, 1002-1014.

Van Tuyl, F.M., 1916. New points on the origin of dolomite. American Journal of Science 42, 249-260.

Vézina, J., Jones, B., Ford, D., 1999. Sea-level highstands over the last 500,000 years: Evidence from the Ironshore Formation on Grand Cayman, British West Indies. Journal of Sedimentary Research 69, 317–327.

Vollbrecht, R., 1990. Marine and meteoric diagenesis of submarine Pleistocene carbonates from the Bermuda Carbonate Platform. Carbonates and Evaporites 5, 13-96.

Vollbrecht, R., Meischner, D., 1996. Diagenesis in coastal carbonates related to Pleistocene sea level, Bermuda Platform. Journal of Sedimentary Research 66, 243-258.

Wang, Z., Shi, Z., Zhang, D., Huang, K., You, L., Duan, X., Li, S., 2015. Microscopic features and genesis for Miocene to Pliocene dolomite in well Xike-1, Xisha Islands. Earth Science-Journal of China University of Geosciences 40, 633-644. [in Chinese]

Ward, W.C., Halley, R.B., 1985. Dolomitization in a mixing zone of near-seawater composition, Late Pleistocene, northeastern Yucatan Peninsula. Journal of Sedimentary Research 55, 407-420.

Warren, J., 2000. Dolomite: occurrence, evolution and economically important associations. Earth-Science Reviews 52, 1-81.

Wei, X., Jia, C., Meng, W., 2008. Dolomitization characteristics of carbonate rock in Xisha Islands and its formation: A case study of well Xichen-1. Journal of Jilin University (Earth Science Edition) 38, 217-224. [in Chinese]

Wei, X., Zhu, Y., Xu, H., Zhao, G., Li, Y., 2006. Discussion on Neogene dolostone forming

condition in Xisha Islands: Evidences from isotope C and O and fluid inclosures. Acta Petrologica Sinica 22, 2394-2404. [in Chinese]

Wheeler, C., Aharon, P. 1997. Chapter 17 Geology and hydrogeology of Niue. In: Vacher, H.L., Quinn, T.M. (Eds.), Geology and Hydrogeology of Carbonate Islands. Elsevier Science, Amsterdam, Netherlands, pp. 537-564.

Wheeler, C.W., Aharon, P., Ferrell, R.E., 1999. Successions of Late Cenozoic platform dolomites distinguished by texture, geochemistry, and crystal chemistry: Niue, South Pacific. Journal of Sedimentary Research 69, 239-255.

Whitaker, F.F., Paterson, R.J., Johnston, V.E., 2006. Meteoric diagenesis during sea-level lowstands: Evidence from modern hydrochemical studies on northern Guam. Journal of Geochemical Exploration 89, 420-423.

Whitaker, F.F., Smart, P., Hague, Y., Waltham, D., Bosence, D., 1997. Coupled two-dimensional diagenetic and sedimentological modeling of carbonate platform evolution. Geology 25, 175-178.

Whitaker, F.F., Smart, P.L., Jones, G.D., 2004. Dolomitization: from conceptual to numerical models. In: Braithwaite, C.J.R., Rizzi, G., Darke, G. (Eds.), The Geometry and Petrogenesis of Dolomite Hydrocarbon Reservoirs. Geological Society of London Special Publication 235, pp. 99-139.

Wignall, B.D., 1995. Sedimentology and Diagenesis of the Cayman (Miocene) and Pedro Castle (Pliocene) Formations at Safe Haven, Grand Cayman, British West Indies. Master Thesis, University of Alberta, 110 pp.

Willson, E.A., 1998. Depositional and Diagenetic Features of the Middle Miocene Cayman Formation, Roger's Wreck Point, Grand Cayman, British West Indies. Master Thesis, University of Alberta, 103 pp.

Wilson, E.N., Hardie, L.A., Phillips, O.M., 1990. Dolomitization front geometry, fluid flow patterns, and the origin of massive dolomite: the Triassic Latemar buildup, northern Italy. American Journal of Science 290, 741-796.

Zhao, H., Jones, B., 2012a. Origin of “island dolostones”: A case study from the Cayman Formation (Miocene), Cayman Brac, British West Indies. Sedimentary Geology 243-244, 191-206.

Zhao, H., Jones, B., 2012b. Genesis of fabric-destructive dolostones: A case study of the Brac Formation (Oligocene), Cayman Brac, British West Indies. Sedimentary Geology 267-268, 36-54.

Zhao, H., Jones, B., 2013. Distribution and interpretation of rare earth elements and yttrium in Cenozoic dolostones and limestones on Cayman Brac, British West Indies. Sedimentary Geology 284-285, 26-38.